

SPECTROSCOPIC STUDIES OF  
SOME SEMIQUINONE RADICAL IONS

By  
Ashley George WHEWAY

Submitted for Degree of Ph.D.  
at the University of Aston in Birmingham

THESIS  
547 567  
WHE

176137. 21 AUG 1974

March 1974.

## SUMMARY

Previous ESR and UV spectroscopic studies of semiquinone cations are reviewed. Cations of 4,4'-biphenosemiquinones prepared by chemical oxidation of the corresponding diols and reduction of the quinones in sulphuric acid, were studied using ESR and UV spectroscopy. Oxidation of biphenyl-4,4'-diol in sulphuric acid leads to either the 4,4'-biphenosemiquinone cation or its 3,3'-disulphonated derivative, whereas, oxidation in aluminium chloride-nitromethane yields only the parent cation. Reduction of 4,4'-biphenoquinone in dideuterio-sulphuric acid initially gives the 4,4'-biphenosemiquinone cation which subsequently undergoes a stepwise exchange of the protons in the 3,3',5 and 5' positions for deuterons. A variable temperature study of this process is reported and discussed. Similar patterns of behaviour are observed in the 1,4-dihydroxybenzene-1,4-benzoquinone system.

The 3,3',5,5'-tetra-*t*-butyl-4,4'-biphenosemiquinone cation under certain conditions undergoes dealkylation to give secondary radicals.

Anions of some alkylated 4,4'-biphenosemiquinones were prepared by the air oxidation of the diols in a variety of solvent mixtures and studied by ESR. The

solvent dependance of the hyperfine coupling constants for the 3,3',5,5'-tetramethyl- derivative are reported and discussed in terms of an equilibrium between semiquinone anions and hydrogen-bonded complexes of such anions with the hydroxylic solvent. The theory of Gendell, Freed and Fraenkel is shown to be quantitatively in agreement with the results. A correlation between the electron-donating power of the solvent and the equilibrium constant for the dissociation of the hydrogen-bonded complexes is also discussed.

Molecular orbital calculations were performed for the 4,4'-biphenosemiquinone system and its 3,3',5,5'-tetramethyl- derivative. Changes in the hyperfine coupling constants between the anion and the cation of 4,4'-biphenosemiquinone are consistent with these qualitative predictions.

Several electron donor compounds were treated with 3,3',5,5'-tetrachloro- and 3,3',5,5'-tetrabromo-4,4'-biphenoquinones. Paramagnetic products were only detected in the case of phenothiazine.

## CONTENTS

	<u>Page</u>
SUMMARY	<u>ii</u>
1. INTRODUCTION .. .. .	1
1.1. SEMIQUINONES .. .. .	1
1.2. BIPHENOSEMIQUINONES .. .. .	3
1.3. SCOPE OF THE PRESENT WORK .. .. .	5
2. EXPERIMENTAL .. .. .	6
2.1. PREPARATION OF COMPOUNDS .. .. .	6
2.1.1. Biphenyl-4,4'-diol .. .. .	6
2.1.2. 3,3',5,5'-Tetrachlorobiphenyl-4,4'-diol .. .. .	6
2.1.3. 3,3',5,5'-Tetrabromobiphenyl-4,4'-diol .. .. .	7
2.1.4. 4,4'-Biphenoquinone .. .. .	7
2.1.5. 3,3',5,5'-Tetrachloro-4,4'-biphenoquinone .. .. .	8
2.1.6. 3,3',5,5'-Tetrabromo-4,4'-biphenoquinone .. .. .	8
2.1.7. 3,3',5,5'-Tetramethyl-4,4'-biphenoquinone .. .. .	9
2.1.8. 3,3',5,5'-Tetraisopropyl-4,4'-biphenoquinone .. .. .	10
2.1.9. 3,3',5,5'-Tetra- <i>t</i> -butyl-4,4'-biphenoquinone .. .. .	10
2.1.10. 3,3',5,5'-Tetra- <i>sec</i> -butyl-4,4'-biphenoquinone .. .. .	10
2.1.11. 3,3',5,5'-Tetraalkylbiphenyl-4,4'-diols .. .. .	11
2.1.12. 3,3'-Dimethylbiphenyl-4,4'-diol .. .. .	11
2.1.13. 3,3',5,5'-Tetramethoxybiphenyl-4,4'-diol .. .. .	12

	<u>Page</u>
2.1.14. 4,4'-Dihydroxybiphenyl-3,3'- disulphonic Acid.. .. .	12
2.1.15. 4,4'-Dihydroxybiphenyl-3,3',5,5'- tetrasulphonic Acid .. .. .	13
2.2. ESR SPECTROSCOPY.. .. .	14
2.2.1. The Spectrometer.. .. .	14
2.2.2. Variable Temperature Accessory ..	15
2.2.3. Sample Preparation .. .. .	17
2.2.3.1. Semiquinone Cations.. ..	17
2.2.3.2. Semiquinone Anions .. ..	19
2.2.3.3. Reactions of Quinones with Donor Molecules ..	19
2.2.4. Measurement of g-Factors.. .. .	20
2.3. OTHER SPECTROSCOPIC TECHNIQUES .. .. .	21
2.4. COMPUTER PROGRAMS .. .. .	22
2.4.1. ESRSIM: A Computer Program for the Simulation of ESR Spectra ..	22
2.4.2. MOLORB 2: A Computer Program for the calculation of $\pi$ -Spin Densities of Conjugated Free Radicals by the HMO and McLachlan Modified HMO Methods.. .. .	27
3. 4,4'-BIPHENOSEMIQUINONE CATIONS .. .. .	31
3.1. PREVIOUS WORK INVOLVING SEMIQUINONE CATIONS .. .. .	31
3.2. 4,4'-BIPHENOSEMIQUINONE CATION, RESULTS AND DISCUSSION .. .. .	37
3.2.1. Oxidation of Biphenyl-4,4'- diol in Concentrated Sulphuric Acid ..	37
3.2.2. Reduction of 4,4'-Biphenoquinone in Concentrated Sulphuric Acid ..	42
3.2.3. Oxidation of Biphenyl-4,4'-diol by an Aluminium Chloride- Nitromethane Mixture.. .. .	47
3.3. HALOGENATED 4,4'-BIPHENOSEMIQUINONE CATIONS, RESULTS AND DISCUSSION.. ..	48
3.4. ALKYL SUBSTITUTED 4,4'-BIPHENOSEMIQUINONE CATIONS, RESULTS AND DISCUSSION.. ..	51

	<u>Page</u>
3.4.1. Reduction of Alkylated 4,4'- Biphenokinones in Concentrated Sulphuric Acid .. .. .	51
3.4.2. Oxidation of Alkylated Biphenyl- 4,4'-diols in Concentrated Sulphuric Acid .. .. .	52
3.4.3. Oxidation of Alkylated Biphenyl- 4,4'-diols by an Aluminium Chloride-Nitromethane Mixture ..	53
3.4.4. Oxidation of 3,3',5,5'-Tetra-t- butylbiphenyl-4,4'-diol by a Concentrated Sulphuric Acid- Nitromethane Mixture.. .. .	56
3.5. g-FACTORS .. .. .	58
3.6. ELECTRONIC ABSORPTION SPECTRA OF 4,4'- BIPHENOSEMIQUINONE CATIONS .. .. .	59
3.6.1. Previous Studies on Semiquinone Cations .. .. .	59
3.6.2. Present Studies .. .. .	60
4. 4,4'-BIPHENOSEMIQUINONE ANIONS .. .. .	63
4.1. PREVIOUS STUDIES.. .. .	63
4.2. RESULTS OF PRESENT WORK .. .. .	66
4.2.1. 3,3',5,5'-Tetramethyl-4,4'- biphenosemiquinone Anion (TMBPSQ Anion) .. .. .	66
4.2.1.1. The Analysis of the ESR Spectra.. .. .	72
4.2.2. 3,3',5,5'-Tetraethoxy-4,4'- biphenosemiquinone Anion.. .. .	73
4.2.3. 3,3',5,5'-Tetraisopropyl-4,4'- biphenosemiquinone Anion (TPBPSQ Anion) .. .. .	73
4.2.4. 3,3',5,5'-Tetra-t-butyl-4,4'- biphenosemiquinone Anion.. .. .	75
4.3. DISCUSSION .. .. .	76
4.3.1. Solvent Effects in Semiquinone Anions .. .. .	76
4.3.2. 3,3',5,5'-Tetramethyl-4,4'- biphenosemiquinone Anion (TMBPSQ Anion) .. .. .	81
5. MOLECULAR ORBITAL CALCULATIONS .. .. .	91

	<u>Page</u>
5.1. SIMPLE MOLECULAR ORBITAL MODELS .. .. .	91
5.2. SPIN DENSITY CALCULATIONS FOR 4,4'- BIPHENOSEMIQUINONE IONS .. .. .	96
6. REACTIONS OF QUINONES WITH DONOR MOLECULES ..	100
6.1. PREVIOUS STUDIES USING ESR SPECTROSCOPY ..	100
6.2. PRESENT STUDIES .. .. .	102
7. CONCLUSIONS .. .. .	105
APPENDICES .. .. .	109
1. NOMENCLATURE.. .. .	109
2. ESRSIM: A Computer Program for the Simulation of ESR Spectra .. .. .	112
3. MOLORB 2: A Computer Program for the Calculation of HMO and McLachlan Modified HMO Spin Densities for Conjugated Free Radicals.. .. .	123
BIBLIOGRAPHY .. .. .	130
ACKNOWLEDGEMENTS .. .. .	137

## 1. INTRODUCTION

### 1.1. SEMIQUINONES

The reduction of quinones to dihydroquinones (commonly referred to as hydroquinones) is a reversible process involving the addition of two electrons and two protons. It is possible to transfer these electrons one at a time thus producing intermediates representing the oxidation state lying half-way between these two compounds. These paramagnetic intermediates are appropriately called semiquinones, their exact nature and stability is largely dependant upon the pH of the solution. In an alkaline medium the semiquinone exists as an anion which gains added stability because of the greater delocalisation of the unpaired electron.

These anion radicals were first discovered by Michaelis (1) in 1931 and his subsequent classic studies (2 - 6) established their nature and also the factors determining the various equilibria. They were also amongst the first radicals examined using the Electron Spin Resonance technique (ESR)(7) and the para- or 1,4-semiquinone anions have been the subject of much research in order to study the effect of structure on the  $\pi$ -electron distribution. The 1,2-isomers (ortho-semiquinones) are much less stable and readily produce



secondary radicals (8 - 10). Although meta- or 1,3-quinones do not exist the ESR spectra of their semiquinones produced by the oxidation of the substituted 1,3-dihydroxybenzenes in a fast flow system have been observed (9, 10).

In neutral or weakly acidic media the semiquinone is present as the neutral monoprotinated species which is much less stable. It tends either to disproportionate directly to mixtures of the quinone and the hydroquinone or produce a quinone-hydroquinone adduct known as a quinhydrone. This substance is apparently a charge-transfer complex with the hydroquinone acting as the electron donor and the quinone as the electron acceptor. Quinhydrones, although not very soluble tend to be considerably dissociated into their components in solution. Neutral semiquinones have been prepared photolytically (11) and have also been observed in dilute acid using an ESR fast flow technique (12).

The doubly protonated species, the semiquinone cation, was first detected by Land and Porter (13) using U.V. spectroscopy. Subsequently, Bolton and Carrington (14) investigated such species in concentrated sulphuric acid using ESR spectroscopy.

The relationships between these various intermediates are shown schematically in figure 1.1 for the 1,4-benzoquinone - hydroquinone system.

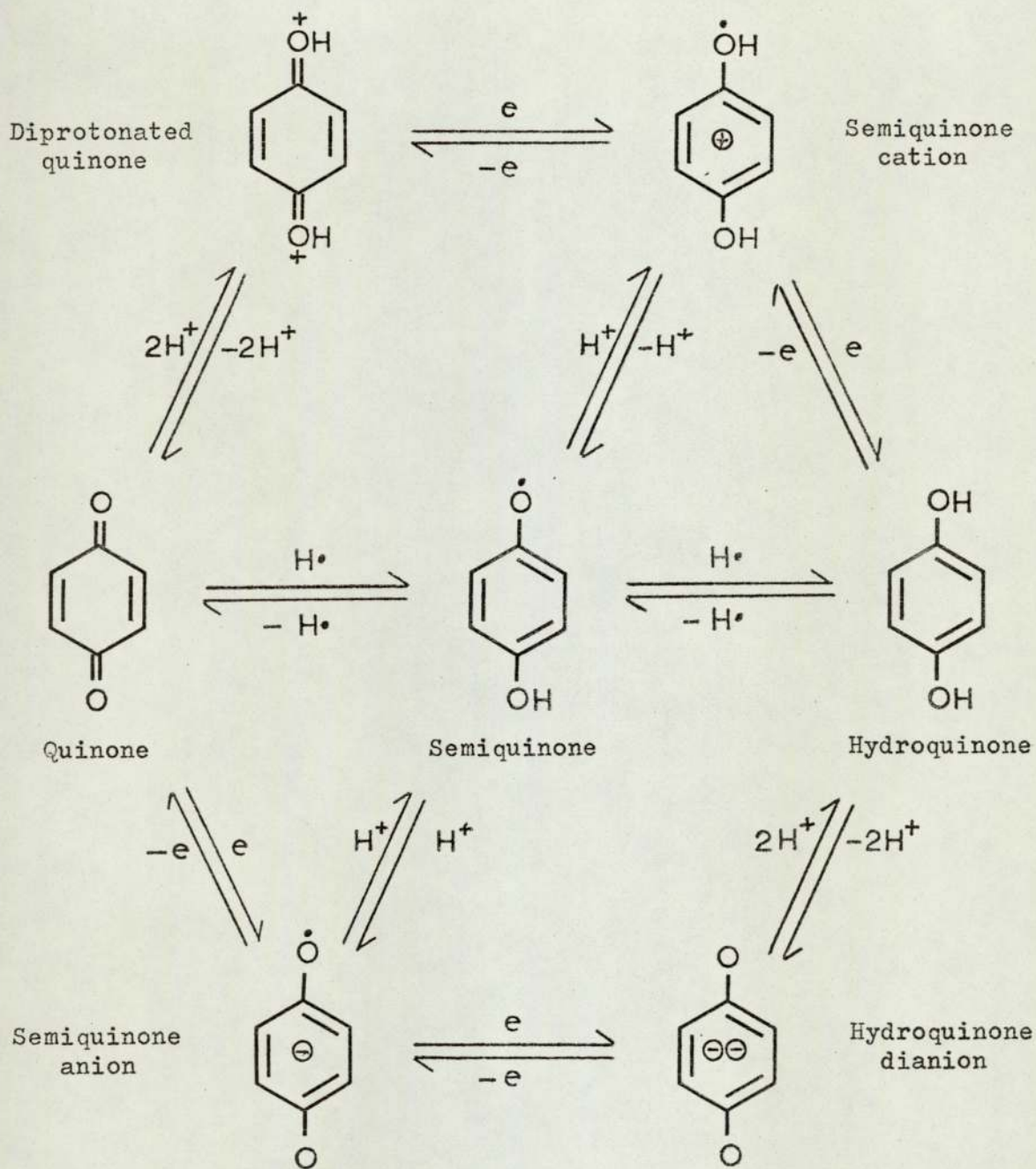
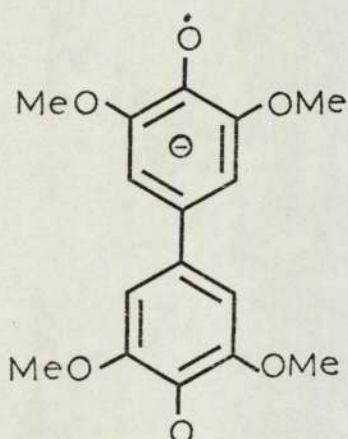


Figure 1.1

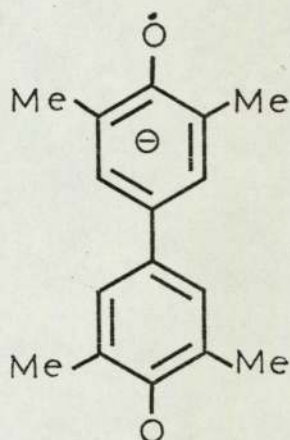
## 1.2. BIPHENOSEMIQUINONES

Although the literature abounds with spectroscopic studies on benzo-, naphtho- and anthrasemiquinones very little had been reported up to 1969 concerning the bipheno- analogues (a note on the nomenclature used for the corresponding quinones and hydroquinones is given in appendix 1).

Matsunaga and McDowell (15) reported the ESR spectra of the 3,3',5,5'-tetramethoxy- and 3,3',5,5'-tetramethyl-4,4'-biphenosemiquinone anions (I, II) prepared by the



(I)

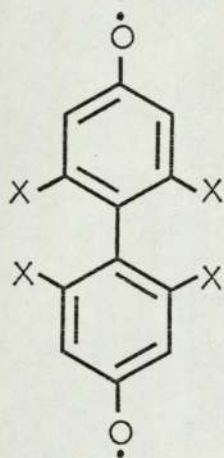


(II)

air oxidation of the respective biphenyldiols in a mixture of aqueous potassium hydroxide and pyridine. However, a subsequent paper by Matsunaga (16) offered an alternative mode of assigning the hyperfine coupling constants for the ring and methyl protons of the tetramethyl derivative.

Forbes and Sullivan (17) in reporting their ESR studies on the cation of 1,4-dimethoxybenzene noted that the oxidation of biphenyl-4,4'-diol with a mixture of aluminium chloride and nitromethane produced a blue paramagnetic solution. They analysed the resulting ESR spectrum in terms of two groups of four equivalent protons and one group of two equivalent protons.

In connection with these compounds it is interesting to note that Bourdon and Calvin (18) attempted to prepare 4,4'-biphenyldiols substituted in the 2,2',6 and 6' positions so that on oxidation a coplanar quinone is not produced but rather a diradical (III) stabilized by resonance.



(III)

Although the work was inconclusive, they showed that a hindered quinone, 2,2'-dimethyl-5,5'-di-t-butyl-4,4'-biphenylquinone could be prepared and was in equilibrium with a small amount of diradical.

### 1.3. SCOPE OF THE PRESENT WORK

The aims of the present work are threefold:

Firstly, to prepare and study using ESR and UV spectroscopy the biphenosemiquinone cation and its halogenated and alkylated derivatives both in concentrated sulphuric acid and in aluminium chloride - nitromethane mixtures with a view to detecting evidence of restricted rotation either of the hydroxyl groups or the aromatic rings.

Secondly, to extend the work of Matsunaga to other alkyl derivatives of biphenosemiquinone anion and perhaps determine the role and effect, if any, of the pyridine on the stability and ESR spectra of the semiquinone anions.

Thirdly, to investigate the electron acceptor properties of the halogenated 4,4'-biphenoquinones by ESR spectroscopy. The redox potential of the 4,4'-biphenoquinone-biphenyl-4,4'-diol system is quite high (0.954V) (19, 20) and halogenated derivatives should be expected to have even higher values and behave as extremely good electron acceptors, possibly even strong enough to completely remove an electron from a suitable donor.

These three topics are discussed in chapters 3, 4 and 6 respectively.

## 2. EXPERIMENTAL

### 2.1. PREPARATION OF COMPOUNDS

#### 2.1.1. Biphenyl-4,4'-diol

A commercial sample (Schukardt) of this compound was recrystallised three times from 70% aqueous ethanol yielding white crystalline plates, m.p. 273-275°C, lit. value 274-275°C (21).

Analysis: Found C 76.94%, H 5.22%

Calculated for  $C_{12}H_{10}O_2$  C 77.50%, H 5.38%

#### 2.1.2. 3,3',5,5'-Tetrachlorobiphenyl-4,4'-diol

The method used by Magatti (22) was employed. Chlorine was passed into a stirred suspension of biphenyl-4,4'-diol in glacial ethanoic acid at room temperature. Gradually the suspension dissolved to give a yellow solution which after a few minutes became hot and a pale yellow crystalline precipitate of crude 3,3',5,5'-tetrachlorobiphenyl-4,4'-diol formed. The slurry was washed several times with glacial ethanoic acid to remove the yellow colour and filtered to yield small white needles which were recrystallised twice from 50% aqueous ethanol, m.p. 239-241°C, lit. value 239-241°C (23).

Analysis: Found                    C 44.40%, H 1.85%, Cl 43.11%  
                  Calculated        C 44.50%, H 1.85%, Cl 43.70%  
                  for  $C_{12}H_6Cl_4O_2$

2.1.3.    3,3',5,5'-Tetrabromobiphenyl-4,4'-diol

This compound was prepared by a modified version of the method employed by Moir (24). 2.5g of biphenyl-4,4'-diol were suspended in 30 cm<sup>3</sup> glacial ethanoic acid at 60°C and bromine was added gradually until a red-brown solution was obtained. The temperature rose to 85°C and after ten minutes a white precipitate formed. The mixture was cooled, filtered and the solid was washed twice with glacial ethanoic acid. Recrystallisation from absolute ethanol produced 4.3g of white needlelike crystals, m.p. 266-267°C, lit. value 266°C (24).

Analysis: Found                    C 28.54%, H 1.24%, Br 63.28%  
                  Calculated        C 28.71%, H 1.20%, Br 63.70%  
                  for  $C_{12}H_6Br_4O_2$

2.1.4.    4,4'-Biphenone

This compound was prepared using the method of König et al. (23). A solution of 2.0g biphenyl-4,4'-diol in 80 cm<sup>3</sup> dry 1,4-dioxan was added with vigorous stirring over a period of five minutes to 7.14g of lead(IV) ethanoate in 140 cm<sup>3</sup> glacial ethanoic acid. The purple-brown mixture was then stirred for a further five minutes at 35°C before cooling in an ice-water bath. The resulting precipitate was filtered off and washed with glacial ethanoic acid and 60-80 light petroleum ether to yield

brown-violet crystals (1.52g). Recrystallisation from benzene produced gold coloured feathery needles whereas when acetone was used as the solvent larger dark red needles were obtained, m.p. ca. 165°C with decomposition, lit. value ca. 160°C with decomposition (25).

Analysis: Found C 77.82%, H 4.40%

Calculated for  $C_{12}H_8O_2$  C 78.30%, H 4.35%

### 2.1.5. 3,3',5,5'-Tetrachloro-4,4'-biphenquinone

This compound was prepared by a similar method to that used for obtaining 4,4'-biphenquinone. However, this time a hot solution of lead(IV) ethanoate in glacial ethanoic acid was added dropwise over a period of thirty minutes to a solution of 3,3',5,5'-tetrachlorobiphenyl-4,4'-diol in 1,4-dioxan. The resulting red-brown solution was cooled and filtered to yield brown-violet leaflets which were washed twice with 1,4-dioxan. The crystalline solid did not melt.

Analysis: Found C 44.40%, H 1.24%, Cl 43.11%

Calculated C 44.75%, H 1.40%, Cl 44.00%

for  $C_{12}H_4Cl_4O_2$

### 2.1.6. 3,3',5,5'-Tetrabromo-4,4'-biphenquinone

Again the method of König et al. (23) was employed but this time the 3,3',5,5'-tetrabromobiphenyl-4,4'-diol solution was added dropwise to the lead (IV) ethanoate solution. The resulting small scarlet crystals were filtered off and washed with 40-60 petroleum ether followed by acetone.



Analysis: Found                    C 28.46%, H 0.89%, Br 64.11%  
                  Calculated            C 28.82%, H 0.80%, Br 64.00%  
                  for  $C_{12}H_4Br_4O_2$

2.1.7.    3,3',5,5'-Tetramethyl-4,4'-biphenoquinone

Silver carbonate - Celite reagent (see footnote) was prepared as follows: 30g of Chromosorb W AW-DCMS (60-85 mesh) were added to a stirred solution of 34g of silver nitrate in 200 cm<sup>3</sup> of distilled water. A solution of 21g potassium hydrogen carbonate in 300 cm<sup>3</sup> distilled water was added slowly to the above suspension and the mixture stirred for a further ten minutes. The yellow-green precipitate was then filtered off, washed with distilled water until neutral and finally dried in a rotary evaporator over a period of four hours. 55g of the Celite reagent (a yellow-green powder) were obtained.

1.2g of 2,6-dimethylphenol were refluxed for thirty minutes in 150 cm<sup>3</sup> benzene with 25.1g Celite reagent. After filtration to remove the spent reagent a red-brown solution was obtained which on evaporation produced 1.1g of small scarlet crystals m.p. 215-216°C with decomposition, lit. value 215°C with decomposition (26). Recrystallisation from benzene did not raise the melting point.

Footnote:

Silver carbonate supported on Celite was found by Balogh et alia (26) to be an excellent reagent for the oxidative coupling of phenols to produce alkyl substituted biphenoquinones.

Analysis: Found C 79.63%, H 6.66%

Calculated for  $C_{16}H_{16}O_2$  C 79.95%, H 6.66%

2.1.8. 3,3',5,5'-Tetraisopropyl-4,4'-biphenquinone

This compound was obtained as violet leaflets by the reaction of the Celite reagent with 2,6-diisopropylphenol in a similar manner to that outlined in section 2.1.7. m.p. 195-198°C, lit. value 196-197°C (27).

Analysis: Found C 81.65%, H 9.12%

Calculated for  $C_{24}H_{32}O_2$  C 81.83%, H 9.09%

2.1.9. 3,3',5,5'-Tetra-t-butyl-4,4'-biphenquinone

Again the method outlined in section 2.1.7. was used to couple 2,6-di-t-butylphenol. The resulting violet crystals had a m.p. of 246-247°C, lit. value 246-247°C (28).

Analysis: Found C 82.02%, H 9.78%

Calculated for  $C_{28}H_{40}O_2$  C 82.30%, H 9.80%

2.1.10. 3,3',5,5'-Tetra-sec-butyl-4,4'-biphenquinone

2,6 di-sec-butylphenol was treated with Celite reagent in the manner outlined in section 2.1.7. to give a red crystalline solid, m.p. ca. 185°C with decomposition.

Analysis: Found C 81.96%, H 9.63%

Calculated for  $C_{28}H_{40}O_2$  C 82.30%, H 9.80%

2.1.11. 3,3',5,5'-Tetraalkylbiphenyl-4,4'-diols

The reduction of the four tetraalkyl quinones mentioned above was carried out in a similar way using zinc and concentrated hydrochloric acid. The quinone was added to isopropanol and the mixture heated to 60°C. The calculated amount of concentrated hydrochloric acid was then poured in followed by the necessary amount of zinc dust which was added gradually over a period of thirty minutes. The initial brightly coloured solution gradually became colourless as the reduction proceeded to completion. The solution was then cooled to 50°C, the insoluble inorganic material removed by filtration and the alkylated biphenyl-4,4'-diol recovered from the filtrate as a very pale crystalline solid by evaporation of the solvent. The solids were still slightly coloured after recrystallisation from aqueous ethanol.

Analysis: Found C 78.92%, H 7.40%

Calculated for

$C_{16}H_{18}O_2$  (tetramethyl-) C 79.30%, H 7.44%

Found C 81.73%, H 10.39%

Calculated for C 81.95%, H 10.25%

$C_{28}H_{42}O_2$  (tetra-t-butyl-)

2.1.12. 3,3'-Dimethylbiphenyl-4,4'-diol

This compound was prepared from 3,3'-dimethylbenzidine by a modified Sandmeyer reaction (29). 11.1g of the benzidine were dissolved in 500 cm<sup>3</sup> of water containing 29.2. cm<sup>3</sup> of concentrated hydrochloric acid

and cooled to 5°C. A cold solution of 7.25g sodium nitrite in 40 cm<sup>3</sup> of water was then added slowly, keeping the temperature below 5°C, until an excess of nitrous acid was present. The diazotised solution was then divided into five equal parts. Each part was then boiled with 1.8 dm<sup>3</sup> of water containing 20 cm<sup>3</sup> phosphoric(V) acid for ten minutes and the cooled solution was extracted with ether. Trituration of the combined extracts with benzene yielded a pale yellow crystalline solid. Recrystallisation from aqueous ethanol yielded very pale yellow crystals, m.p. 163-164°C.

Analysis: Found C 78.33%, H 6.54%  
Calculated for C<sub>14</sub>H<sub>14</sub>O<sub>2</sub> C 78.50%, H 6.54%

#### 2.1.13. 3,3',5,5'-Tetramethoxybiphenyl-4,4'-diol

The 3,3',5,5'-tetramethoxy-4,4'-biphenylquinone was first prepared from 2,6-dimethoxyphenol by dissolving it in glacial ethanoic acid followed by treatment with sodium nitrite. The quinone separated as purple needle-like crystals (30). Reduction of the quinone in the usual way (see section 2.1.11) yielded the diol which upon recrystallisation from ethanol gave almost white crystals, m.p. 192-193°C.

Analysis: Found C 62.77%, H 5.83%  
Calculated for C<sub>16</sub>H<sub>18</sub>O<sub>2</sub> C 62.72%, H 5.88%

#### 2.1.14. 4,4'-Dihydroxybiphenyl-3,3'-disulphonic Acid

The method outlined by Moir (31) was used to prepare a sample of this compound. 1g of biphenyl-

4,4'-diol was dissolved in 5 cm<sup>3</sup> concentrated sulphuric acid at 60°C. After about ten minutes the white micro-crystalline solid was formed which was filtered off on a sintered glass crucible.

2.1.15. 4,4'-Dihydroxybiphenyl-3,3',5,5'-  
tetrasulphonic Acid

A solution of this compound in concentrated sulphuric acid was prepared in a similar way to that of the disulphonic acid (2.1.14.) but this time the reaction mixture was kept at 160°C for thirty minutes (31).

All other solid organic compounds used were obtained commercially and were used either without further purification or if necessary recrystallised from a suitable solvent.

## 2.2. ESR SPECTROSCOPY

### 2.2.1. The Spectrometer

All ESR spectra were recorded on a Hilger and Watts Microspin X-Band (9.4 GHz) ESR Spectrometer with the magnet and power supply from Newport Instruments Ltd. The spectrometer provides two methods of viewing the electron spin resonance of unpaired electrons in an external magnetic field. The one, known as crystal video detection enables the absorption signal to be viewed on a cathode-ray tube as the external magnetic field is swept at 50 Hz. The second method, giving a much better sensitivity, utilizes a small amplitude high frequency field modulation (100 kHz) and together with a phase sensitive detector enables the output to be monitored by a pen recorder (a Servoscribe RE 511.20). The spectrum obtained in this later case is the first derivative of the absorption curve.

An automatic frequency control accessory, W.956 was also employed with the basic Microspin spectrometer. This enabled the klystron frequency to be locked to the sample cavity as reference instead of to the separate reference cavity. A detailed description of the spectrometer is given elsewhere (32).

A cylindrical reflection cavity (W.932), 4 cm in diameter, having a  $H_{011}$  mode and a selectivity factor (Q) of 8000 when operational was used throughout the work.

After setting up, the magnitude of the modulation current, and thus the amplitude of the modulating field, was made small enough (usually 0.005 A) to minimise lack of resolution by modulation current broadening and the scan speed and amplitude set to display the signal. When recording a signal a time constant of 1.5 sec. was usually employed.

The recorder chart was calibrated after each spectrum to be measured, which was scanned over a 2 mT range in twenty minutes using a recorder chart speed of 3 cm. min<sup>-1</sup>. A dilute solution of Fremy's salt, potassium peroxyamine disulphonate, in saturated potassium hydrogen carbonate solution which gives an ESR spectrum consisting of three equally intense hyperfine lines was used for the calibration, the separation of these lines was taken to be 1.3091 mT. This solution was contained in a sealed melting point capillary placed in the cavity alongside the solutions of the radicals under investigation.

#### 2.2.2. Variable Temperature Accessory

We had received as a gift a part of a Microspin variable temperature gas flow system (W.910) comprising a control unit (FA.999), liquid nitrogen dewar (W.972) and an evacuated feed and heater assembly (W.973). The basic system was designed to provide a stream of nitrogen gas at a pre-determined stabilized temperature in the range -180°C to +120°C.

In order to use this equipment a quartz dewar

assembly for the cavity (W.932) was constructed as shown in figure 2.1. A Cryoproducs 25 dm<sup>3</sup> capacity standard container was used to pressure feed the liquid nitrogen into W.972 (liquid nitrogen dewar) for use in obtaining the lower part of the temperature range. For temperatures greater than room temperature nitrogen gas from a cylinder was passed directly into the heater assembly. The nitrogen gas from the heater assembly was supplied to the quartz dewar by a dewar tube connected to it via the ball joint (figure 2.1.) and covered with ceramic insulating wool. The temperature inside the quartz dewar was monitored by the control unit using a thermistor inserted in the bottom of the dewar. The temperature recorder on the control unit was calibrated using a copper-constantan thermocouple inserted in the top of the dewar. In the upper range (30°C to 120°C) the temperature stability was  $\pm 0.5^{\circ}\text{C}$  whereas in the lower range (-140°C to +30°C) it was only  $\pm 2^{\circ}\text{C}$ .

When using the assembly in the lower range it was found necessary to surround it with a polythene sleeve so that the cavity could be flushed with a stream of dry nitrogen gas to prevent the accumulation of water and ice which would otherwise have led to a loss in sensitivity.

A more detailed description of the gas flow system and its operating instructions is given elsewhere (33).



DEWAR ASSEMBLY

3/4 ACTUAL  
SIZE

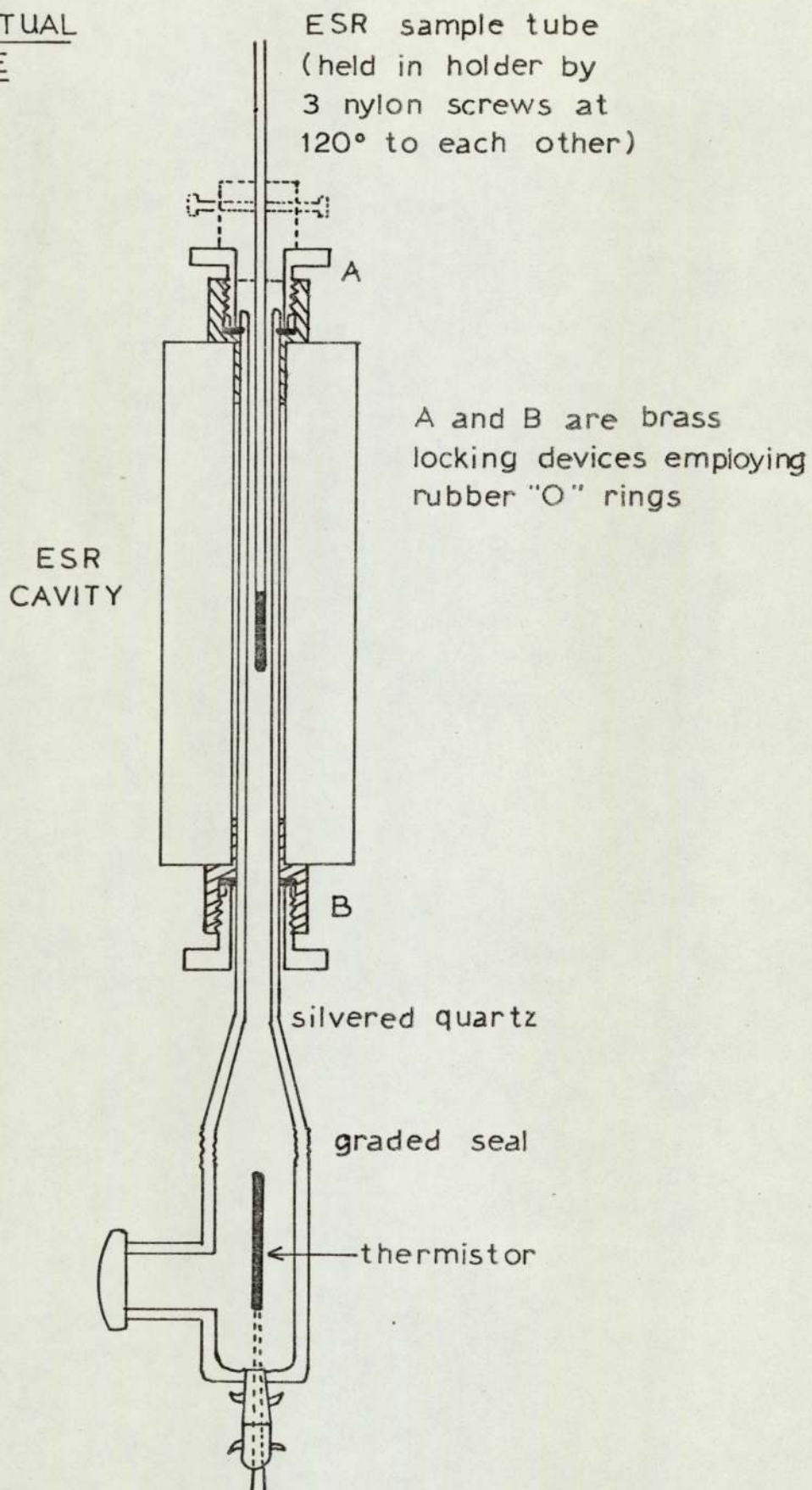


Figure 2.1

### 2.2.3. Sample Preparation

The ESR sample tubes used throughout this work were made from thin walled quartz tubing ("Spectrosil" grade) having a maximum outside diameter of 3mm. To facilitate their use on the vacuum line they were topped with B10 ground glass cones thus enabling vacuum taps to be fitted to them.

#### 2.2.3.1. Semiquinone Cations

The dihydroxy compounds were oxidised in 98% sulphuric acid or dideuteriosulphuric acid (Koch-Light) by pipetting 2.0 cm<sup>3</sup> acid onto a known mass of the substrate so as to give a concentration in the range 0.001 - 0.005M. A trace of hydrogen peroxide or potassium persulphate was then added with stirring. Oxygen was removed from the resulting highly coloured solution by bubbling dry nitrogen gas through it followed by degassing a sample of the solution in an ESR tube by a repetitive freeze-thaw technique on the vacuum line. The ESR sample was then kept under vacuum.

Cation radicals were produced from the quinones by the addition of 2.0 cm<sup>3</sup> acid, again a similar concentration of substrate was used. A trace of sodium dithionite was added to the solution if the radical concentration was too low for adequate observation by ESR spectroscopy. Finally the acid solutions were degassed in the same way as outlined above.

The reaction of 4,4'-biphenoquinone with dideutero-sulphuric acid at temperatures in the range 22 - 50°C was studied in the apparatus shown in figure 2.2. A known mass of the quinone was placed in bulb A and the required amount of acid, through which dry nitrogen gas had been bubbled, pipetted into side-arm B. The acid was then degassed in the usual way and the apparatus evacuated before immersing it in a water bath at the reaction temperature for twenty minutes. The reactants were then mixed together and a small amount of the mixture poured into the quartz side-arm of the apparatus which was then placed in the cavity of the spectrometer also at the reaction temperature.

A similar apparatus (figure 2.2.) was also used for the oxidation of the dihydroxy compounds using aluminium chloride and nitromethane. However, in this case, no direct access to the side-arm B was necessary. About 30 mg anhydrous aluminium chloride and 5 mg dihydroxy compound were placed in bulb A and the apparatus connected to the vacuum line where 2 cm<sup>3</sup> nitromethane were distilled into side-arm B. The reactants were mixed at room temperature under vacuum and some of the solution was subsequently transferred into the quartz capillary tube. The nitromethane was dried by distillation from phosphorus(V) oxide and deoxygenated by passing dry nitrogen gas through the liquid, followed by degassing under vacuum.

Cation radicals were also produced from biphenyl-4,4'-diol and some of its alkylated derivatives by the addition of nitromethane to a mixture of 98% sulphuric

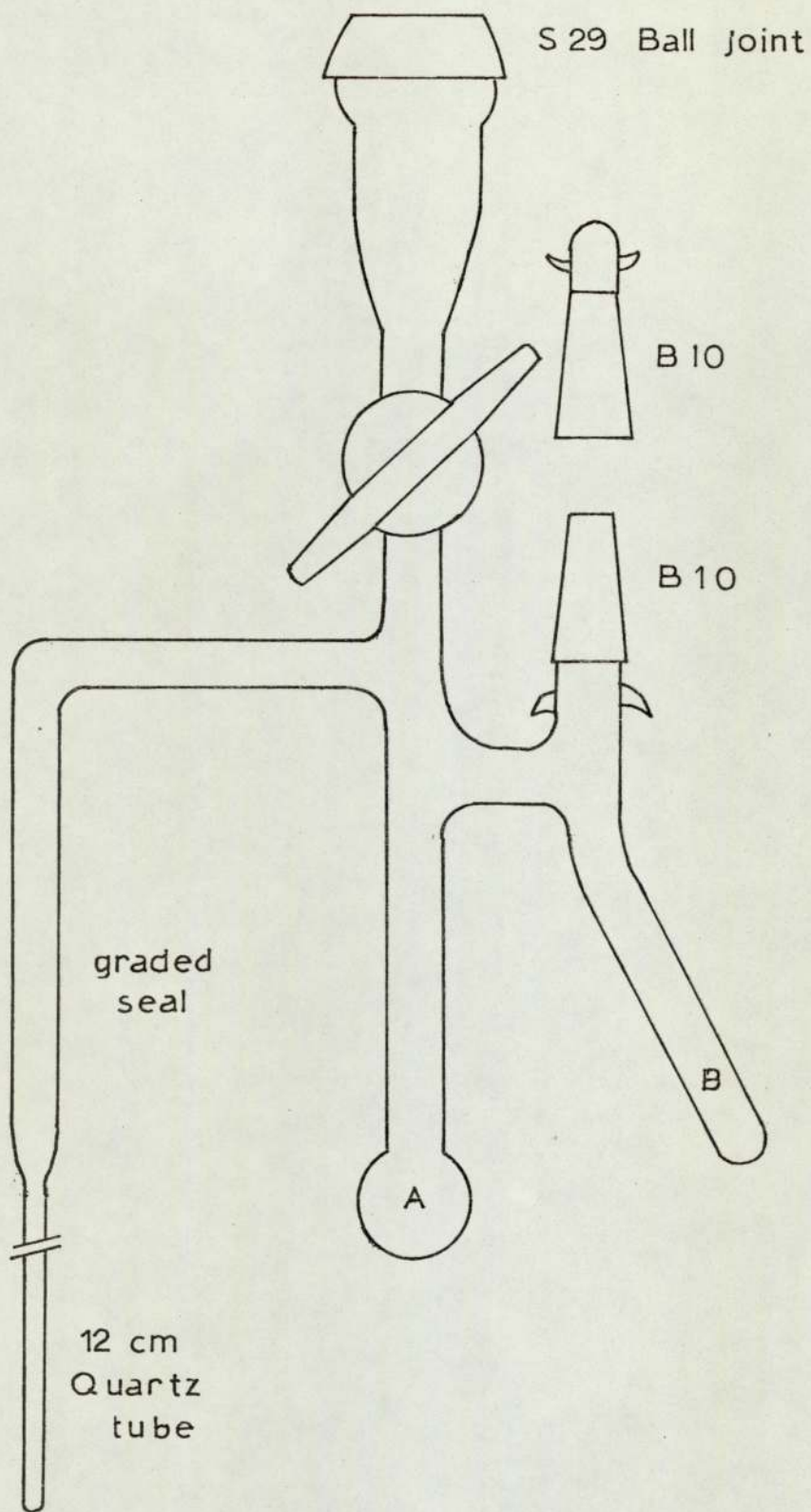


Figure 2.2

acid and the diol. The reactants were mixed in an apparatus similar to that shown in figure 2.2. but without the side-arm B. Nitromethane was distilled on the vacuum line onto a frozen matrix of the diol and acid and the reaction then allowed to proceed at room temperature before transfer of the solution to the quartz capillary.

#### 2.2.3.2. Semiquinone Anions

A known mass of the alkylated biphenyl-4,4'-diol, sufficient to give an overall concentration of 0.01M was mixed with a known volume of solvent. The volume of the mixture was then made up to 2.00 cm<sup>3</sup> with either aqueous or ethanolic potassium hydroxide solution (concentration 0.5 - 2.0M). The resulting yellow coloured solution, containing the semiquinone anion, was then deoxygenated by passing a slow stream of dry nitrogen gas through it and a sample sealed in an ESR tube. The solvents used, acetonitrile, benzene, diethylamine, N,N'-dimethylformamide, 1,4-dioxan, 2-picoline, pyridine and tetrachloromethane were purified by distillation before use.

#### 2.2.3.3. Reactions of Quinones with Donor Molecules

Solutions of the 3,3',5,5' tetrachloro- and tetrabromo-4,4'-biphenylquinones (0.005M) in a variety of organic solvents were treated with solutions in the same solvent of suitable electron donor compounds in an apparatus similar to that in figure 2.2. The two

solutions were degassed, mixed under vacuum and a small amount of the resulting mixture poured into the ESR quartz side-arm.

#### 2.2.4. Measurement of g-Factors

In order to determine the g-factors of the ESR spectra a solution containing the dianion, peroxyamine disulphonate (see section 2.2.1. for method of preparation) was inserted in the cavity simultaneously with the sample under investigation. The magnetic field ( $H_R$ ) corresponding to the central peak of the resonance absorption of this reference standard was then determined using the proton resonance method described elsewhere (34). Recording the combined spectra and taking the nitrogen hyperfine coupling constant in the peroxyamine disulphonate as 1.3091 mT enabled the field separation ( $\Delta H$ ) of the two signals to be calculated ( $\Delta H$  being taken as positive if the sample absorption signal occurred at the high field side of the reference). Using a value of 2.0055 for the g-factor of peroxyamine disulphonate the g-factor of the sample ( $g_s$ ) is then given by equation (2.1.).

$$g_s = 2.0055 (H_R / (H_R + \Delta H)) \quad (2.1.)$$

Using this technique a value of 2.0036 was consistently obtained for the g-factor of diphenylpicrylhydrazyl (DPPH).

### 2.3. OTHER SPECTROSCOPIC TECHNIQUES

The ultra-violet and visible absorption spectra recorded at room temperature were determined in 1cm quartz cells on a Unicam SP700 and a Perkin Elmer model 137UV spectrophotometer. Spectra at higher temperatures were determined on the 137UV incorporating a variable temperature attachment.

The nuclear magnetic resonance spectrum of 4,4'-dihydroxybiphenyl-3,3'-disulphonic acid was obtained on a Perkin Elmer R10 spectrometer operating at 60MHz using a saturated solution of the substrate in acetone.

The compounds referred to in section 2.1. were also characterised by infra-red spectroscopy using a Perkin Elmer model 237 spectrophotometer.

## 2.4. COMPUTER PROGRAMS

The programs, written in Algol, were designed for use on an ICL 1905 computer and are consequently given in 1900 series Algol. Program and data input was by cards unless otherwise stated. Graphical outputs were generated using a modified version of a set of procedures known as PAGE (35) and produced by means of a Calcomp Ltd. graph plotter associated with the 1905 computer.

### 2.4.1. ESRSIM: A Computer Program for the Simulation of ESR Spectra

A copy of the program is given in appendix 2. The program is designed to simulate the ESR spectra arising from one to four groups of equivalent atoms with a nuclear spin of a  $\frac{1}{2}$  or 1. Provision is made for a Gaussian or a Lorentzian line shape to be reproduced. The equations describing the overall spectrum were determined using the method outlined by Ayscough (36). The data for a single simulation is read into the computer in the following order:

1. Q - The number of groups of equivalent atoms.
2. N [D] - The number of atoms in each group commencing with the largest number.
3. SPIN [D] - The nuclear spin of each group of equivalent atoms (either 0.5 or 1).
4. K [D] - The hyperfine coupling constant in mT of each type of equivalent atom, keeping the same order as in 2 above.



5. XA, DX, XB - The parameters XA and XB determine the range over which the maximum and minimum values of the simulated ESR curve will be calculated. The magnetic field corresponding to the centre of the spectrum is taken as zero and all lines on the left hand side as having negative values. DX, again in mT units, determines how often the calculation is performed. Thus for a spectrum with its largest peak at the centre typical values of these parameters might be - 0.03, 0.0001, 0.03.
6. LW - The line width of the spectrum in mT.
7. C - An integer, 1 to 6, which determines the lineshape i.e. Gaussian or Lorentzian type and also depends on Q. For Gaussian curves with Q = 2, 3 and 4, C = 1, 2 and 3 respectively, whereas for Lorentzian curves with Q = 2, 3 and 4, C = 4, 5 and 6 respectively.
8. XMIN, XMAX - These two parameters expressed in mT determine the spread of the simulated spectrum e.g. for the simulation of an ESR spectrum with a total width of 2.6 mT the values of XMIN and XMAX would have to be at least - 1.3 and 1.3 respectively.
9. NUMBER - A spectrum reference number, an integer in the range 1 to 999.
10. CONTROL - An integer which controls the rest of the program after the first

simulation.

IF CONTROL = 6 then the program is terminated  
for other integers (1 to 5) the subsequent  
program is modified as follows,

CONTROL = 1,

Alters the overall width of the  
spectrum new data required for XMIN, XMAX  
and NUMBER only.

CONTROL = 2,

Alters the line shape, i.e.  
either from Gaussian to Lorentzian or  
vice versa, new data required for C to  
NUMBER.

CONTROL = 3,

Alters the linewidth, new data  
required for XA to NUMBER.

CONTROL = 4,

Alters the hyperfine coupling  
constants, new data required for K [D] to  
number.

CONTROL = 5,

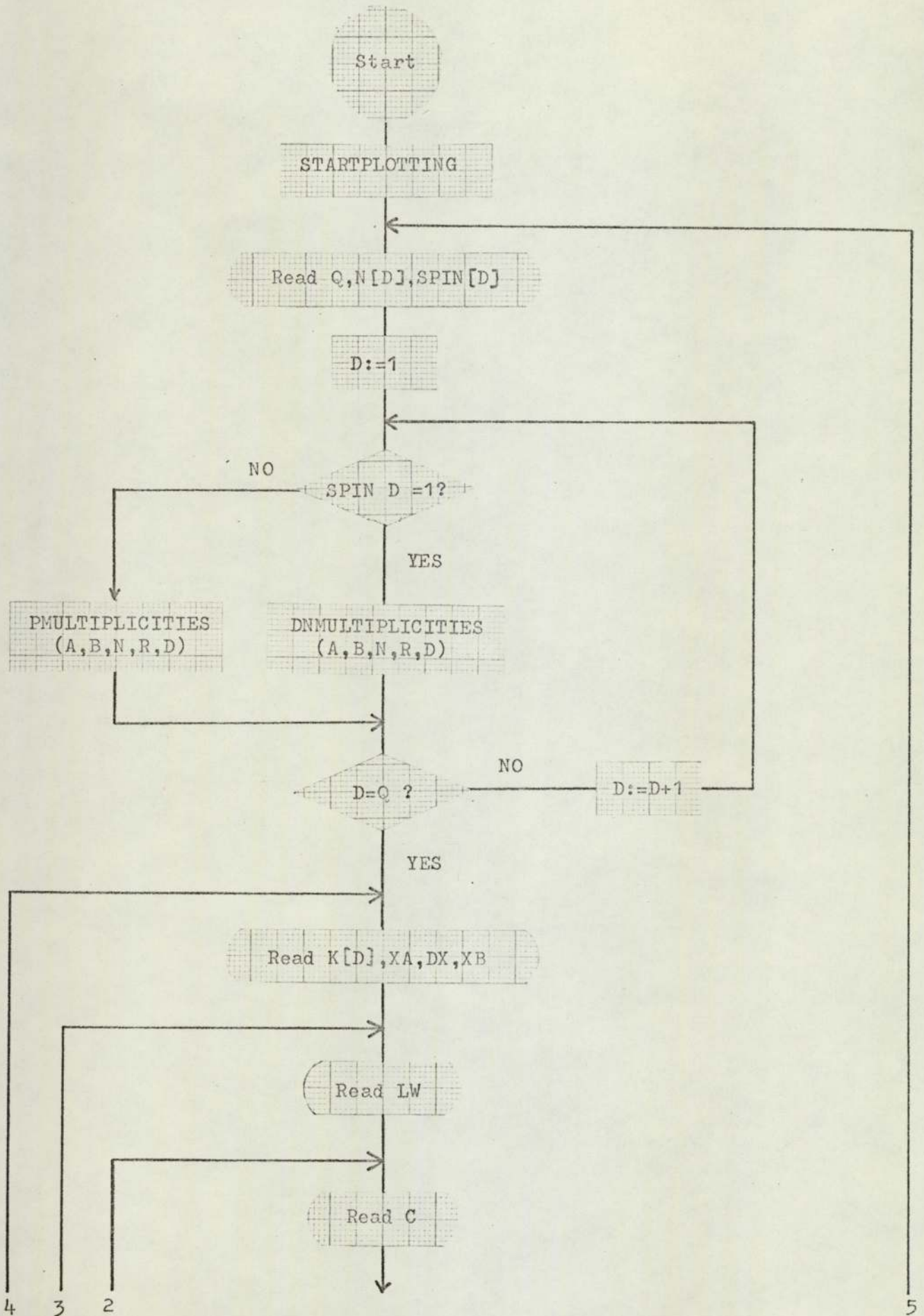
Produces a completely new spectrum,  
new data required for Q to NUMBER.

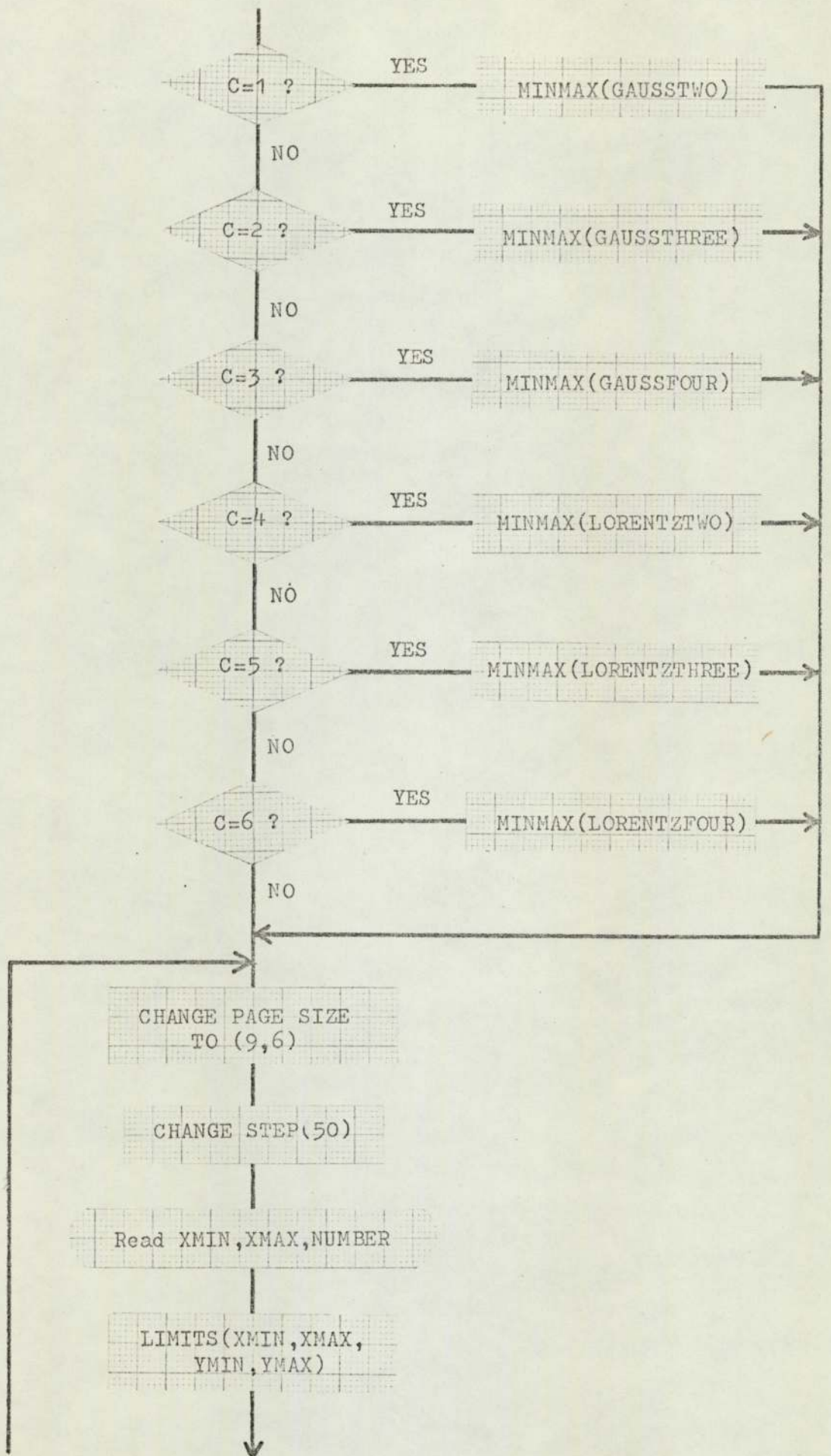
The following brief notes about the program organ-  
isation refer to the simplified flow diagram for ESRSIM  
(Figure 2.3.).

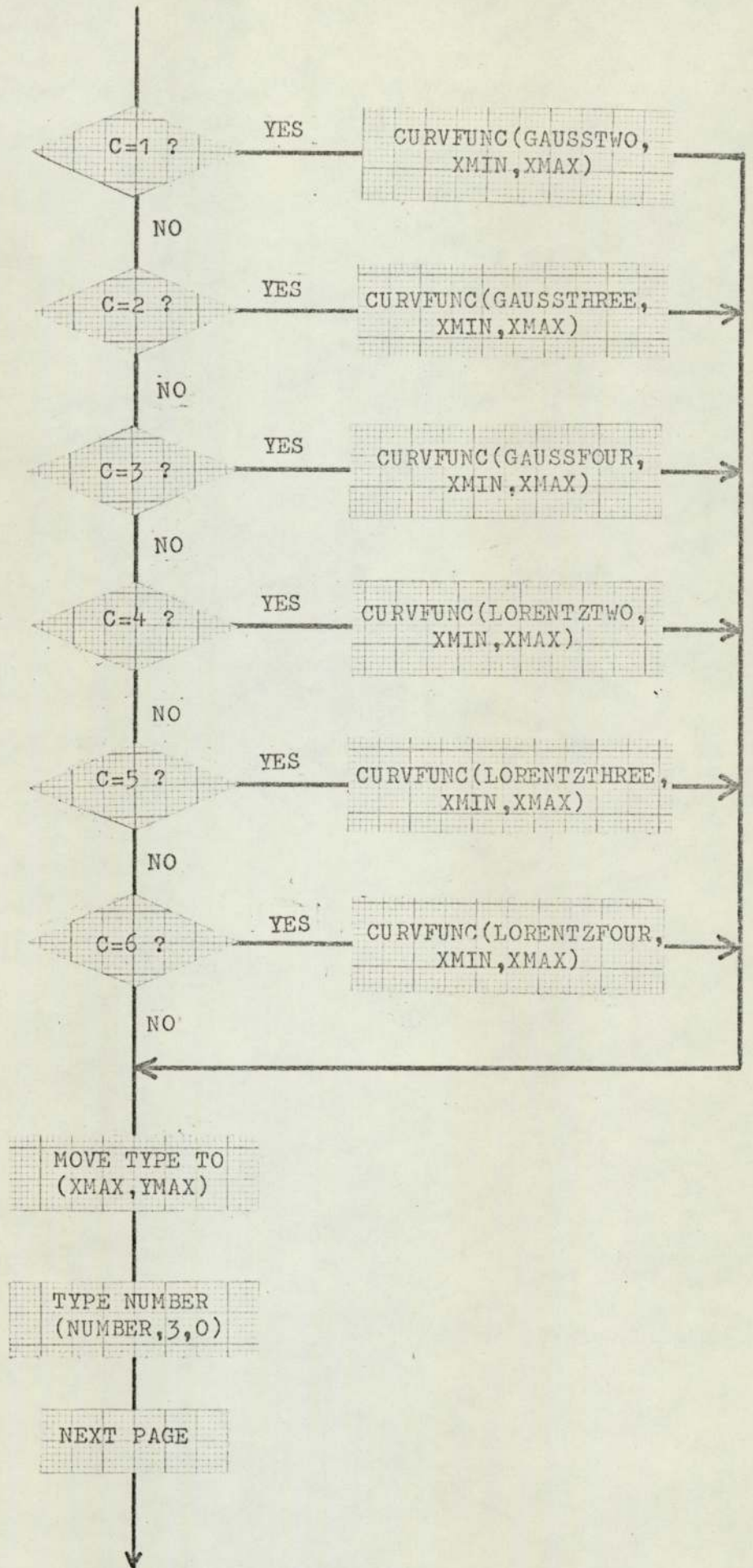
START PLOTTING is a control procedure which initial-  
ises the values of certain global variables required in  
subsequent plotting and activates the necessary computer

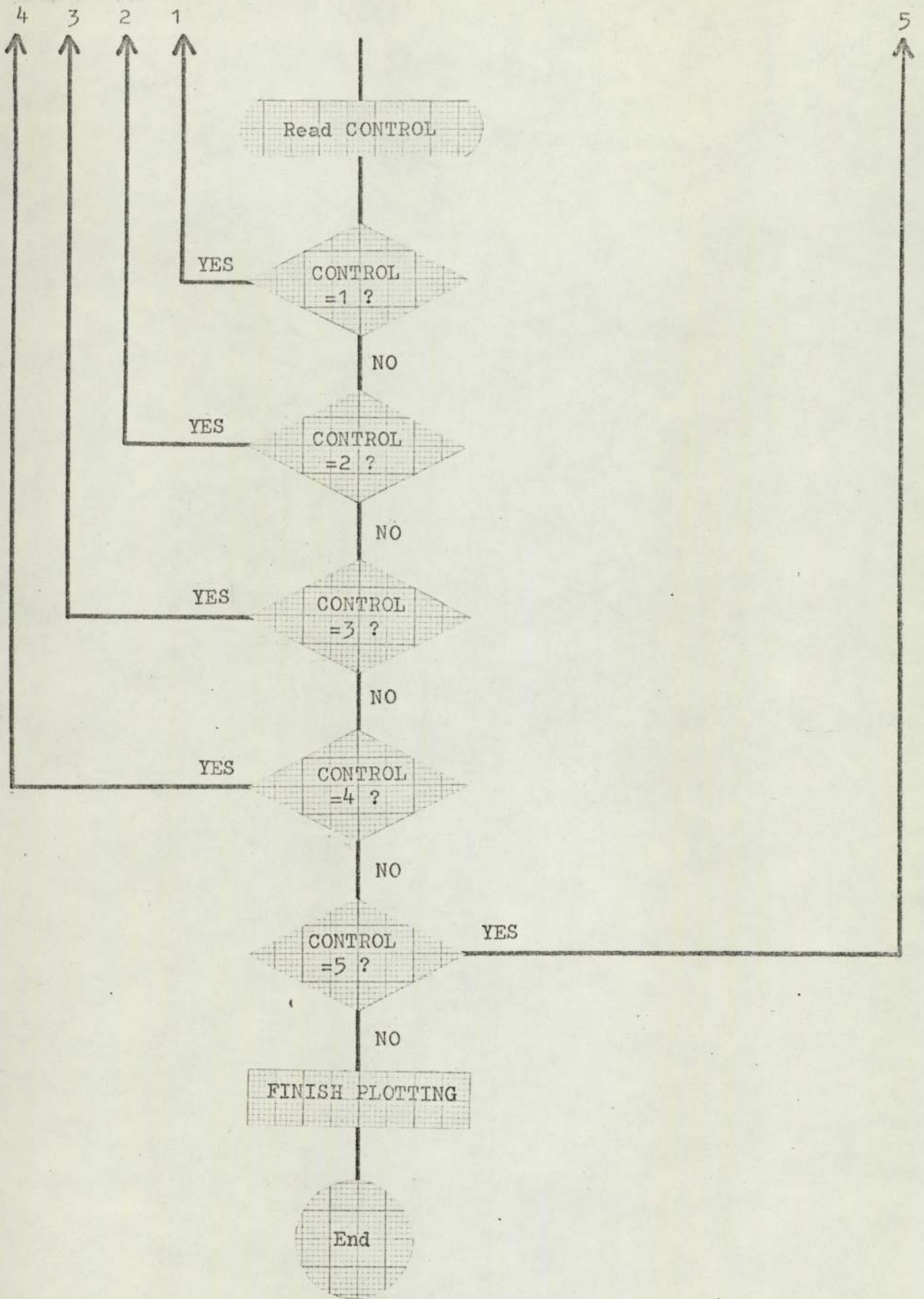
Figure 2.3

Flow diagram for ESRSIM









operations required for the use of the graph plotter.

The required nuclear multiplicities for atoms with spin  $1/2$  or 1 are then calculated using the procedures PMULTIPLICITIES and DNMULTIPLICITIES respectively.

The procedures that define the equations for the shape of the spectra are named GAUSS TWO, GAUSS THREE, GAUSS FOUR, LORENTZ TWO etc. the number part of the name refers to the number of groups of equivalent atoms involved. Although the program is only designed to deal with spectra involving up to four different types of nuclei it is an easy matter to insert extra procedures to cope with greater numbers. The one required is now called together with MINMAX in order to calculate maximum and minimum values of the spectrum shape.

The size of the graphical output is normally 7.5 inches square. To alter this the procedure CHANGE PAGE SIZE TO (XINCHES, YINCHES) can be called, XINCHES and YINCHES being the required length and height of the page in inches. XINCHES can have any value up to a maximum of 100 whereas YINCHES cannot be greater than 25.

The procedure CHANGE STEP (N) determines the distance between successive points joined up by the graph plotter and hence the smoothness of the curve, which increases with the value of N.

The simulated curve is scaled to fit the defined

page size by the procedure LIMITS (XMIN, XMAX, YMIN, YMAX).

The spectrum is now plotted by calling CURVFUNC (F, XMIN, XMAX) where F is the procedure defining the shape of the curve.

The reference number of the spectrum is plotted at the top right-hand corner of the page by calling the procedures MOVE TYPE TO (XMAX, YMAX) and TYPE NUMBER (NUMBER, 3, 0).

The procedure NEXT PAGE automatically produces a new page for the output of the next spectrum.

When the program is completed the control procedure FINISH PLOTTING completes the graph plotter operations and prints out on the line printer a message giving the number of pages of graphical output produced.

A spectrum arising from a single type of atom is produced in the normal manner except that a second value of  $N[D] = 0$  and  $C = 1$  or  $4$  depending on the line shape required.

The simulated spectra in this thesis were all calculated using a Lorentzian line shape function since this gave a better comparison with the experimental results. The spectra referred to in section 4.2.1. were reproduced using a page size of 15.5 inches x 7.5 inches and XMIN and YMIN values of  $-1.4$  and  $1.4$  mT respectively. These values enabled the simulated spectra to be compared easily with the experimental ones.



2.4.2. MOLORB 2: A Computer Program for the Calculation of  $\pi$ -Spin Densities of Conjugated Free Radicals by the HMO and McLachlan Modified HMO Methods

Given the secular determinant of the molecule under investigation the program utilizes a procedure developed by Rutishauser (37), which uses the Jacobi method (38) of matrix diagonalisation to calculate the eigenvalues and eigenvectors. The HMO  $\pi$ -spin densities are then determined from these eigenvectors. A subsequent calculation of the atom-atom polarisabilities (39) and application of McLachlan's approximation (40) enables these simple HMO spin densities to be corrected for  $\pi$  -  $\pi$  spin polarisation.

The copy of the program given in appendix 3 is for a specific structure, the diphenoquinodimethane system. The numbering of the atoms in this system is shown in figure 2.4. The perturbation resulting from the replacement of the carbon atomic orbitals of atoms 13 and 14 by those of oxygen is expressed in the usual way by two parameters  $h_o$  and  $k_{co}$  defining the Coulomb integral ( $\alpha_o$ ) and the Resonance integral ( $\beta_{co}$ ) as shown in equations (2.2), where  $\alpha$  and  $\beta$  are the

$$\alpha_o = \alpha + h_o\beta \quad \text{and} \quad \beta_{co} = k_{co}\beta \quad (2.2.)$$

integrals for the carbon atomic orbitals. The non zero elements of the secular determinant are inserted in the program rather than as data, the parameters  $h_o$  and  $k_{co}$

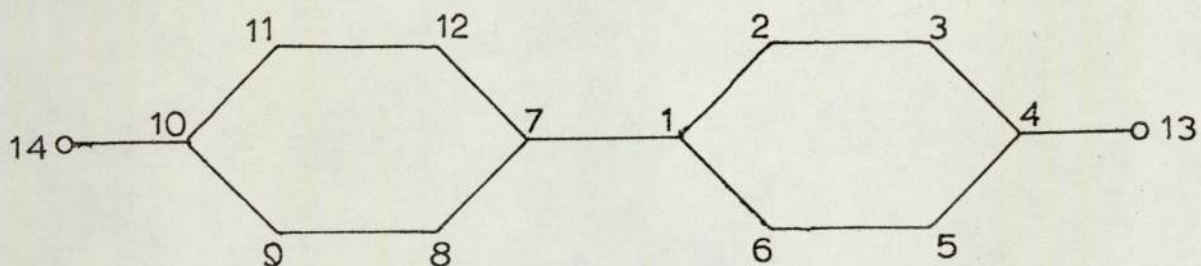


Figure 2.4.

being represented by the identifiers H and K.

The following data is required by the program:

1. N - The number of atomic centres involved in the molecular orbitals, in this case  $N = 14$ .
2. ORB - The orbital containing the unpaired electron, again in this case  $ORB = 8$ .
3. H1,DH,H2 - These parameters define the range of values of  $h_0$  for which the calculations will be performed. H1 represents the initial value, DH the interval added on after each calculation until the final value H2 is reached.
4. K1,DK,K2 - These parameters

define  $k_0$  as the parameters in 3 above

define  $h_0$ .

5. EIVEC, EIGENVEC, RHOVAL - These are Boolean identifiers.

If EIVEC := FALSE, then the eigenvalues only are calculated and printed out.

If EIGENVEC := TRUE, then the eigenvalues and eigenvectors are printed out.

If RHOVAL := TRUE, then the RHO VALUES (the McLachlan modified spin densities) are calculated and printed out whereas

If RHOVAL := FALSE (and provided EIVEC := TRUE) both the simple and modified HMO spin densities for atoms 1,2,3,4 and 13 are calculated and printed out.

The program was slightly modified to give a tape output of the ratio of RHO VALUES for atoms 2 and 3 over a range of H and K values. Thus the ratio of the modified spin densities of atoms 2 and 3 could be plotted against K for each value of H. However, this was done automatically and cubic equations for each of the curves determined by processing the data contained on the output tape using a curve-fit program. This was done using a Digico Micro 16 computer and a further tape output suitable for use as a data tape for the ICL 1905

computer obtained. This tape was incorporated into a program with the PAGE procedures (35) which enabled the curves to be drawn by the graph plotter.

In order to use the program for systems with a different number of atoms the procedures ATOM POLARISABILITY (M,N,S,R), and RHO VALUE (I,J) require a slight alteration where the integers 7 and 14 are used and obviously the output procedures would have to be modified.

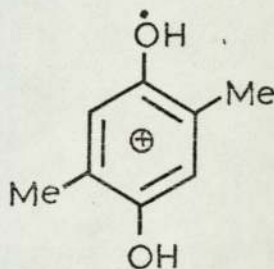
### 3. 4,4'-BIPHENOSEMIQUINONE CATIONS

#### 3.1. PREVIOUS WORK INVOLVING SEMIQUINONE CATIONS

The classical method for the production of radical cations in solution is by the oxidation of the parent compound, often an aromatic hydrocarbon, in concentrated sulphuric acid (41-43). In 1961, Bolton and Carrington (44), investigating the reaction of 1,4-dimethylbenzene in concentrated sulphuric acid containing potassium persulphate obtained an ESR spectrum which they attributed to the 1,4-dimethylbenzene positive ion (IV). However the



(IV)

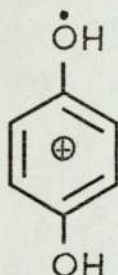


(V)

measured value of the proton hyperfine coupling constant associated with the methyl group, 0.389 mT was considerably lower than the predicted value of 0.6 mT (45) and in a

subsequent paper (14) the spectrum was reassigned to the semiquinone cation (V), the hydroxyl-proton hyperfine coupling constant being virtually identical to that of the ring protons.

Evidence in support of this conclusion was obtained by producing solutions exhibiting the same ESR spectrum from the oxidation of methoxybenzene, phenol and 1,4-dihydroxybenzene with potassium persulphate in concentrated sulphuric acid and from the reduction of 1,4-benzoquinone with sodium dithionite also in concentrated sulphuric acid. This spectrum, consisting of five lines arising from four ring protons each of which is further split into a triplet, was attributed to the 1,4-benzosemiquinone cation (VI). Further, spectra identical to that obtained



(VI)

from the dissolution of 1,4-dimethylbenzene in sulphuric acid containing potassium persulphate were obtained by the reduction of 2,5-dimethyl-1,4-benzoquinone with sodium dithionite and by the potassium persulphate oxidation of the corresponding quinol, both in concentrated

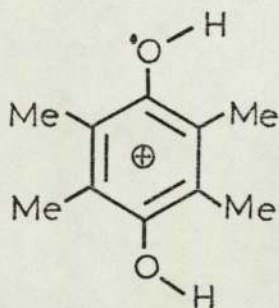
sulphuric acid.

Subsequently Bolton, Carrington and Santos-Veiga (46) reported their ESR studies on the cations of 2,5-dihydroxy-1,4-benzosemiquinone, 1,4-naphthosemiquinone and 9,10-anthrasemiquinone. The first two were produced by the sodium dithionite reduction of the corresponding quinones in sulphuric acid whereas the 9,10-anthraquinone was only successfully reduced using zinc dust and the resulting spectrum consisted of twenty-one rather broad lines. On replacing the sulphuric acid by its dideuterated analogue these hyperfine lines became much sharper and careful analysis showed that only the hydroxyl protons are exchanged for deuterons. The lack of resolution of the spectrum in sulphuric acid was attributed to a more rapid exchange of the hydroxyl protons.

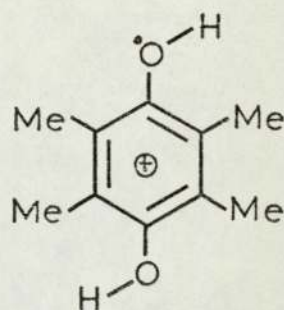
An interesting feature of the spectra of semiquinone cations is that in all the cases so far studied hyperfine splitting was observed for the protons attached to the oxygen atoms. Furthermore the spectra all exhibited a linewidth broadening effect, there being a gradual increase in the linewidth towards high field and is a consequence of the rather high viscosity of the sulphuric acid (47).

Later work involving the cations of tetramethyl-1,4-benzosemiquinone (48), 1,4,5,8-tetrahydroxynaphthalene (49) and 1,4-dimethoxybenzene (50) provided evidence for the existence of cis- and trans- rotational isomers (e.g. VII, VIII) and enabled the potential barrier to rotation

in the case of the cation of 1,4,5,8-tetrahydroxynaphthalene to be calculated. If the rate of isomerisation is slow compared with the hyperfine frequency separations



(VII)



(VIII)

the observed spectrum would be a superposition of the individual spectra of the cis- and trans-isomers.

Whereas, if the isomerisation is rapid the hyperfine couplings will be the average of the extreme values in the two isomers and a simple spectrum will result.

However at intermediate rates of isomerisation a marked alternating linewidth effect is often observed.

In their search for methods of preparing positive ions of aromatic molecules Buck and his co-workers (51) discovered that nitro compounds in combination with acids possessed extremely good electron attracting properties. Subsequently Forbes and Sullivan (17) found that the use of a mixture of aluminium chloride and nitromethane had several advantages over sulphuric acid for the production of cation radicals by oxidation. For a number of radicals e.g. the cation of 1,4-dimethoxy-



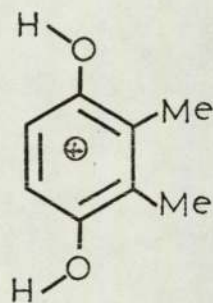
benzene the radical concentration approximated to 100% whereas with sulphuric acid it was considerably less than 1%. Since the viscosity of aluminium chloride in nitromethane is much less than for concentrated sulphuric acid there are no significant contributions to the linewidths due to anisotropic dipolar interactions hence the phenomena of high field broadening observed in sulphuric acid is absent. Furthermore the lower melting point of the system permits the study of temperature effects over a wider range.

They also observed that the aluminium chloride-nitromethane system sometimes enabled the oxidation to go beyond the one-electron stage. Thus biphenyl-4,4'-diol gave initially a blue paramagnetic solution. Using an excess of aluminium chloride the solution became yellow in colour and diamagnetic. The further oxidation was able to be reversed by either dilution with nitromethane or by the addition of more substrate. The ESR spectrum of the blue solution was analysed in terms of three groups of four, four and two equivalent protons having hyperfine coupling constants of 0.195 mT, 0.073 mT and 0.164 mT respectively.

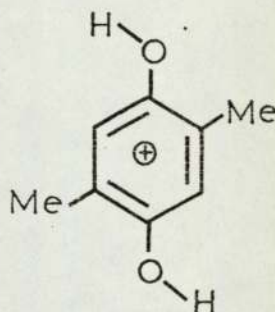
Further studies by Sullivan and his co-workers on the cations of 1,4-benzosemiquinone (52), tetramethyl-1,4-benzosemiquinone (53) and 4,4'-dimethoxybiphenyl (54) showed that these radicals exist as cis- and trans-isomers and that the ESR spectra at certain temperatures exhibit the linewidth alternation phenomena characteristic of the hindered rotation of the hydroxyl groups

about the carbon-oxygen bonds. On the other hand no such behaviour was observed for 1,4-dimethoxy-2,3,5,6-tetramethylbenzene (53) which was shown to exist as a single species in aluminium chloride-nitromethane solution. However, in concentrated sulphuric acid dimethoxydurene gives an ESR spectrum corresponding to the cation of tetramethyl-1,4-benzosemiquinone.

The ESR spectrum of the cation of 2,6-dimethylbenzosemiquinone (55) also exhibits an alternating linewidth effect whereas neither the 2,3-nor the 2,5-dimethyl derivatives produce spectra showing this effect. This behaviour was interpreted by assuming that the 2,3- and 2,5-dimethyl-1,4-benzosemiquinone cations are stabilised in the cis- and trans- conformations respectively (IX, X).



(IX)



(X)

### 3.2. 4,4'-BIPHENOSEMIQUINONE CATION, RESULTS AND DISCUSSION

#### 3.2.1. Oxidation of Biphenyl-4,4'-diol in Concentrated Sulphuric Acid

When biphenyl-4,4'-diol is oxidised by hydrogen peroxide or potassium persulphate in 98% sulphuric acid coloured solutions are obtained which exhibit paramagnetism. The colour of the solution and its characteristic ESR spectrum depends on the technique and conditions employed. If the biphenyl-4,4'-diol is added to the acid containing a trace of the oxidising agent at room temperature or below, a deep blue solution giving the ESR spectrum shown in figure 3.1. is obtained. However if the substrate is first dissolved in the sulphuric acid either by being left to stand at room temperature or warming to about 35°C and then cooling prior to the addition of the oxidising agent then a sea-green coloured solution having the ESR spectrum shown in figure 3.2a results. In both cases the concentration of the substrate is in the range 0.001M - 0.005M.

The seventeen line ESR spectrum obtained from the blue solution can be analysed in terms of two groups of four equivalent protons having hyperfine coupling constants of 0.205 mT and 0.071 mT respectively. The computed spectrum is shown in figure 3.3. On repeating the experiment with dideuterosulphuric acid in place of sulphuric acid the observed ESR spectrum consists of a quintet of broad lines with a hyperfine coupling constant

Biphenyl-4,4'-diol in 98% sulphuric acid containing a trace of hydrogen peroxide  
(blue solution)

---

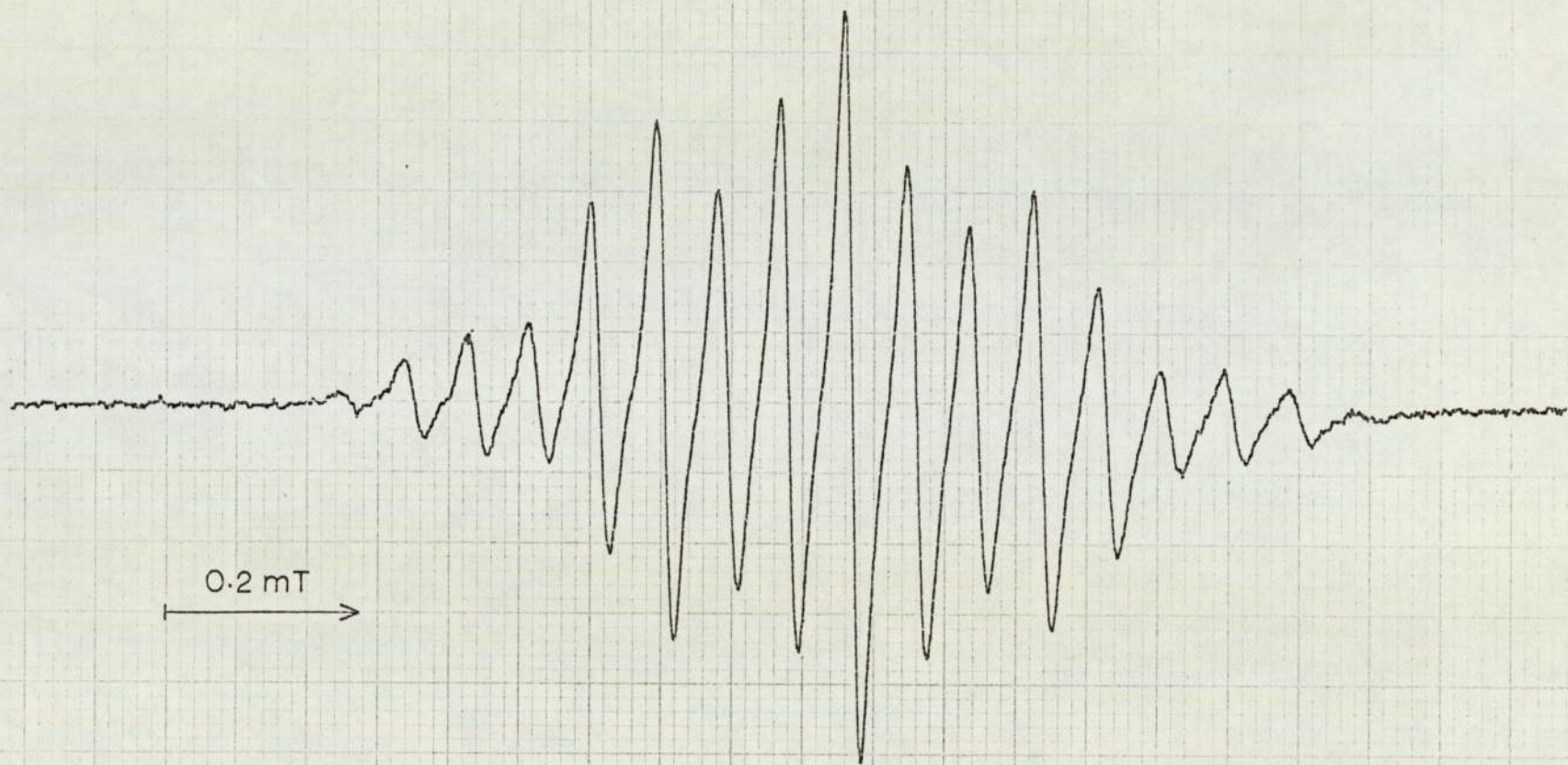


Figure 3.1

Biphenyl-4,4'-diol dissolved in (a) 98% sulphuric acid and (b) dideuterosulphuric acid, followed by the addition of a trace of hydrogen peroxide (green solution)

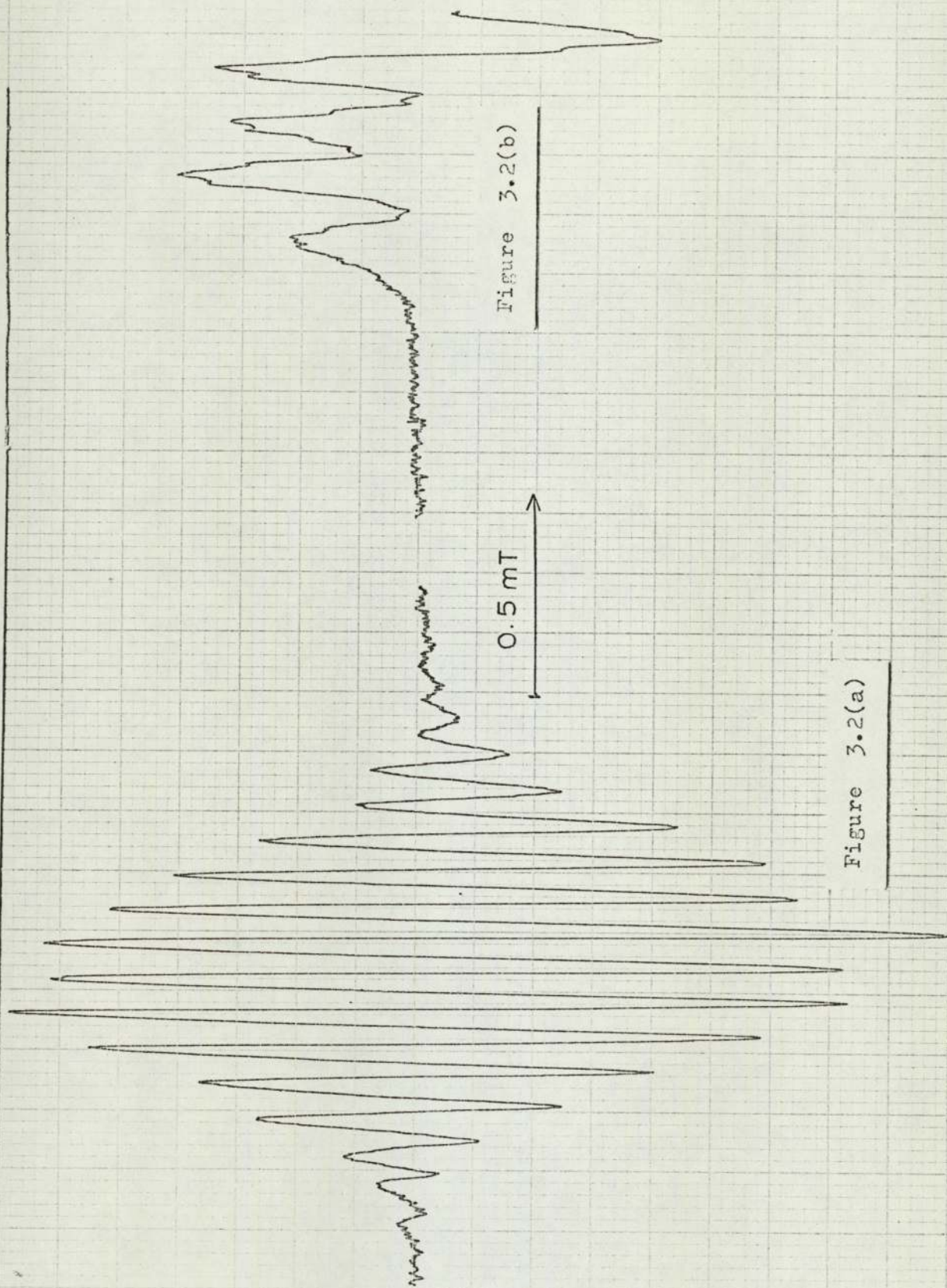


Figure 3.2(a)

Figure 3.2(b)

Computer Simulated Spectrum

4 equivalent protons  $a^H = 0.205$  mT

4 equivalent protons  $a^H = 0.071$  mT

Linewidth = 0.016 mT

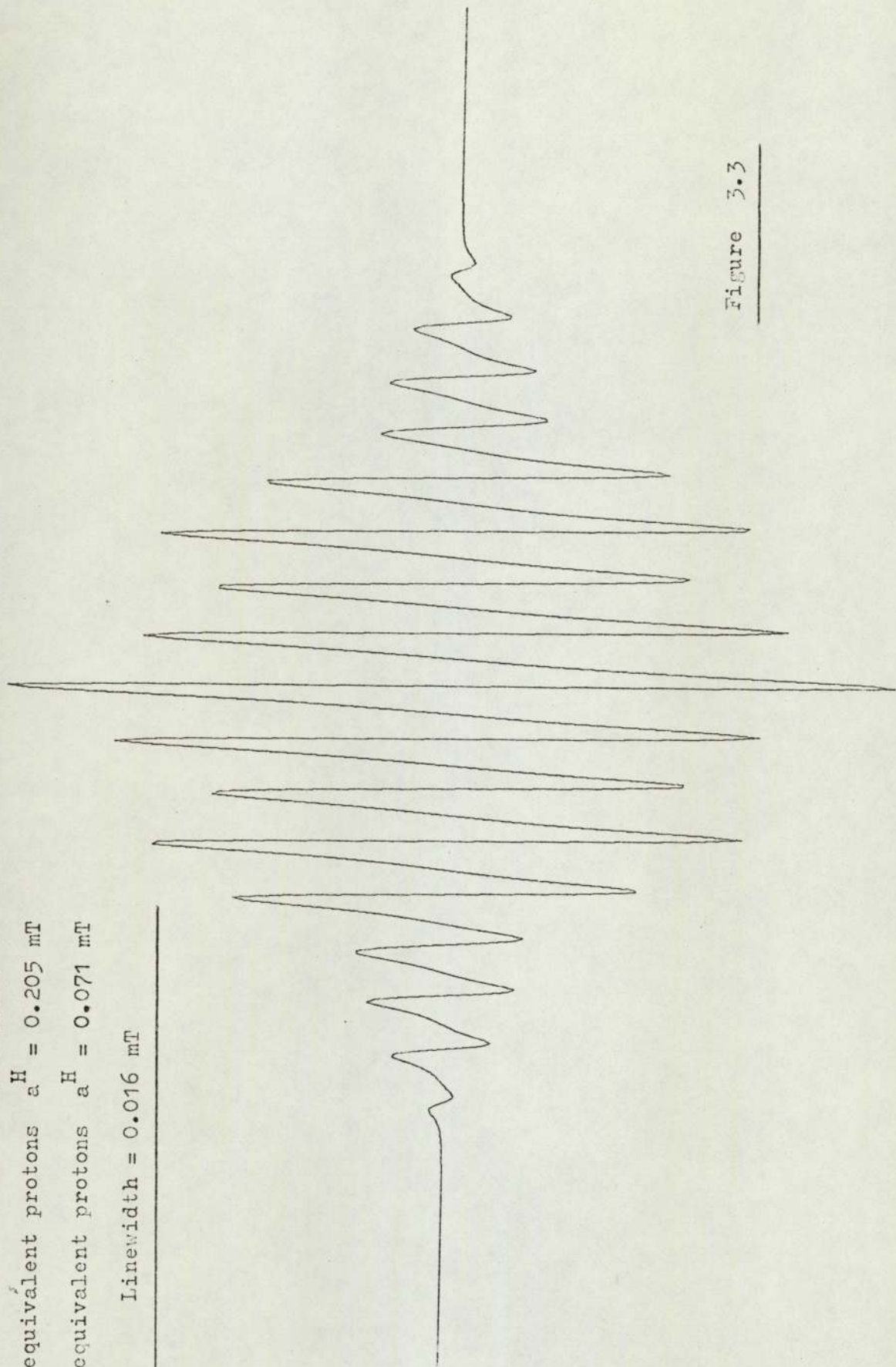
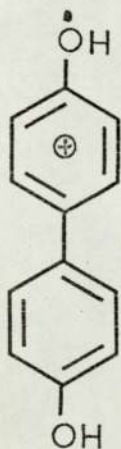


Figure 3.3

of 0.205 mT (figure 3.4). The ESR spectrum is thus attributed to the 4,4'-biphenosemiquinone cation (XI).



(XI)

Because of steric hindrance the protons in the 2 and 6 positions in each ring do not exchange with the protons (or deuterons) of the acid thus the hyperfine coupling constant for the quintet obtained in dideuterosulphuric acid can be assigned to the protons in these positions. Furthermore the lack of any hydroxyl-proton hyperfine coupling can be accounted for by assuming that the lifetime of the cation with a particular proton on an oxygen must be short compared with the time for the ESR transition i.e. the rate of the hydroxyl proton exchange is fast compared with the hyperfine coupling.

Attempts to slow down sufficiently the rate of exchange by cooling the sample so as to try and observe any hyperfine coupling by the hydroxyl protons only results in the spectra becoming extremely asymmetric

Biphenyl-4,4'-diol in 98% dideuterosulphuric acid containing a trace of hydrogen peroxide

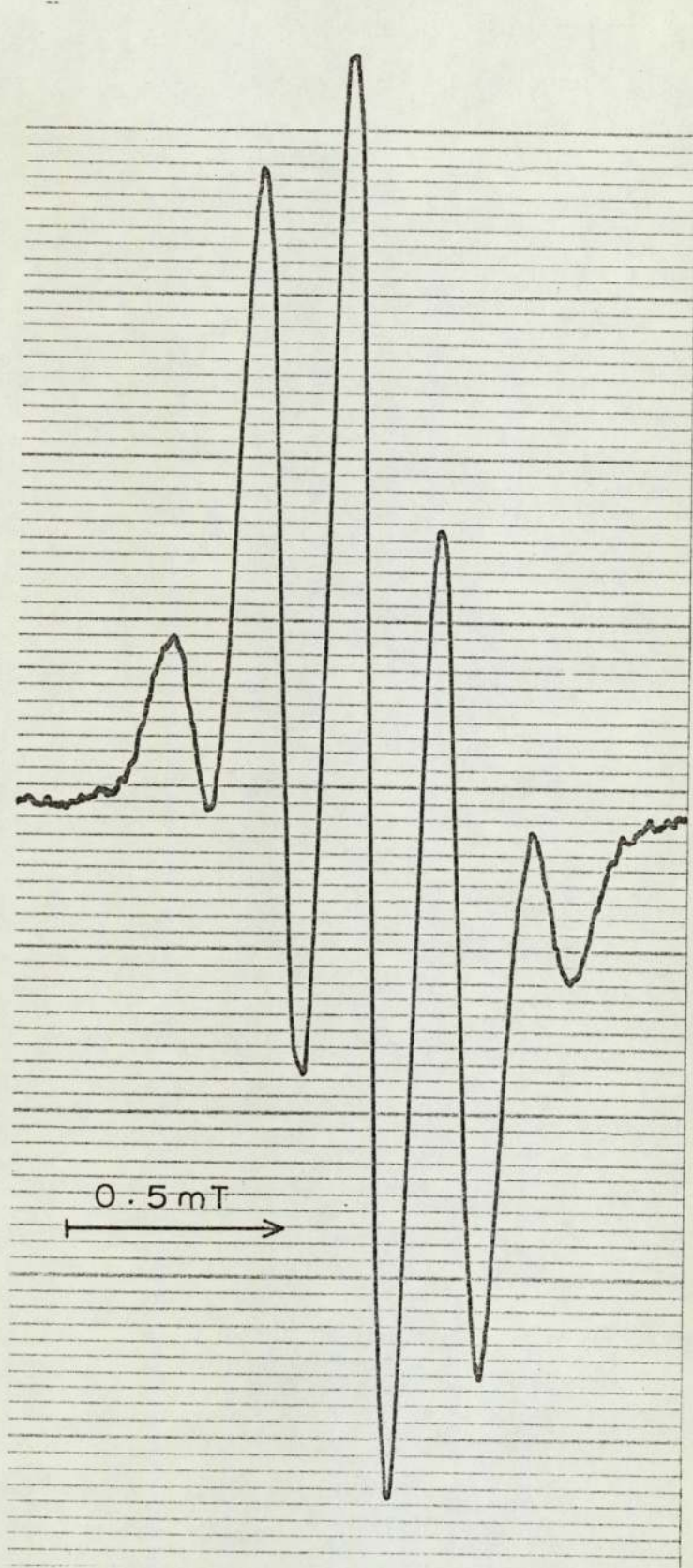
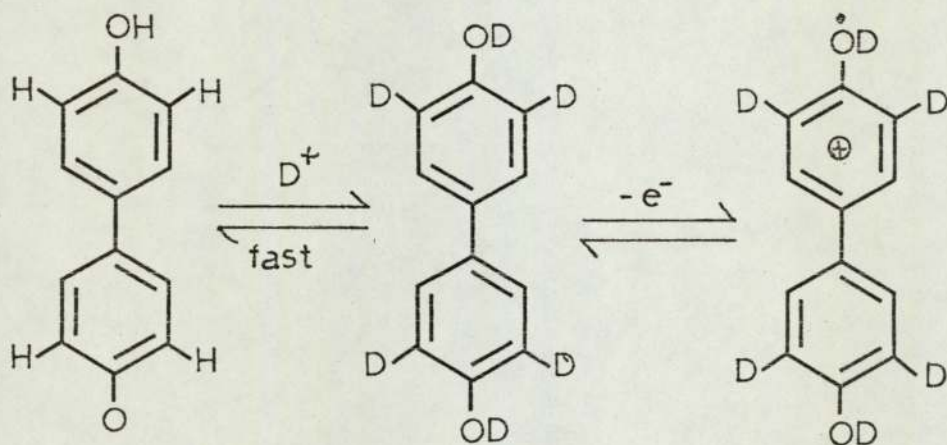


Figure 3.4



due to the increased viscosity of the solution. Dilution of the sulphuric acid with trifluoroethanoic acid also leads to a loss of resolution.

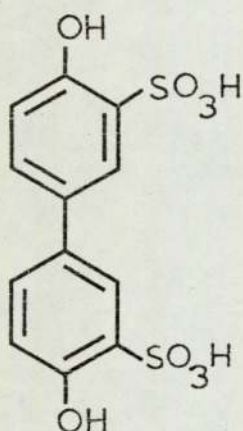
A similar ESR spectrum to that of figure 3.1 is exhibited by the dark brown-green coloured solution obtained when 4,4'-biphenoquinone is reduced in concentrated sulphuric acid containing a trace of sodium dithionite. Further, the same spectrum is initially observed when the deuterated analogue of the acid is used. These results suggest that the exchange of the ring protons by deuterons in positions 3 and 5 of the diol takes place prior to the oxidation process. Thus we can consider the following sequence to apply.



The ESR spectrum of the sea-green coloured solution being both asymmetric and only partially resolved proved much more difficult to interpret. The corresponding spectrum using dideuterosulphuric acid is shown in figure

3.2b. When a much higher concentration of biphenyl-4,4'-diol (approximately 1M) is used a white precipitate gradually forms in the solution. This white solid on addition to cold concentrated sulphuric containing a trace of hydrogen peroxide produces a sea-green solution exhibiting the same ESR spectrum as that in figure 3.2a.

The white solid appears to be identical to the 4,4'-dihydroxybiphenyl-3,3'-disulphonic acid prepared by Moir (31). Both of these white solids when dissolved in acetone give the same NMR spectrum (the ring protons fine structure is shown in figure 3.5.). This spectrum is consistent with the structure (XII). Thus we consider



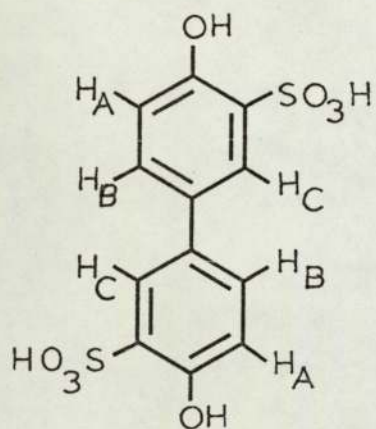
(XII)

the ESR spectrum of such solutions to be due to the cation of 4,4'-biphenosemiquinone-3,3'-disulphonic acid.

If it is true that all the diol is sulphonated prior to the oxidation reaction then it should be

Figure 3.5

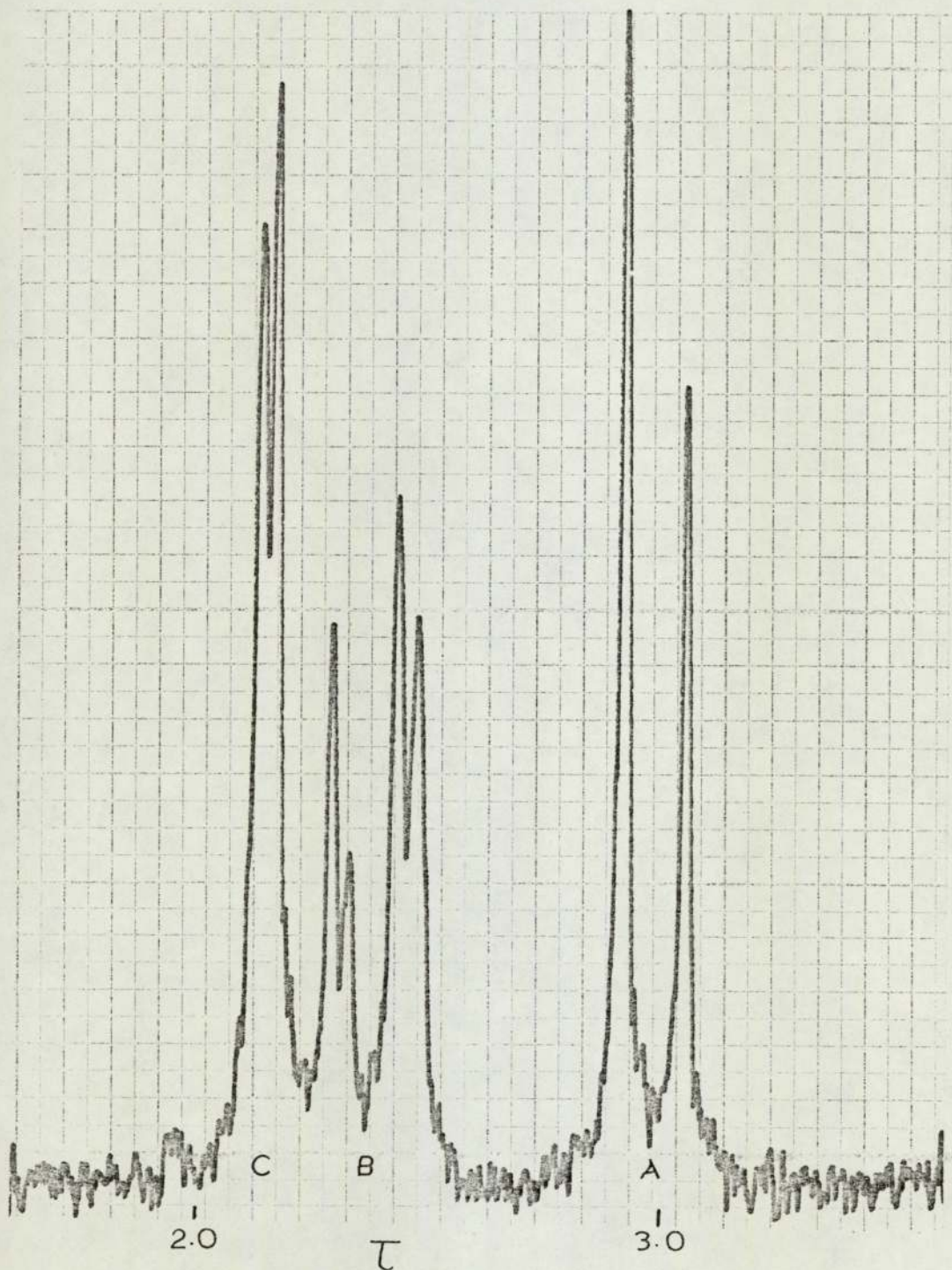
Proton resonance (at 60 MHz) of  
4,4'-dihydroxybiphenyl-3,3'-disulphonic acid in acetone



Spin-Spin Coupling Constants

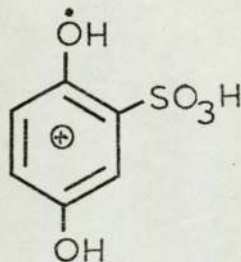
$$J_{AB} = 8.5 \text{ Hz}$$

$$J_{BC} = 2.5 \text{ Hz}$$



possible to produce other sulphonated radical cations in concentrated sulphuric acid provided the substrate is not oxidised in the presence of the acid alone. When 1,4-dihydroxybenzene is dissolved in concentrated sulphuric acid by heating and a trace of oxidising agent added a yellow solution is produced. Provided the ESR spectrum of this solution is recorded within ten minutes of mixing as the radical species decays rapidly, the spectrum shown in figure 3.6. can be recorded. The ESR spectrum of 1,4-benzosemiquinone cation produced by the normal mode of oxidation of 1,4-dihydroxybenzene in concentrated sulphuric acid is shown for comparison in figure 3.7.

The spectrum illustrated in figure 3.6 can be approximately analysed in terms of one group of two equivalent protons having a hyperfine coupling constant of 0.205 mT and a further group of three equivalent protons having a value of 0.334 mT. A computed spectrum using these values is shown in figure 3.8. This analysis is thus in accordance with a monosulphonated 1,4-benzoquinone cation (XIII), the three ring protons having



(XIII)

1,4-dihydroxybenzene (quinol) dissolved in 98% sulphuric acid and a trace of hydrogen peroxide added

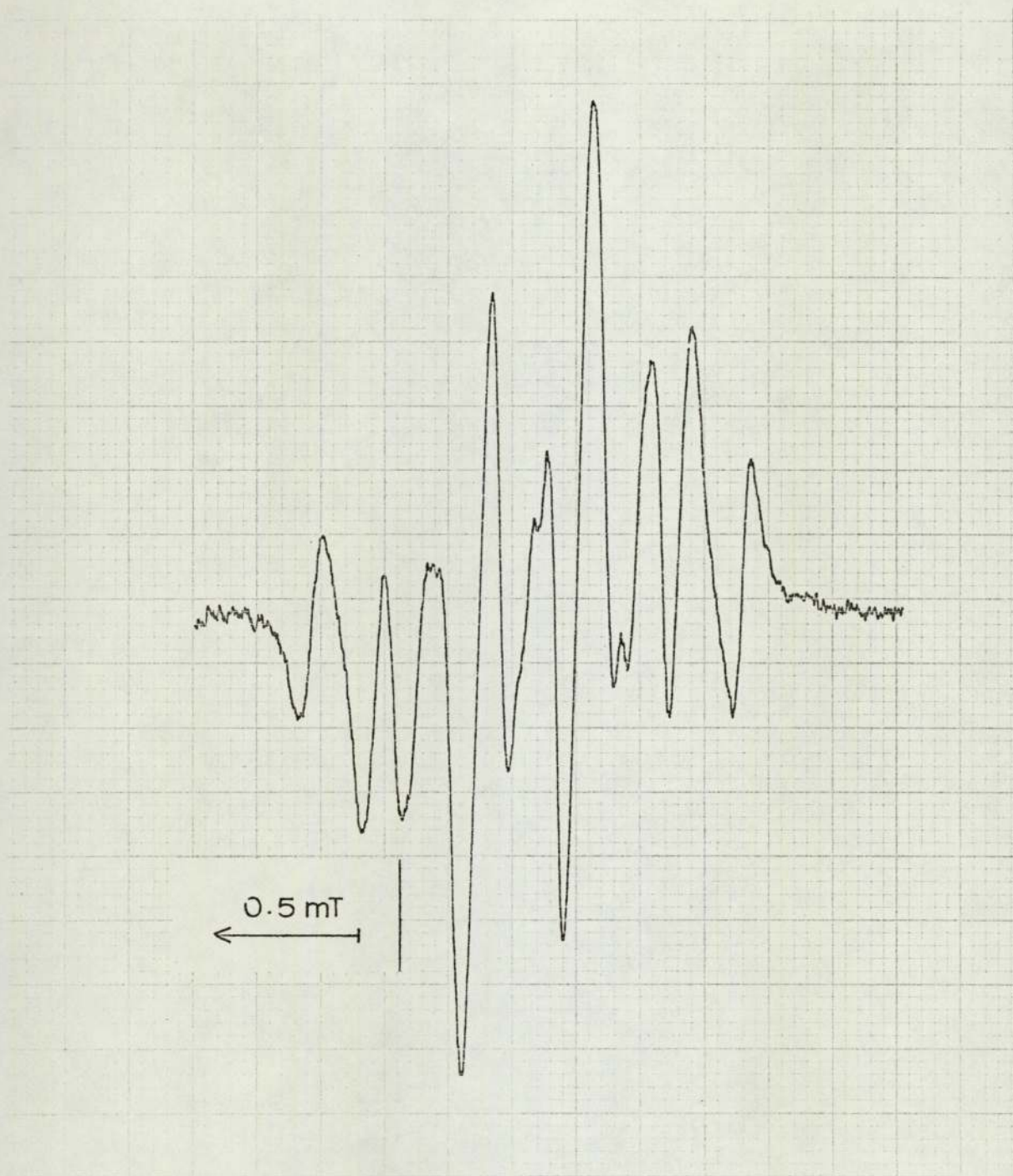


Figure 3.6

1,4-Dihydroxybenzene (quinol) in 98% sulphuric acid  
containing a trace of hydrogen peroxide



$$a^{\text{H}} (\text{ring H}) = 0.234 \text{ mT}$$

$$a^{\text{H}} (\text{hydroxyl H}) = 0.344 \text{ mT}$$

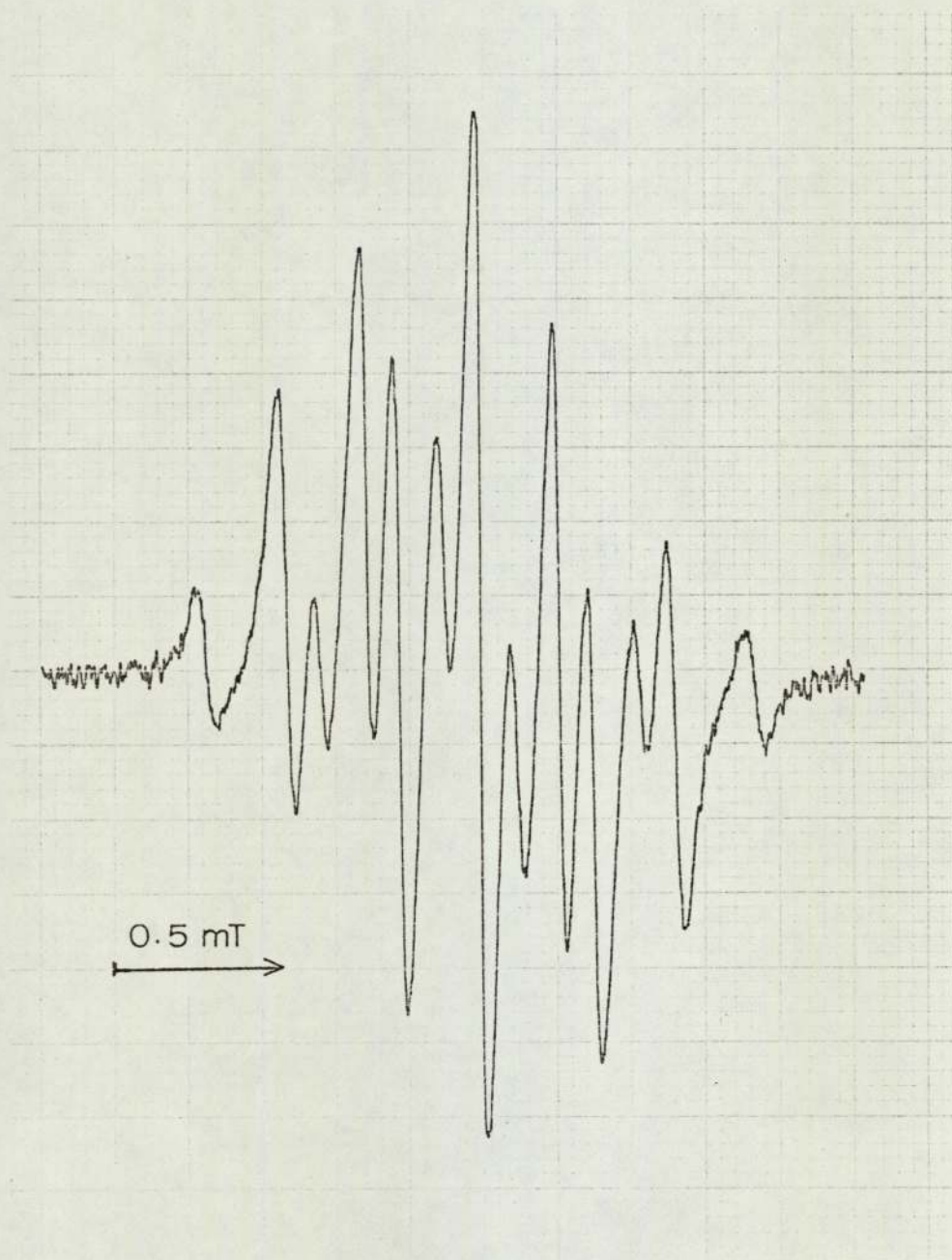


Figure 3.7

Computer Simulated Spectrum

3 equivalent protons  $a^H = 0.334$  mT

2 equivalent protons  $a^H = 0.205$  mT  
Linewidth = 0.05 mT

---

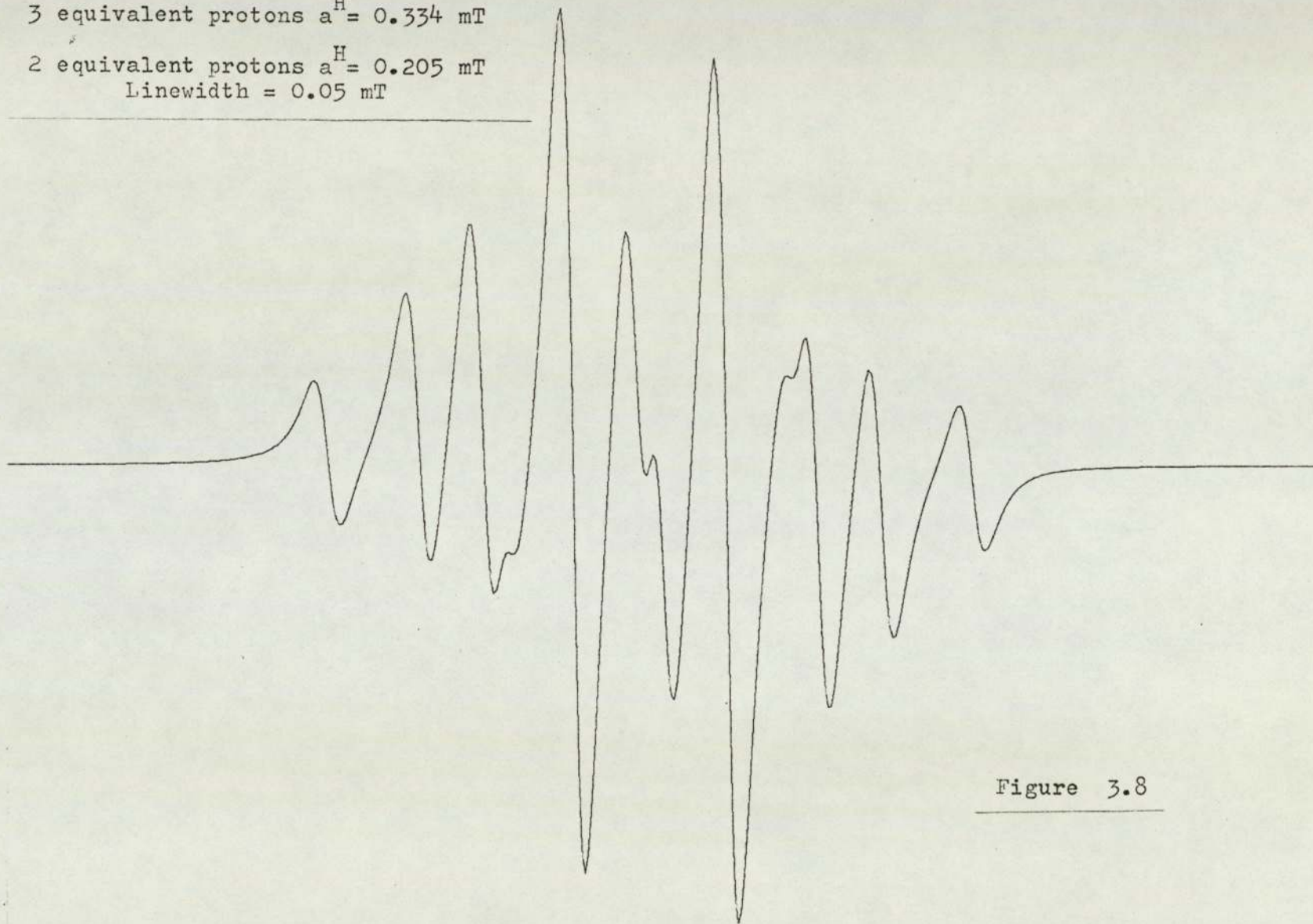


Figure 3.8

similar hyperfine coupling constants (ca. 0.334 mT). The fact that 2,5-dihydroxybenzene sulphonic acid (56) when added to concentrated sulphuric acid containing a trace of hydrogen peroxide produces a similar ESR spectrum provides further evidence in support of this interpretation.

The conditions necessary for the sulphonation of biphenyl-4,4'-diol to occur were further investigated and there appears to be a clear demarcation between the formation of two types of radical. The biphenyl-4,4'-diol was allowed to stand in contact for differing periods of time with sulphuric acid prior to oxidation at a variety of temperatures. Thus the time required to change the ESR spectrum of the oxidised acid solution from that due to the 4,4'-biphenosemiquinone cation to that due to its disulphonated derivative was determined. The results for a 0.005M substrate concentration in a range of sulphuric acid concentrations are shown in graphical form in figure 3.9.

No radical species could be detected when 4,4-dihydroxybiphenyl-3,3',5,5'-tetrasulphonic acid was added to concentrated sulphuric acid containing a trace of oxidising agent.

### 3.2.2. Reduction of 4,4'-Biphenoquinone in Concentrated Sulphuric Acid

As mentioned in the previous section a solution of 4,4'-biphenoquinone in concentrated sulphuric acid



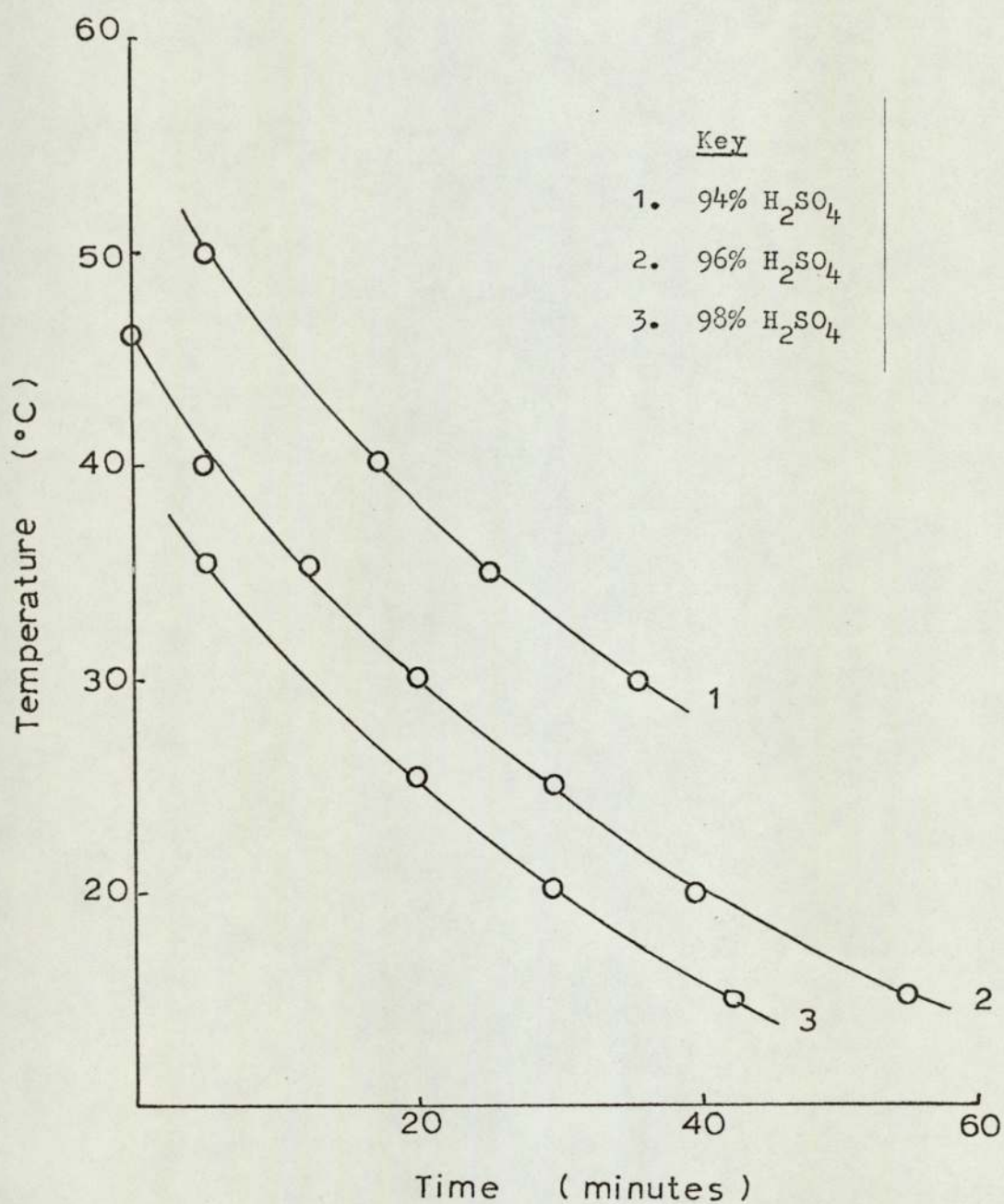
containing a trace of sodium dithionite exhibits the ESR spectrum shown in figure 3.1 which is attributed to the 4,4'-biphenosemiquinone cation. However, the use of sodium dithionite often leads to the occurrence of ESR signals from sulphur species at low fields and although usually of a weak intensity they tend to obscure the wing of the spectrum under consideration. Fortunately, in this case the addition of sodium dithionite is found to be unnecessary. The substrate in concentrated sulphuric acid results in a brown solution which when degassed produces an adequately resolved ESR spectrum.

On changing the reagent to dideuterosulphuric acid the initial ESR spectrum is the same. However, over a period of time it gradually changes both in intensity and in the number of hyperfine components. Figures 3.10 to 3.14 show this change for a 0.005M solution at 30°C.

The change in the number of hyperfine lines can be interpreted in terms of a slow, stepwise replacement of the ring protons in positions 3,3',5 and 5' by deuterium nuclei. The proposed reaction sequence is outlined in figure 3.15. The 4,4'-biphenoquinone (XIV) undergoes fast deuteration of the oxygen atoms followed by reduction to produce the cation (XV). The ESR spectrum of this cation will be similar to that obtained from the cation (XI) produced by reduction of the quinone (XIV) in sulphuric acid.

Figure 3.9

Plot of reaction temperature against the reaction time for the sulphonation of biphenyl-4,4'-diol in sulphuric acid



4,4'-Biphenoquinone in dideuterosulphuric acid  
at 30°C after 11 minutes

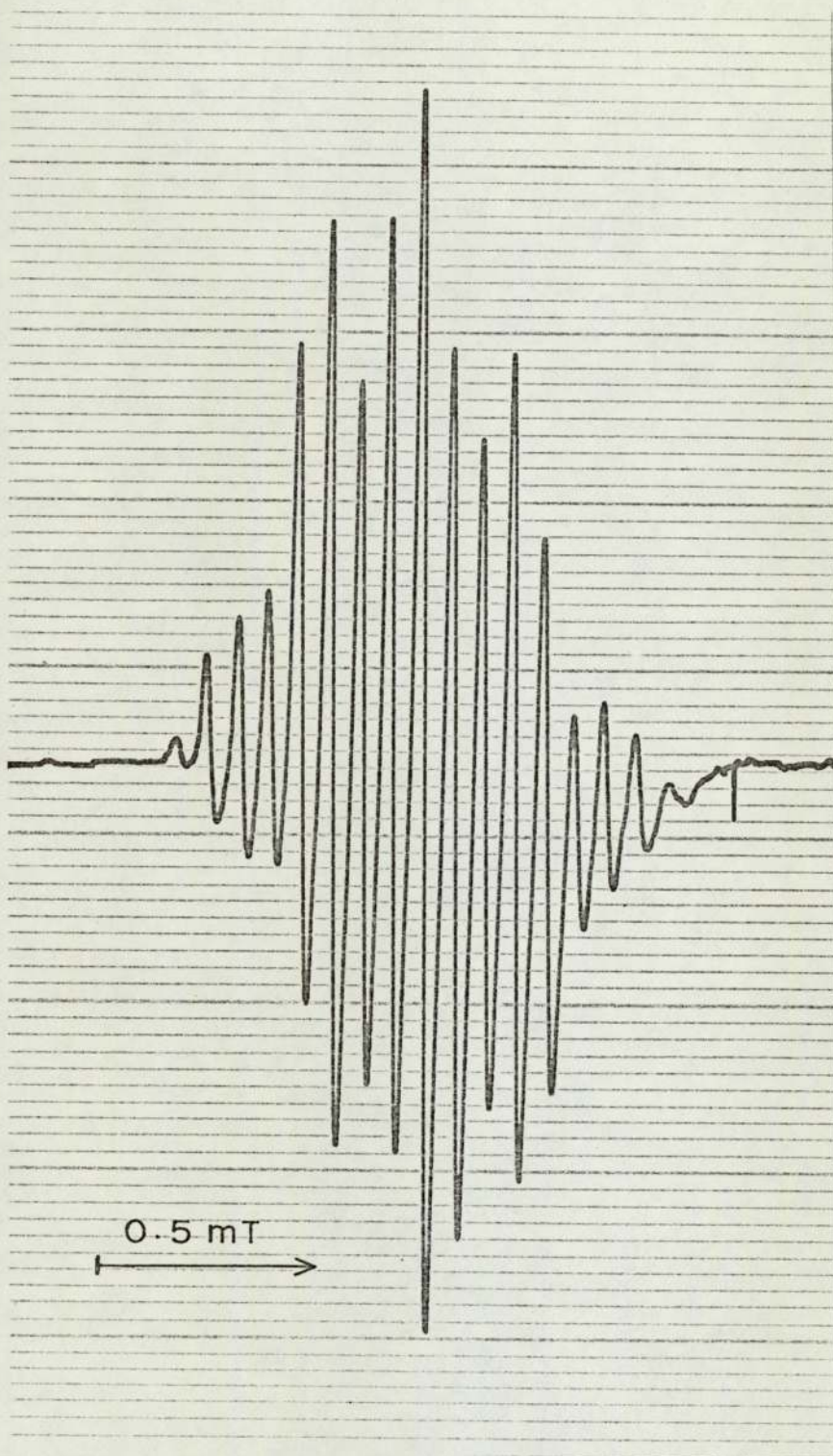


Figure 3.10

4,4'-Biphenylquinone in dideuterosulphuric acid  
at 30°C after 33 minutes

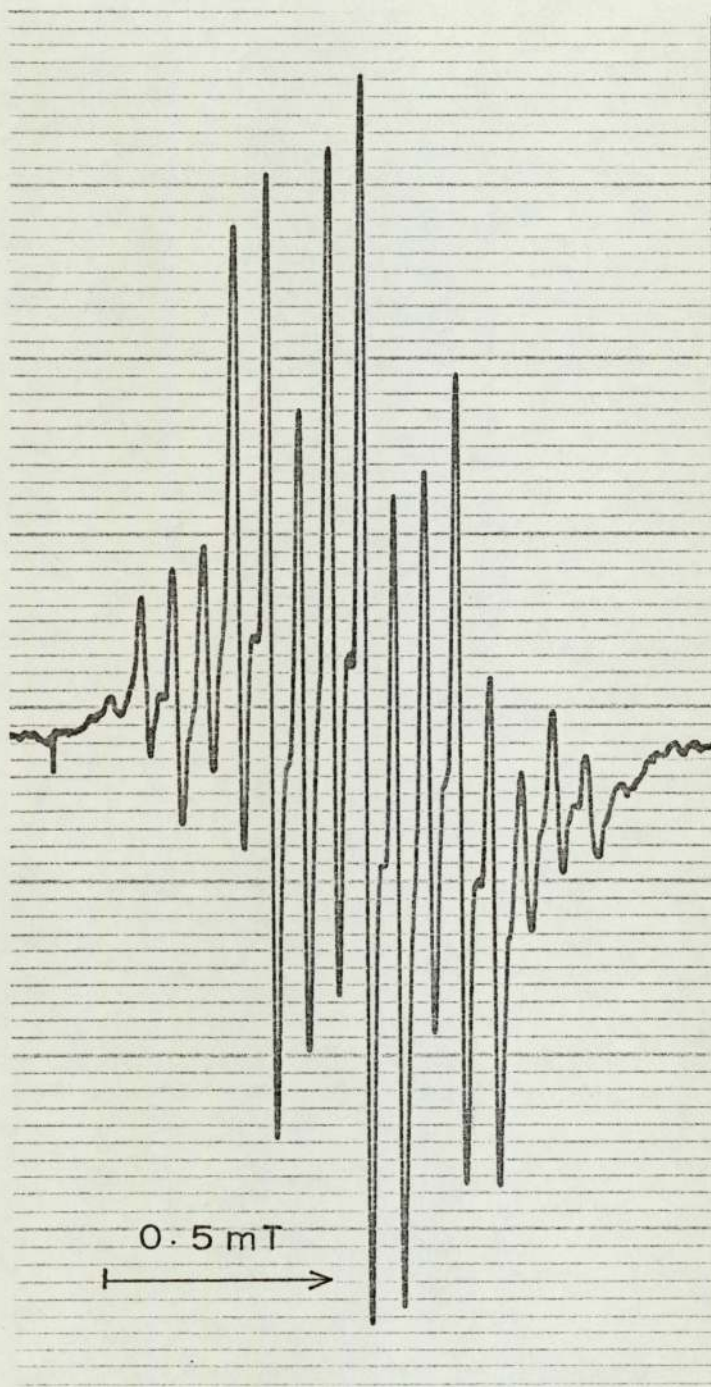


Figure 3.11

4,4'-Biphenoquinone in dideuterosulphuric acid  
at 30°C after 43 minutes

---

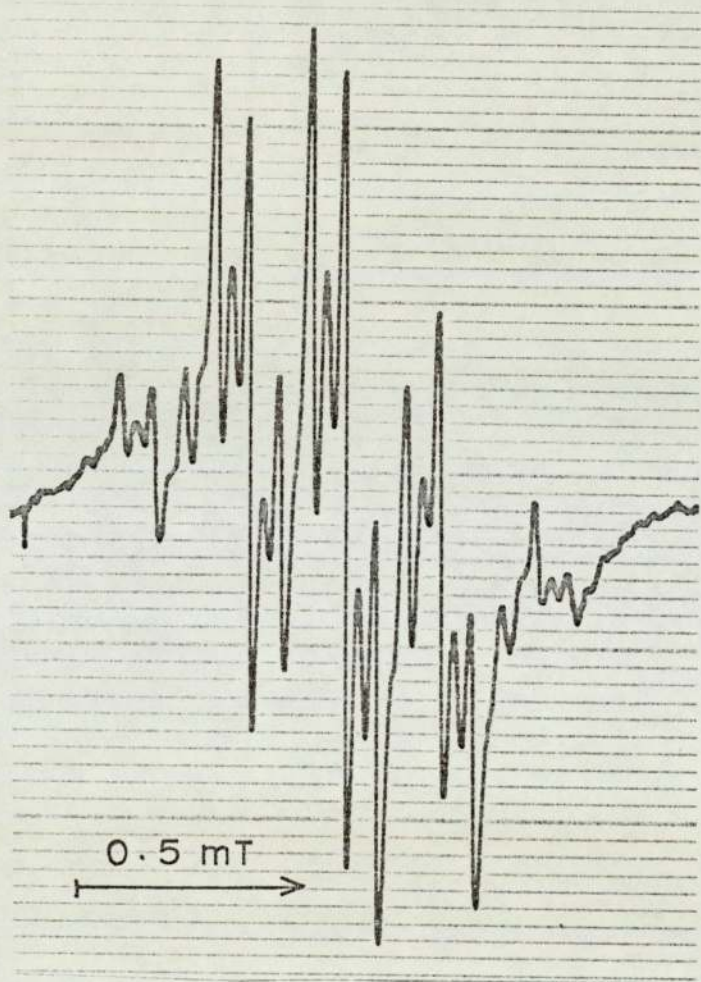


Figure 3.12

4,4'-Biphenoquinone in dideuterosulphuric acid  
at 30°C after 60.5 minutes

---

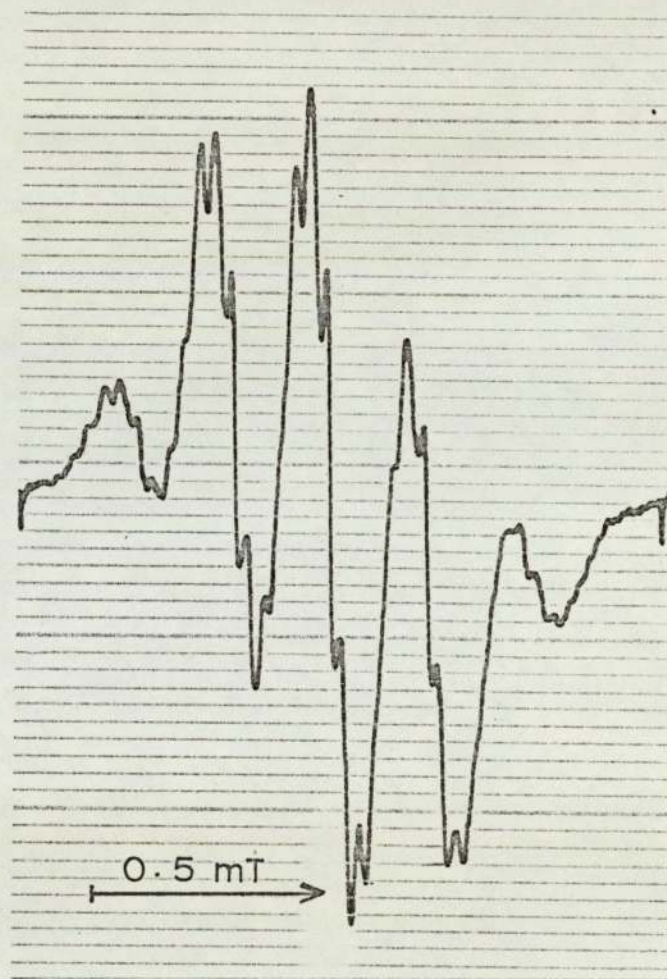


Figure 3.13

4,4'-Biphenoquinone in dideuteriosulphuric acid  
at 30°C after 83.5 minutes

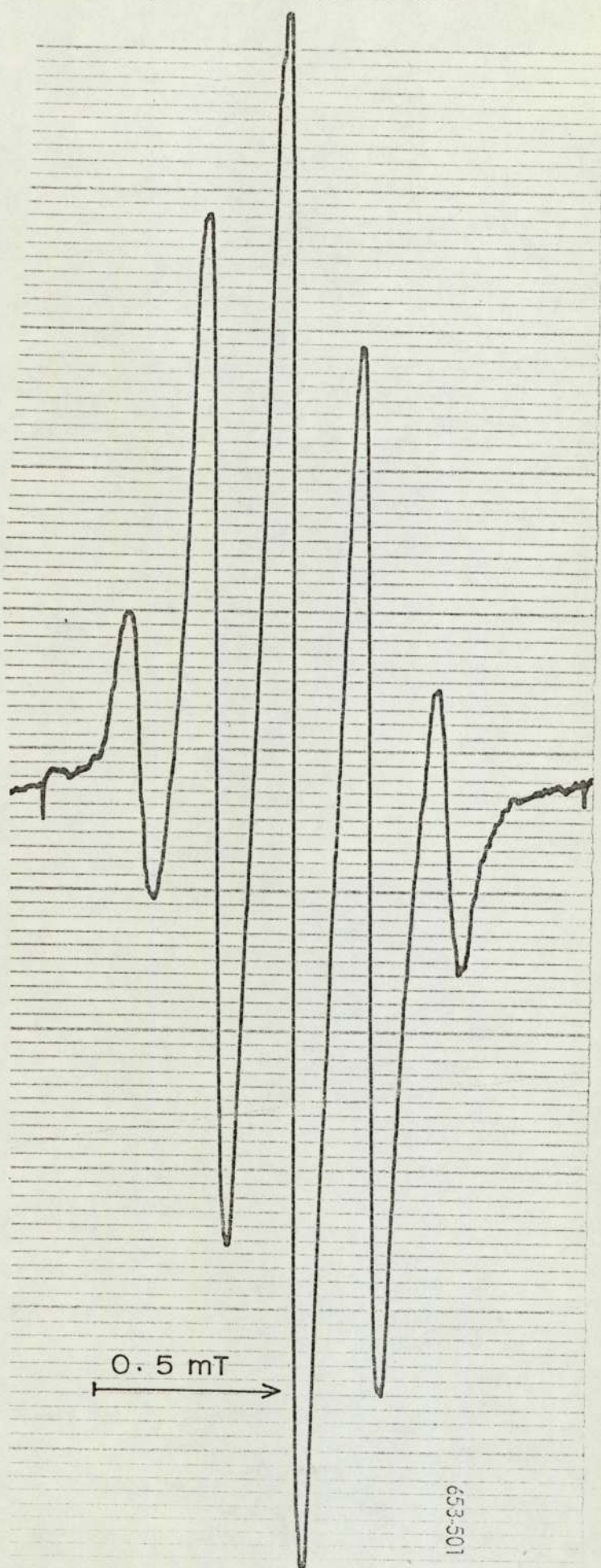


Figure 3.14

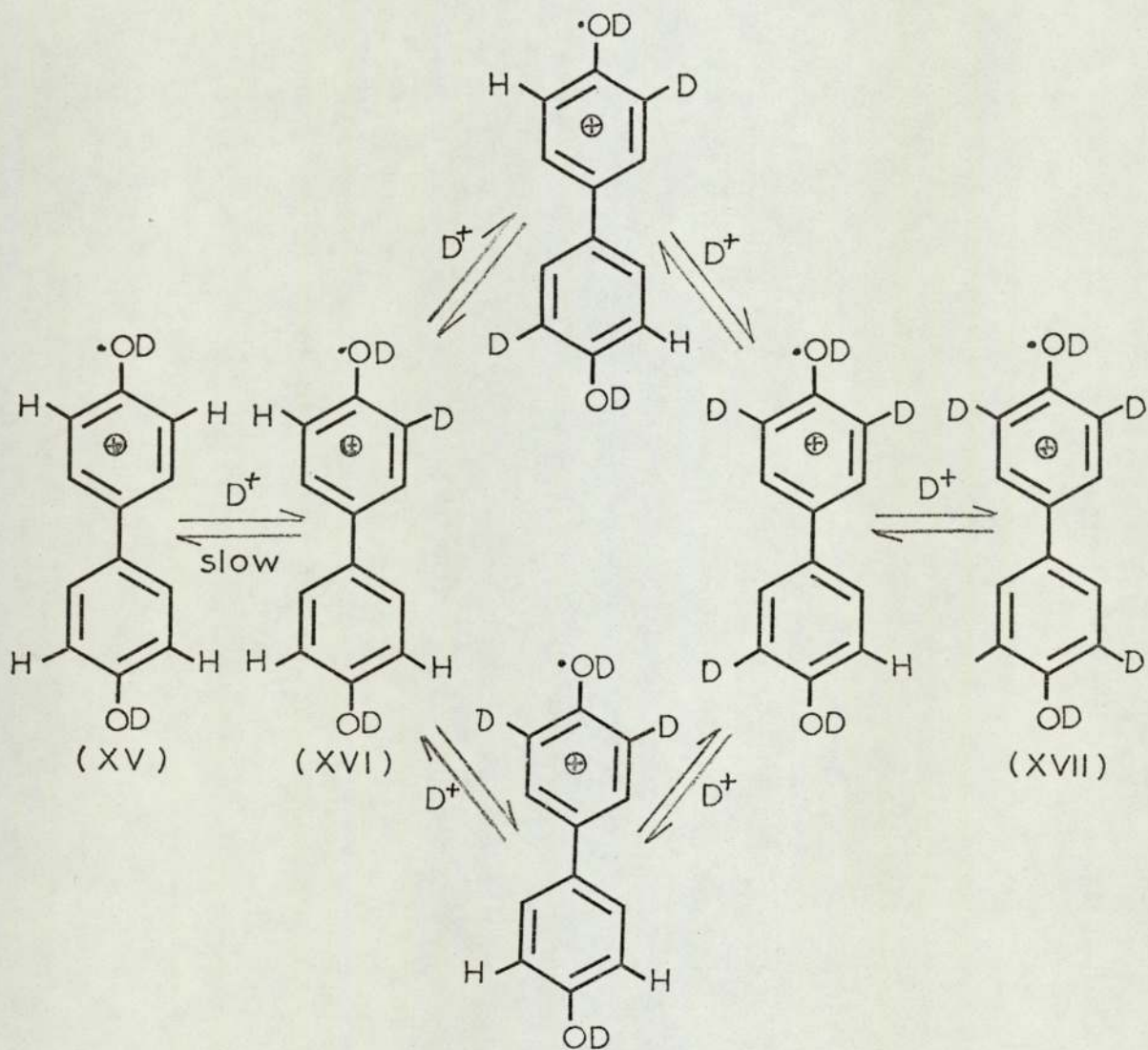
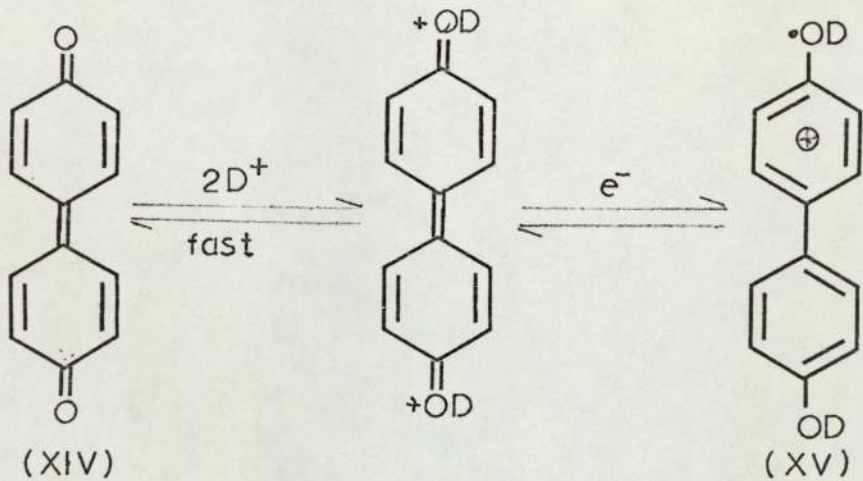


Figure 3.15

Replacement of the proton in the 3 position in the cation (XV) by a deuteron produces the cation (XVI). However since the nuclear moments of hydrogen and deuterium differ by a factor of 6.5 this ring deuterium nuclei will only be expected to have a hyperfine coupling constant of about 0.01 mT. This is much less than the linewidth (ca. 0.02 mT) and hence no line splitting due to the deuterium atoms will be observed. The three remaining ortho hydrogen atoms will thus give rise to a quartet splitting of the main quintet (assuming that  $a_5^H = a_3^H = a_5^H$ ). The appearance of these new lines can be observed in figure 3.11. Subsequent replacement of the remaining protons will eventually lead to the broad quintet of figure 3.14 due to the cation (XVII). The time taken from when the reactants were mixed until this replacement is complete decreases with an increase in temperature. The results for a quinone concentration of 0.005M are summarised in table 3.1. Furthermore when the concentration of the quinone is doubled there is

TABLE 3.1

Temperature (°C)	Time for completion of deuteration. (minutes)
22	180
30	83.5
40	33
50	13

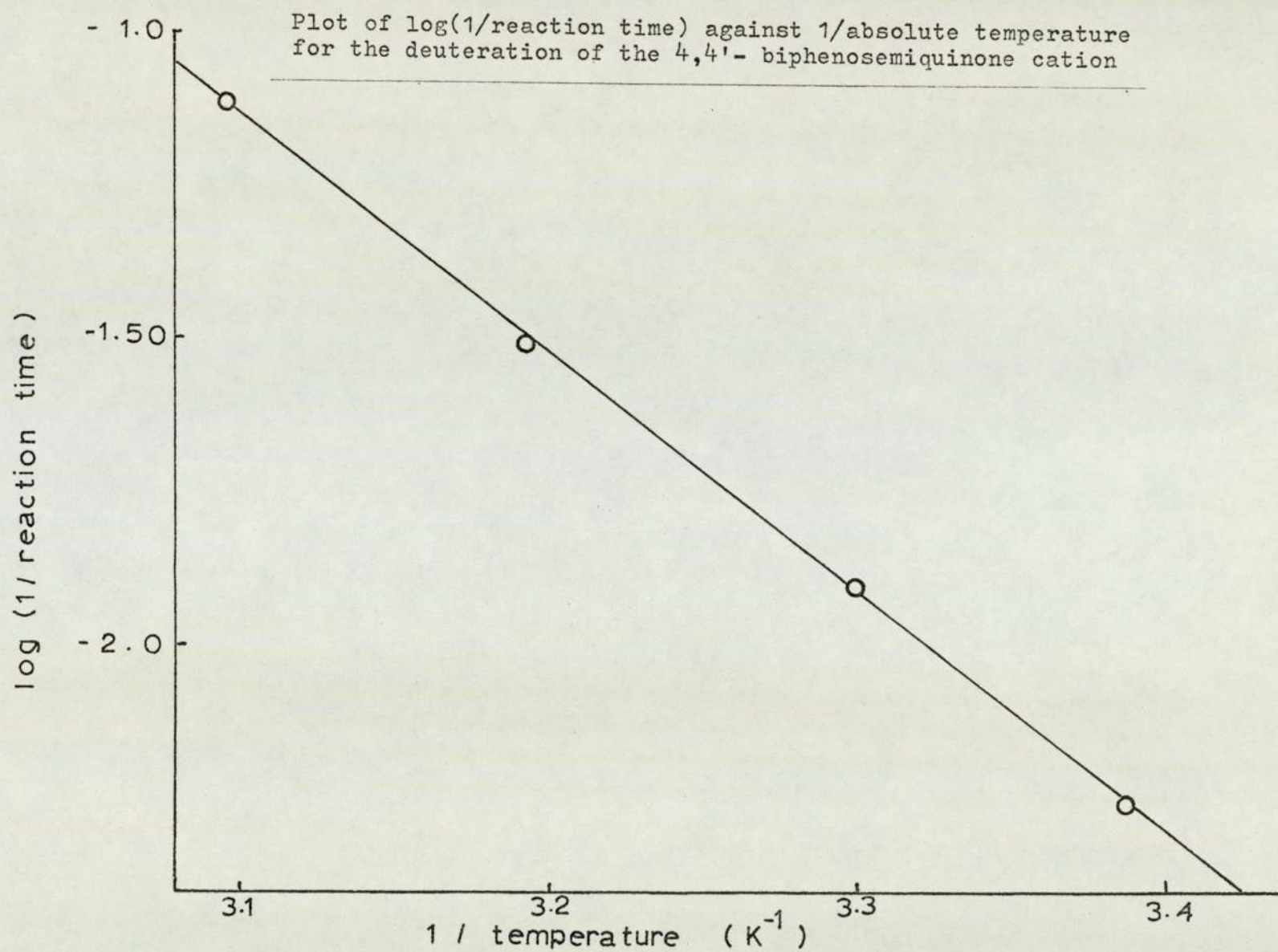


very little change in this time. An arrhenius plot of this data (figure 3.16) yields an activation energy for the reaction of  $73.5 \text{ kJ mol}^{-1}$ .

At all temperatures at which the system was studied the intensity of the ESR signal behaves in the same way. After an initial decrease the intensity remains reasonably constant until the broad quintet stage is approached when it increases and reaches a maximum at the appearance of this quintet after which it decays rather rapidly. As no integrator was available and so that this phenomena could be studied quantitatively a double integrator was built based on the circuit described by Randolph (57) but using operational amplifiers. However the stability obtained was rather poor and such a study was abandoned.

When the experiment is repeated with 1,4-benzoquinone as the substrate the reaction is much faster, all the ring protons are replaced by deuterons within ten minutes of mixing. The ESR spectrum, as one would expect is an unresolved broad band. However, by cooling the reactants slightly to about  $10^{\circ}\text{C}$  before mixing it is possible to record the initial ESR signal in which the fine structure is partially resolved although extremely asymmetric (figure 3.17). This spectrum can be partly explained by the four ring protons producing the main quintet which is further split into smaller quintets with an intensity ratio of 1:2:3:2:1 by the two deuterons on the oxygenatoms. However, the splitting of the five lines of the main quintet (label as 1,4,6,-4,-1) appear to be unequal, the splitting between lines 4 and 6 is

Figure 3.16



1,4-Benzoquinone in cold dideuterosulphuric acid  
immediately after mixing

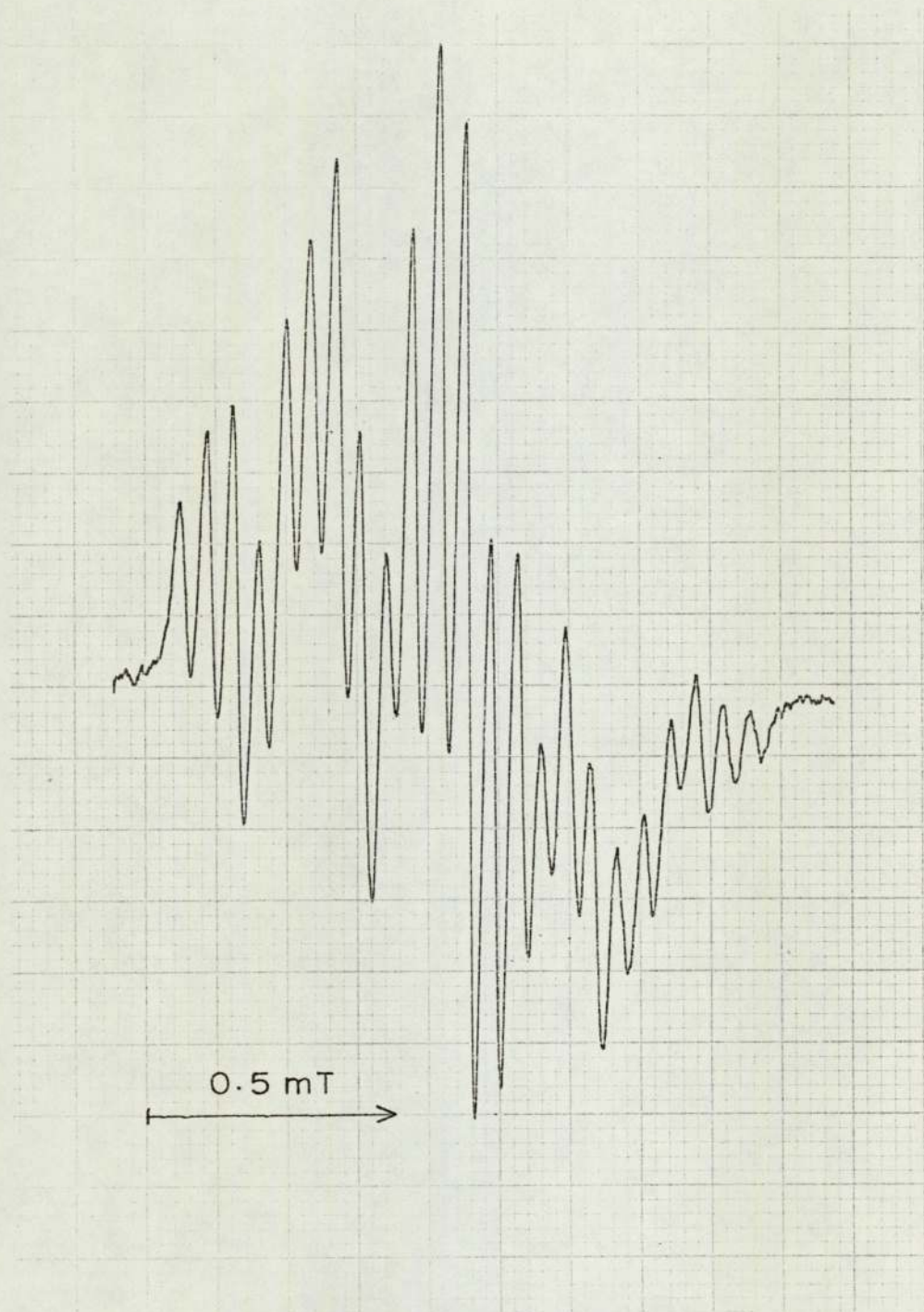


Figure 3.17

greater than between 1 and 4 although the total splitting between 1 and 6 is what one would expect, 0.468 mT. The hyperfine coupling constant of the deuterium nuclei ( $a_{OD}^D$ ) is 0.53 mT which gives a value of 6.50 for the  $a_{OH}^H/a_{OD}^D$  ratio. Subsequent deuteration of the aromatic rings leads to a loss in resolution.

On the addition of a small amount of water the brown solution of 4,4'-biphenquinone in 98% sulphuric acid develops a deep blue colour, the ESR signal remaining unchanged. The addition of further amounts of water cause the precipitation of a pale blue solid leaving a colourless solution. The blue solid is paramagnetic whereas the solution is not and produces an ESR spectrum consisting of a single narrow line having a g-value of 2.0030 (figure 3.18). Furthermore, the filtered solid gradually becomes white on standing and no longer paramagnetic. However, on dissolution in 98% sulphuric acid it reforms the blue paramagnetic solution once more. The white solid after recrystallisation has the same melting point as biphenyl-4,4'-diol. The blue solid is also formed by heating a solution of the quinone in sulphuric acid of concentration not greater than 90%.

Possibly the pale blue solid is a mixture of biphenol and the 4,4'-biphenosemiquinone cation salt of the acid, the salt decomposing to give the biphenol on standing. The blue solid is somewhat more stable in acid solution (longer than seven days).

The ESR spectrum of the paramagnetic blue solid obtained by diluting a solution of 4,4'-biphenoquinone in 98% sulphuric acid with water

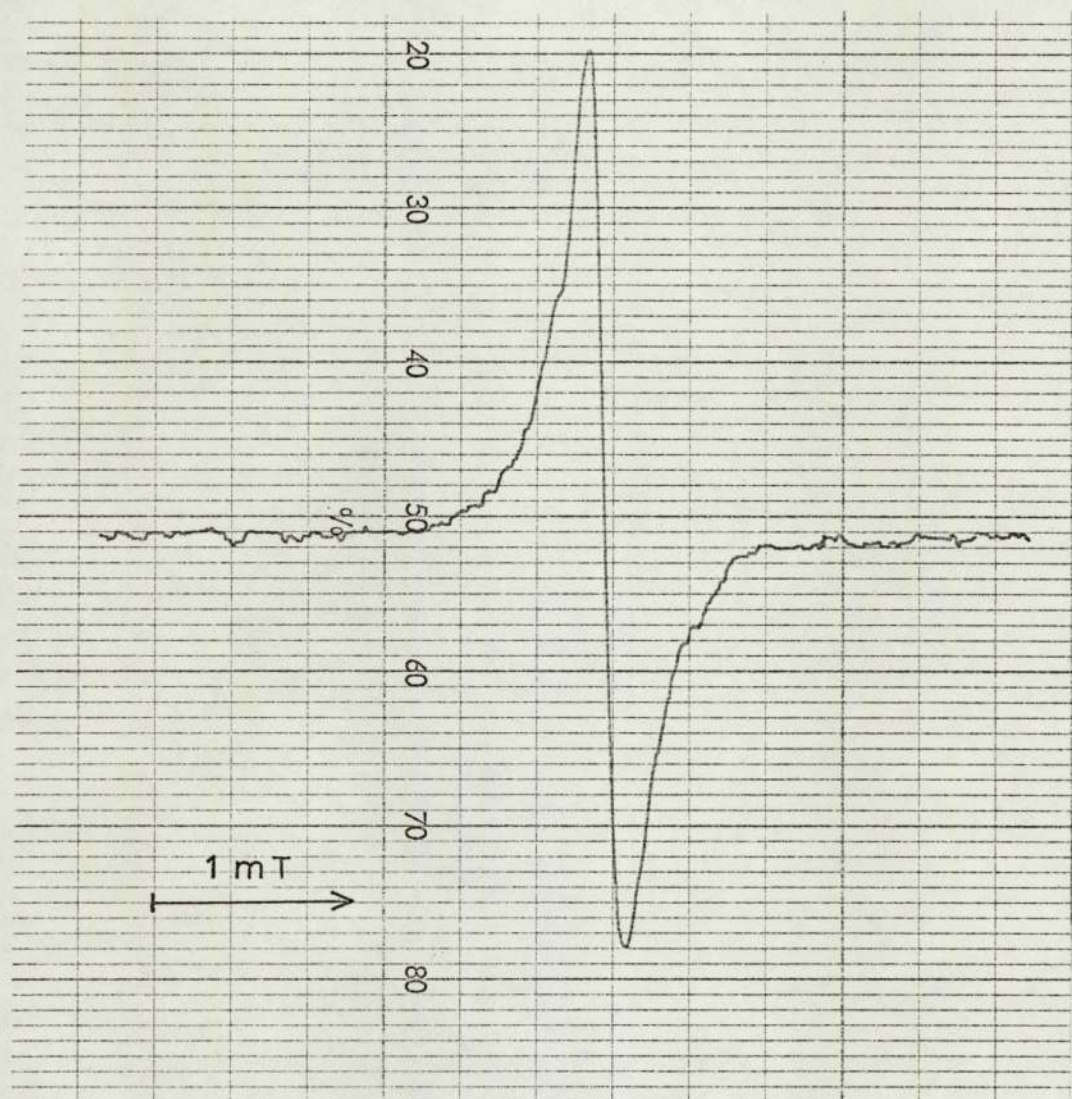


Figure 3.18

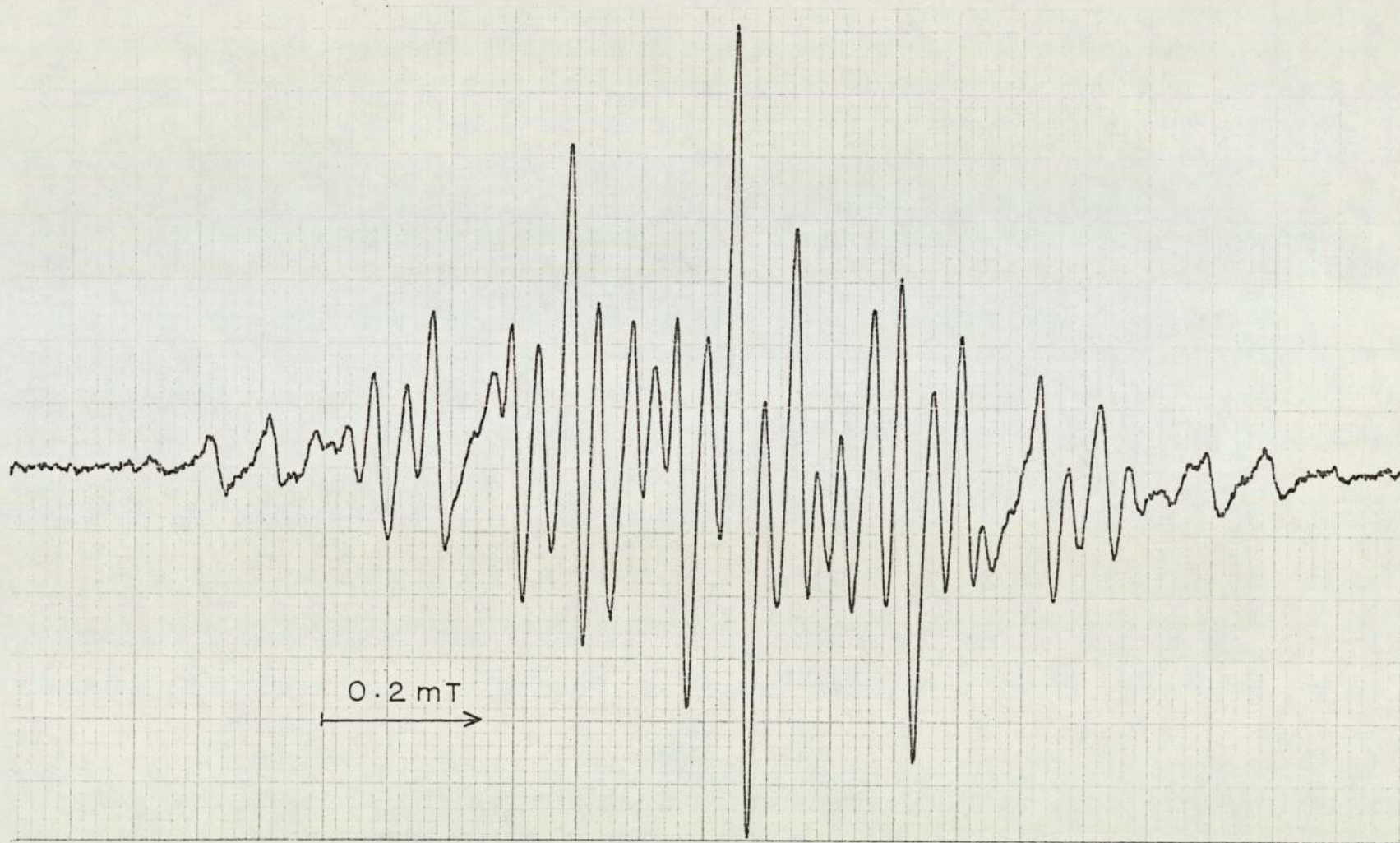
### 3.2.3. Oxidation of Biphenyl-4,4'-diol by an Aluminium

#### Chloride - Nitromethane Mixture

A paramagnetic pale blue-purple solution is obtained when nitromethane is distilled onto a mixture of biphenyl-4,4'-diol and aluminium chloride in vacuo. The observed ESR spectrum (figure 3.19) is attributed to the 4,4'-biphenosemiquinone cation having the following hyperfine coupling constants,  $a_2^H = 0.197$  mT,  $a_3^H = 0.073$  mT and  $a_{OH}^H = 0.166$  mT. These values are very similar to those reported by Barabas, Forbes and Sullivan (52), but by comparison with the sulphuric acid results we are now able to assign the ring proton hyperfine coupling constants to the specific protons. Attempts to detect anomalous linewidths due to any cis-trans isomerism of the hydroxyl groups or restricted rotation of the phenyl rings, by cooling the sample only led to a loss of resolution.

Figure 3.19

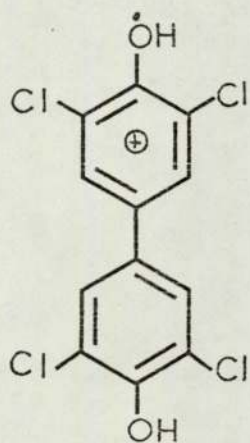
Biphenyl-4,4'-diol in aluminium chloride-nitromethane



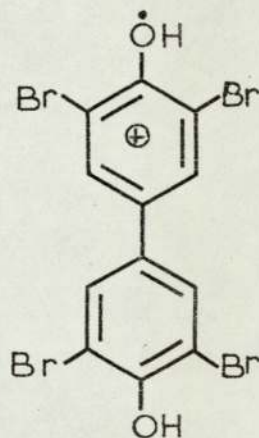
3.3. HALOGENATED 4,4'-BIPHENOSEMIQUINONE CATIONS,  
RESULTS AND DISCUSSION

3,3',5,5'-Tetrachloro-4,4'-biphenoquinone produces a red coloured paramagnetic solution when added to 98% sulphuric acid. The resulting ESR spectrum consists of seven equally spaced lines in the intensity ratio 1:6:15:20:15:6:1 with a hyperfine coupling constant of 0.177 mT (figure 3.20(a)). The 3,3',5,5'-tetrabromo-derivative yields a purple solution from which a similar spectrum is obtained, although the individual lines are much broader and the hyperfine coupling constant is 0.182 mT (figure 3.21).

These spectra are attributed to the respective semiquinone cations (XVIII) and (XIX), the seven lines



(XVIII)



(XIX)

arising from six equivalent protons. This means that the



3,3',5,5'-Tetrachloro-4,4'-biphenoquinone  
in (a), (b) dideuterosulphuric acid  
and (c) 98% sulphuric acid

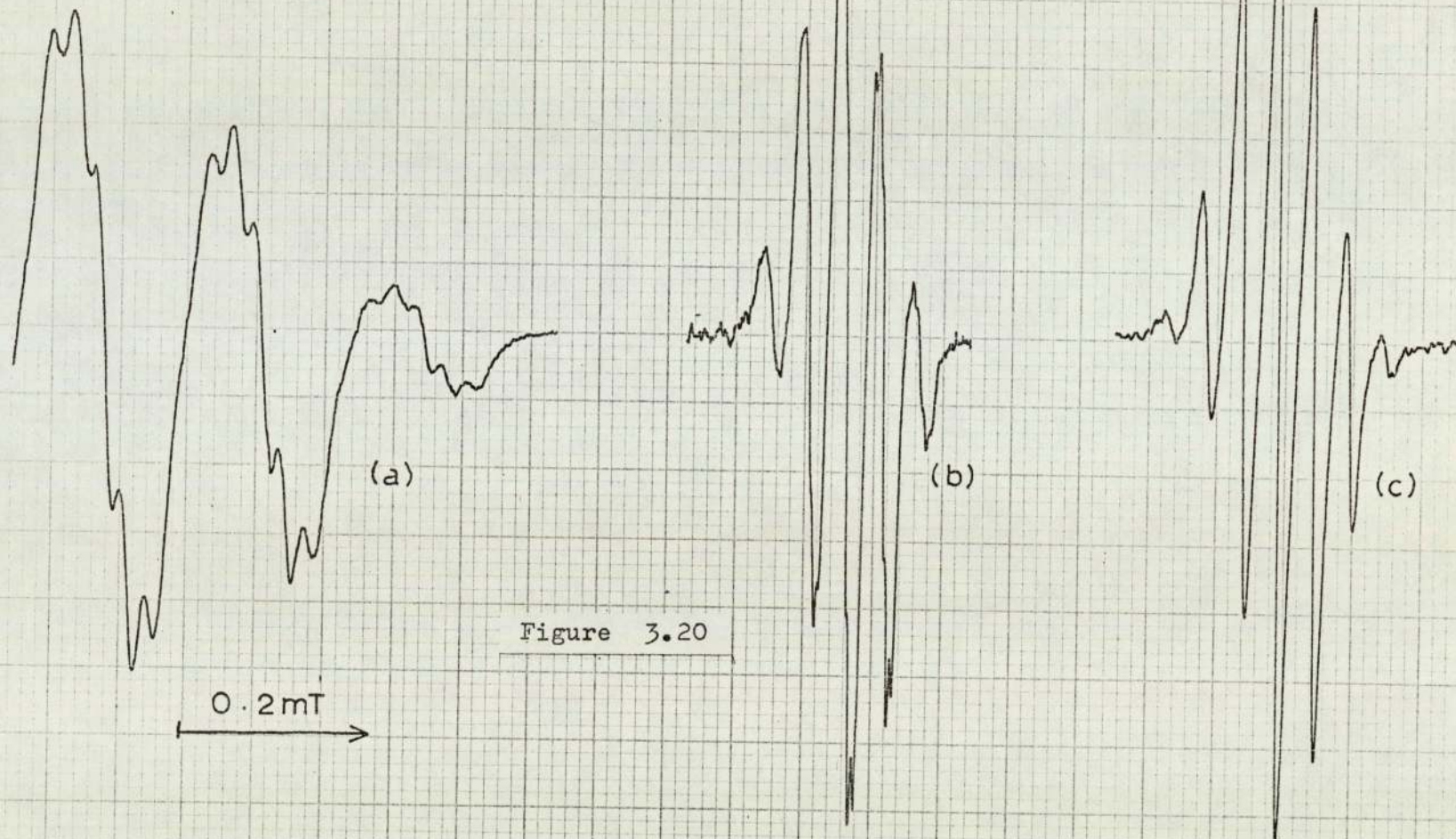
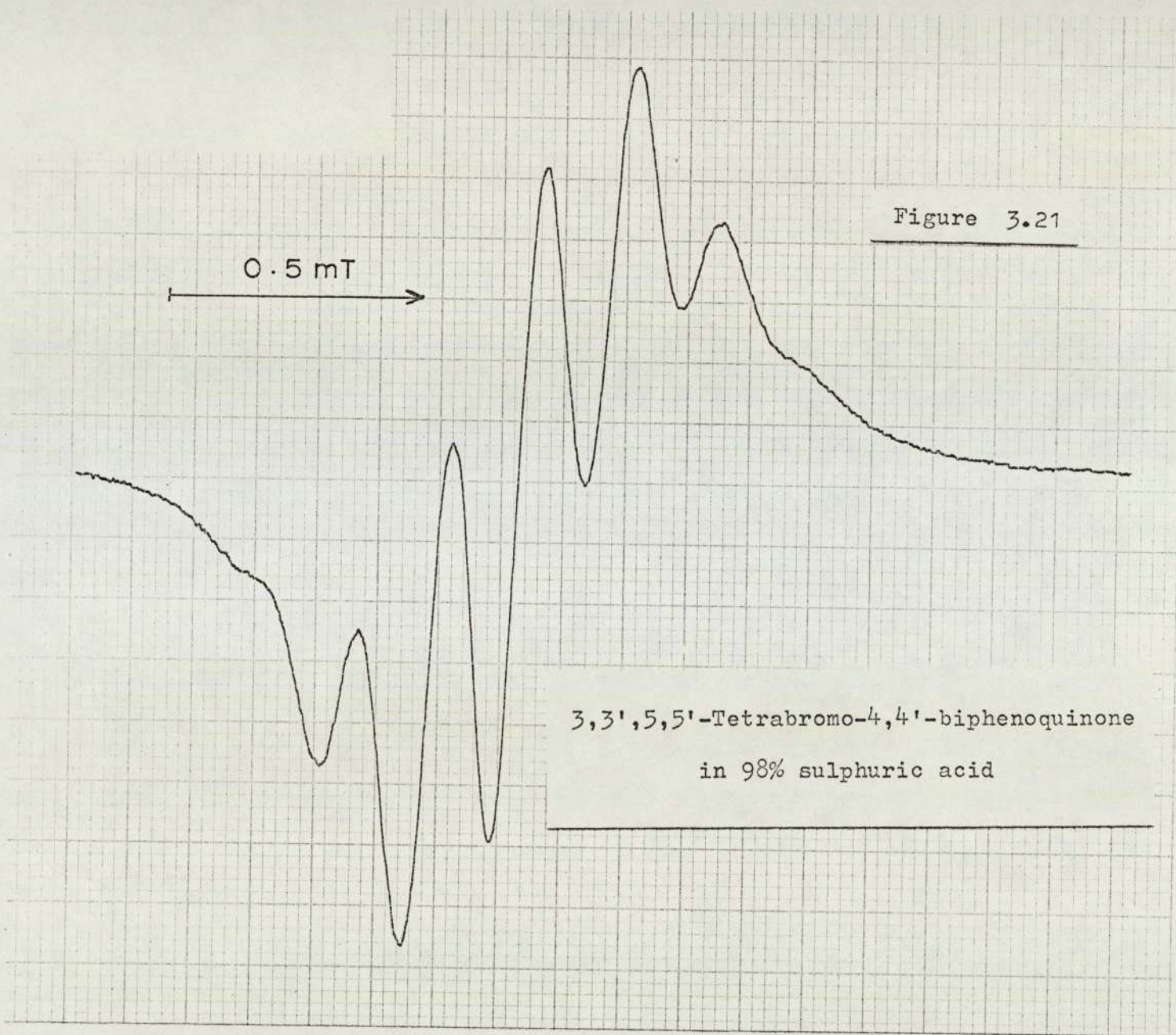


Figure 3.20



protons of the hydroxyl groups, unlike those in the parent cation (section 3.2.1), give rise to hyperfine coupling and furthermore the coupling constants are identical to those of the ring protons.

This interpretation is confirmed by using concentrated dideuterosulphuric acid as the reaction medium. The resulting spectrum of the tetrachloro-derivative consists of a quintet of lines (intensity ratio 1:4:6:4:1) with the same coupling constant as before (figure 3.20(b)). However, it is possible to observe fine structure due to the replacement of the hydroxyl protons by deuterons, the value of the deuterium hyperfine coupling constant being 0.027 mT (figure 3.20(c)). In the case of the tetrabromo-compound the spectrum consists of five poorly resolved lines, having a hyperfine coupling constant of 0.182 mT.

Addition of sodium dithionite to the radical solutions produces white solid precipitate and colourless diamagnetic solutions. The white materials have the same melting points as the corresponding diols and are oxidised to the coloured paramagnetic cation solutions again by sulphuric acid containing hydrogen peroxide. The halogenated diols are much more resistant to oxidation than the parent compound, heat being required in the case of the tetrachloro-analogue to produce even a weak signal. When the coloured acid solutions of the quinones are poured onto ice the quinones are recovered unchanged.

From the foregoing it is concluded that sulphuric

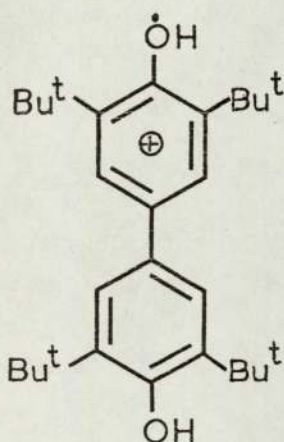
acid alone leads to a one-electron reduction of the quinones whereas when sodium dithionite is present as well a two-electron reduction takes place.

Oxidation of 3,3',5,5'-tetrachlorobiphenyl-4,4'-diol by an aluminium chloride-nitromethane mixture produces a pale orange-brown solution exhibiting a weak poorly resolved ESR signal. No reaction was detected when the tetrabromo-compound was used.

3.4. ALKYL SUBSTITUTED 4,4'-BIPHENOSEMIQUINONE  
CATIONS, RESULTS AND DISCUSSION

3.4.1. Reduction of Alkylated 4,4'-Biphenquinones in  
Concentrated Sulphuric Acid

3,3',5,5'-Tetra-*t*-butyl-4,4'-biphenquinone produces a red-brown coloured paramagnetic solution with 98% sulphuric acid. The ESR spectrum, illustrated in figure 3.22(a) can be analysed as five lines arising from four equivalent protons having a hyperfine coupling constant of 0.188 mT which are further split into triplets by a group of two equivalent protons with a coupling constant of 0.149 mT. If dideuterosulphuric acid is used instead of sulphuric acid then the ESR spectrum consists of five broad lines, hyperfine coupling constant 0.189 mT (figure 3.22(b)). Thus the ESR spectrum in concentrated sulphuric acid is considered to arise from the radical cation (XX).



$$a_3^H = 0.188 \text{ mT}$$

$$a_{OH}^H = 0.149 \text{ mT}$$

(XX)

3,3',5,5'-Tetra-*t*-butyl-4,4'-biphenquinone  
in (a) 98% sulphuric acid  
and (b) dideuterosulphuric acid

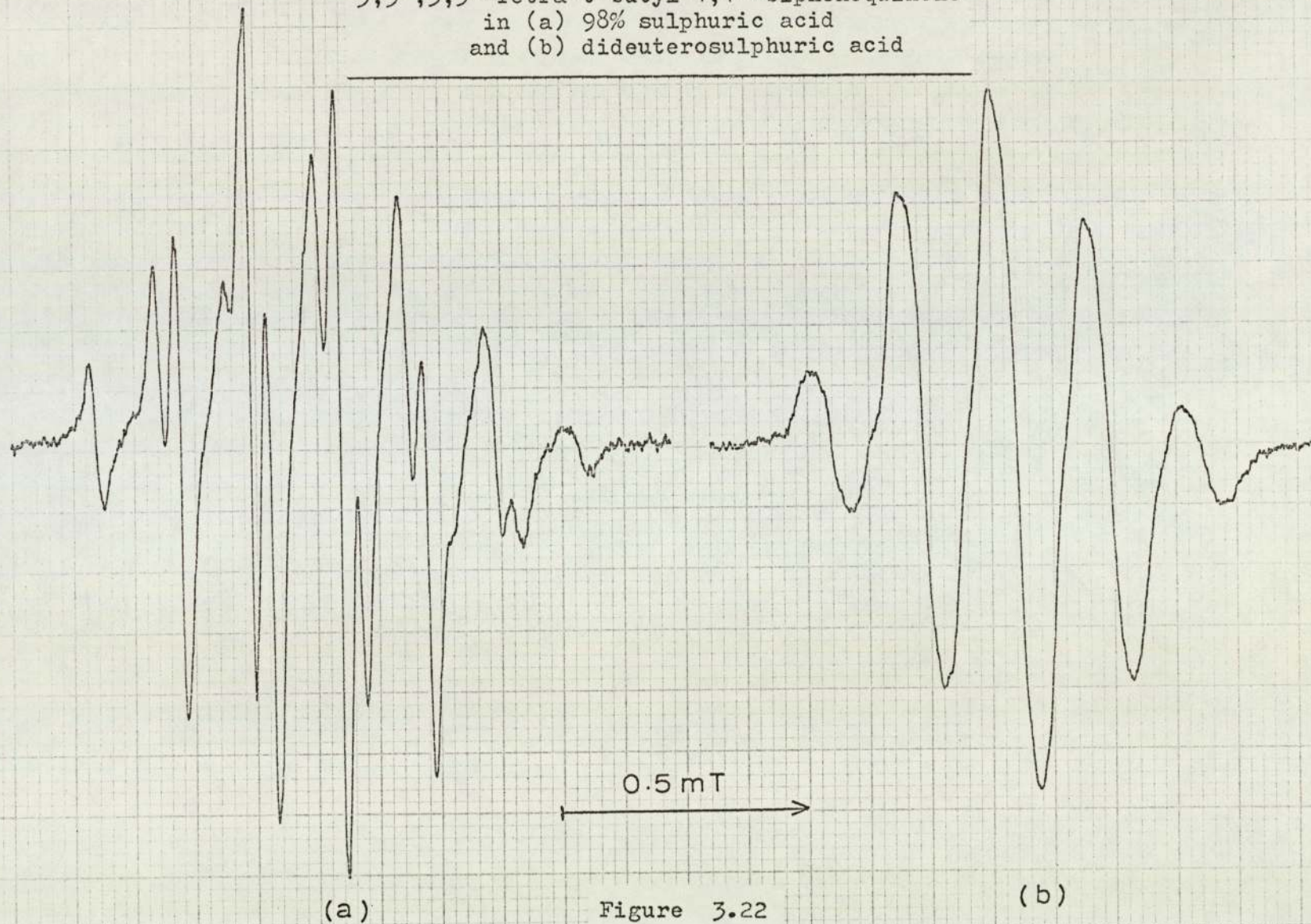


Figure 3.22

Other alkyl substituted 4,4'-biphenyloquinones give coloured paramagnetic solutions in sulphuric acid, the 3,3',5,5'-tetraisopropyl and tetra-sec-butyl solutions are red-brown. However their ESR signals consist of a single unresolved broad line. The solution of the tetramethyl derivative is not paramagnetic unless sodium dithionite is present.

#### 3.4.2. Oxidation of Alkylated Biphenyl-4,4'-diols in Concentrated Sulphuric Acid

Provided a trace of the oxidising agent is added to a cold mixture of the 3,3',5,5'-tetra-t-butylbiphenyl-4,4'-diol in 98% sulphuric acid the same results are obtained as outlined in the previous section for the reduction of the quinone. However, if the mixture is warm, a sea-green coloured solution is produced which exhibits the same spectrum as that shown in figure 3.2a which was attributed to the semiquinone cation of the disulphonic acid (XII). Thus a complete dealkylation and a partial sulphonation of the substrate occurs in the second case. Nishinaga and his co-workers (58) in studying the electron transfer of 1,4-dimethoxybenzene and its alkyl substituted derivatives in concentrated sulphuric acid showed that the dealkylation of 2,5-di-t-butyl-1,4-dimethoxybenzene takes place only in the neutral molecule whilst the radical cation is stable against dealkylation.

The semiquinone cation ( XX ) is also produced when 2,6-di-t-butylphenol is dissolved in 98% sulphuric

acid at room temperature. At first the solution is green in colour but after about thirty seconds it darkens to a red-brown colour exhibiting the ESR signal of the cation (XX). Presumably a cation radical formed by a one-electron oxidation of the phenol is initially produced and subsequently reacts with another molecule of the phenol to produce the cation (XX).

Oxidation of the 3,3',5,5'-tetramethyl, tetraisopropyl and tetra-sec-butylbiphenyl-4,4'-diols gives the same results as for the reduction of the corresponding quinones. 3,3'-Dimethylbiphenyl-4,4'-diol produces a paramagnetic blue coloured solution, the ESR signal of which is a single broad line.

#### 3.4.3. Oxidation of Alkylated Biphenyl-4,4'-diols by an Aluminium Chloride-Nitromethane Mixture

3,3',5,5'-Tetramethylbiphenyldiol gives a blue-green paramagnetic solution when oxidised with aluminium chloride in nitromethane. The resulting ESR spectrum (figure 3.23) is attributed to the semiquinone cation (XXI), the hyperfine coupling constant of the hydroxyl and ring protons being the same yet larger than the methyl proton hyperfine coupling constant.

The 3,3'-dimethyl compound produces a blue paramagnetic solution when oxidised. The observed ESR spectrum (figure 3.24) consists of at least twenty-three equally spaced (0.073 mT) broad lines. Such a spectrum could arise if the methyl protons and ring



3,3',5,5'-Tetramethylbiphenyl-4,4'-diol  
in aluminium chloride-nitromethane

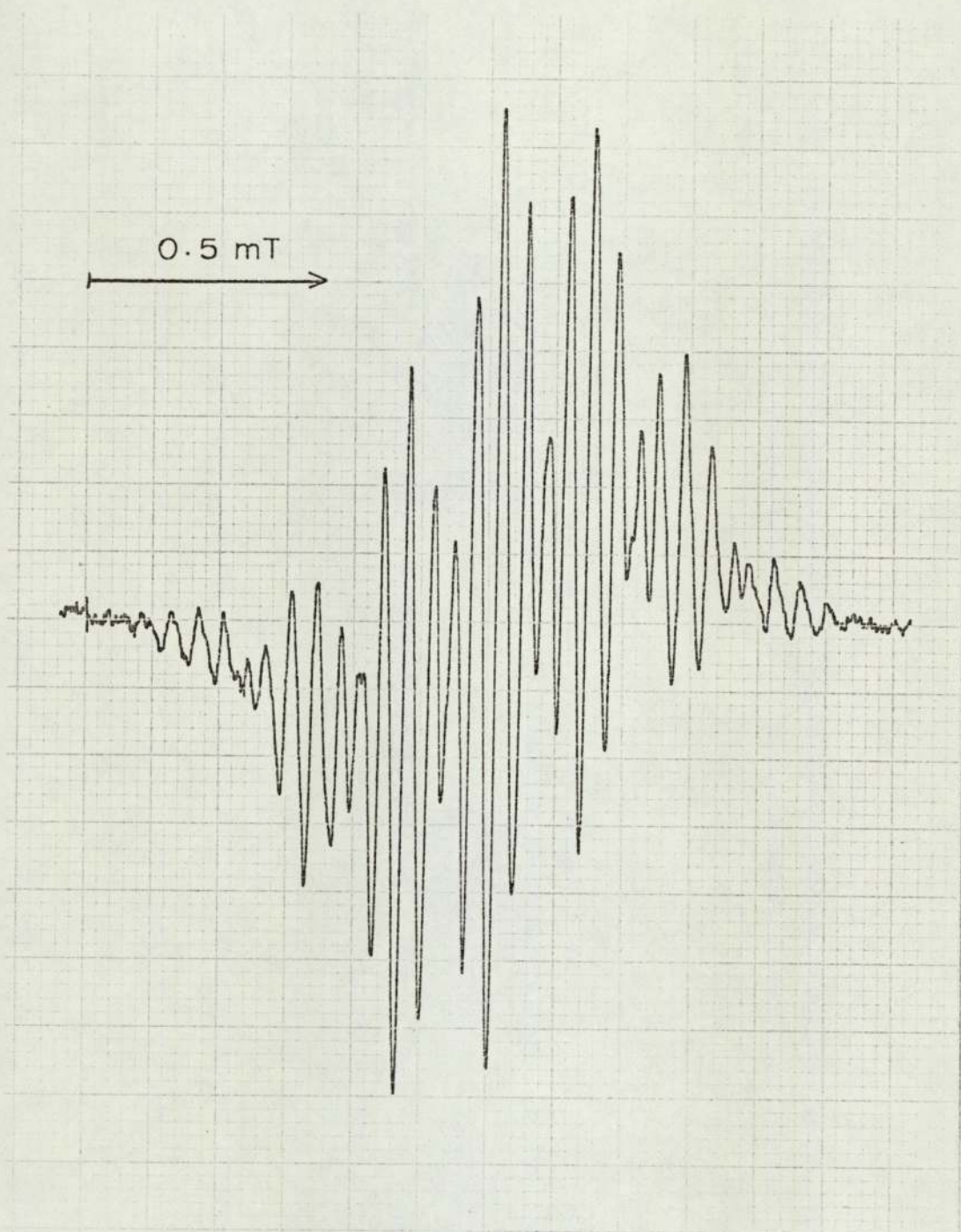


Figure 3.23

3,3'-Dimethylbiphenyl-4,4'-diol  
in aluminium chloride-nitromethane

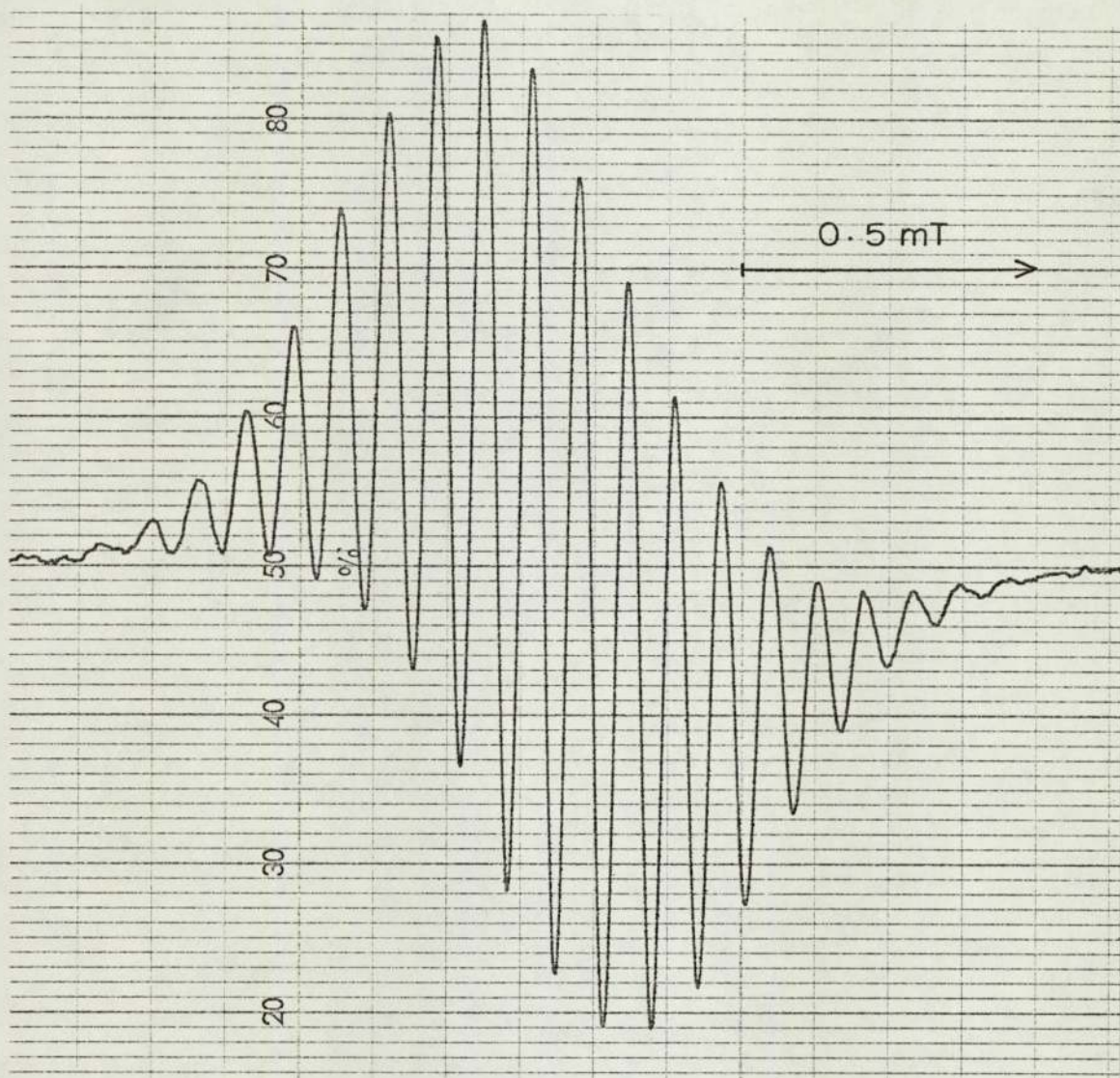
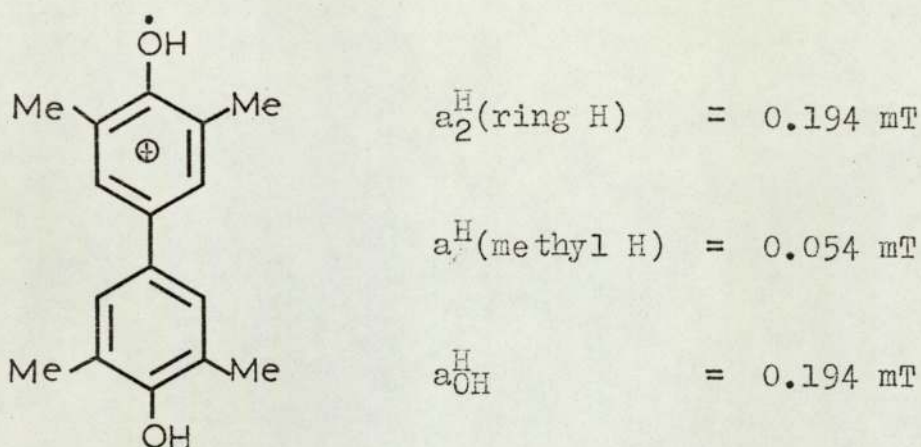


Figure 3.24



(XXI)

protons in position 3 have coupling constants of about 0.073 mT and the hydroxyl and remaining ring protons have a value of about 0.146 mT, which from a comparison with the other semiquinone cations are quite reasonable assignments.

The corresponding ESR spectrum obtained using the 3,3',5,5'-tetraisopropyl compound cannot be resolved at all. However, although the ESR signal obtained from the red solution produced by oxidation of the 3,3',5,5'-tetra-sec-butyl derivative is extremely weak, this could be partially resolved. Assuming that the radical species present is the semiquinone cation of the substrate, then analysis of the spectrum (figure 3.25) gives the following hyperfine coupling constants,  $a_2^{\text{H}}(\text{ring H}) = 0.180 \text{ mT}$ ,  $a_{\text{OH}}^{\text{H}} = 0.145 \text{ mT}$  and  $a_{\text{CH}}^{\text{H}} = 0.033 \text{ mT}$ . The latter value is the hyperfine coupling constant for the methin proton

3,3',5,5'-Tetra-sec-butylbiphenyl-4,4'-diol  
in aluminium chloride-nitromethane

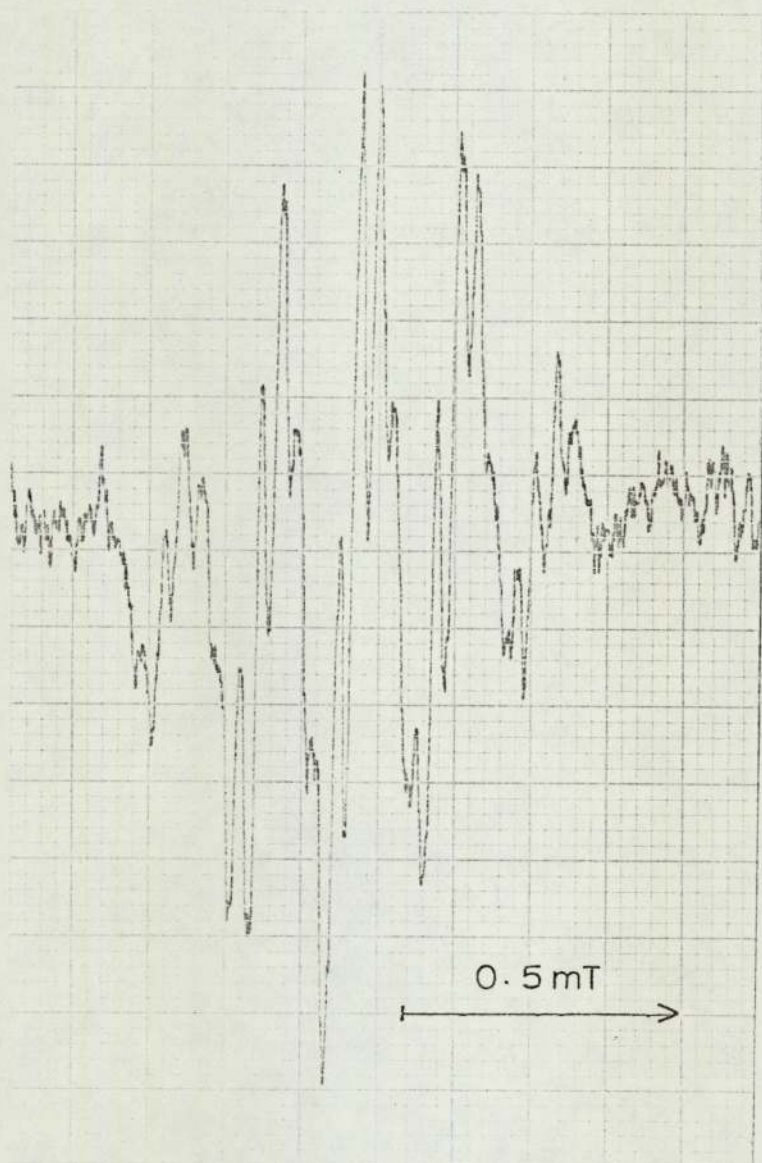


Figure 3.25

of the sec-butyl group.

3,3',5,5'-Tetra-*t*-butylbiphenyl-4,4'-diol is anomalous in its behaviour on oxidation. On mixing the reactants at room temperature, a dark red-brown coloured paramagnetic solution is formed, which after about thirty seconds becomes pale green darkening gradually until after a few hours it is deep blue. At the same time the ESR spectrum of the solution changes, figures 3.26 to 3.28 illustrate this transition. By mixing the reactants at  $-20^{\circ}\text{C}$  and recording the ESR spectrum of the solution at the same temperature, the production of the secondary radicals is halted and the spectrum of the red-brown coloured solution is obtained (figure 3.29). This much simpler spectrum is due to the semiquinone cation (XX). Unfortunately the resolution at this temperature is not sufficient to distinguish the separate hydroxyl and ring proton hyperfine coupling constants and the spectrum approximates to one due to six equivalent protons.

Although the intermediate spectra (figures 3.26 and 3.27) obtained at room temperature are difficult to analyse, the final spectrum (figure 3.28) is that of the 4,4'-biphenosemiquinone cation (section 3.2.3) indicating that dealkylations are taking place.

Recently, Sullivan (59) has also shown that a cation radical containing a hydroxyl group flanked by two ortho *t*-butyl substituents, the 2,6-di-*t*-butyl-1,4-benzosemiquinone cation is only stable at reduced temperatures. The cation, produced by oxidation of the hydroquinone with

3,3',5,5'-Tetra-*t*-butylbiphenyl-4,4'-diol  
in aluminium chloride-nitromethane  
at 25°C after 10 minutes

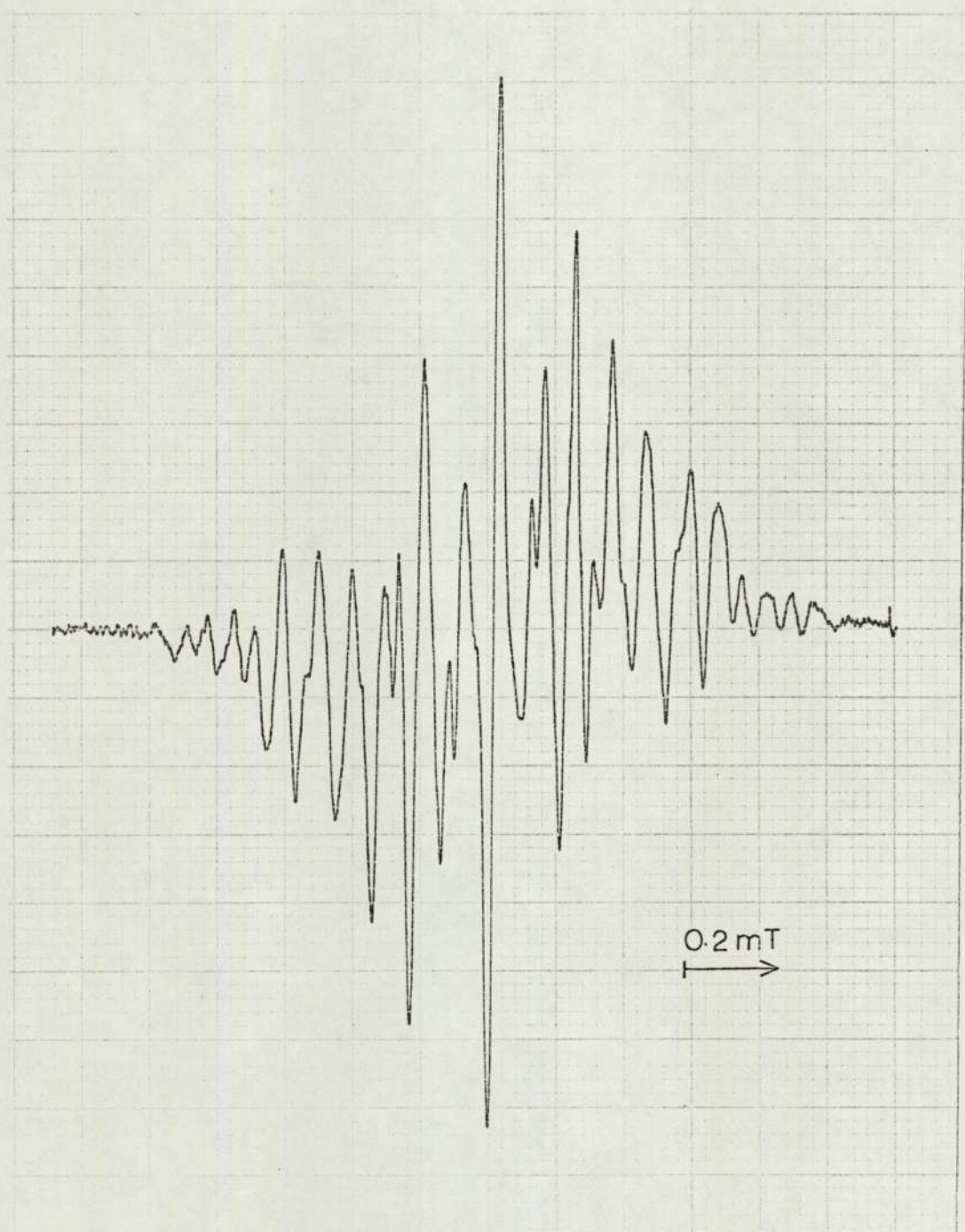


Figure 3.26

3,3',5,5'-Tetra-*t*-butylbiphenyl-4,4'-diol  
in aluminium chloride-nitromethane  
at 25°C after 2.25 hours

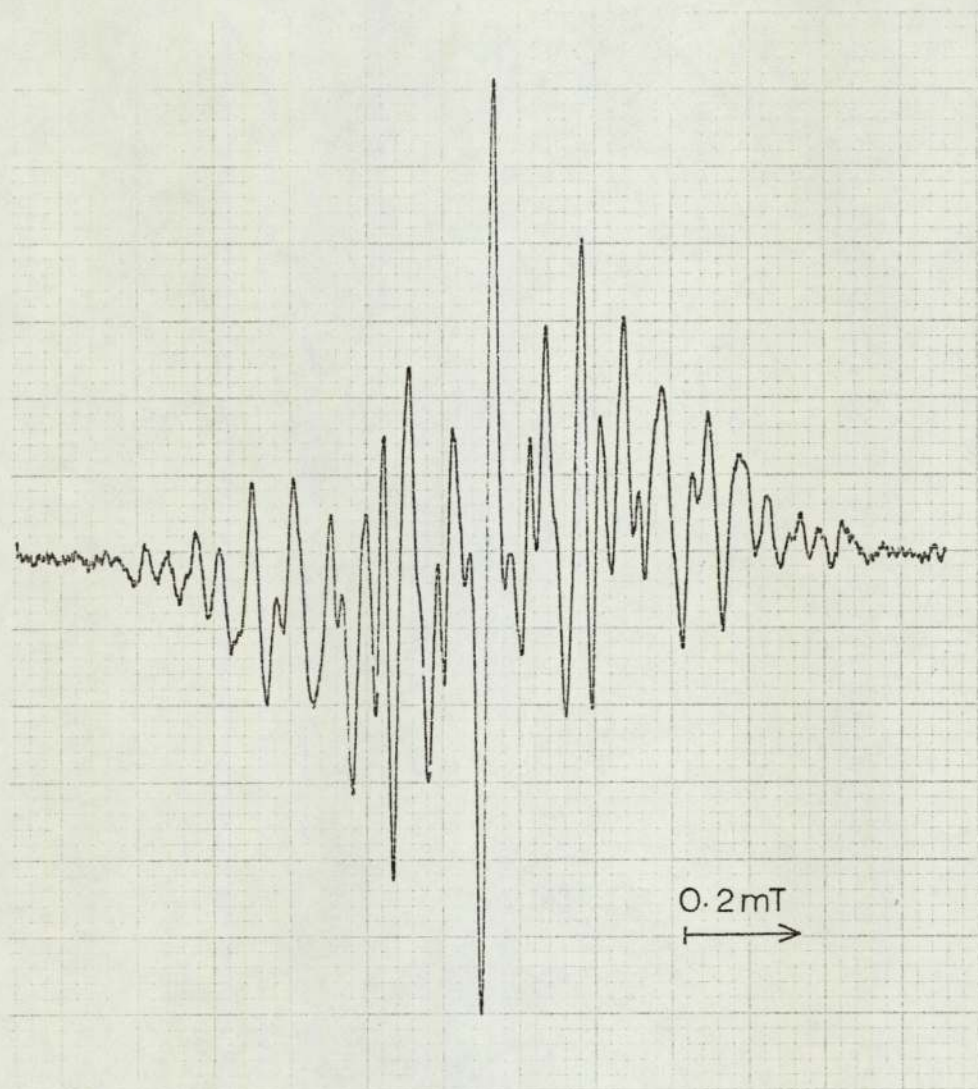


Figure 3.27

3,3',5,5'-Tetra-*t*-butylbiphenyl-4,4'-diol  
in aluminium chloride-nitromethane  
at 25°C after 8 hours

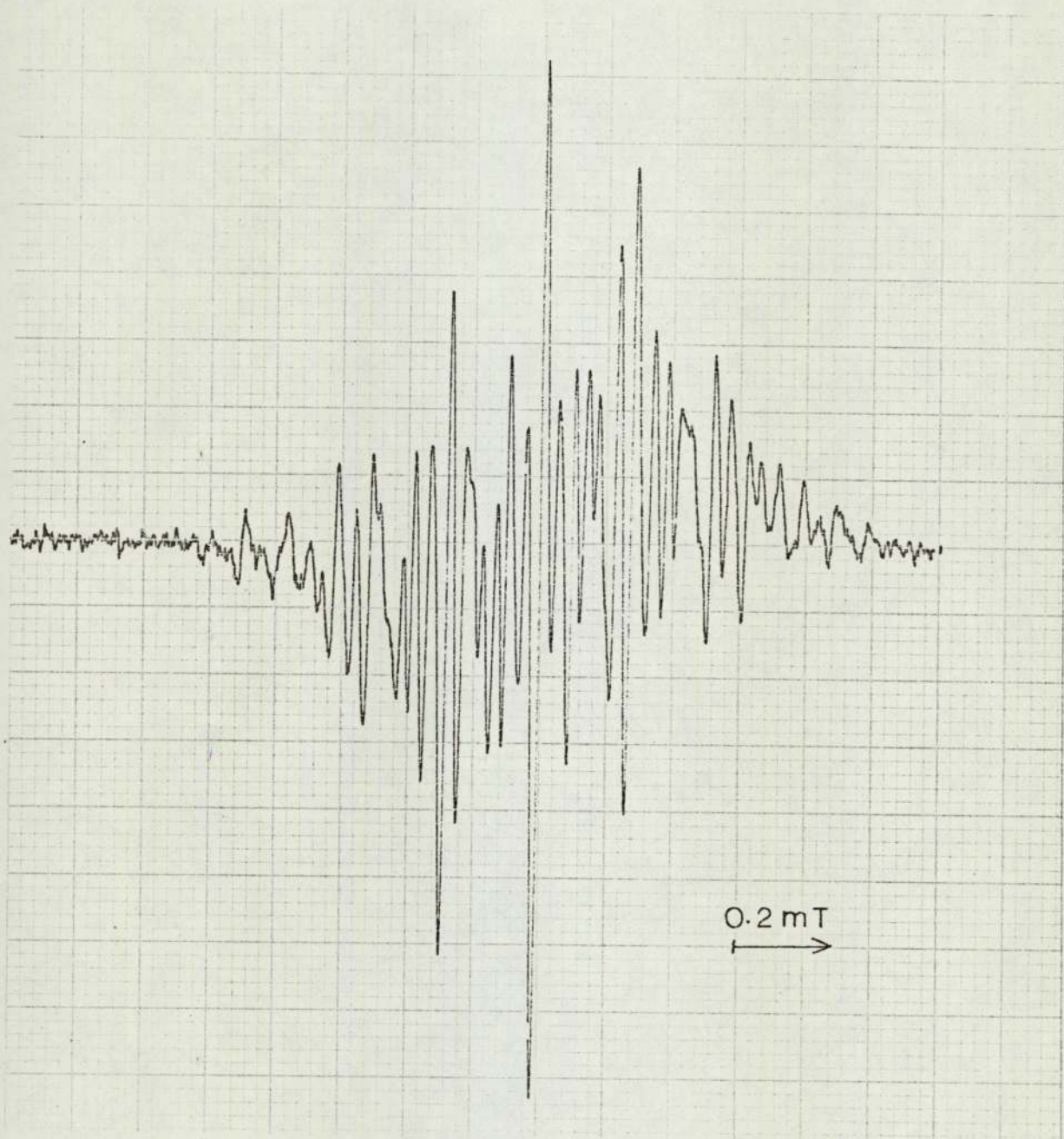


Figure 3.28



3,3',5,5'-Tetra-*t*-butylbiphenyl-4,4'-diol  
in aluminium chloride-nitromethane  
at  $-20^{\circ}\text{C}$

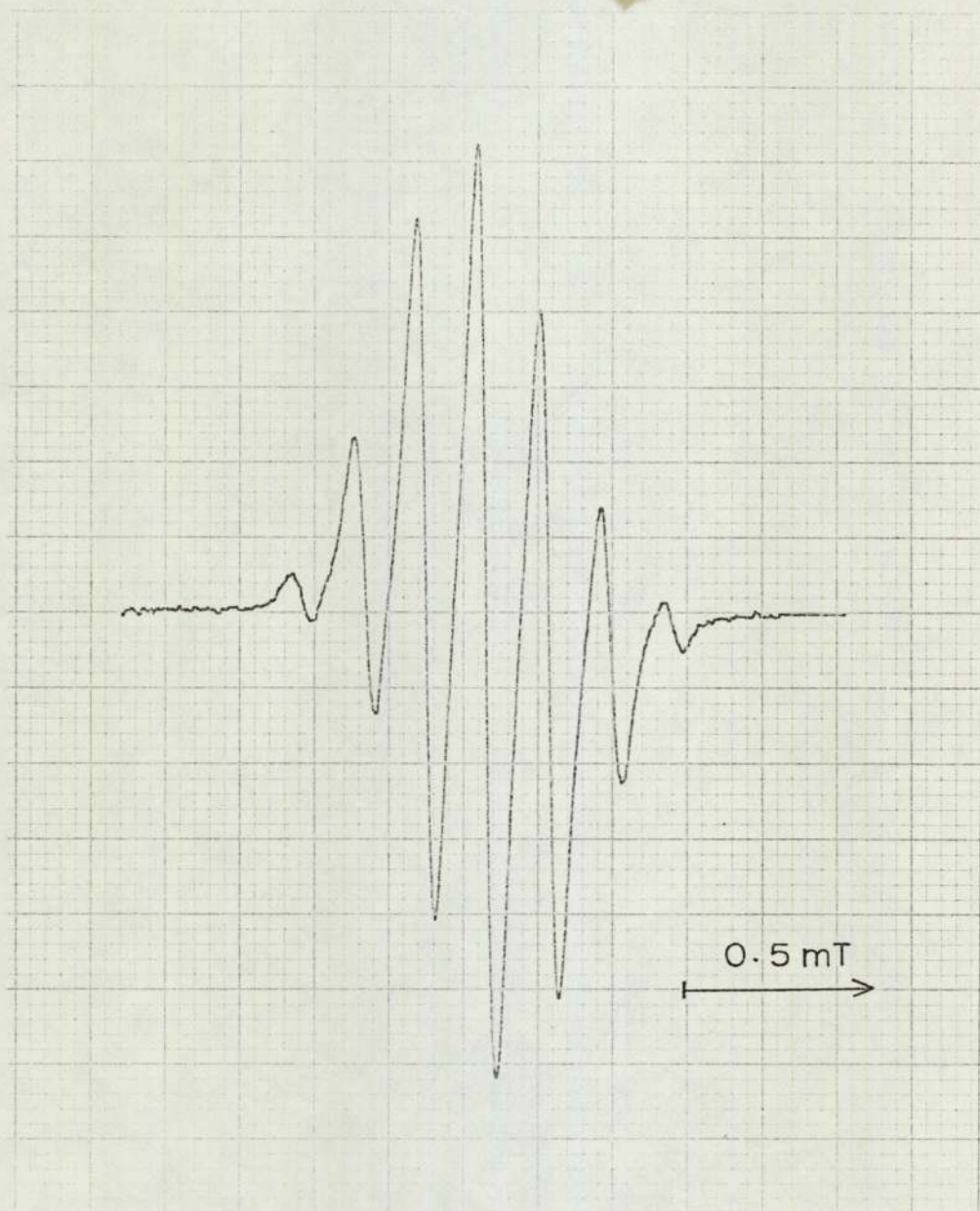


Figure 3.29

aluminium chloride-nitromethane undergoes an alkyl-group migration to form the 2,5-di-t-butyl-1,4-benzosemiquinone cation. Sullivan also analysed the ESR spectra of 2-alkyl substituted 4,4'-biphenosemiquinone cations also obtained using aluminium chloride-nitromethane. The 3,3',5,5'-tetra-t-butyl derivative yielded a spectrum composed of broad lines consistent with interaction of only the hydroxyl and ring protons ( $a_2^H = 0.183$  mT,  $a_{OH}^H = 0.146$  mT). However, in the case of the 3,3'-dimethyl-5,5'-di-t-butyl substituted cation even the t-butyl splittings were easily resolved ( $a_2^H = 0.178$  mT,  $a_{CH_3}^H = 0.059$  mT,  $a_{t-Bn}^H = 0.004$  mT,  $a_{OH}^H = 0.1465$  mT).

#### 3.4.4. Oxidation of 3,3',5,5'-Tetra-t-butylbiphenyl-4,4'-diol by a Concentrated Sulphuric Acid-Nitromethane Mixture

The t-butyl compound is the only alkylated diol studied that behaves differently when a mixture of concentrated sulphuric acid and nitromethane (20% - 80% by volume) is used to perform the oxidation rather than aluminium chloride and nitromethane. On mixing the reactants at room temperature an initial pale green colouration of the solution rapidly gives way to a red-brown solution which gradually changes to orange and finally becomes dark green. Again secondary radicals are produced but at a slower rate than with aluminium chloride. The red-brown solution initially yields the ESR spectrum of the semiquinone cation (XX) ( $a_2^H(\text{ringH}) = 0.185$  mT,  $a_{OH}^H = 0.146$  mT) but it is gradually replaced by more complex spectra (figure 3.30) and after standing

3,3',5,5'-Tetra-*t*-butylbiphenyl-4,4'-diol  
in 98% sulphuric acid-nitromethane  
at 25°C after 10 minutes

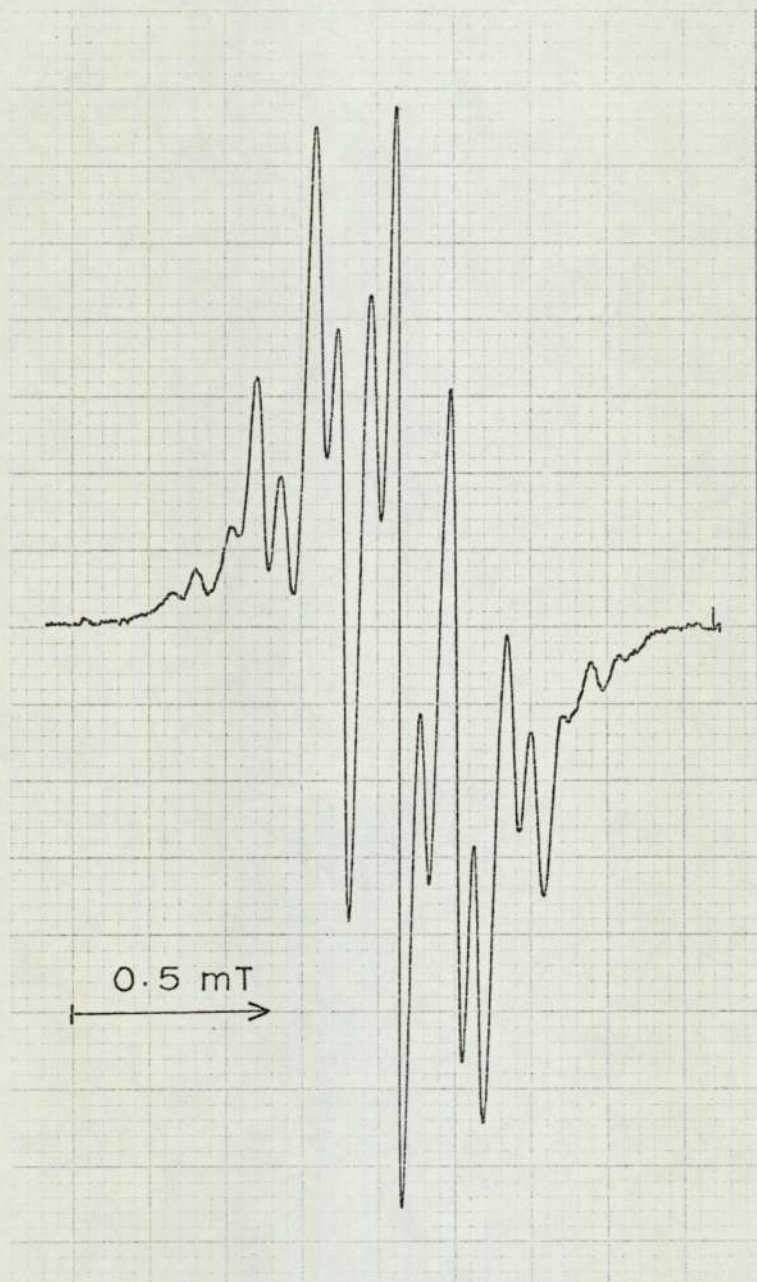


Figure 3.30(a)

3,3',5,5'-Tetra-*t*-butylbiphenyl-4,4'-diol  
in 98% sulphuric acid-nitromethane  
at 25°C after 18 minutes

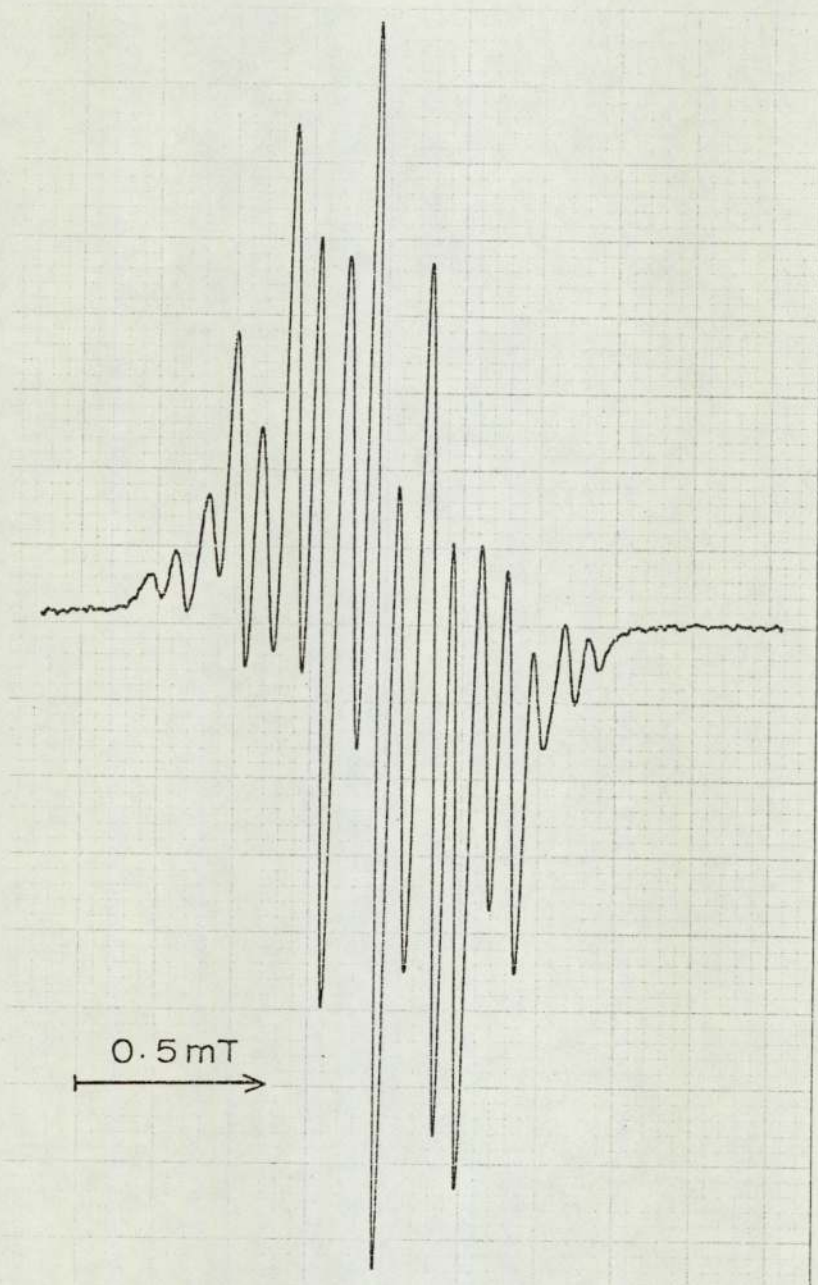


Figure 3.30(b)

3,3',5,5'-Tetra-*t*-butylbiphenyl-4,4'-diol  
in 98% sulphuric acid-nitromethane  
at 25°C after 40 minutes

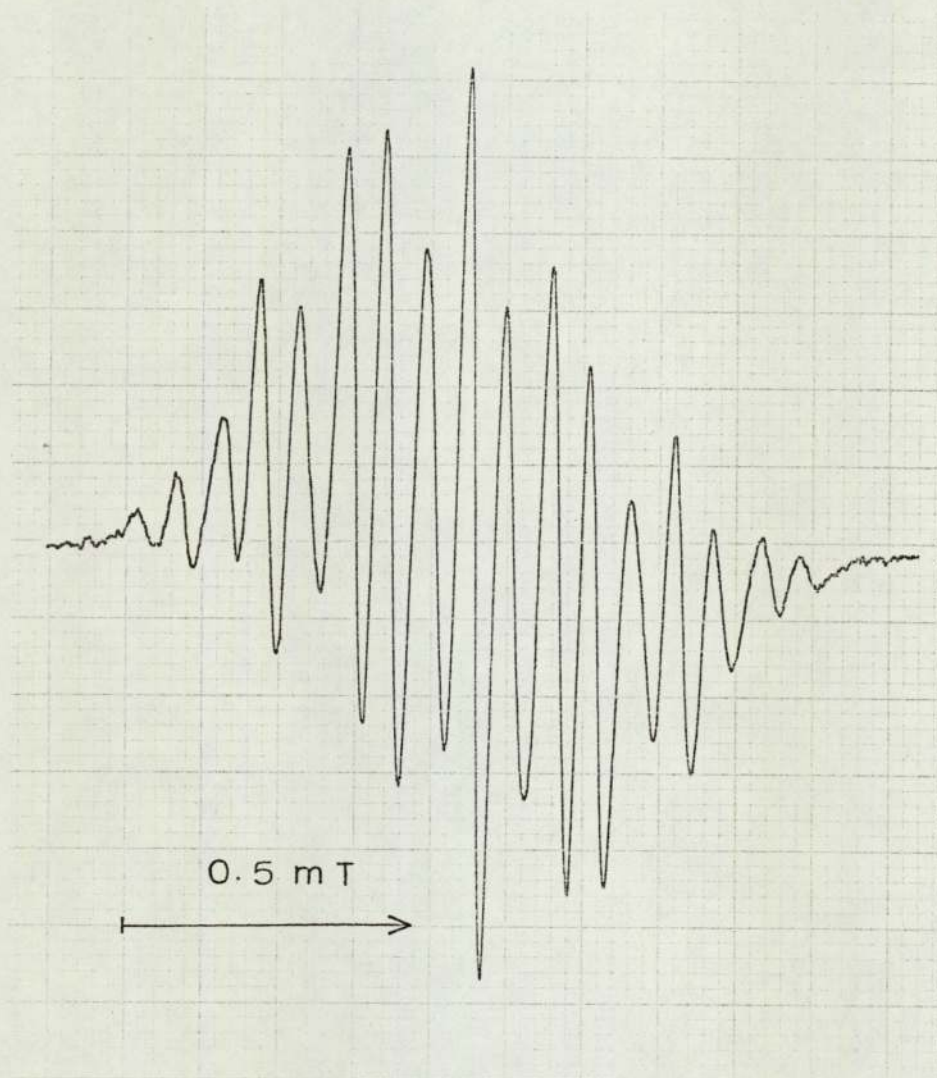


Figure 3.30(c)

overnight yields a spectrum having a greater width and also a much better resolution (figure 3.31). This last spectrum can be analysed in terms of four equivalent protons with  $a^H = 0.288$  mT, two equivalent protons with  $a^H = 0.182$  mT and a further two equivalent protons with  $a^H = 0.143$  mT.

3,3',5,5'-Tetra-*t*-butylbiphenyl-4,4'-diol  
in 98% sulphuric acid-nitromethane  
at 25°C after 16 hours

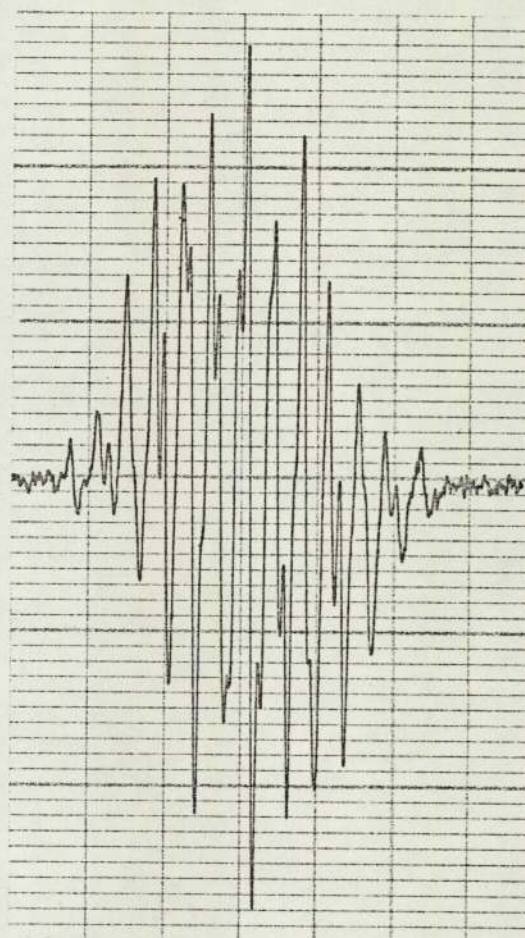
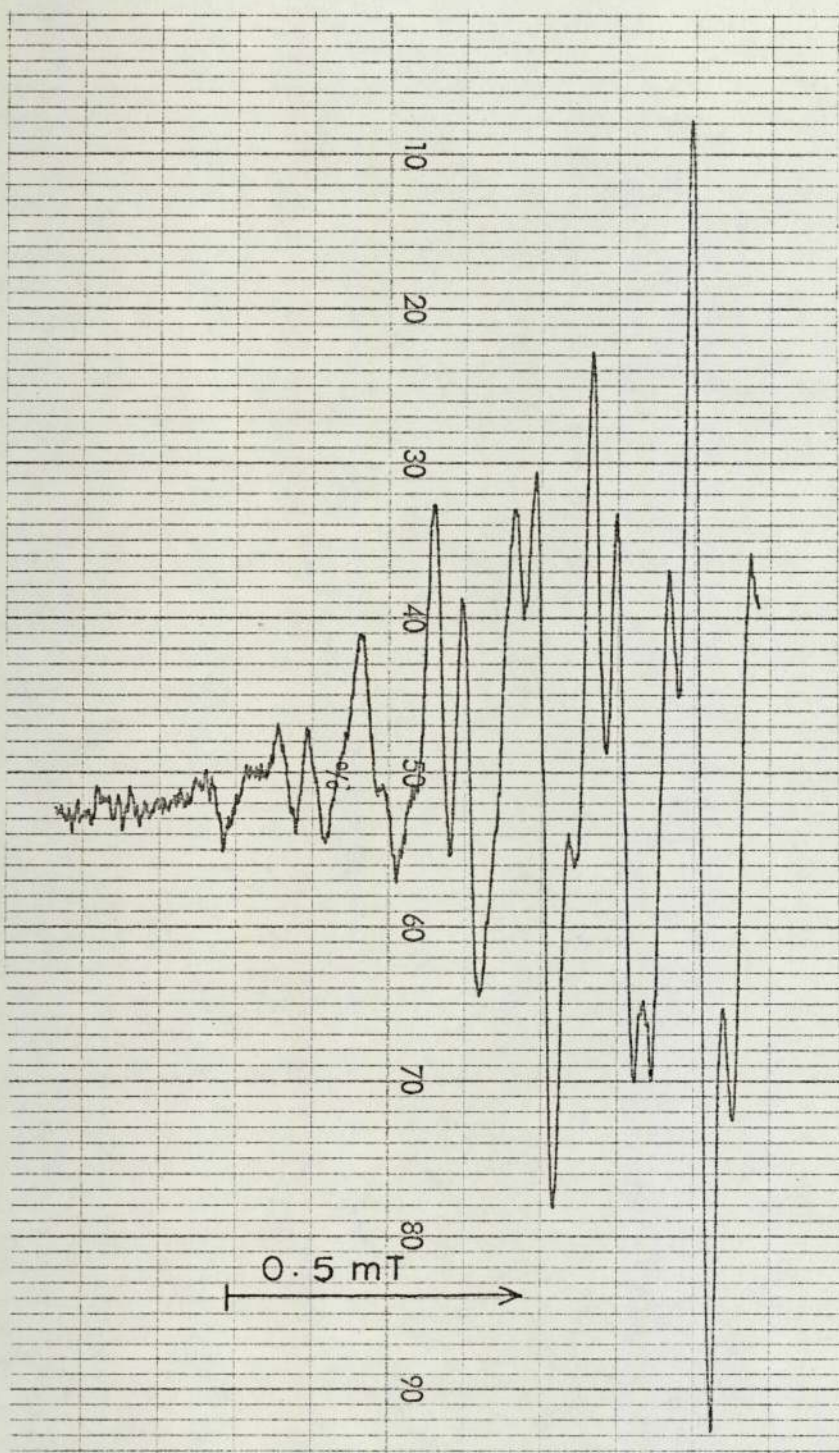


Figure 3.31

### 3.5. g-FACTORS

Table 3.2 summarises the *g*-factors of the 4,4'-biphenosemiquinone cations produced by dissolution of the quinone in sulphuric acid.

TABLE 3.2

4,4'-Biphenosemiquinone Cations	<i>g</i> -Factor
Unsubstituted	2.0030
Alkyl derivatives	2.0030
3,3',5,5'-Tetramethoxy-	2.0032
3,3',5,5'-Tetrachloro-	2.0036
3,3',5,5'-Tetrabromo-	2.0061

The variation in the *g*-factors of the methoxy-, chloro- and bromo- substituted radicals is in accordance with the increased spin-orbit coupling of the unpaired electron caused by such substituents (60).



3.6. ELECTRONIC ABSORPTION SPECTRA OF  
4,4'-BI(HEMOSEMIOQUINONE CATIONS)

3.6.1. Previous Studies on Semiquinone Cations

Only a few studies have been reported on electronic absorption spectra for the cations of 1,4 -benzosemiquinones and the related 1,4 -dialkoxybenzenes. Land and Porter (13) showed that the absorption band in the region of 410-445 m $\mu$  in the electronic absorption spectra of flash photolysed mixtures of sulphuric acid-alcohol-water containing duroquinone could be attributed to the durosemiquinone cation (2,3,5,6-tetramethyl-1,4 -benzosemiquinone cation). The spectrum of a solution of 1,4 -dimethoxybenzene in concentrated sulphuric acid shows intense bands at 280 m $\mu$  which were ascribed by Forbes and Sullivan (50) to 1,4-dimethoxybenzene and its three-sulphonic acid derivative. Less intense bands at 434 and 463 m $\mu$  were ascribed to free radical and (or) protonated species.

More recently Yamada et al. (61,62) have shown that the solutions produced by dissolving 1,4-dihydroxybenzene, 4-methoxyphenol, 4-ethoxyphenol, 1,4-dimethoxybenzene, 1,4-diethoxybenzene and 2,3,5-trimethyl-1,4-dihydroxybenzene in concentrated sulphuric acid all exhibit electronic absorption bands in the region of 400-470 m $\mu$ . They ascribed these bands to the cations of the 1,4-dialkoxybenzenes. Furthermore, when the sulphuric acid solutions were frozen at 77 K, new absorption bands appeared in the region of 500-650 m $\mu$ . They found that

this phenomenon was reversible, the bands disappearing on warming the solutions, and explained the new bands as due to dimer formation by the cation radicals.

### 3.6.2. Present Studies

The UV absorption spectra of both biphenyl-4,4'-diol and its 3,3'-disulphonic acid in 98% sulphuric acid ( $10^{-5}M$ ) show intense bands at 210 and 263  $m\mu$  and a weak band at around 430  $m\mu$  (figure 3.32). If the diol is dissolved in acid containing a trace of hydrogen peroxide the intensity of the weak band is greatly enhanced having absorption maxima at 414 and 435  $m\mu$ . A new band in the region of 630  $m\mu$  also appears if a higher concentration of the diol is used. However, if hydrogen peroxide is added to a solution of the diol, or its disulphonic acid, in the acid then the intensity of the weak band is again enhanced but has a different shape (absorption maximum at 426  $m\mu$ ) and a new band appears at around 670  $m\mu$  (figure 3.33).

The paramagnetic solution of 4,4'-biphenylquinone in 98% sulphuric acid ( $10^{-5}M$ ) exhibits a similar UV absorption spectrum (figure 3.34). On standing the weak bands in the region of 200-280  $m\mu$  are intensified, absorption maxima appearing at 210 and 263  $m\mu$ , at the same time the stronger bands at 414 and 435  $m\mu$  decrease in intensity. When a small amount of water is added to the solution it changes colour from yellow to blue (section 3.2.2) and a new absorption peak occurs in the visible region around 600  $m\mu$ .

UV Spectra

1. Biphenyl-4,4'-diol or 4,4'-dihydroxybiphenyl-3,3'-disulphonic acid in 98% sulphuric acid ( $10^{-5}M$ )
2. Biphenyl-4,4'-diol in 98% sulphuric acid ( $10^{-5}M$ ) containing a trace of hydrogen peroxide
3. As 2 but using a higher concentration of the diol

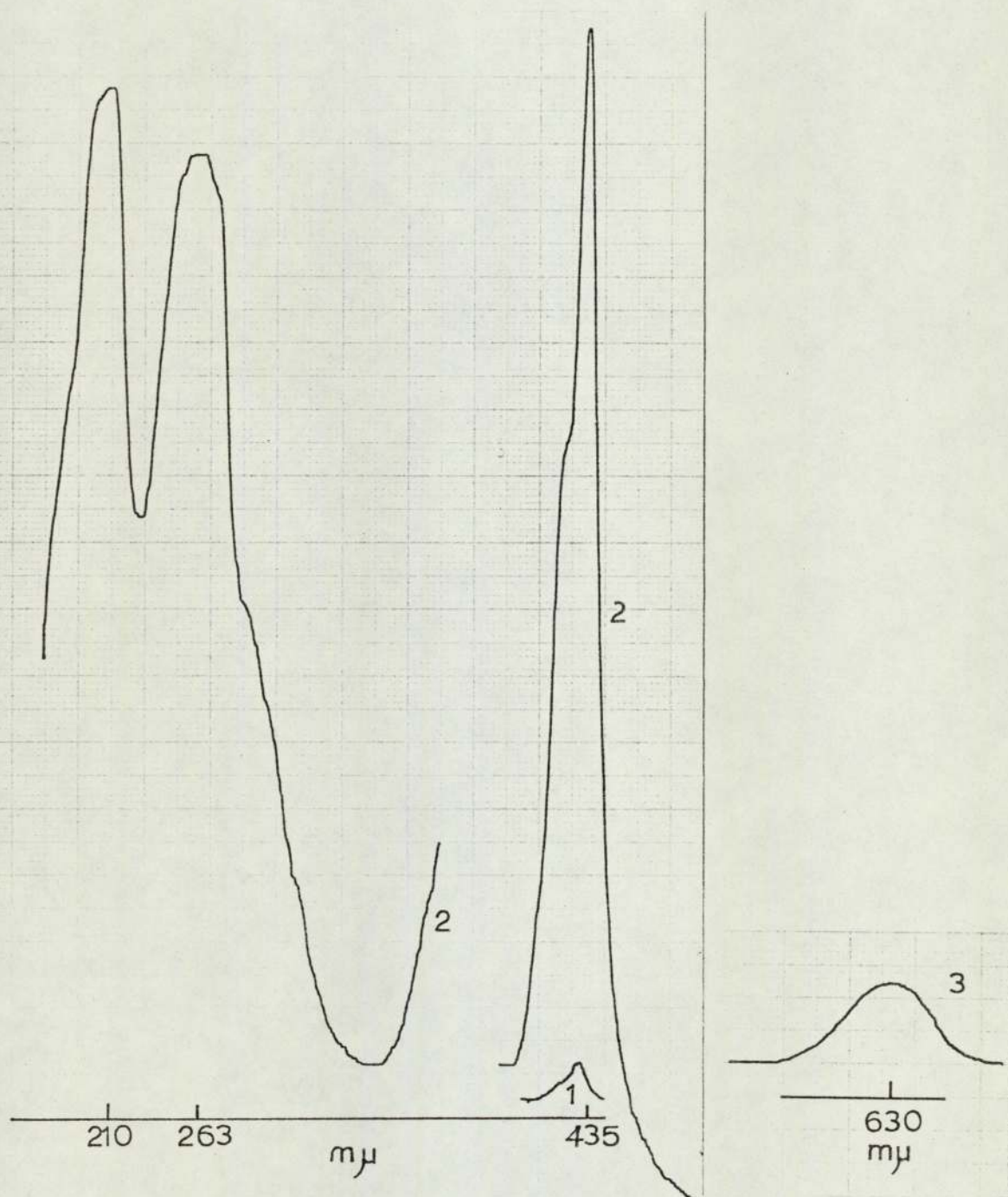
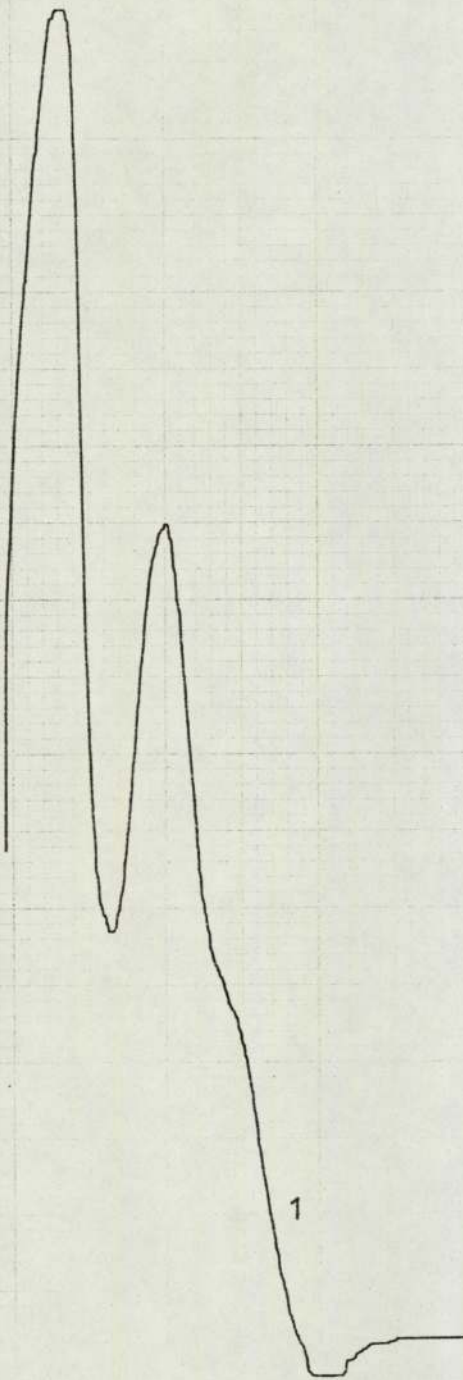


Figure 3.32

UV Spectra

1. Biphenyl-4,4'-diol dissolved in 98% sulphuric acid
2. Biphenyl-4,4'-diol dissolved in 98% sulphuric acid followed by the addition of hydrogen peroxide

210 263  $m\mu$



426 670  $m\mu$

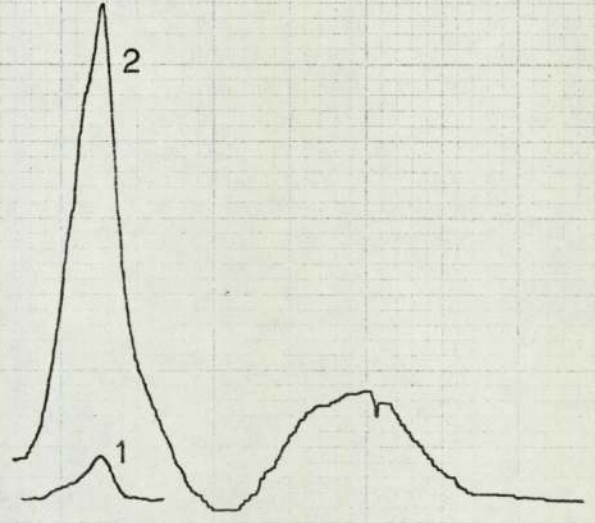


Figure 3.33

UV spectra of 4,4'-biphenoquinone in sulphuric acid

1. Initial spectrum (yellow solution)
2. After 30 minutes (yellow solution)
3. After the addition of water (blue solution)

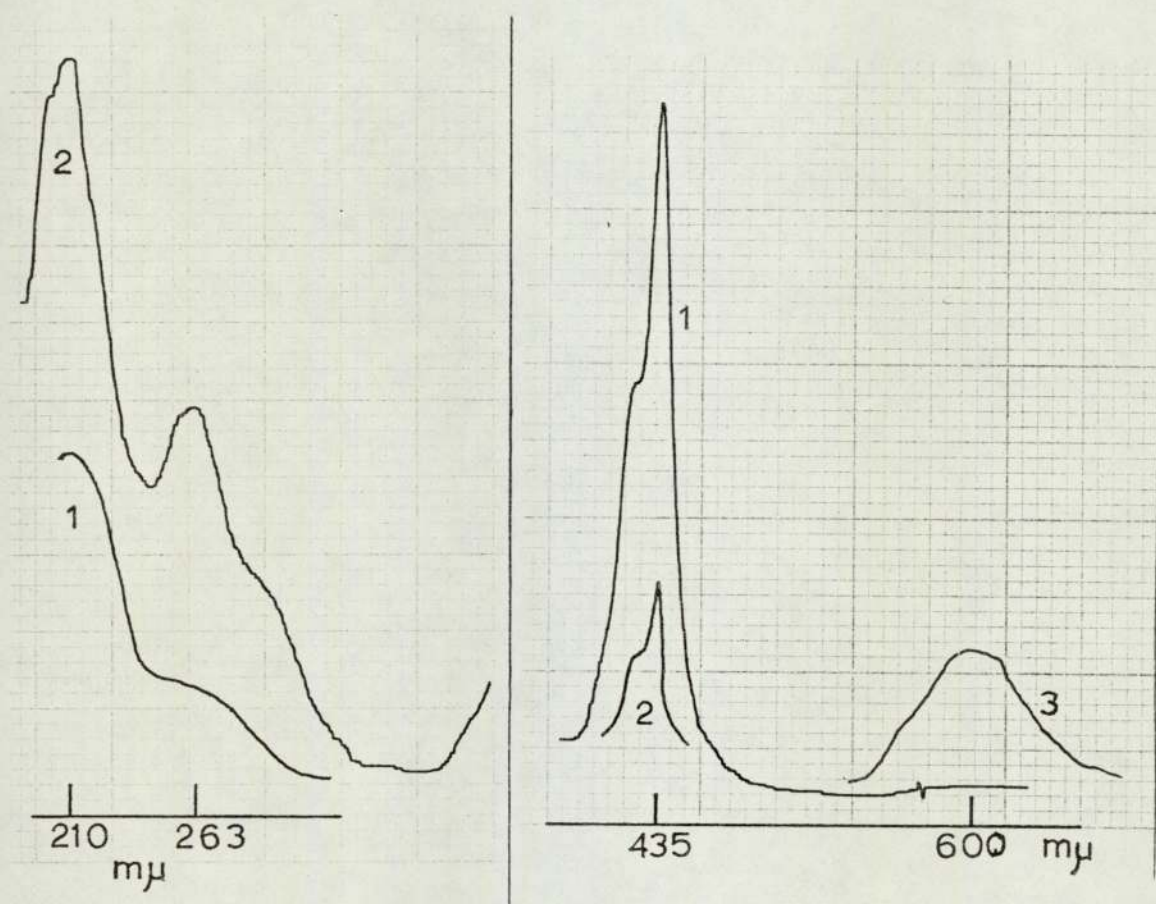
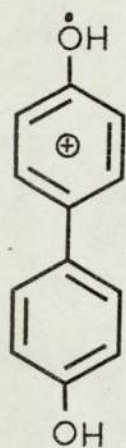
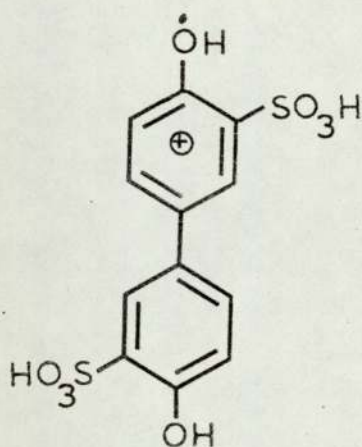


Figure 3.34

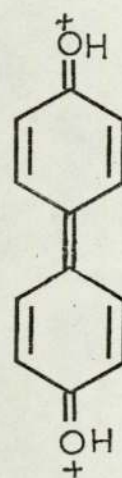
The intense bands at 210 and 263  $\mu$  are ascribed to biphenyl-4,4'-diol and its disulphonic acid derivative. By comparison with the ESR studies outlined in sections 3.2.1 and 3.2.2 and the UV data presented in section 3.6.1 it seems reasonable to ascribe the bands at 414 and 435  $\mu$  to the cation (XI) and the band at 426  $\mu$  to its disulphonic acid derivative (XXII).



(XI)



(XXII)



(XXIII)

However, the intensity ratio of the absorption band at 435  $\mu$  to the one at 414  $\mu$  is much greater (about 3) when 4,4'-biphenol is freshly dissolved in the acid, the 435  $\mu$  band decaying rapidly to give the more usual ratio of about 1.7. Further, a study of the absorption spectrum of the quinone in dideuterosulphuric acid at temperatures of 30°, 40° and 50°C indicate that the intensity changes of this band do not coincide with the ESR results (section 3.2.2). The position of the absorption maxima are somewhat altered by using dideutero-

sulphuric acid as shown in figure 3.3.5. Buck and his co-workers (51) appear to assign the absorption in the region 414-435  $\mu$  to the dication (XXIII). Thus we are led to the conclusion that this complex band should be assigned to the radical cation (XI) and (or) the dication (XXIII).

The bands which appear in the region of 600-700  $\mu$  are possibly due to charge-transfer transitions.

UV spectrum of 4,4'-biphenolquinone  
in dideuterosulphuric acid at 40°C

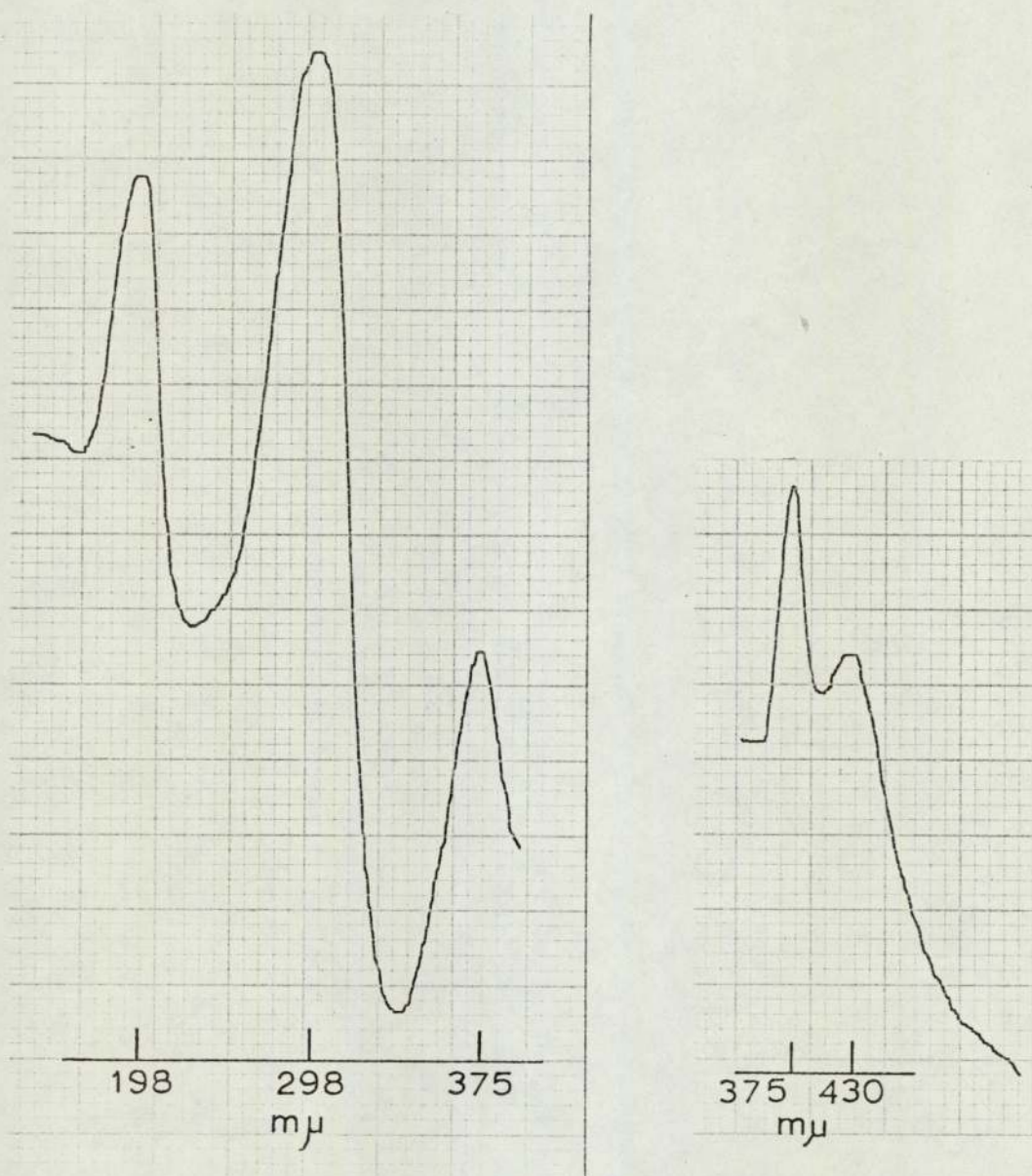


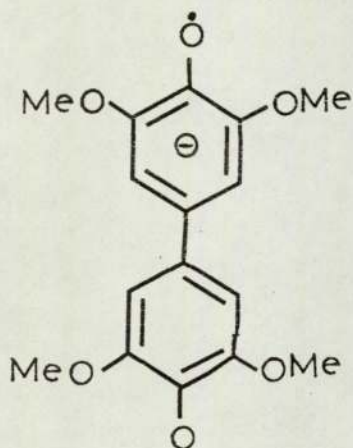
Figure 3.35



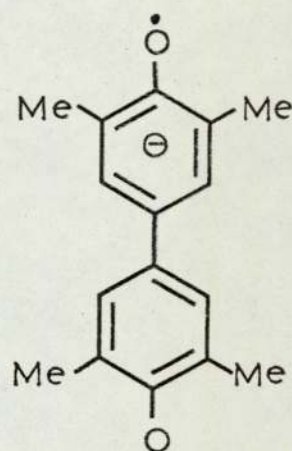
#### 4. 4,4'-BIPHENOSEMIQUINONE ANIONS

##### 4.1. PREVIOUS STUDIES

In his ESR studies on alkoxy derivatives of semiquinone anions, Matsunaga (15) prepared the 3,3',5,5'-tetramethoxy- and 3,3',5,5'-tetramethyl-4,4'-biphenosemiquinone anions (I, II) by the air oxidation of the respective biphenyldiols in a mixture of 2M potassium



(I)



(II)

hydroxide and pyridine (1:1 by volume). The observed thirteen-line spectrum of the methoxy derivative was explained by assigning a hyperfine coupling constant of 0.049 mT to both the ring and the methoxy protons. The two lines at each end of the spectrum were expected

to be too low in intensity to be detectable.

The spectrum from the tetramethyl derivative consisted of twenty-one lines with equidistant spacings. This was explained by assigning values of 0.234 mT and 0.078 mT to the hyperfine coupling constants for the ring and methyl protons respectively with the two lines at each end of the spectrum again too weak to be detected.

However, later work (16) indicated that in 4,4'-biphenosemiquinone salts the unpaired electron density given by the simple LCAO-MO method for carbon atom 3 is at least 1.5 times larger than that on carbon atom 2. Thus an alternative assignment was suggested of 0.078 mT for the ring protons and 0.156 mT for the methyl protons.

More recently, Petranek, Pilar and Ryba (63) in their studies on the oxidation-reduction properties of alkyl substituted polynuclear phenols used ESR spectroscopy to identify the radical anions produced by the electrochemical reduction of 4,4'-biphenolquinone and several of its alkyl derivatives. Acetonitrile was used as the solvent and it was found necessary to use flow techniques to detect the semiquinone anions from the parent quinone and its disubstituted derivatives. Their results are summarised in Table 4.1.

Table 4.1

HYPERFINE COUPLING CONSTANTS OF SOME  
BIPHENO-4,4'-SEMIQUINONE ANIONS

	Hyperfine Coupling Constants (mTesla)					
	$A_2^H$ ring H	$A_6^H$ ring H	$A_3^H$ ring H	$A_5^H$ ring H	$A_3^H$ (d) alkyl H	$A_5^H$ (d) alkyl H
4,4'-biphenosemiquinone						
Unsubstituted (a)	0.056	0.056	0.236	0.236	-	-
3,3'-dimethyl-	0.048	0.078	-	0.236	0.196(b)	-
3,3'-di-t-butyl-	0.040	0.062	-	0.230	-	-
3,3',5,5'-tetramethyl-	0.054	0.054	-	-	0.188(b)	0.188(b)
3,3',5,5'-tetraisopropyl-	0.056	0.056	-	-	0.111(c)	0.111(c)
3,3',5,5'-tetra-t-butyl-	0.046	0.046	-	-	-	-
3,3'-dimethyl-5,5'-di-t-butyl-	0.056	0.042	-	-	0.200(b)	-
3,3'-diisopropyl-5,5'-di-t-butyl-	0.056	0.056	-	-	0.100(c)	-

(a) Gerson quotes similar values,  $a_2^H = 0.053$  mT and  $a_3^H = 0.229$  mT (64)

(b) Hyperfine coupling constants of the methyl group protons.

(c) Hyperfine coupling constants of the methin proton of the isopropyl group.

(d) The subscript in the notations for the hyperfine coupling constants refers to the atom to which the alkyl group is attached.

## 4.2. RESULTS OF PRESENT WORK

The large differences in the hyperfine coupling constants obtained for the 3,3',5,5'-tetramethyl-4,4'-biphenosemiquinone anion (hereafter referred to as the TMBESQ anion) by the chemical oxidation of 3,3',5,5'-tetramethyl-4,4'-biphenyldiol (TMBPD) and the electrochemical reduction of the corresponding quinone (TMBPQ) led us to re-investigate the work done by Matsunaga (15, 16) with a view to extending it to other alkyl derivatives. The results obtained are given under the name of the semiquinone anion.

The experimental details for the preparation of the anion radicals and the subsequent recording of their ESR spectra are outlined in sections 2.2.3.2. and 2.2.1. respectively.

### 4.2.1. 3,3',5,5'-Tetramethyl-4,4'-biphenosemiquinone Anion (TMBESQ Anion)

When TMBPD is oxidised by air in a solvent mixture of pyridine and 2M aqueous potassium hydroxide solution a yellow paramagnetic solution is obtained. The ESR spectrum of this solution depended upon the ratio of the pyridine to potassium hydroxide solution used. The spectra recorded using 57% and 90% of pyridine are shown in figures 4.1 and 4.2 respectively.

The spectra can be explained on the basis that the TMBESQ anion is formed and its hyperfine coupling

3,3',5,5'-Tetramethylbiphenyl-4,4'-diol in pyridine-aqueous  
potassium hydroxide (57%-43% by volume)

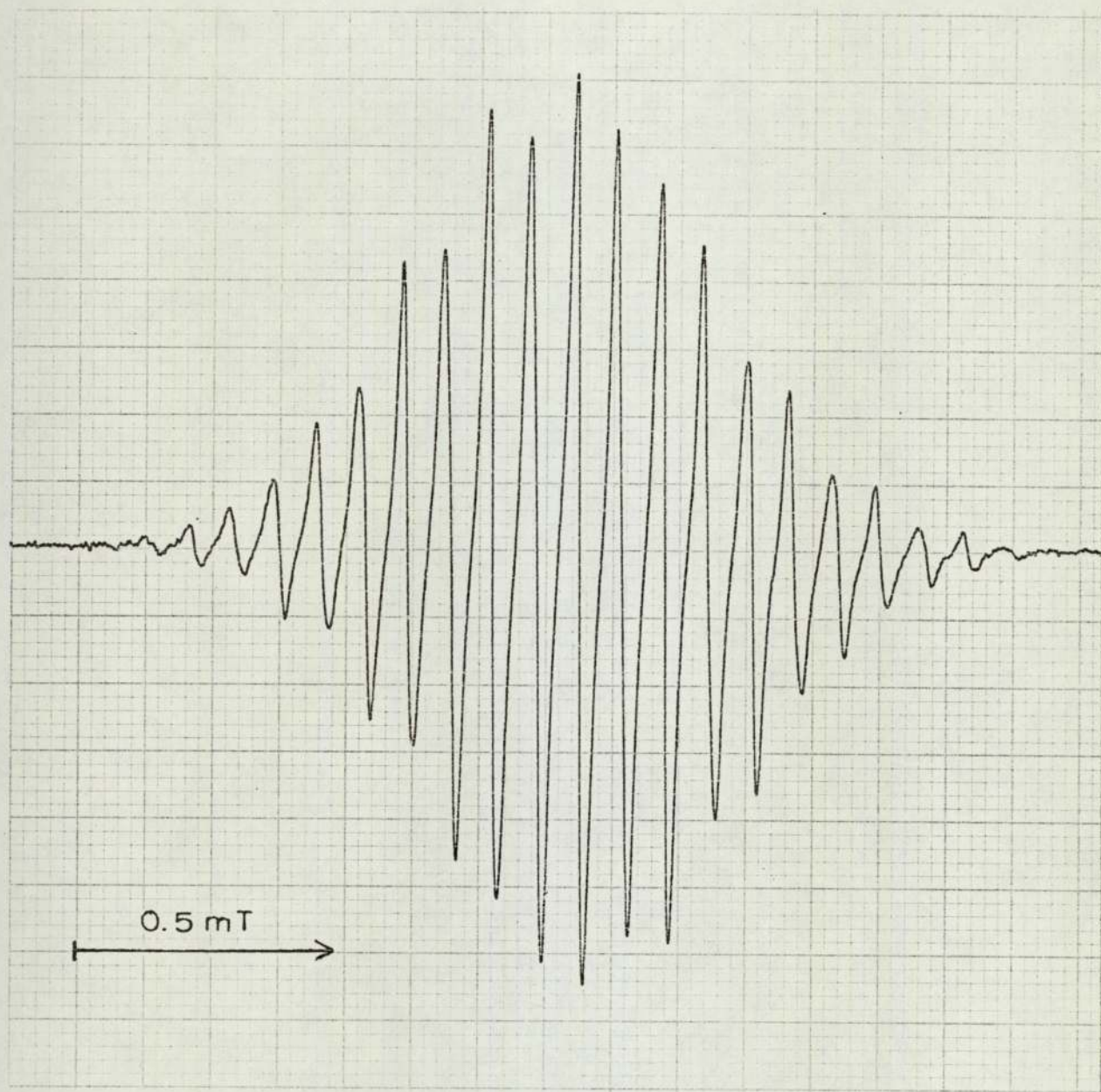


Figure 4.1

3,3',5,5'-Tetramethylbiphenyl-4,4'-diol in pyridine-aqueous  
potassium hydroxide (90%-10% by volume)

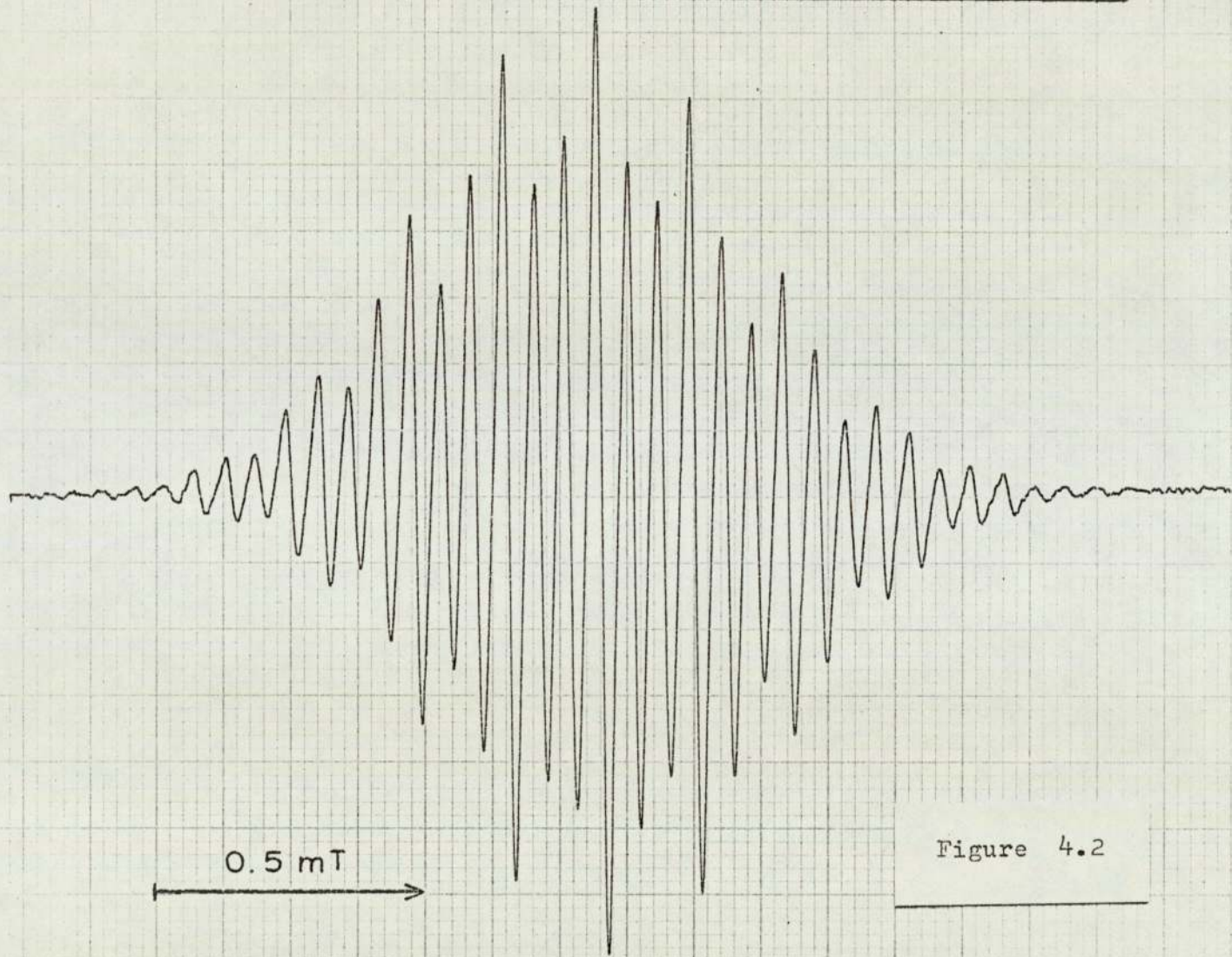


Figure 4.2

constants are sensitive to the solvent mixture. In 57% pyridine  $a_2^H(\text{ring H}) = 0.074 \text{ mT}$  and  $a_3^H(\text{Methyl H}) = 0.166 \text{ mT}$ , whereas in 90% pyridine the corresponding values are 0.062 mT and 0.178 mT. Spectra simulated using these values and a linewidth of 0.0175 mT are shown in figures 4.3 and 4.4.

In an attempt to rationalise these results a more detailed investigation was undertaken varying the solvent mixture. As the concentration of the potassium hydroxide did not affect the ESR results, a more dilute solution, 0.5M was used throughout the experiments. The results are summarised below in tabular form.

Computer Simulated Spectrum

12 Equivalent protons  $a^H = 0.166\text{mT}$

4 Equivalent protons  $a^H = 0.074\text{mT}$

Linewidth  $0.0175\text{mT}$

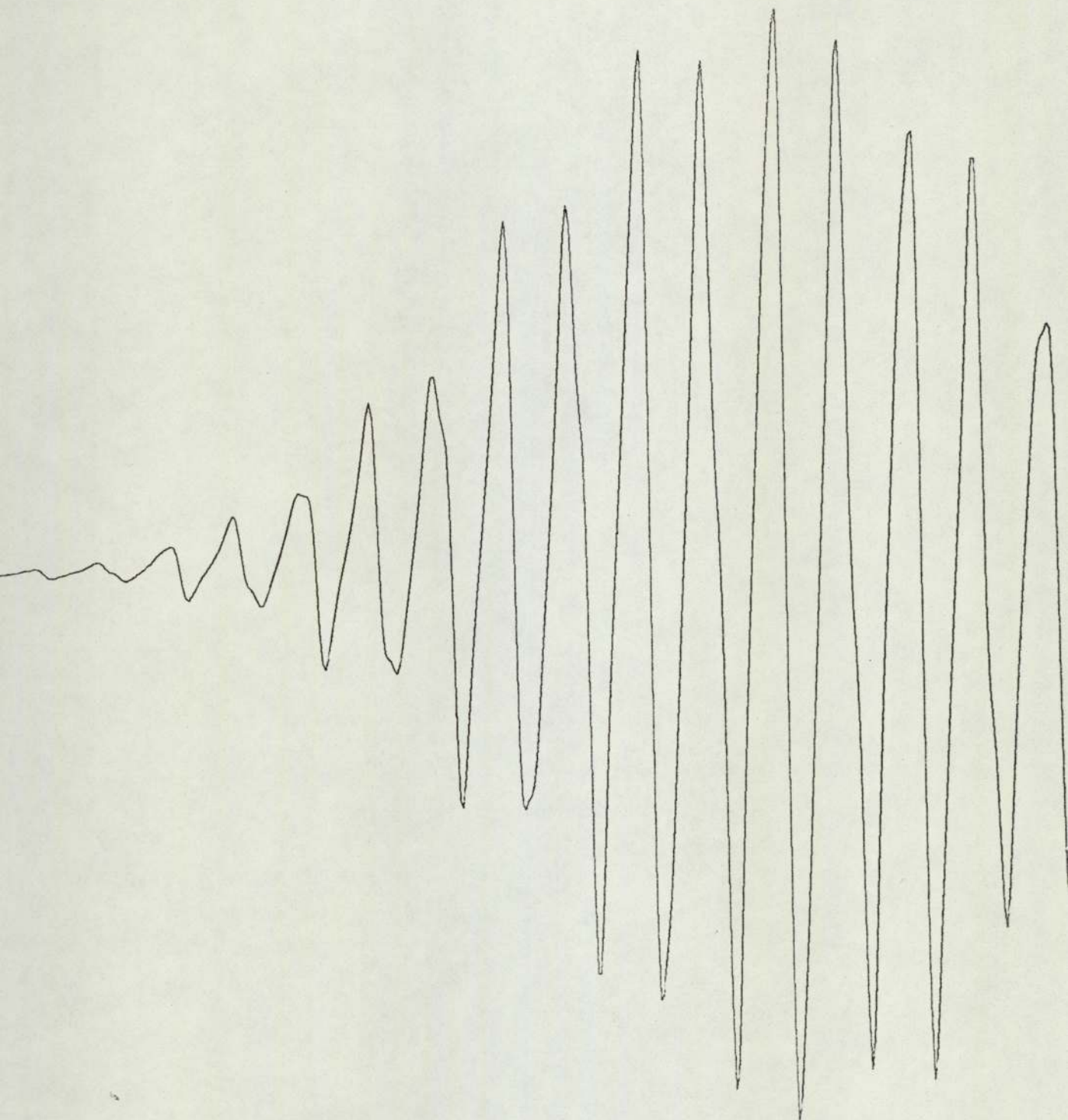
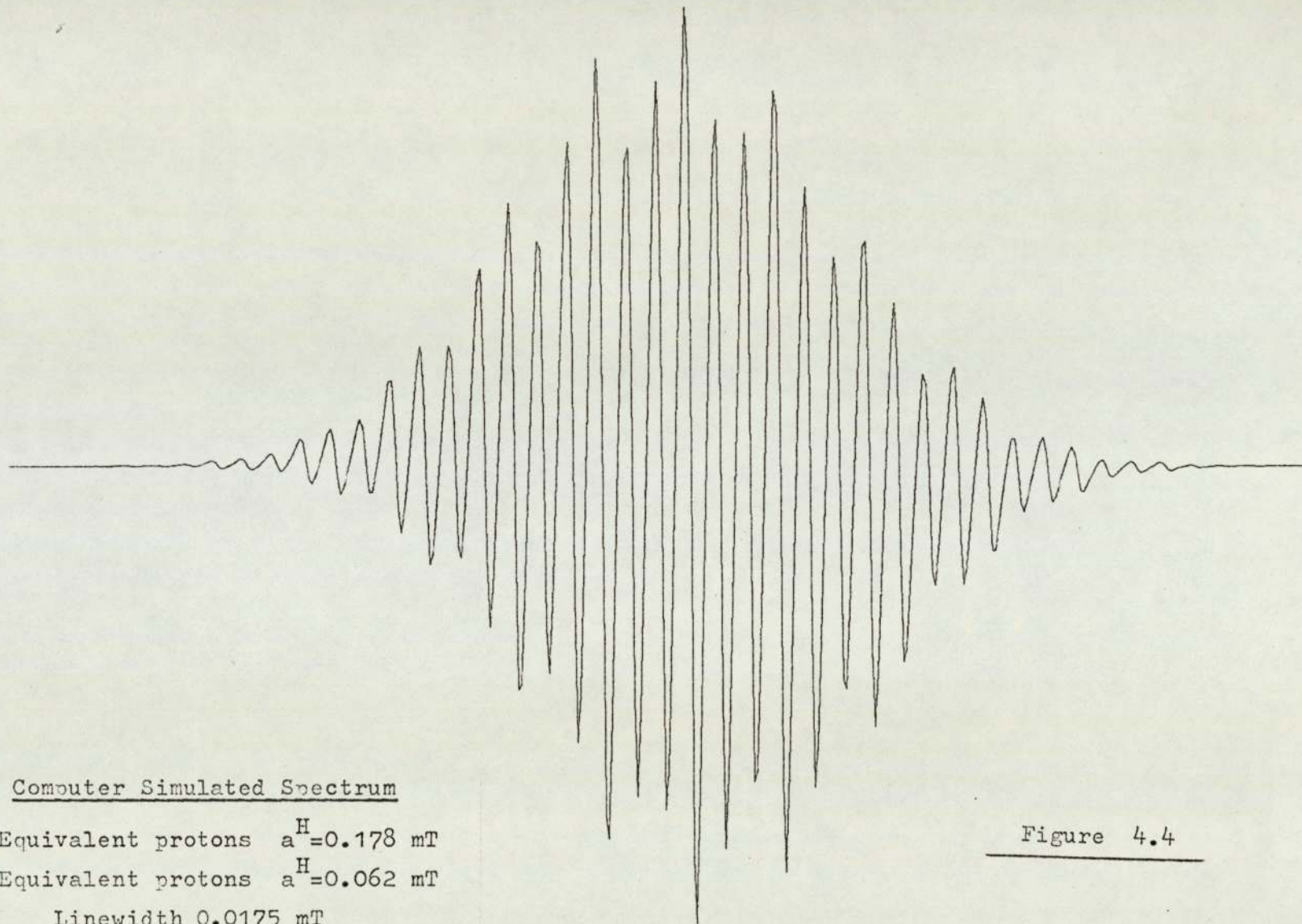


Figure 4.3





Computer Simulated Spectrum

12 Equivalent protons  $a^H = 0.178$  mT

4 Equivalent protons  $a^H = 0.062$  mT

Linewidth 0.0175 mT

Figure 4.4

TABLE 4.2

HYPERFINE COUPLING CONSTANTS FOR 3,3',5,5'-TETRAMETHYL-  
4,4'-BIPHENOSEMIQUINONE ANION IN VARIOUS PYRIDINE-AQUEOUS  
POTASSIUM HYDROXIDE MIXTURES

Mole Fraction		Hyperfine Coupling Constants		$\frac{a_3^H}{a_2^H}$
Water	Pyridine	$a_2^H$ (ring H) mT	$a_3^H$ (methyl) mT	
0.93	0.07(a)	0.078	0.162	2.08
0.87	0.13	0.076	0.164	2.16
0.82	0.18	0.075	0.165	2.20
0.77	0.23	0.074	0.166	2.25
0.75	0.25	0.0735	0.1665	2.27
0.725	0.275	0.0725	0.1675	2.31
0.68	0.32	0.0715	0.1685	2.36
0.64	0.36	0.070	0.170	2.43
0.61	0.39	0.0695	0.1705	2.45
0.60	0.40	0.069	0.171	2.48
0.58	0.42	0.0685	0.1715	2.51
0.545	0.455	0.0675	0.1725	2.56
0.50	0.50	0.0665	0.1735	2.61
0.44	0.56	0.065	0.175	2.69
0.33	0.67(b)	0.062	0.178	2.87

(a) No radicals are detected with a lower pyridine concentration.

(b) Weak ESR signal when the pyridine concentration is increased.

TABLE 4.3

HYPERFINE COUPLING CONSTANTS FOR 3,3',5,5'-TETRAMETHYL-4,4'-BIPHENOSEMIQUINONE ANION IN VARIOUS PYRIDINE-ETHANOLIC POTASSIUM HYDROXIDE MIXTURES.

Mole Fraction		Hyperfine Coupling Constants		$\frac{a_3^H}{a_2^H}$
Ethanol	Pyridine	$a_2^H$ (ring H) mT	$a_3^H$ (methyl H) mT	
0.805	0.195	0.075	0.165	2.20
0.65	0.35	0.071	0.169	2.38
0.58	0.42	0.069	0.171	2.48
0.47	0.53	0.066	0.174	2.64
0.32	0.68	0.062	0.178	2.87
0.24	0.76	0.060	0.180	3.00
0.14	0.86	0.058	0.182	3.14
0.065	0.935	0.056	0.184	3.28
0.03	0.97	0.055	0.185	3.36

TABLE 4.4.

HYPERFINE COUPLING CONSTANTS FOR 3,3',5,5'-TETRAETHYL-4,4'-BIPHENOSEMIQUINONE ANION IN VARIOUS SOLVENT-AQUEOUS POTASSIUM HYDROXIDE MIXTURES.

Solvent	Mole Fraction		Hyperfine Coupling Constants		$\frac{a_3^H}{a_2^H}$
	Water	Solvent	$a_2^H$ (ring H) mT	$a_3^H$ (methyl H) mT	
Acetonitrile	0.92	0.08	0.080	0.160	2.00
	0.31	0.69	0.76	0.164	2.16
	0.225	0.775	0.074	0.166	2.25
Diethylamine	0.855	0.145	0.074	0.166	2.25
	0.805	0.195	0.072	0.168	2.33
	0.765	0.235	0.070	0.170	2.42
	0.74	0.26	0.069	0.171	2.48
	0.715	0.285	0.068	0.172	2.53
	0.645	0.355	0.0665	0.1735	2.61
	0.59	0.41	0.065	0.175	2.69
	0.39	0.61	0.060	0.180	3.00
N,N-Dimethylformamide	0.975	0.025	0.080	0.160	2.00
	0.88	0.12	0.078	0.162	2.08
	0.70	0.30	0.075	0.165	2.20
	0.62	0.38	0.073	0.167	2.29
	0.53	0.47	0.071	0.169	2.39
	0.50	0.50	0.070	0.170	2.42
	0.40	0.60	0.0675	0.1725	2.60
	0.27	0.73	0.064	0.176	2.75

TABLE 4.4 CONTINUED

Solvent	Mole Fraction		Hyperfine Coupling Constants		$\frac{a_3^H}{a_2^H}$
	Water	Solvent	$a_2^H$ (ring H) mT	$a_3^H$ (methyl H) mT	
1,4-Dioxan	0.96	0.04	0.080	0.160	2.00
	0.75	0.25	0.077	0.163	2.12
	0.60	0.40	0.075	0.165	2.20
	0.545	0.455	0.074	0.166	2.25
2-Picoline	0.65	0.35	0.068	0.172	2.53
	0.61	0.39	0.067	0.173	2.59
	0.545	0.455	0.066	0.174	2.64
	0.49	0.51	0.064	0.176	2.75
	0.375	0.625	0.061	0.179	2.94
Benzene or Tetra-chloro-methane	Saturated with aqueous potassium hydroxide		0.080	0.160	2.0

#### 4.2.1.1. The Analysis of the ESR Spectra

Some of the spectra were impossible to analyse accurately, however, those in which the ratio of the hyperfine coupling constants  $a_3^H : a_2^H$  was in the region 2.25 to 2.75 could be analysed without too much difficulty. A selection of these spectra are shown in figures 4.5 to 4.9.

If a plot of the hyperfine coupling constants for the methyl protons is made against the corresponding values of the ring protons, as in figure 4.10, then a straight line relationship is obtained. This fact was made use of in facilitating the analysis of subsequent spectra. The graph was replotted as  $a_3^H$  (methyl H) against  $a_3^H$  (methyl H) :  $a_2^H$  (ring H) (see figure 4.11).

A series of simulated spectra was prepared for various ratios of the hyperfine coupling constants which could then be compared with the experimental spectra and reasonably accurate assignments made assuming that the relationship still holds in the region where accurate measurements were difficult.

A selection of the computerized spectra are shown in figures 4.12 to 4.17. Figures 4.18 to 4.20 show some of the spectra having their ratios of hyperfine coupling constants outside the range 2.25 to 2.75.

Practical details have been discussed previously in section 2.4.1.

3,3',5,5'-Tetramethyl-4,4'-biphenosemiquinone anion in N,N-dimethylformamide-aqueous potassium hydroxide (75%-25% by volume)

$$a_2^H (\text{ringH}) = 0.073 \text{ mT}$$

$$a_3^H (\text{methylH}) = 0.167 \text{ mT}$$

$$\text{Ratio } a_3^H : a_2^H = 2.29$$

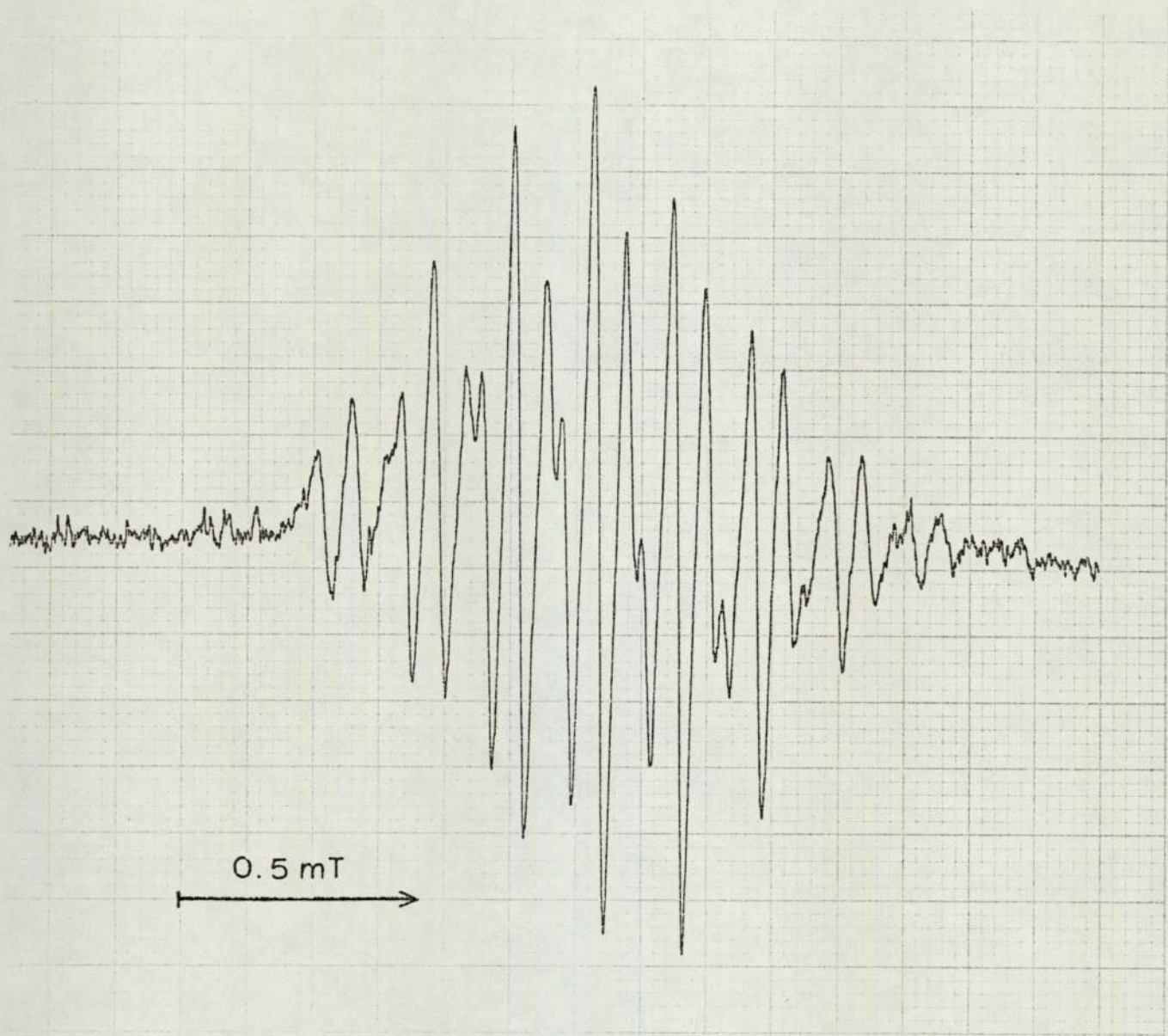


Figure 4.5

3,3',5,5'-Tetramethyl-4,4'-biphenosemiquinone anion in pyridine-  
aqueous potassium hydroxide (78%-22% by volume)

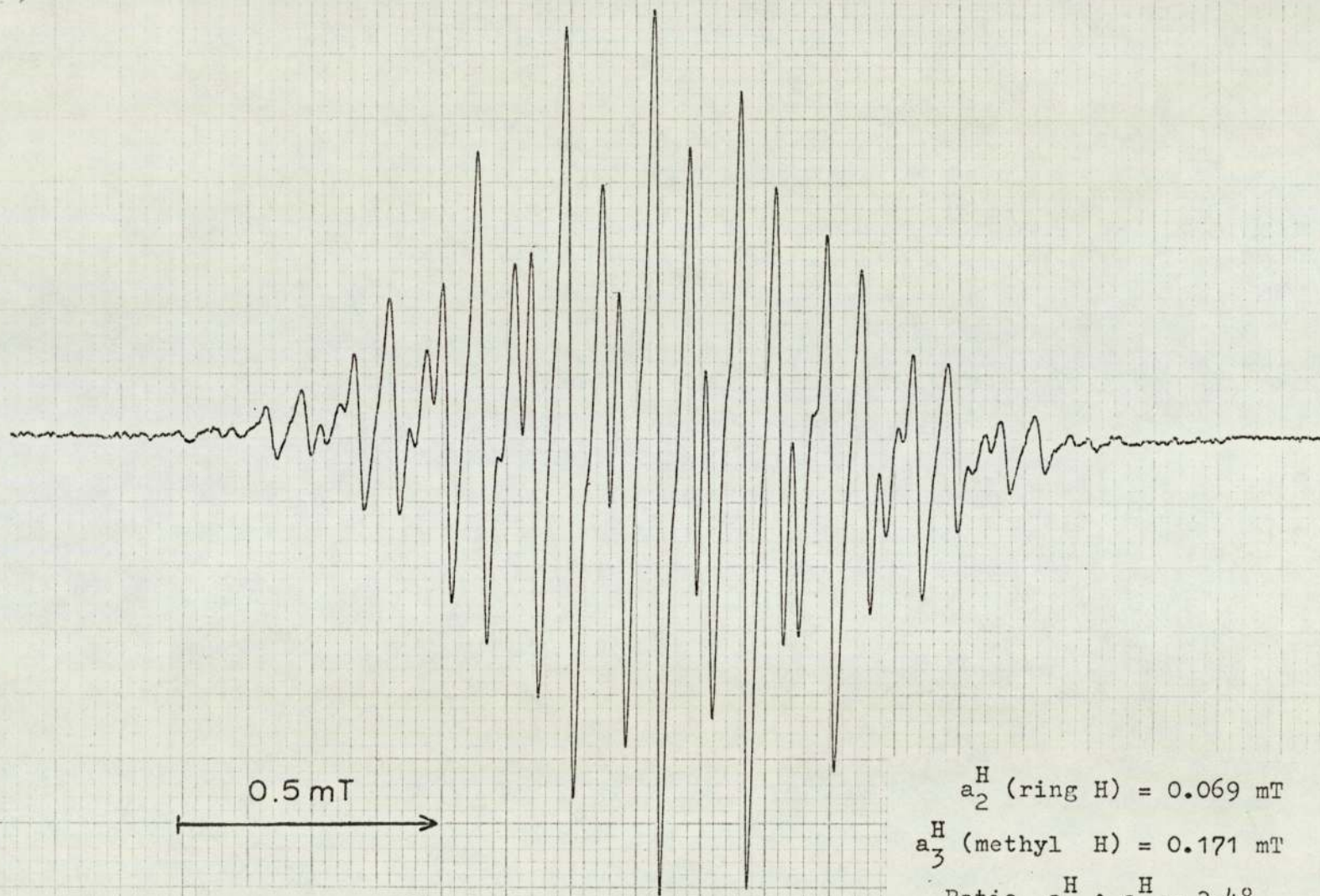


Figure 4.6

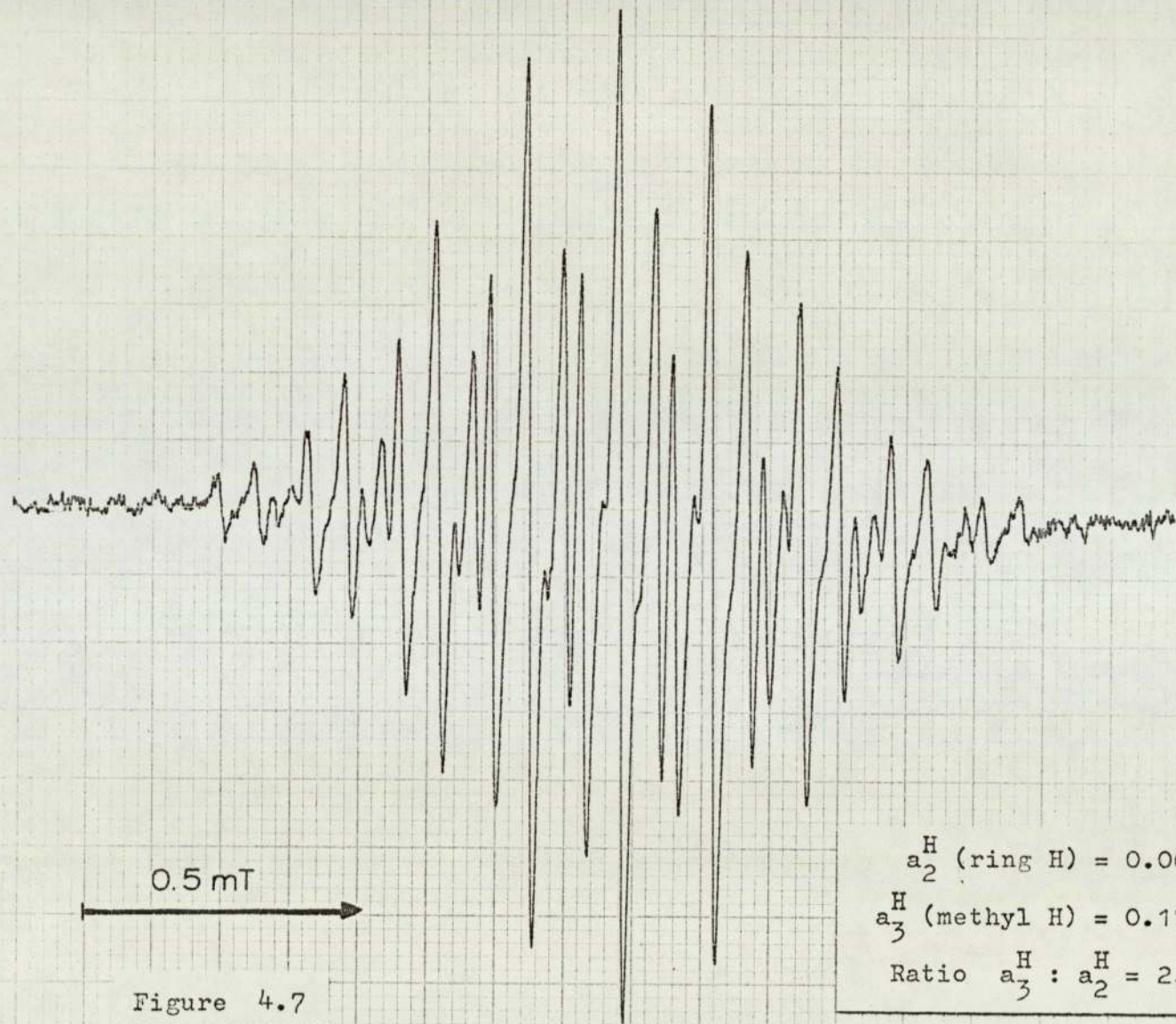
$$a_2^H \text{ (ring H)} = 0.069 \text{ mT}$$

$$a_3^H \text{ (methyl H)} = 0.171 \text{ mT}$$

$$\text{Ratio } a_3^H : a_2^H = 2.48$$



3,3',5,5'-Tetramethyl-4,4'-biphenosemiquinone anion in diethylamine-  
aqueous potassium hydroxide (70%-30% by volume)



3,3',5,5'-Tetramethyl-4,4'-biphenosemiquinone anion in pyridine-ethanolic potassium hydroxide (60%-40% by volume)

$$a_2^H \text{ (ring H)} = 0.066 \text{ mT}$$

$$a_3^H \text{ (methyl H)} = 1.74 \text{ mT}$$

$$\text{Ratio } a_3^H : a_2^H = 2.64$$

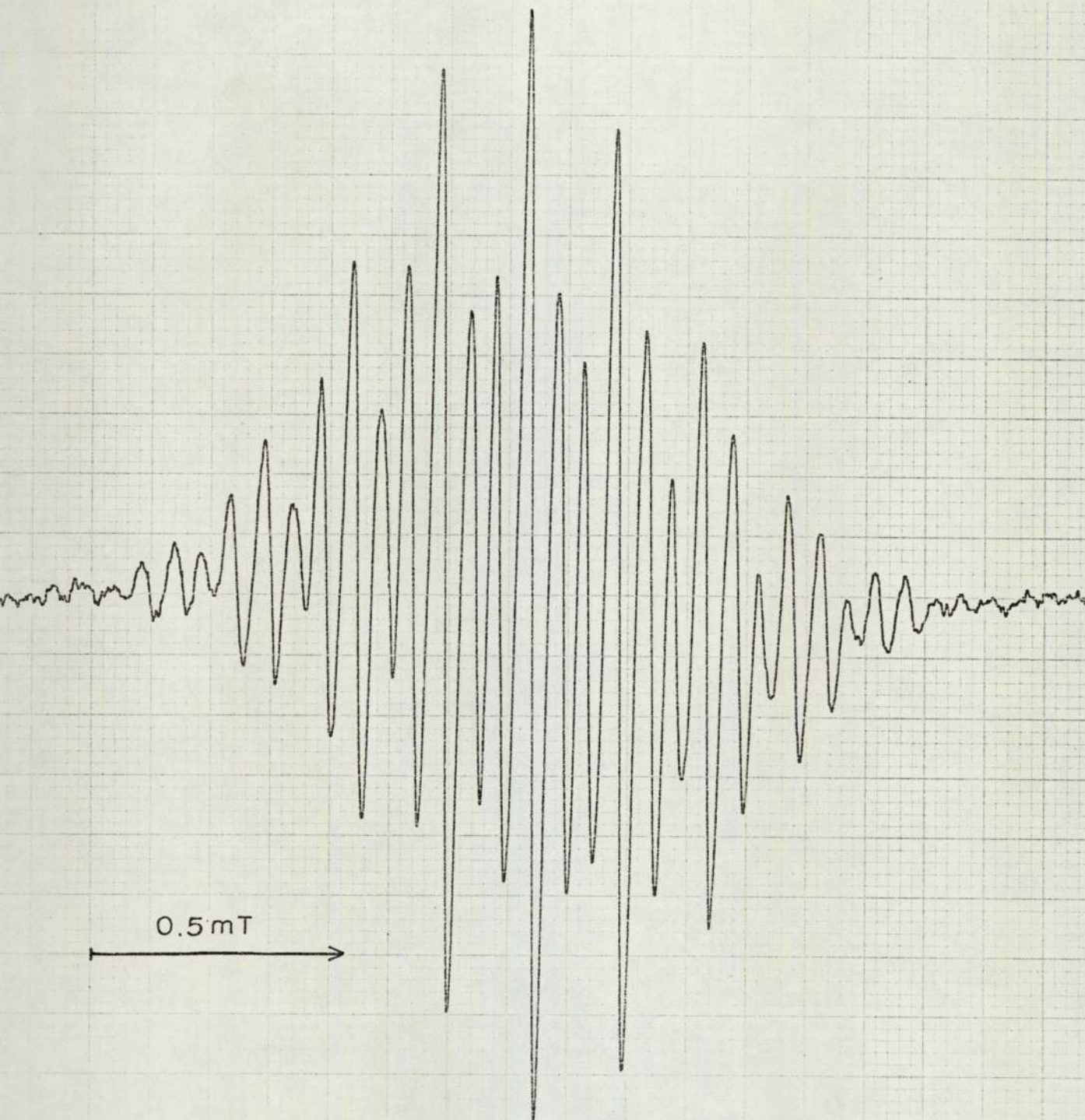
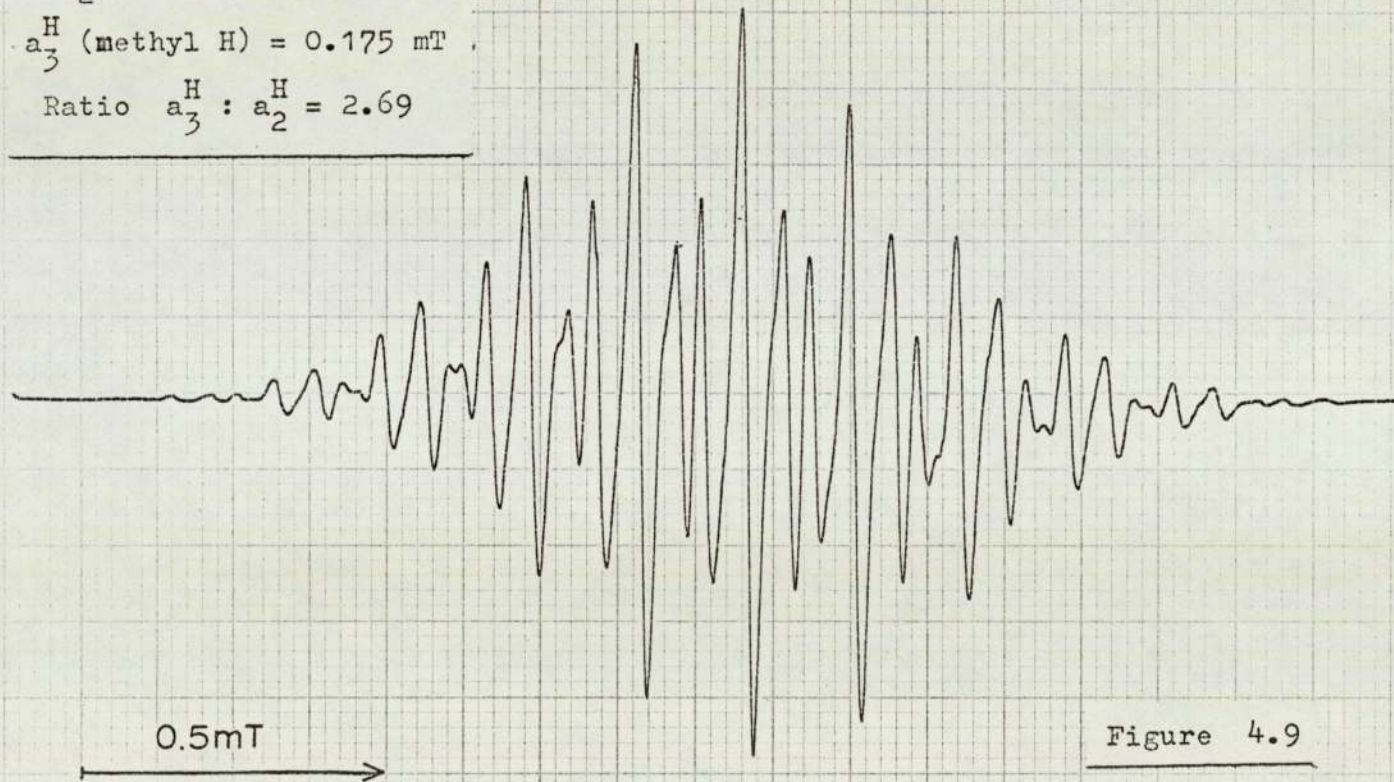


Figure 4.8

3,3',5,5'-Tetramethyl-4,4'-biphenosemiquinone anion in 2-picoline-  
aqueous potassium hydroxide (85%-15% by volume)

$a_2^H$  (ring H) = 0.065 mT  
 $a_3^H$  (methyl H) = 0.175 mT  
Ratio  $a_3^H : a_2^H = 2.69$



Plot of  $a_3^H$  against  $a_2^H$  for the spectra  
shown in figures 4.5 to 4.9

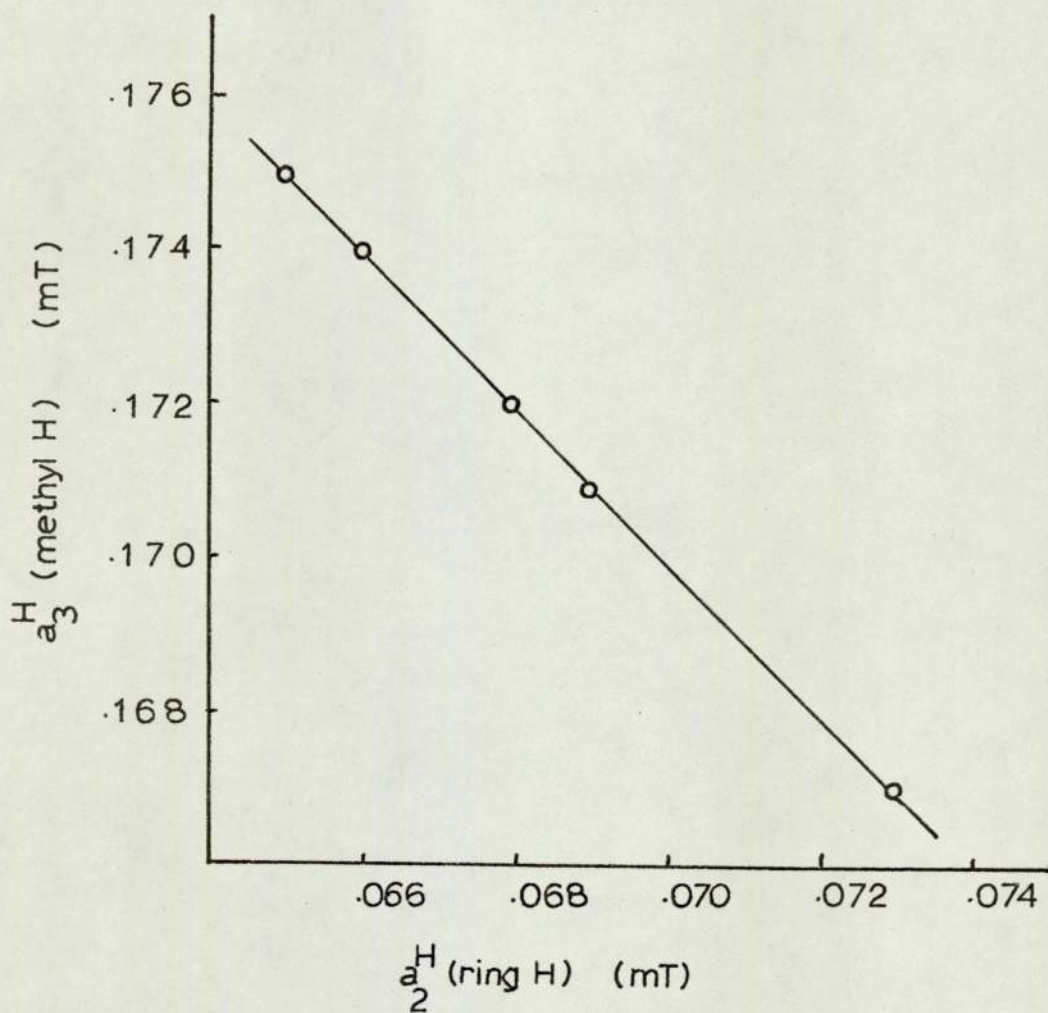


Figure 4.10

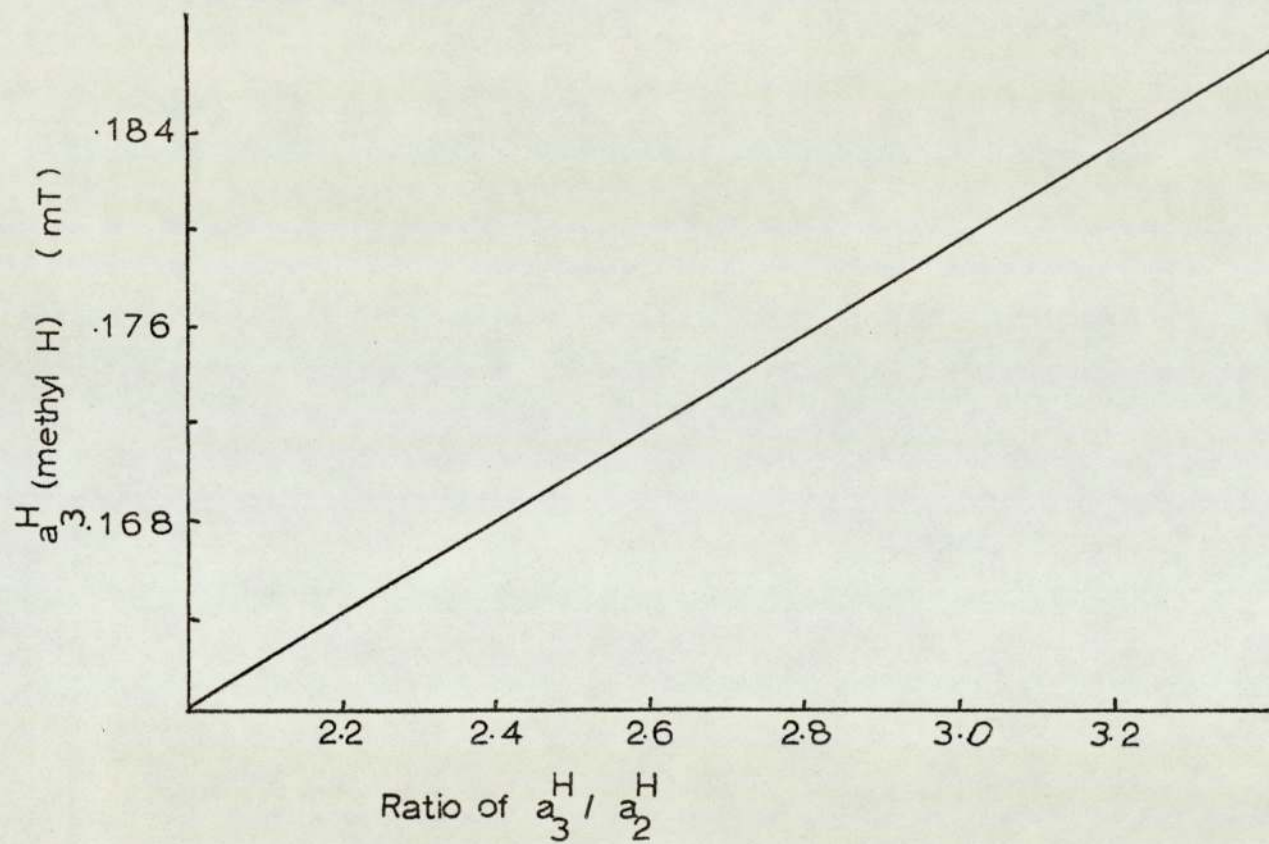


Figure 4.11

Graph for the determination of  $a_3^H$  (methyl H) in conjunction with the computer simulated spectra

Computer Simulated Spectrum

12 equivalent protons  $a_3^H = 0.160$  mT

4 equivalent protons  $a_2^H = 0.080$  mT

Linewidth = 0.0175 mT

Ratio  $a_3^H : a_2^H = 2.00$

---

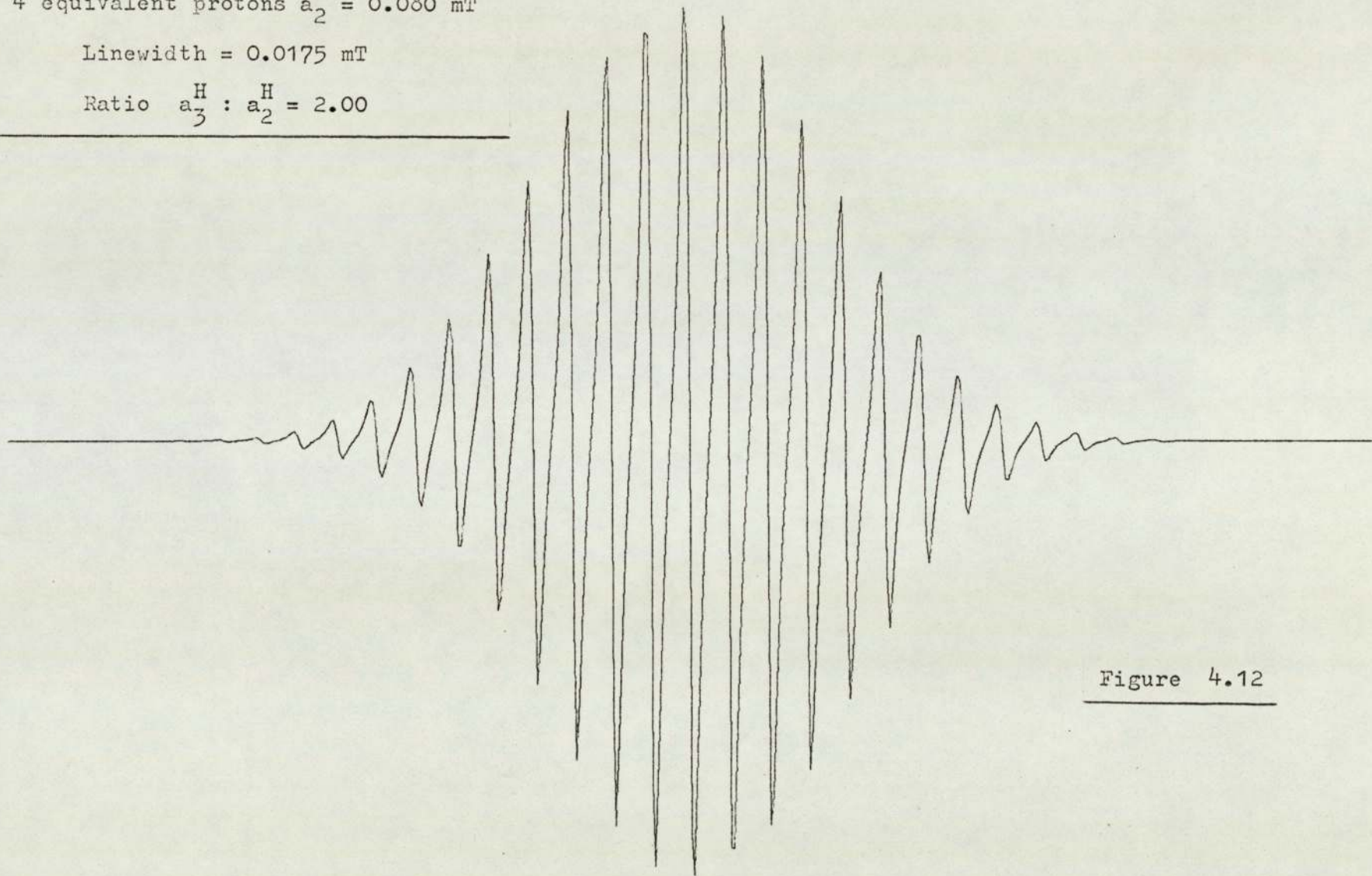


Figure 4.12

Computer Simulated Spectrum

12 equivalent protons  $a_3^H = 0.167$  mT

4 equivalent protons  $a_2^H = 0.073$  mT

Linewidth = 0.0175 mT

Ratio  $a_3^H : a_2^H = 2.29$

---

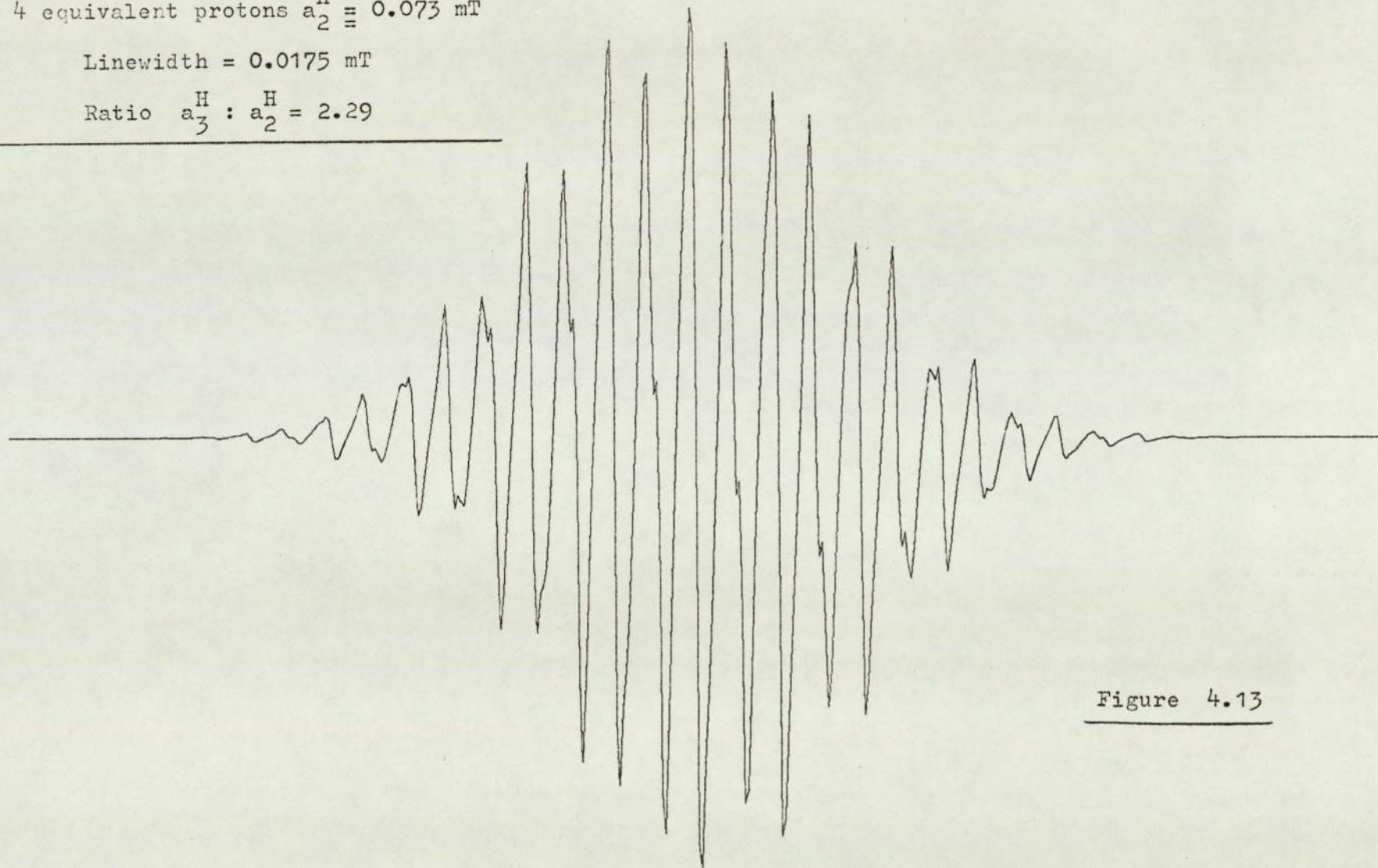


Figure 4.13

Computer Simulated Spectrum

12 equivalent protons  $a_3^H = 0.169$  mT

4 equivalent protons  $a_2^H = 0.071$  mT

Linewidth = 0.0175 mT

Ratio  $a_3^H : a_2^H = 2.38$

---

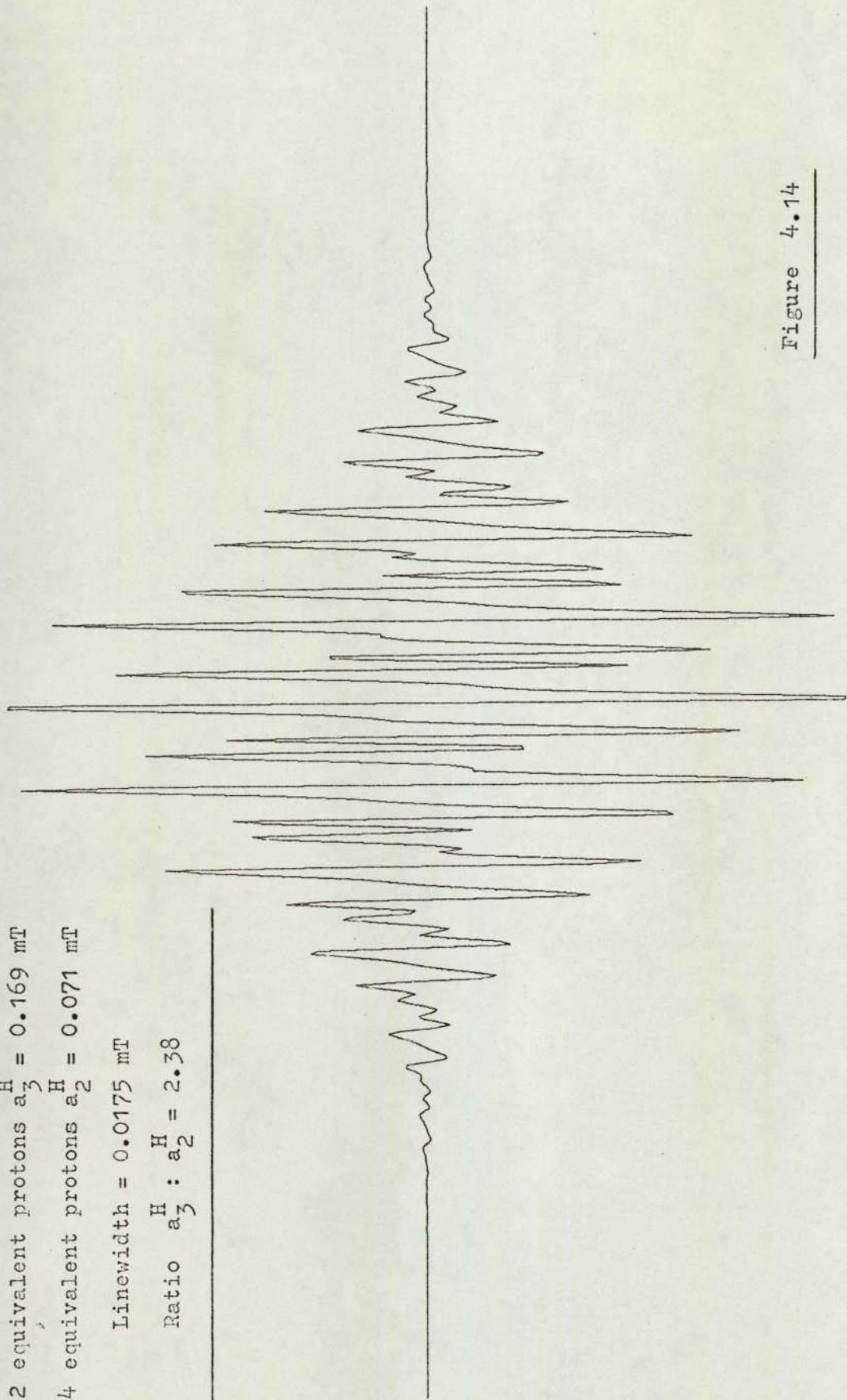
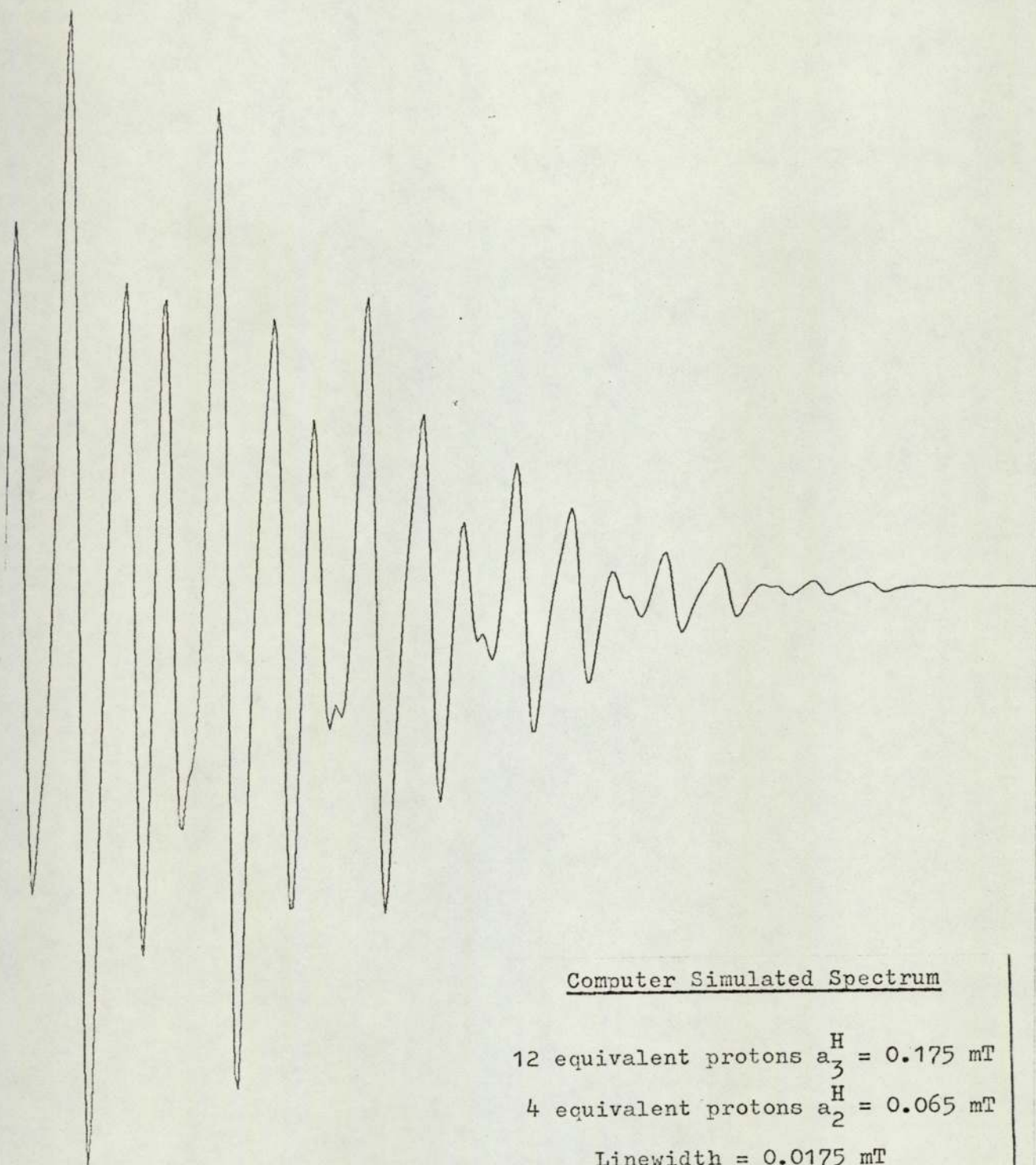


Figure 4.14





Computer Simulated Spectrum

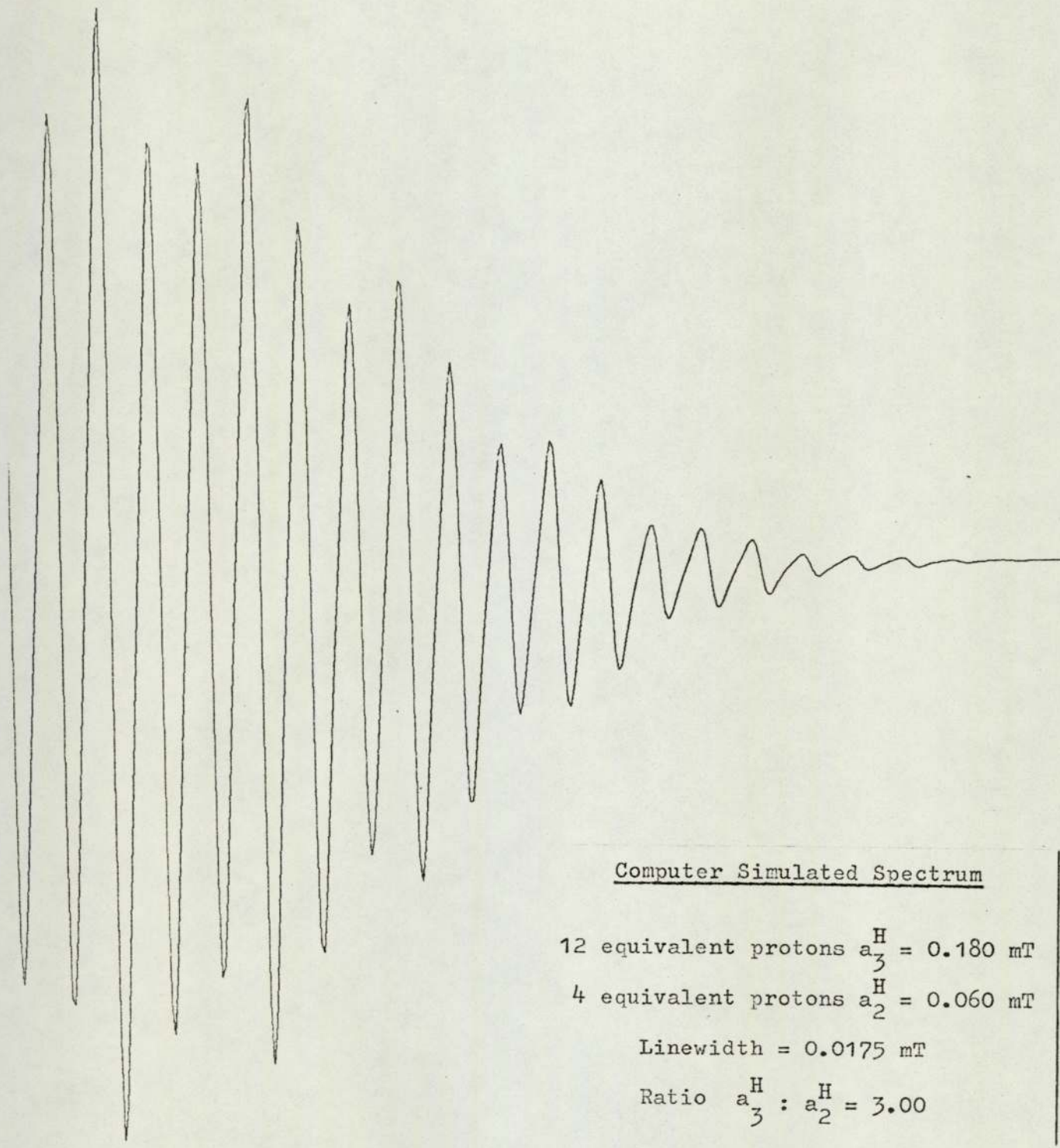
12 equivalent protons  $a_3^H = 0.175$  mT

4 equivalent protons  $a_2^H = 0.065$  mT

Linewidth = 0.0175 mT

Ratio  $a_3^H : a_2^H = 2.69$

Figure 4.15 |



Computer Simulated Spectrum

12 equivalent protons  $a_3^H = 0.180$  mT

4 equivalent protons  $a_2^H = 0.060$  mT

Linewidth = 0.0175 mT

Ratio  $a_3^H : a_2^H = 3.00$

Figure 4.16 |

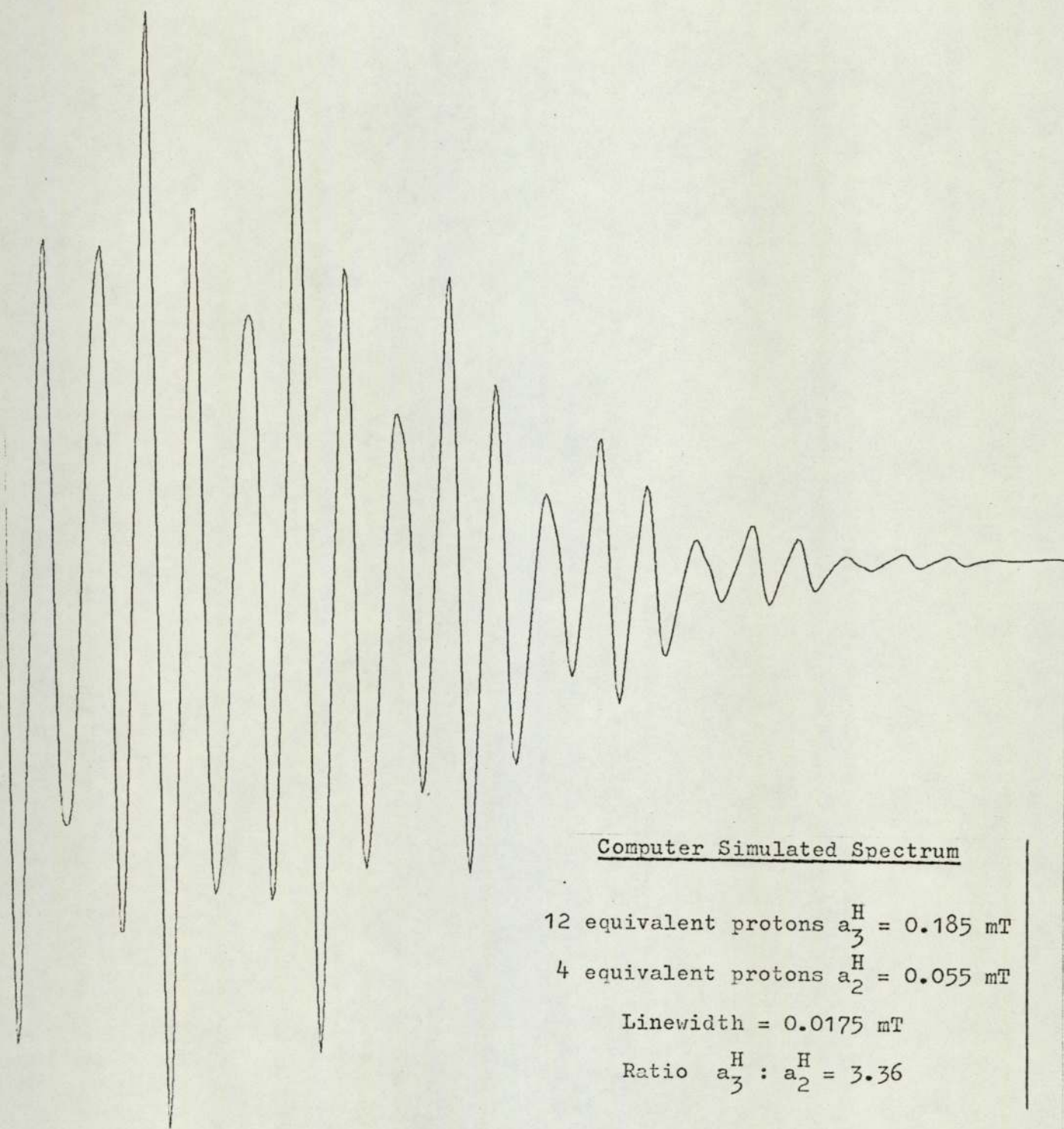


Figure 4.17 |

3,3',5,5'-Tetramethyl-4,4'-benzosemiquinone anion in acetonitrile-  
aqueous potassium hydroxide (94%-6% by volume)

$$a_2^H \text{ (ring H)} = 0.080 \text{ mT}$$
$$a_3^H \text{ (methyl H)} = 0.160 \text{ mT}$$

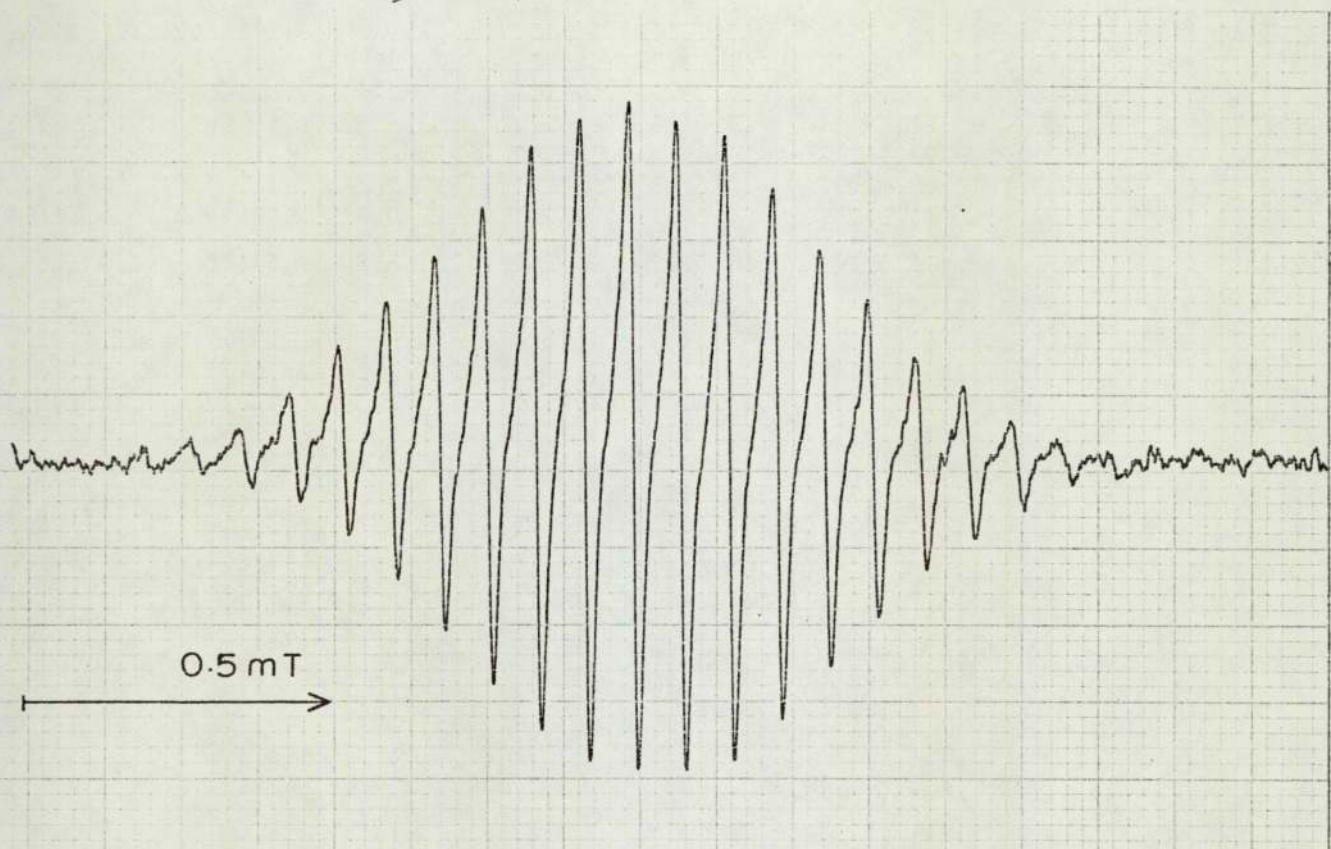


Figure 4.18

3,3',5,5'-Tetramethyl-4,4'-benzosemiquinone anion in carbon tetra-  
chloride saturated with aqueous potassium hydroxide

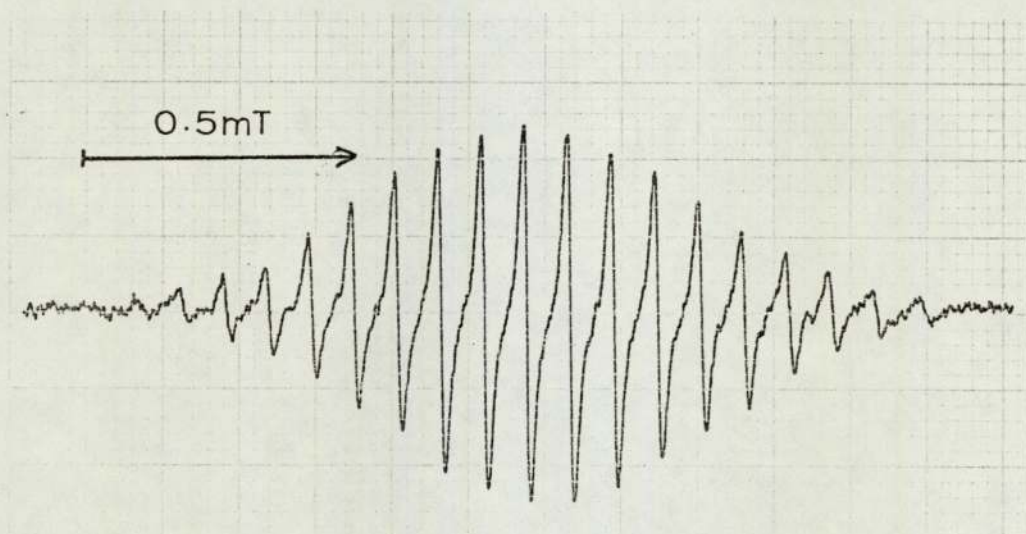


Figure 4.19

3,3',5,5'-Tetramethyl-4,4'-benzosemiquinone anion in pyridine-ethanolic potassium hydroxide (80%-20% by volume)

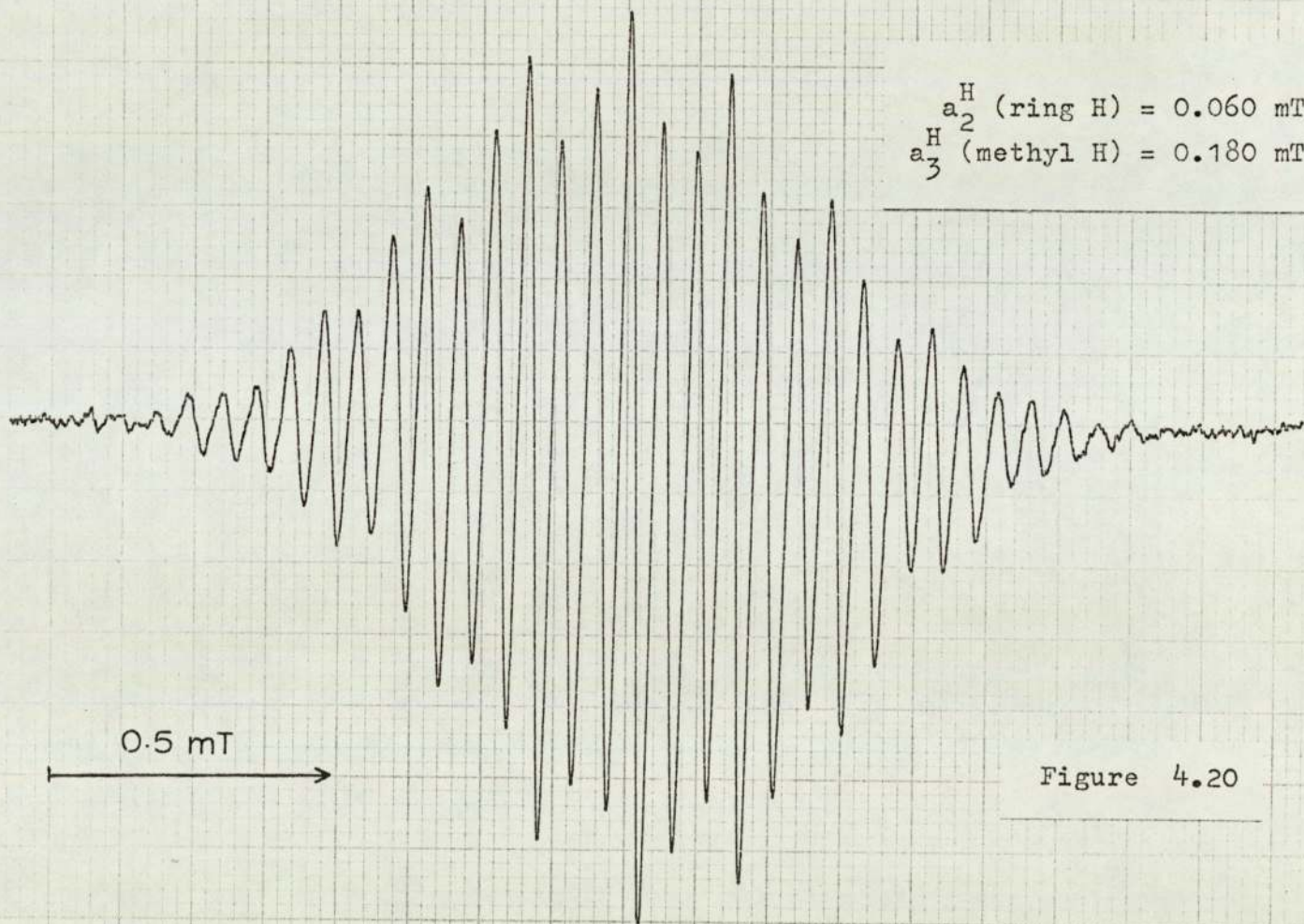


Figure 4.20

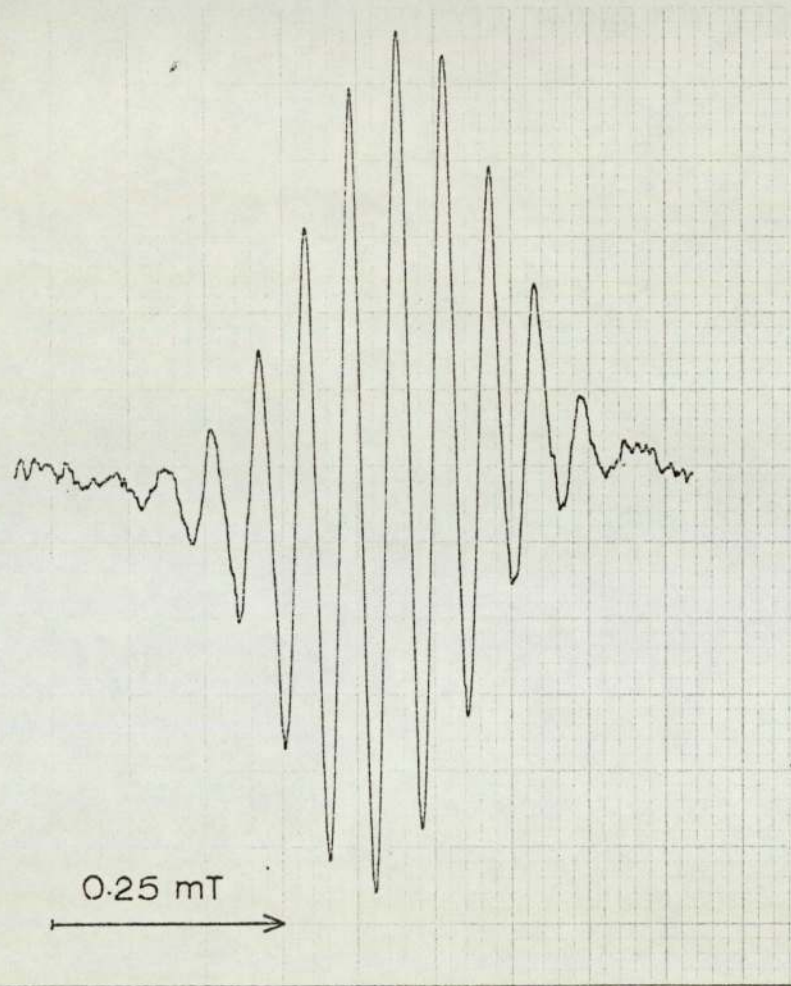
4.2.2. 3,3',5,5'-Tetramethoxy-4,4'-biphenosemiquinone  
Anion

No solvent effect is exhibited by this radical. The thirteen-line spectrum obtained by Matsunaga (15) is observed when a variety of solvent-potassium hydroxide mixtures are used. However, using a high initial concentration of the diol (greater than 0.05M compared with the more usual 0.002 to 0.004M) a simpler spectrum, as shown in figure 4.21 is observed. The five equally spaced lines have an intensity ratio of 1:4:6:4:1 and a hyperfine coupling constant of 0.049 mT.

4.2.3. 3,3',5,5'-Tetraisopropyl-4,4'-biphenosemiquinone  
Anion (TPBFSQ Anion)

When TPBPD is oxidised in pyridine-alcoholic potassium hydroxide mixtures a yellow-orange paramagnetic solution is obtained. As in the case of the tetramethyl derivative the resultant spectrum depends on the composition of the solvent mixture. Typical spectra are shown in figure 4.22, they can be analysed in terms of two groups of four equivalent protons, the ring protons and the methin protons of the isopropyl group.

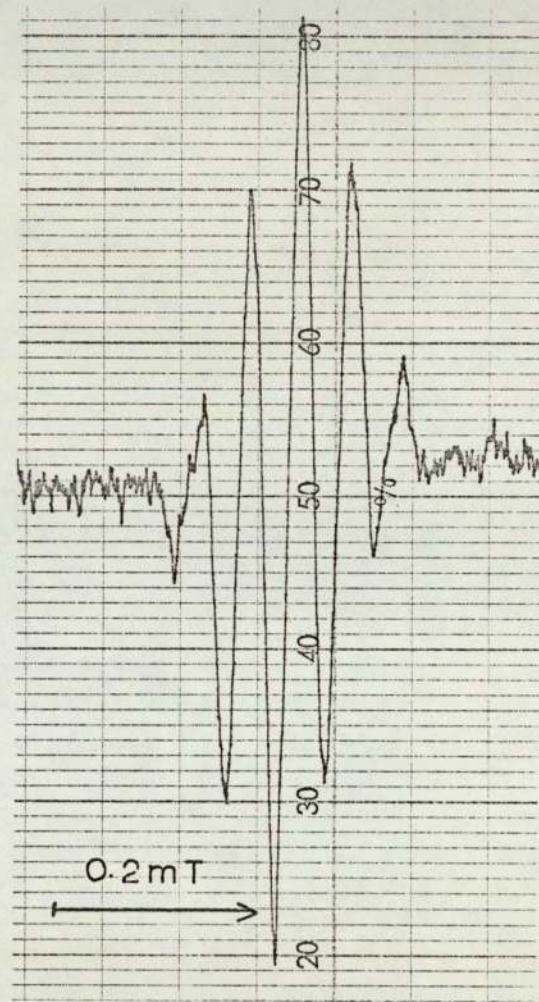
Unlike the tetramethyl derivative radicals are observed in the absence of any pyridine. The results are summarised in table 4.5.



3,3',5,5'-Tetramethoxy-4,4'-biphenyl-  
semiquinone anion

$$a_2^H (\text{ring H}) = a_3^H (\text{methyl H}) = 0.049 \text{ mT}$$

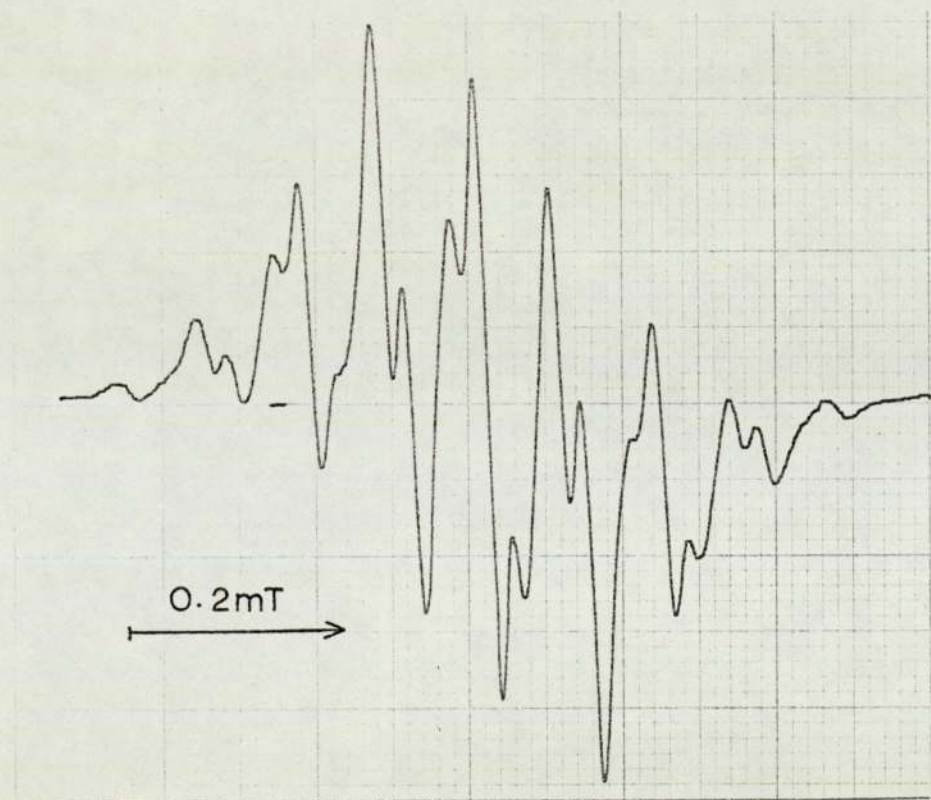
Figure 4.21



The ESR spectrum when a high concentration of 3,3',5,5'-tetramethoxybiphenyl-4,4'-diol is dissolved in pyridine-ethanolic potassium hydroxide (50%-50% by volume)

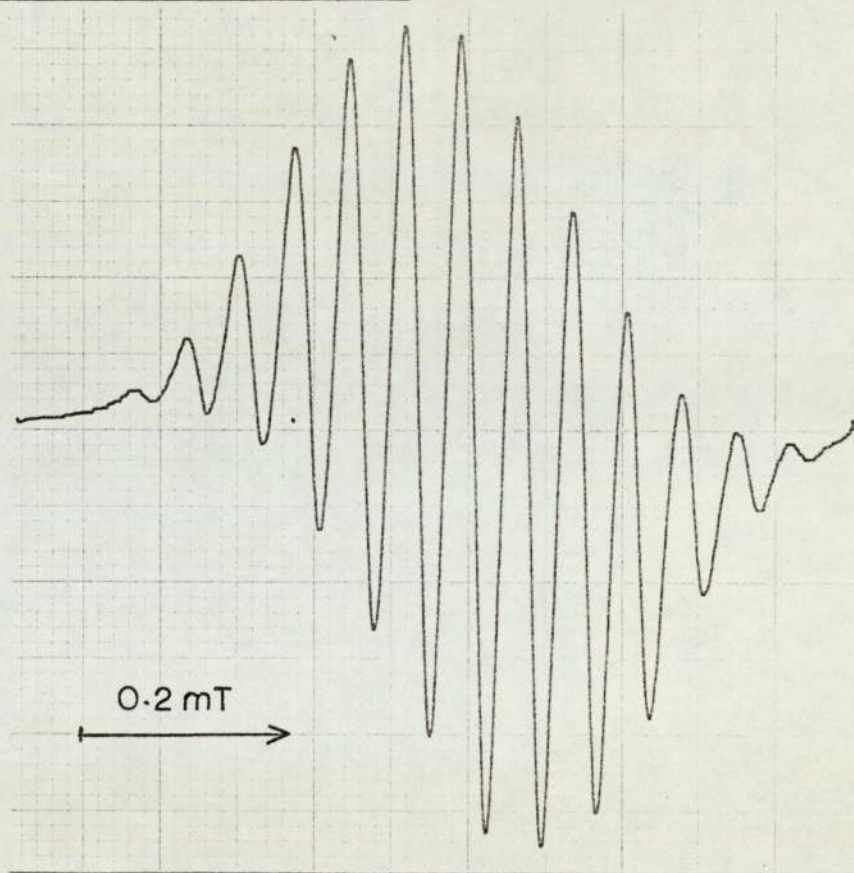
$$a^H = 0.049 \text{ mT}$$

3,3',5,5'-Tetraisopropyl-4,4'-biphenosemiquinone anion



(a) in ethanolic potassium hydroxide solution

$$a_2^H \text{ (ring H)} = 0.070 \text{ mT}$$
$$a_3^H \text{ (methin H)} = 0.097 \text{ mT}$$



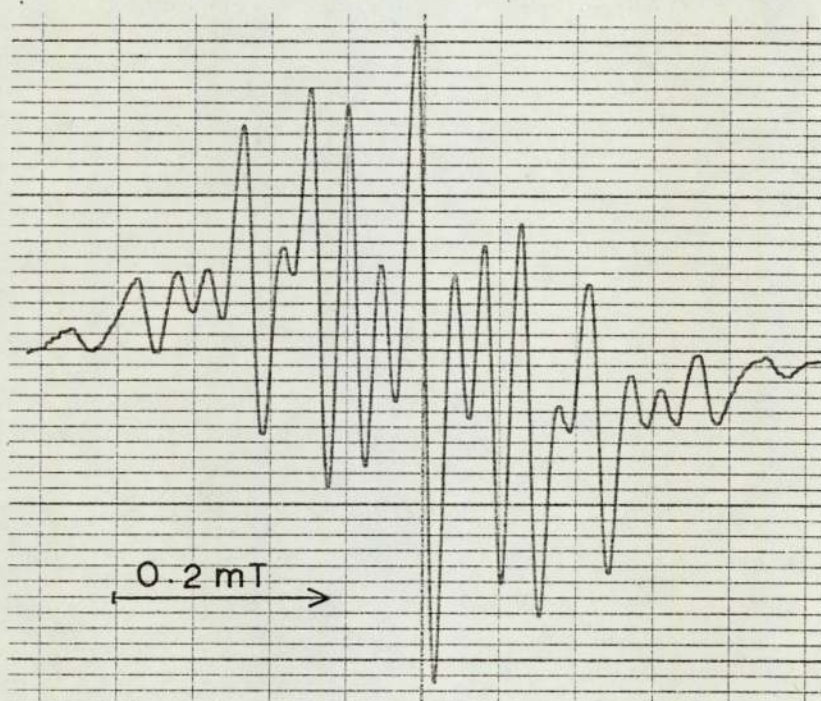
(b) in pyridine-ethanolic potassium hydroxide solvent mixture (0.98-0.02 mole fractions)

$$a_2^H \text{ (ring H)} = 0.055 \text{ mT}$$
$$a_3^H \text{ (methin H)} = 0.110 \text{ mT}$$

Figure 4.22



3,3',5,5'-Tetraisopropyl-4,4'-biphenosemiquinone anion



(c) in pyridine ethanolic potassium hydroxide solvent mixture (0.20-0.80 mole fractions)

$$a_2^H \text{ (ring H)} = 0.065 \text{ mT}$$

$$a_3^H \text{ (methin H)} = 0.101 \text{ mT}$$

Figure 4.22

TABLE 4.5.

HYPERFINE COUPLING CONSTANTS FOR 3,3',5,5'-TETRAISOPROPYL-4,4'-BIPHENOSEMIQUINONE ANION IN PYRIDINE-ALCOHOLIC POTASSIUM HYDROXIDE MIXTURES.

MOLE FRACTION		HYPERFINE COUPLING CONSTANTS	
Ethanol	Pyridine	$a_2^H$ (ring H) mT	$a_3^H$ (methin H) mT
1.0	0.0	0.070	0.097
0.80	0.20	0.065	0.101
0.58	0.42	0.059	0.105
0.02	0.98	0.055	0.110

4.2.4. 3,3',5,5'-Tetra-t-butyl-4,4'-biphenosemiquinone  
Anion

A yellow-orange paramagnetic solution is obtained by oxidation of the diol with alcoholic potassium hydroxide solution. The ESR spectrum consists of a quintet of lines, intensity ratio 1:4:6:4:1 with an hyperfine coupling constant of 0.05 mT. There is no evidence of any solvent effect when pyridine or diethylamine is added to the solution.

A similar spectrum is obtained when the tetra-sec-butyl derivative is oxidised, the hyperfine coupling constant is 0.048 mT. Again there is no evidence for a solvent effect.

No radicals are detected when the 3,3'-di-sec-butyl derivative is used.

### 4.3. DISCUSSION

#### 4.3.1. Solvent Effects in Semiquinone Anions

Stone and Maki (65) were the first to report a solvent effect on the proton hyperfine coupling constants in the anions of 2-methyl-1,4-benzosemiquinone, 1,4-naphthosemiquinone and 9,10-anthrasemiquinone when the solvent is changed from a protic type (ethanol-water) to an aprotic (dimethylsulphoxide, DMSO). However, the protons in the parent ion, 1,4-benzosemiquinone anion, were remarkably insensitive to the nature of the solvent. They also obtained a value for the  $^{13}\text{C}$  hyperfine coupling constant for the C atom in the carbonyl position with DMSO as solvent, which was widely different from that obtained by Das and Venkataraman (66) using alkaline ethanol.

These results prompted Gendell, Freed and Fraenkel (67) to develop a general theory of solvent-ion interaction. They assumed that the changes in hyperfine coupling constants arise entirely from a redistribution of the  $\pi$ -electron spin density and that this is effected only by localised complexes produced between the solvent and any polar substituents in the radical. In the case of the semiquinones, the solvent, by complexing with the carbonyl group, alters the effective electronegativity of the oxygen atom. Thus, in changing the solvent from an aprotic to a hydroxylic one there will be an increase in the total charge on the oxygen atom (shared by solvent).

Subsequent calculations by Das and Fraenkel (68) indicated that the  $\pi$ -electron spin density on this atom decreases whilst there is a small increase in the spin density on the carbonyl carbon atom. These changes result in a decreased spin polarisation at the oxygen nucleus (69). This means that the magnitude of an  $^{17}\text{O}$  hyperfine coupling constant will be reduced whereas a  $^{13}\text{C}$  hyperfine coupling constant would become more positive. Both these conclusions have been confirmed by experimental results (70 - 72).

Broze et al. (72) observed only small variations in the  $^{17}\text{O}$  hyperfine coupling constant ( $a^{\text{O}}$ ) of the 1,4-benzosemiquinone anion between different aprotic solvents. However, on changing to water there was a relatively large drop (about 10%) in the magnitude of  $a^{\text{O}}$ . These results together with the  $^{13}\text{C}$  hyperfine coupling constants were correlated by Oakes and Symons (73, 74) with the Z-value of the solvent. This empirical parameter is based on shifts in the ultraviolet spectra of the charge-transfer band of 1-alkyl-pyridinium iodide complexes in various solvents and so provides a measure of the ion-solvating power of that solvent (75).

Later, Ackermann, Germain and Robert (76) measured the hyperfine coupling constants due to  $^{13}\text{C}$  in natural abundance in the 1,4-benzosemiquinone anion. Their results indicated a large variation in the magnitude of the  $a^{\text{C}}$  for the carbon atom of the carbonyl group between protic and aprotic solvents. However the  $a^{\text{C}}$  values for the carbon atom in site 2 (carbon to hydrogen) were

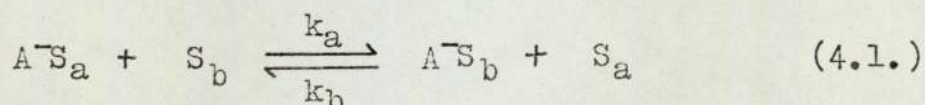
practically constant.

Symons et al. also extended the  $a^H$  measurements to the 2,3-, 2,5- and 2,6-dimethyl derivatives of 1,4-benzosemiquinone anion together with the durosemiquinone anion. The low sensitivity for  $a^H$  in both the anions of 1,4-benzosemiquinone and its tetramethyl derivative was explained in terms of a compensation, the effect of a change in spin density within one carbonyl group being exactly balanced by the change in the other group. The  $a^H$  values for the 2,3- and 2,5-dimethyl anions were found to be slightly more solvent sensitive. However, the  $a^H$  (ring H) and  $a^H$  (methyl H) values for the 2,5-dimethyl anion varied markedly with the solvent, although the correlation with the Z-values was poor, which suggested that other factors such as ion-pair formation may play some part.

In order to explain these observations Symons et al. (74) postulated an asymmetric solvation in which the unhindered end of the ion is preferred. This idea was supported by the  $a^H$  values of the 2,6-di-*t*-butyl anion being even more highly sensitive to solvent changes, than the corresponding dimethyl analogue. Subsequently a theoretical study by Claxton and McWilliams (77) supported this postulate and attributed the effect of solvent on  $a^H$  values to a combination of molecular asymmetry and asymmetric solvation.

Gendell et al. (67) aware of the observations of Adams regarding the variation in  $a^N$  when water is added

to an acetonitrile solution of the nitrobenzene anion showed that a simple model for a radical ion with only one functional group which can interact with the solvent could account for the observed variations in hyperfine coupling constants as a function of a binary solvent mixture. They assumed that the radical ion ( $A^-$ ) forms relatively stable 1:1 complexes with each of the pure solvents ( $S_a$  and  $S_b$ ) so that the predominant species present in the mixed solvent are  $A^-S_a$  and  $A^-S_b$ . These localised complexes were further assumed to exchange solvent molecules according to equation (4.1.). Generally



the hyperfine coupling constant arising from nucleus  $i$  in complex  $A^-S_a$ , say  $a_a^i$  will be different from  $a_b^i$  in complex  $A^-S_b$ . Thus the spectrum obtained will depend on the rate of the exchange reaction.

Assuming that the reaction is fast, i.e., that the lifetimes of the radical species are short compared to the difference in hyperfine coupling constants, Gendell et al. showed that the average observed coupling constant ( $a_{obs}^i$ ) is given by equation (4.2.), where  $x_a$  and  $x_b$  are

$$a_{obs}^i = x_a \cdot a_a^i + x_b \cdot a_b^i \quad (4.2.)$$

the fractions of the total amount of radical ion in the forms  $A^-S_a$  and  $A^-S_b$ , respectively. The fractions  $x_a$  and  $x_b$  were then replaced in equation (4.2.) by expressions involving the equilibrium constant  $K$ , where  $K = k_a/k_b$

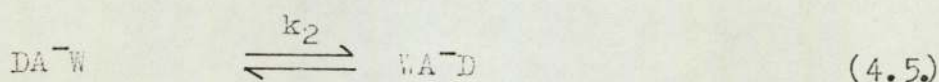
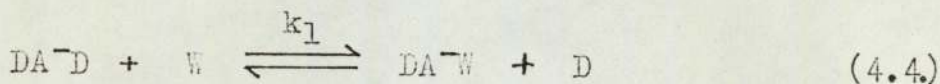
and the solvent concentrations  $[S_a]$  and  $[S_b]$ . The resulting equation related a function of the change in hyperfine coupling constant to the ratio of the solvent concentration and is thus open to confirmation by comparison with the experimental results.

For the case where there are several complexes, say  $j$ , present in solution equation (4.2.) can be generalised to equation (4.3.), which applies only for the

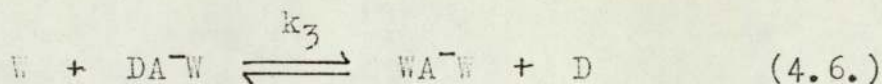
$$a_{\text{Obs}}^i = \sum_j x_j \cdot a_j^i \quad (4.3.)$$

limit of fast exchange. Thus a careful analysis of the results should be able to provide information regarding the various equilibrium constants.

Such an analysis was attempted by Stone and Maki (70) for the variation in  $^{13}\text{C}$  hyperfine coupling constants of the carbonyl carbon atom ( $a^{\text{C}}$ ) in 1,4-benzosemiquinone anion in various water - DMSO and water-acetonitrile mixtures. In the former solvent mixture a good agreement between the experimental and theoretical results was obtained assuming that the only relevant equilibria are the ones represented by equations (4.4.) to (4.6.). In these equations D represents a molecule of the aprotic solvent whilst a water molecule is represented by W and the equilibrium constants are written as  $K_1$  etc.







This scheme ignored mono- and non-solvated species and is surprising in that Gendell et al. (67) had previously suggested that the anion radical did not complex with the aprotic solvent since they had observed similar values for  $a^G$  in both acetonitrile and DMSO.

When applied to the water-acetonitrile results no agreement was obtained. Burgess and Symons (73) suggested that the shifts in the values of  $a^G$  are due to a complex mixture of solvation and ion-pairing effects. Since the radical ions were prepared electrolytically bulky alkyl ammonium ions are present and these are known to form ion-pairs even in protic solvents. Oakes and Symons (74) also put this argument forward to explain the poor correlation obtained between the Z-value of the solvent and the  $^{17}O$  and  $^{13}C$  hyperfine coupling constants of 2,6-dimethyl-1,4-benzosemiquinone anions.

#### 4.3.2. 3,3',5,5'-Tetramethyl-4,4'-biphenosemiquinone Anion (TMBFSQ Anion)

Since no radicals can be detected in the absence of an organic solvent the TMBFSQ anion must be stabilised by the solvent in some way. Michaelis and Granick (6) have shown that when phenanthraquinone or its 3-sulphonated derivative is partially reduced in alkaline solution the resulting paramagnetic semiquinone anion is in equilibrium with its diamagnetic dimer. Further they

found that this dimerisation is suppressed by the addition of an organic solvent such as pyridine. Thus it would seem reasonable to suppose that the organic solvent is providing a solvent cage for the semiquinone anions.

The variation of the hyperfine coupling constants of the TMBPSQ anion with solvent compositions are expressed in figure 4.23 as a plot of ( $a_{\frac{H}{3}}$  (methyl H) -  $a_{\frac{H}{2}}$  (ring H)) against mole fraction of the aprotic solvent ( $x_a$ ). In order to explain these results we shall further assume that any redistribution of the  $\pi$ -electron spin density due to interactions between the TMBPSQ anion and the solvent cage is small and may be neglected. Support for this assumption is provided by the tendency of the hyperfine coupling constants in certain solvent - water mixtures (see tables 4.2 to 4.4) at high solvent concentrations to approach the values obtained by Petranek et al. (63) of 0.188 mT for  $a_{\frac{H}{3}}$  (methyl H) and 0.054 mT for  $a_{\frac{H}{2}}$  (ring H) using acetonitrile as a single solvent. Furthermore, on application of the solvent effect theory of Gendell et al. (67) no quantitative agreement could be obtained if complexing between the semiquinone anion and the aprotic solvent was postulated.

Qualitatively, the results may be explained as follows. The solvent surrounded TMBPSQ anions, which will be referred to as solvated and represented as (TMBPSQ<sup>-</sup>) are able to form hydrogen bonded complexes via the oxygen atoms with protic solvents. Thus the electronegativity of the oxygen atoms are altered and a redistribution of

the  $\pi$ -electron spin density within the solvated TMBESQ anions occurs.

According to McConnell's (78) relationship (equation (4.6.)), the hyperfine coupling constant  $a_i^H$  of a ring

$$a_i^H (\text{ring H}) = Q_{C-H}^H \cdot \rho_i^C \quad (4.6.)$$

proton attached to a carbon atom  $C_i$  is proportional to the  $\pi$ -electron spin density,  $\rho_i^C$  at this carbon.  $Q_{C-H}^H$  is a parameter, sometimes referred to as the  $\sigma - \pi$  interaction parameter, its absolute value lies between 2.0 and 3.0 mT. Molecular orbital theory has indicated that it has a negative sign (79) which has been confirmed by experiment (80). Thus any effect which alters the value of  $\rho_i^C$  will alter  $a_i^H$ . Equation (4.7) can also be

$$a_i^H (\text{methyl H}) = Q_{C-CH_3}^H \cdot \rho_i^C \quad (4.7.)$$

applied to the methyl protons.

The various hydrogen bonded complexes together with the solvated TMBESQ anions are in equilibrium with each other, and assuming that the rate of exchange between these species is rapid a single spectrum is obtained. The appearance of this spectrum will depend upon the relative concentrations of the various paramagnetic species present and therefore upon the concentration of the protic solvent and the equilibrium constants for the exchange reactions. We should expect the equilibrium constants to vary with the ability of the aprotic solvent

to undergo hydrogen bonding with the protic solvent.

Recently Kagiya, Sumida and Inoue (30) have measured the frequency of the O - D vibrational bands of mono-deuteromethanol in a variety of solvents using infra red spectroscopy. Taking benzene as a standard, they have used the frequency shift observed in changing to another solvent as a measure of the electron-donating power ( $\Delta\nu_D$ ) or proton attracting force for that solvent. The  $\Delta\nu_D$ -values for the solvents used in the present work are given in table (4.6.).

A comparison of figure 4.23 with the  $\Delta\nu_D$ -values of table 4.6. shows that as the electron-donating power of the solvent increases so does the difference between the methyl and ring proton hyperfine coupling constants for the same mole fraction of solvent. Assuming that when  $x_a = 0$  only hydrogen bonded species are present, whereas when  $x_a = 1.0$  no hydrogen bonded complexes are present only solvated TMBESQ anions, then the above comparison can be interpreted in terms of a decrease in the concentration of hydrogen bonded complexes as the electron-donating power of the solvent is increased keeping the solvent concentration constant.

The solvent effect theory (67) was then applied quantitatively to these results. When both doubly and singly hydrogen bonded complexes as in equations (4.8.) to (4.10.) were considered no quantitative agreement could

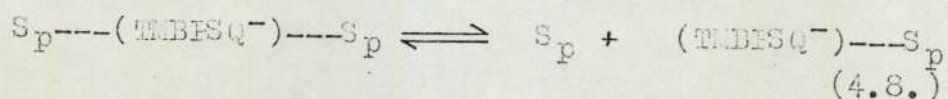


Figure 4.23

Plot of the difference in the methyl and ring proton hyperfine coupling constants against the solvent-water composition

(The values for the pyridine-ethanol mixture are indicated with a x )

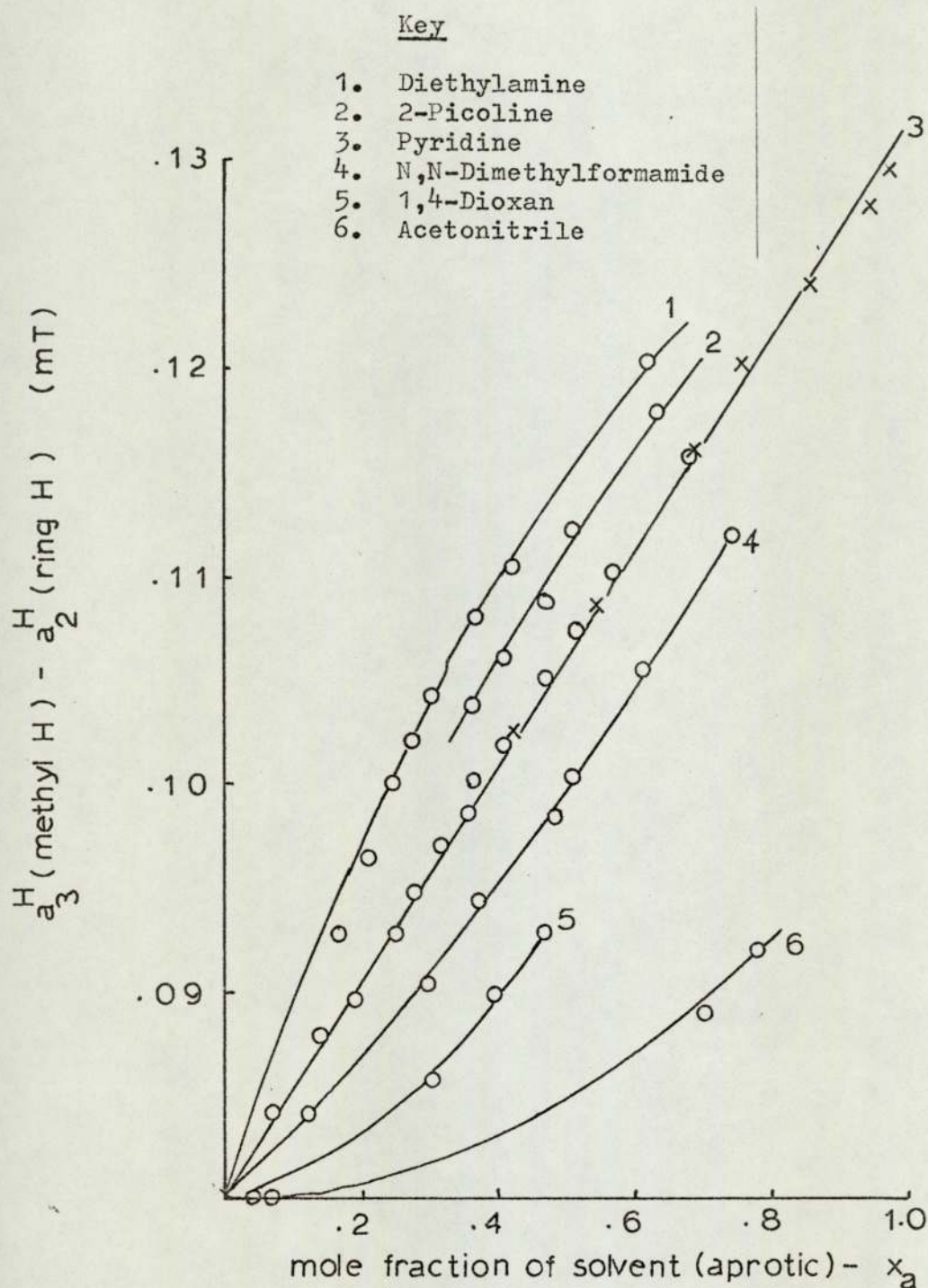
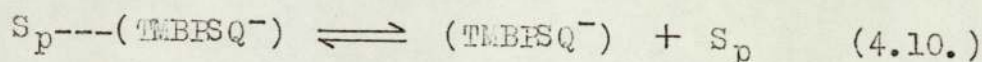
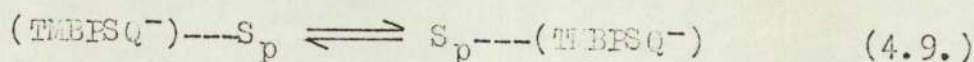


TABLE 4.6.

THE ELECTRON-DONATING POWERS OF SOME LIQUID ORGANIC  
COMPOUNDS

Compound	Electron-donating power $\Delta\nu_D$ ( $\text{cm}^{-1}$ )
Tetrachloromethane	-21
Benzene	0
Acetonitrile	49
1,4-Dioxan	77
N,N -Dimethylformamide	107
Pyridine	168
2-Picoline	183
Diethylamine	238 (a)

(a) The value for diethylamine was not measured by Kagiya et al. (81), however, they give the values for ethylamine and triethylamine as 233 and 238 respectively.



be obtained.  $\text{S}_p$  represents a molecule of a protic solvent. However a reasonable fit is obtained if a simpler model involving only single hydrogen bonded complexes as in equation (4.10.) is used.

The application of the theory of Gendell et al. yields equation (4.11.).

$$(a_i^H)_{\text{obs}} = \frac{(a_i^H)_a + (a_i^H)_p}{2} + \frac{(\frac{k}{[\text{S}_p]} - 1)((a_i^H)_a - (a_i^H)_p)}{2(\frac{k}{[\text{S}_p]} + 1)} \quad (4.11.)$$

where  $(a_i^H)_{\text{obs}}$  = the observed proton hyperfine coupling constant in the mixed solvent.

$(a_i^H)_a$  = the proton hyperfine coupling constant in pure aprotic solvent.

$(a_i^H)_p$  = the proton hyperfine coupling constant in pure protic solvent.

$K$  = the equilibrium constant for equation (4.10.).

$[\text{S}_p]$  = the concentration of protic solvent.

It should be noted that although the hydrogen bonded complex,  $(\text{TMBFSQ}^-) \cdots \text{S}_p$ . is asymmetric there are an equal number of the oppositely solvated species  $\text{S}_p \cdots (\text{TMBFSQ}^-)$  and since the rate of exchange is fast the inequivalence is averaged out.

Equation (4.11.) may be rewritten as equation (4.12).

$$\frac{2((a_i^H)_{\text{obs}} - \frac{1}{2}((a_i^H)_a + (a_i^H)_p))}{(a_i^H)_a - (a_i^H)_p} = \frac{[\frac{k}{S_p}] - 1}{[\frac{k}{S_p}] + 1} \quad (4.12.)$$

The quantity  $((a_i^H)_{\text{obs}} - \frac{1}{2}((a_i^H)_a + (a_i^H)_p))$  is the difference of the average observed hyperfine coupling constant from the arithmetic mean and will be re-written as  $\delta a$ .

$$\frac{2 \delta a}{(a_i^H)_a - (a_i^H)_p} = \frac{[\frac{k}{S_p}] - 1}{[\frac{k}{S_p}] + 1} \quad (4.13.)$$

In order to test the validity of equation (4.13.) we required values for the hyperfine coupling constants  $(a_i^H)_a$  and  $(a_i^H)_p$  neither of which were we able to measure directly. However, the values of the methyl and ring proton hyperfine coupling constants in a pyridine - ethanol mixture in which the mole fraction of pyridine is 0.97 are 0.185 and 0.055 mT respectively, whereas Petranek et al. (63) obtained values of 0.188 and 0.054 mT using acetonitrile. Therefore, we consider 0.186 mT to be a reasonable value for  $a_{\frac{H}{3}}$  (methyl H) in the absence of a protic solvent. In the absence of any data for  $(a_i^H)_p$  these values were taken as 0.160 and 0.30 mT for the methyl and ring protons respectively. These are the lowest values which are observed at low aprotic solvent concentrations, particularly where the solvent also has a low  $\Delta\nu_D$ -value.



These extreme values for the methyl hyperfine coupling constants were then inserted in equation (4.12).

$$\frac{(a_{\frac{H}{2}}^{\text{methyl H}})_{\text{obs}} - 0.173}{0.013} = \frac{\frac{k}{[S_p]} - 1}{\frac{k}{[S_p]} + 1} \quad (4.14.)$$

Thus the observed values for the left hand side of equation (4.14.) can be plotted against  $1/[S_p]$  and if the relationship is valid for the equilibrium, constant K can be determined from the experimental results thus allowing a theoretical curve to be calculated and compared with the experimental one.

Figure 4.24 shows the results of such a procedure applied to the observed methyl hyperfine coupling constants in pyridine-ethanol mixtures. The concentration of protic solvent is expressed in terms of molality. These results are then compared in figure 4.25 with those obtained from the pyridine-water mixtures. It can be seen that water and ethanol behave similarly indicating that they both, when complexing with the semiquinone anion, bring about a similar redistribution in the  $\pi$ -electron spin density.

The results for the other solvent-water mixtures are shown in figure 4.26, the dotted lines represent theoretical results calculated using the values for K given in table 4.7.

These equilibrium constants can be correlated as

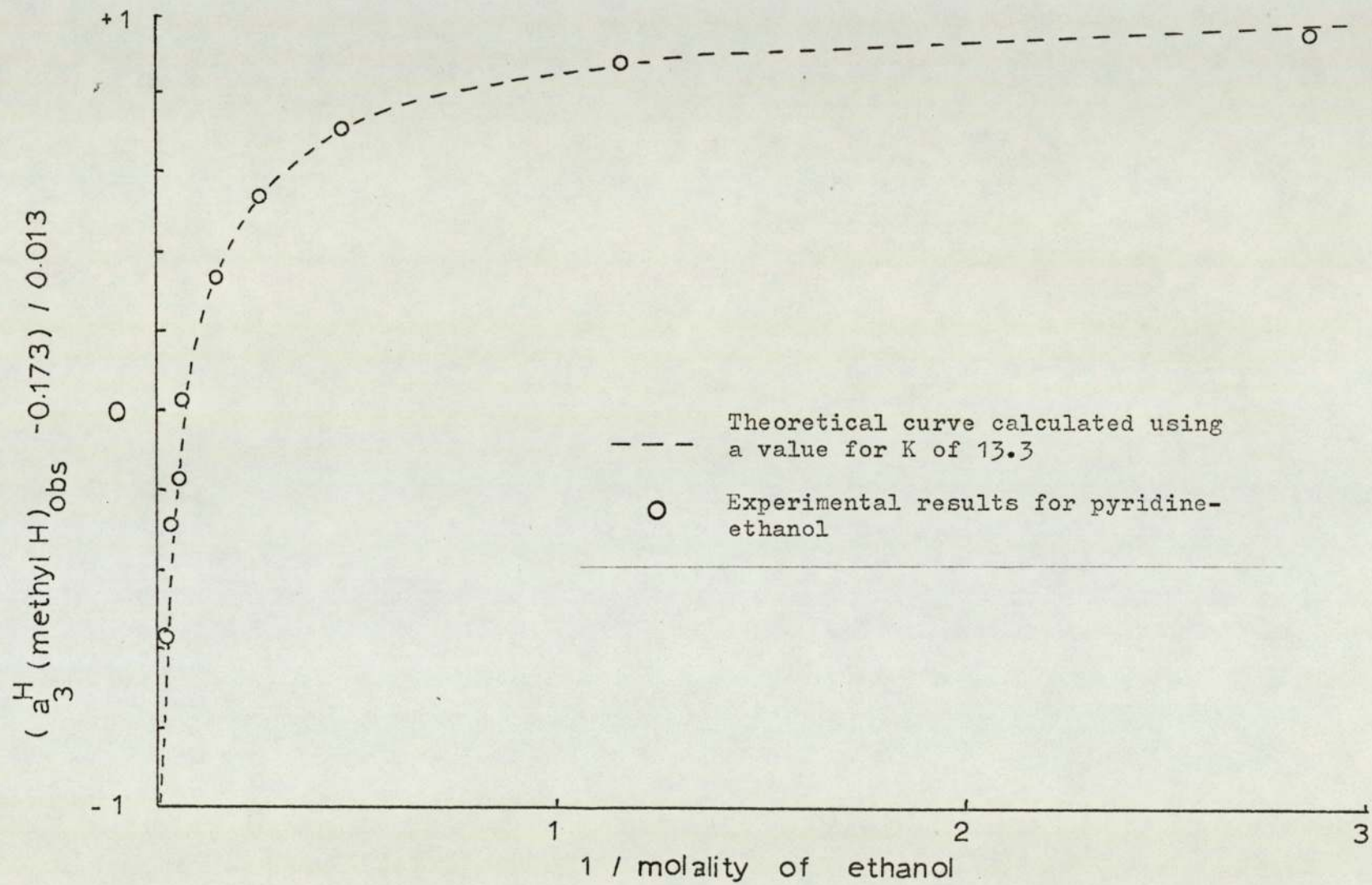


Figure 4.24

Figure 4.25

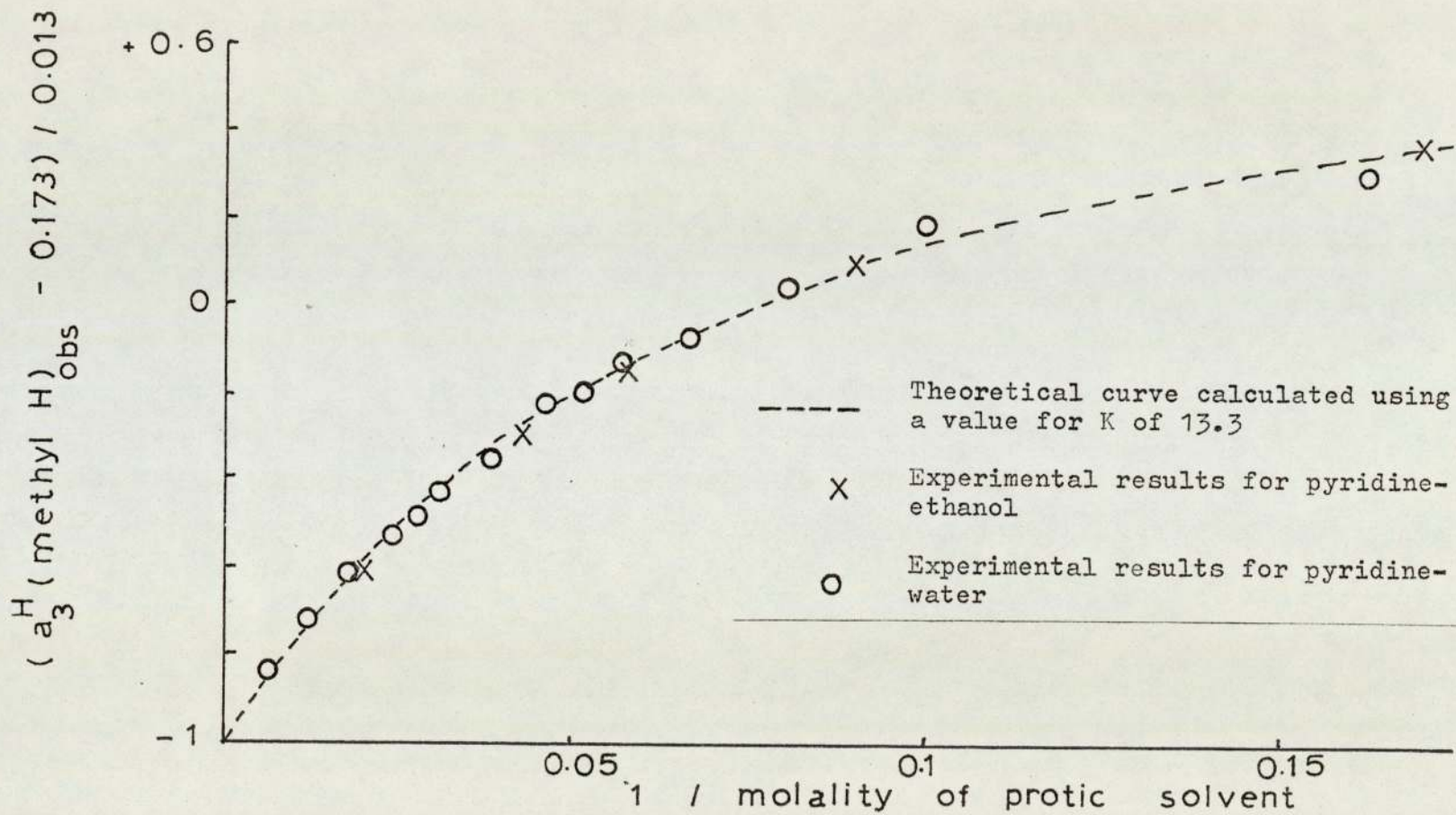


Figure 4.26

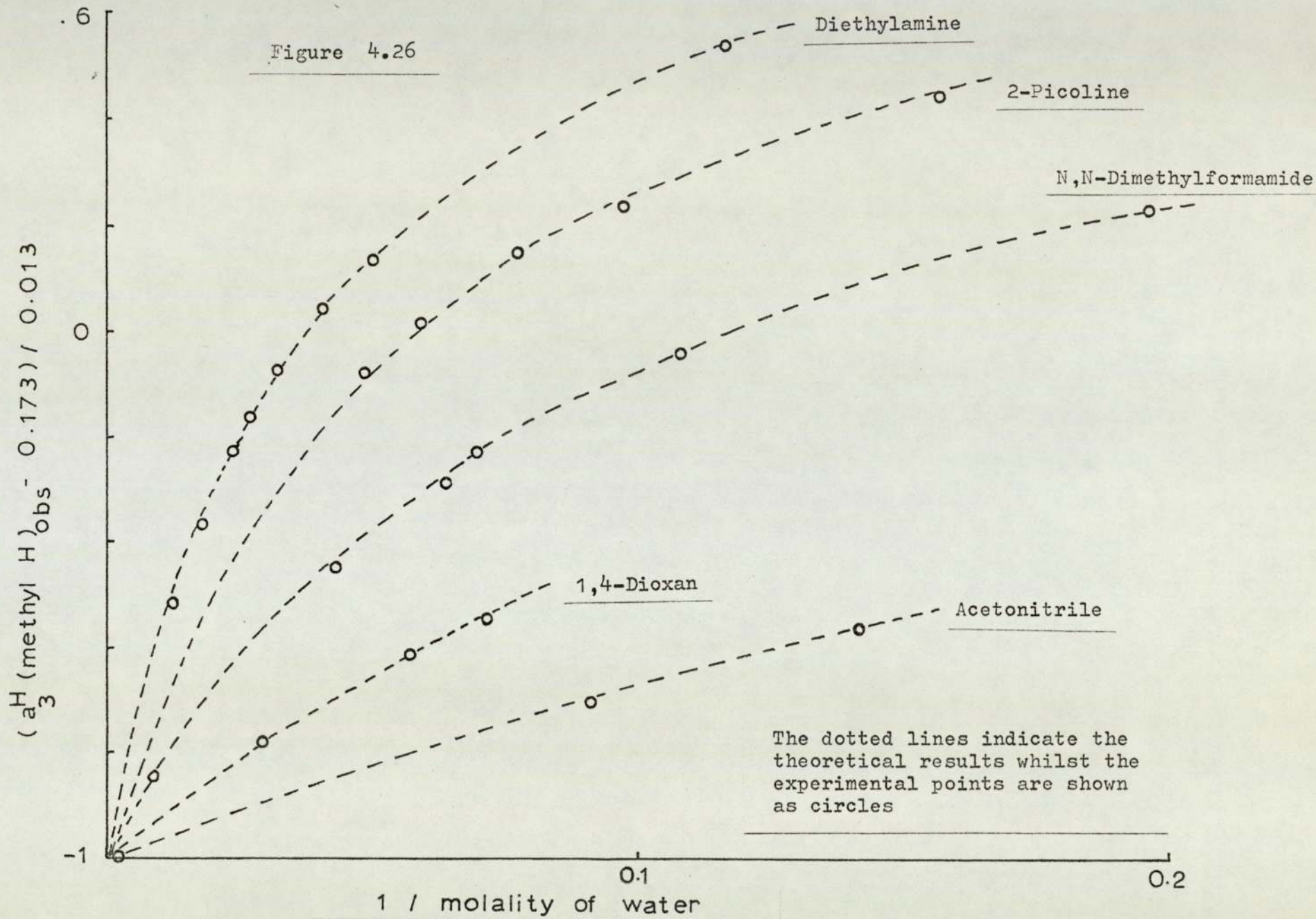


TABLE 4.7.

THE VALUES OF THE EQUILIBRIUM CONSTANT, K OBTAINED  
FROM THE EXPERIMENTAL RESULTS

Solvent	K(a)
Acetonitrile	2.08
1,4-Dioxan	4.17
N,N'-Dimethylformamide	8.3
Pyridine	13.3
2-Picoline	16.7
Diethylamine	26.7

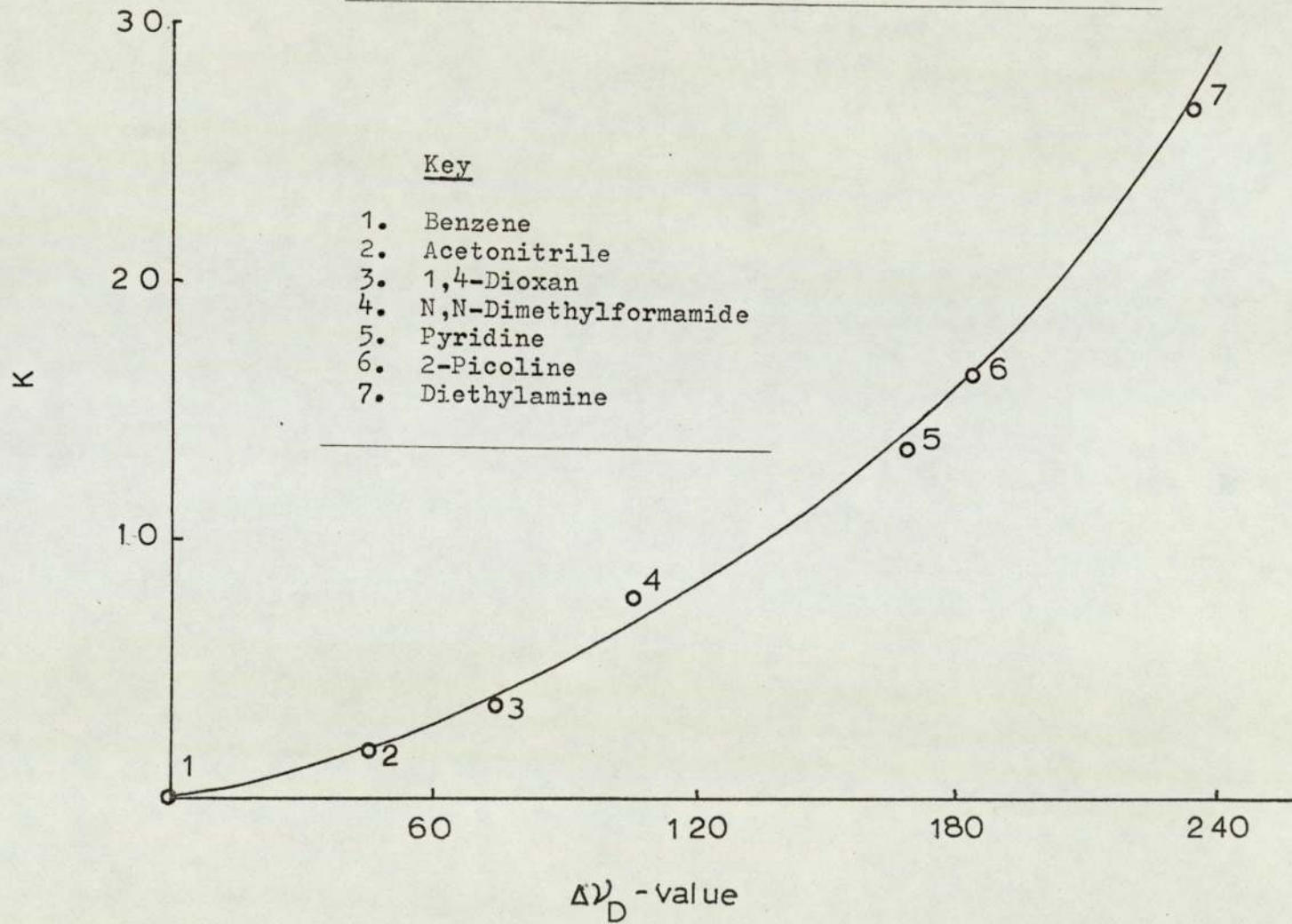
(a) K will have the same units as  $[S_p]$  i.e. in this case it will be expressed in terms of the molality.

one would expect with the electron-donating powers of Kagiya et al. (see figure 4.27), thus when the  $\Delta\nu_D$ -value of the solvent is low the value of K will also be low indicating the presence in solution of a preponderance of the hydrogen bonded complexes.

The solvent dependance of the proton hyperfine coupling constants exhibited by the tetraisopropyl-derivative can also be explained qualitatively in a similar way. Whilst the absence of any measurable solvent effect with the tetra-t-butyl- derivative is presumably due to the large steric factors involved preventing the formation of strongly hydrogen bonded complexes.

Figure 4.27

Plot of K against electron-donating power ( $\Delta\nu_D$ )



## 5. MOLECULAR ORBITAL CALCULATIONS

### 5.1. SIMPLE MOLECULAR ORBITAL MODELS

The hyperfine coupling observed due to ring protons in a  $\pi$  system has been attributed to a polarisation of the sigma electrons in the C-H bonds by the unpaired electrons in the delocalised  $\pi$ -orbital (73, 81 - 84). Thus there should be a close connection between the distribution of the unpaired  $\pi$ -electron over the individual carbon atoms ( $C_i$ ) and the magnitude of the polarised spin density on the adjacent ring protons ( $H_i$ ).

According to McConnell's relationship (77) (equation (5.1)), the hyperfine coupling constant  $a_i^H$  of a ring proton attached to a carbon atom  $C_i$  is proportional to the  $\pi$ -spin density  $\rho_i$  at this carbon:

$$a_i^H = Q_{CH} \cdot \rho_i \quad (5.1.)$$

where  $Q_{CH}$  is a parameter whose absolute value lies between 2 and 3 mT. Molecular orbital theory indicates that this parameter has a negative sign, which agrees with the idea that the polarised spin density in the  $\sigma$ -orbital at the ring proton  $H_i$  has an opposite sign to that in the  $\pi$ -orbital of the adjacent carbon atom  $C_i$  (see figure 5.1.). This negative sign has subsequently been confirmed



C-H section of an aromatic radical-ion

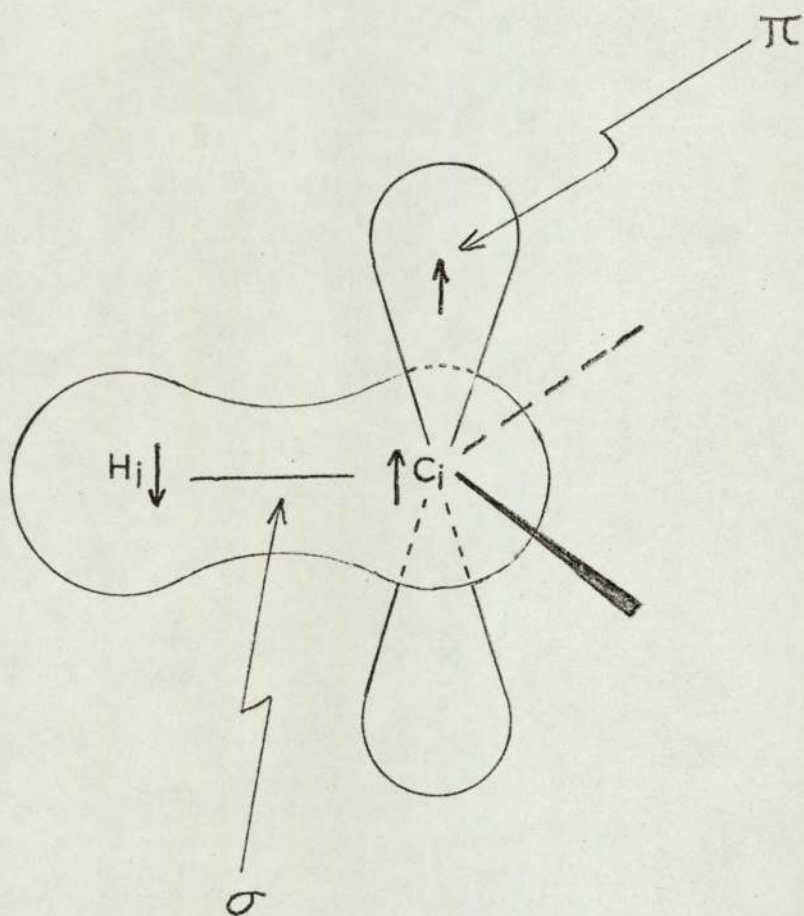


Figure 5.1

experimentally (79, 85). Thus McConnell's relationship enables the experimental results ( $a_i^H$ ) to be compared with theoretical values ( $\rho_i$ ).

The simplest method of computing spin densities involves the Huckel Molecular Orbital (HMO) treatment (86). The HMO model describes the eigenvalues of the molecular orbitals in terms of 2 parameters, the Coulomb integral  $\alpha$  of a 2p atomic orbital and the C-C bond or Resonance integral  $\beta$ , both of which have a negative sign. Since there is no interaction between  $\pi$ -electrons in the Huckel model the spin density on the  $i$ th carbon atom is determined solely by the contribution of the singly occupied HMO and is equal to the square of the eigenvector for that atom.

The simple HMO model has been refined by McLachlan (40) to take into account  $\pi$ - $\pi$  spin polarisation. This treatment allows for the interaction between the unpaired electron spin and the paired spins of the other  $\pi$ -electrons. In some cases it leads to negative spin densities which have been confirmed experimentally. According to McLachlan, the  $\pi$ -spin density  $\rho_i$  of the  $i$ th carbon atom can be calculated as in equation (5.2.).

$$\rho_i = c_{oi}^2 + \lambda \sum_j \pi_{ij} c_{oj}^2 \quad (5.2.)$$

Where  $c_{oi}$  and  $c_{oj}$  are the HMO eigenvectors of the  $i$ th atom and the other atoms  $j$  in the system, respectively, for the singly occupied  $\pi$ -orbital 0. Furthermore, the

$\pi_{ij}$  terms represent the HMO atom-atom polarisabilities of the neutral diamagnetic system (39). The value of the parameter  $\lambda$  has been estimated at 1.2 (87).

Both models outlined above can be used to calculate the spin densities in semiquinone ions. The perturbation resulting from the replacement of a carbon atomic orbital by that of an oxygen is expressed by 2 parameters  $h_o$  and  $k_{co}$  defining the Coulomb integral  $\alpha_o$  and the Resonance integral  $\beta_{co}$  (equation (5.3.)).

$$\alpha_o = \alpha + h_o\beta \quad \text{and} \quad \beta_{co} = k_{co}\beta \quad (5.3.)$$

The values of these parameters used by the various workers studying semiquinone ions are summarised in table 5.1 for the HMO model and in table 5.2 for the McLachlan modified HMO treatment.

In the semiquinone anion the unpaired electron occupies the lowest vacant antibonding HMO of the quinone. The semiquinone cations can be considered as diprotonated semiquinone anions from the viewpoint of their  $\pi$ -electron structure. This protonation leads to an increase in the electronegativity of the oxygen atoms and a decrease in the double bond character of the carbon-oxygen linkage. This effect can be taken into account in the spin density calculation by using a higher value for  $h_o$  and a lower value for  $k_{co}$  with the unpaired electron again occupying the lowest available orbital of the quinone.

TABLE 5.1.

h AND k PARAMETERS USED IN HMO CALCULATIONS  
OF SEMIQUINONE IONS

Semiquinone Ion	$h_0$	$k_{CO}$	Ref.
The anions of 1,4-benzosemiquinone, 1,4-naphthosemiquinone, 9,10-anthrasemiquinone and their derivatives.	1.2	1.56	88
The anions of 1,4-benzosemiquinone, 1,4-naphthosemiquinone and 9,10-anthrasemiquinone in (a) ethanol-water mixtures and (b) DMSO	0.90 0.80 0.40 0.40	1.40 1.38 1.40 1.38	66 71 66 71
The cations of 1,4-benzosemiquinone, 1,4-naphthosemiquinone and 9,10-anthrasemiquinone	2.0	1.1	46

TABLE 5.2.

h AND k PARAMETERS USED IN McLACHLAN MODIFIED  
HMO CALCULATIONS OF SEMIQUINONE IONS

Semiquinone Ion	$h_0$	$k_{co}$	Ref.
The anions of 1,4-benzosemiquinone, 1,4-naphthosemiquinone and 9,10-anthrasemi- quinone in (a) ethanol-water mixtures and (b) DMSO	1.60	1.55	66
	1.42	1.46	71
	1.26	1.55	66
	1.17	1.46	71
The anions of 2,3-, 2,5- and 2,6-dimethyl- 1,4-benzosemiquinone	0.80	1.25	55
The cations of 2,3-, 2,5- and 2,6-dimethyl- 1,4-benzosemiquinone	1.65	1.20	55

5.2. SPIN DENSITY CALCULATIONS FOR 4,4'-  
BIPHENOSEMIQUINONE IONS

The McLachlan method was employed in the spin density calculations. The values of the parameters  $h_0$  and  $k_{CO}$  were both varied in the range 0.8 to 1.9. Acceptable values of these parameters must yield spin densities consistent with the experimental hyperfine coupling constants. A further requirement is that the value of the parameter  $Q_{CH}$  should lie in the range -2 to -3 mT. Using McConnell's relationship (equation (5.1.)) the ratio of the hyperfine coupling constants of the ring protons in position 2 and 3 (see figure 5.2.) can be equated with the ratio of the spin densities on these carbon atoms.

The variation of the ratio of the calculated spin densities  $\rho_2/\rho_3$  with the parameter  $k_{CO}$  for various values of the parameter  $h_0$  is shown in figure 5.3. Values of these parameters which satisfy the two criteria outlined above are indicated in figure 5.3. for both the anion and the cation of 4,4'-biphenosemiquinone by broken horizontal lines. The range of the parameters investigated was not sufficiently wide enough to determine the upper limits, however, the minimum values are summarised in table 5.3.

Although it is not possible to select specific pairs of the parameters  $h_0$  and  $k_{CO}$  on the basis of the results to date, the changes in the parameters necessary to represent the change in coupling constants in going

The numbering of the atoms in the  
diphenoquinodimethane system

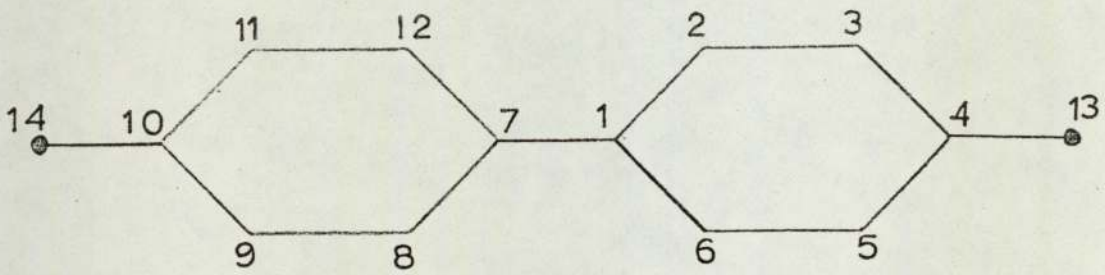


Figure 5.2

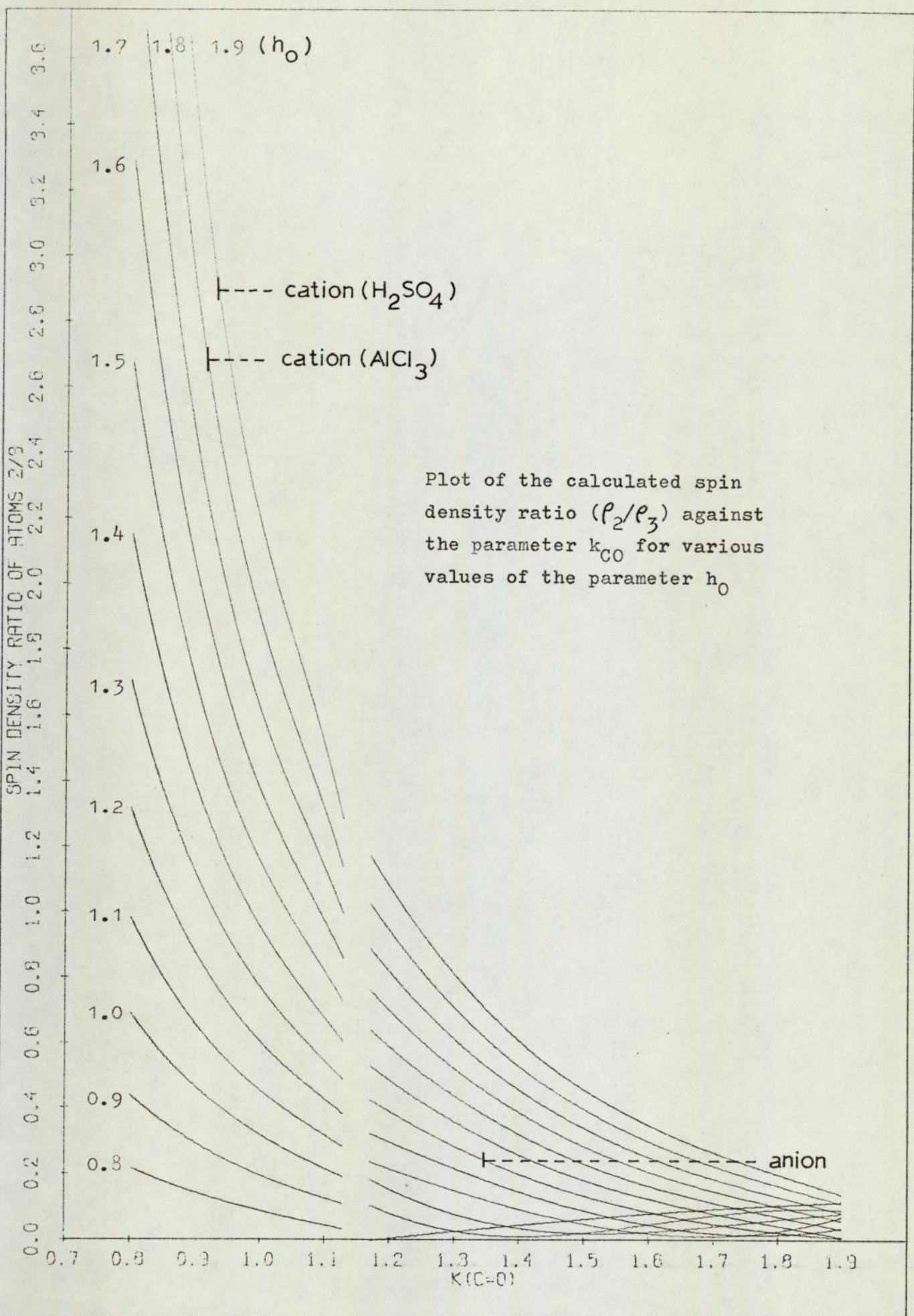


Figure 5.3



from the anion to the cation are quite reasonable and in the right directions.

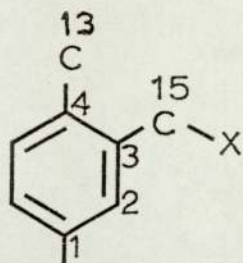
TABLE 5.3.

MINIMUM VALUES OF THE  $h_0$  and  $k_{CO}$  PARAMETERS WHICH WILL SATISFY THE EXPERIMENTAL DATA FOR 4,4'-BIPHENOSEMISQUINONE IONS AND YIELD  $Q_{CH}$  VALUES IN THE RANGE 2 - 3 mT.

Ion	Experimental ratio of spin densities on atoms 2 and 3	$h_0$	$k_{CO}$
Anion in Acetonitrile	0.238 (a)	1.3	1.35
Cation in aluminium chloride-nitromethane	2.70	1.8	0.9
Cation in concentrated sulphuric acid	2.89	1.9	0.95

(a) reference (63).

A hyperconjugative model (39) was used to describe the effect of the methyl group on the spin density distribution of the 3,3',5,5'-tetramethyl derivative of 4,4'-biphenosemiquinone anion. The methyl group is assumed to be rotating freely and treated as a two-centre grouping (XXIIIa). The values suggested by Coulson and



(XXIIIa)

Crawford (90) were used for the methyl group parameters,

$$\begin{aligned}
 h_{\text{C}(3)} &= -0.1 \\
 h_{\text{C}(15)} &= -0.1 \\
 h_{\text{X}} &= -0.5 \\
 k_{\text{CC}} &= 0.70 \\
 k_{\text{CX}} &= 2.5.
 \end{aligned}$$

Huckel calculations gave a better fit with the experimental data than the McLachlan treatment. The HMO spin densities calculated using the parameters suggested by Gendell et alia are given in table 5.4.

The effect on the spin density distribution of changing the solvent from a protic type to one which is largely aprotic (pyridine) can be accounted for by decreasing the value of the parameter  $h_{\text{O}}$ . This decrease in the effective electronegativity of the oxygen atom is in agreement with the model outlined in section 4.3.

TABLE 5.4.

Parameters	Calculated HMO spin densities	Hyperfine coupling constants
$h_o = 0.40$ $k_{CO} = 1.40$	Atom 2 : 0.0169 Atom 3 : 0.0854	$a_2 = 0.055 \text{ mT}$ $a_{CH_3} = 0.185 \text{ mT}$ (a)
$h_o = 0.90$ $k_{CO} = 1.40$	Atom 2 : 0.0251 Atom 3 : 0.0773	$a_2 = 0.080 \text{ mT}$ $a_{CH_3} = 0.160 \text{ mT}$ (b)

(a) determined in pyridine-ethanol (mole fraction of ethanol = 0.03).

(b) determined in acetonitrile-water (mole fraction of water = 0.92).

## 6. REACTIONS OF QUINONES WITH DONOR MOLECULES

### 6.1. PREVIOUS STUDIES USING ESR SPECTROSCOPY

The formation of free radical ions by the dissociation of the charge-transfer complex of tetrachloro-1,4-benzoquinone and N,N,N',N',-tetramethylbenzene-1,4-diamine (hereafter referred to as TMBD) has been demonstrated by two groups of workers (92, 93). Whilst no ESR signal was observed for solutions of the complex in solvents of low ionizing power such as benzene, a strong signal was obtained in acetonitrile. Immediately after mixing the substrates in acetonitrile the ESR absorption was consistent with the presence of the anion of tetrachloro-1,4-benzo-semiquinone and the positive ion of TMBD in the solution. However the intensity of the absorption due to the semiquinone anion rapidly decreased.

More recently Kolodny and Bowers (94) have studied the dissociation of charge-transfer complexes of 2,3-dichloro-5,6-dicyano-1,4-benzoquinone (DDQ) with benzene-1,4-diamine (BD) and TMBD using ESR spectroscopy in conjunction with a fast flow system. Again both radical cations and anions were observed in solution. However, in the system BD-DDQ in acetonitrile a third paramagnetic species was observed which was identified as either

$(\text{BD-DDQ})\cdot^-$  or  $(\text{BD}-(\text{DDQ})_2)\cdot^-$ .

Further, Maruyama et alia (95) have shown that spontaneous electron transfer from simple amines such as diethylamine to quinones such as phenanthraquinone, potassium phenanthraquinone-2-sulphonate and acenaphthene-quinone can occur in a deaerated aqueous medium. The radical anions derived from these quinones were detected using ESR spectroscopy.

## 6.2. PRESENT WORK

Iida (96) in his studies of the paramagnetic anion radical salts of 3,3',5,5'-tetrachloro- and 3,3',5,5'-tetrabromo-4,4'-biphenoquinone (hereafter referred to as TCBQ and TBBQ) has estimated that their electron affinities are 1.64 and 1.71 eV respectively. Thus TCBQ and TBBQ are good electron-acceptor molecules and should be capable of reacting with suitable donor molecules to produce radical ions. In order to test this possibility we investigated, using the ESR technique, mixtures of TCBQ or TBBQ (0.005M) with the following donor molecules (0.005M), benzene-1,4-diamine, benzidine, N,N,N',N',-tetramethylbenzidine and phenothiazine. 1,4-dioxan, dimethoxyethane, acetonitrile and ethanol were used as solvents.

Except in the case of phenothiazine the solutions did not exhibit any ESR spectra. However, benzene-1,4-diamine with both quinones gave a brown coloured solution containing a black solid, which has recently been identified by Matsunaga and Narita (97) as a 1:2 complex between the diamine and quinone. They formulated the complex as an anion-radical salt.

However, when phenothiazine and TCBQ or TBBQ are mixed in acetonitrile, dioxane or ethanol the ESR spectrum shown in figure 6.1 is obtained. This spectrum is identical to that obtained by Jackson and Patel (98) from the oxidation of phenothiazine in benzene which they attributed to the phenothiazinyl radical XXIV. They further reported that the oxidation of phenothiazine in

The ESR spectrum of an acetonitrile solution of phenothiazine  
and 3,3',5,5'-tetrachloro-4,4'-biphenylquinone

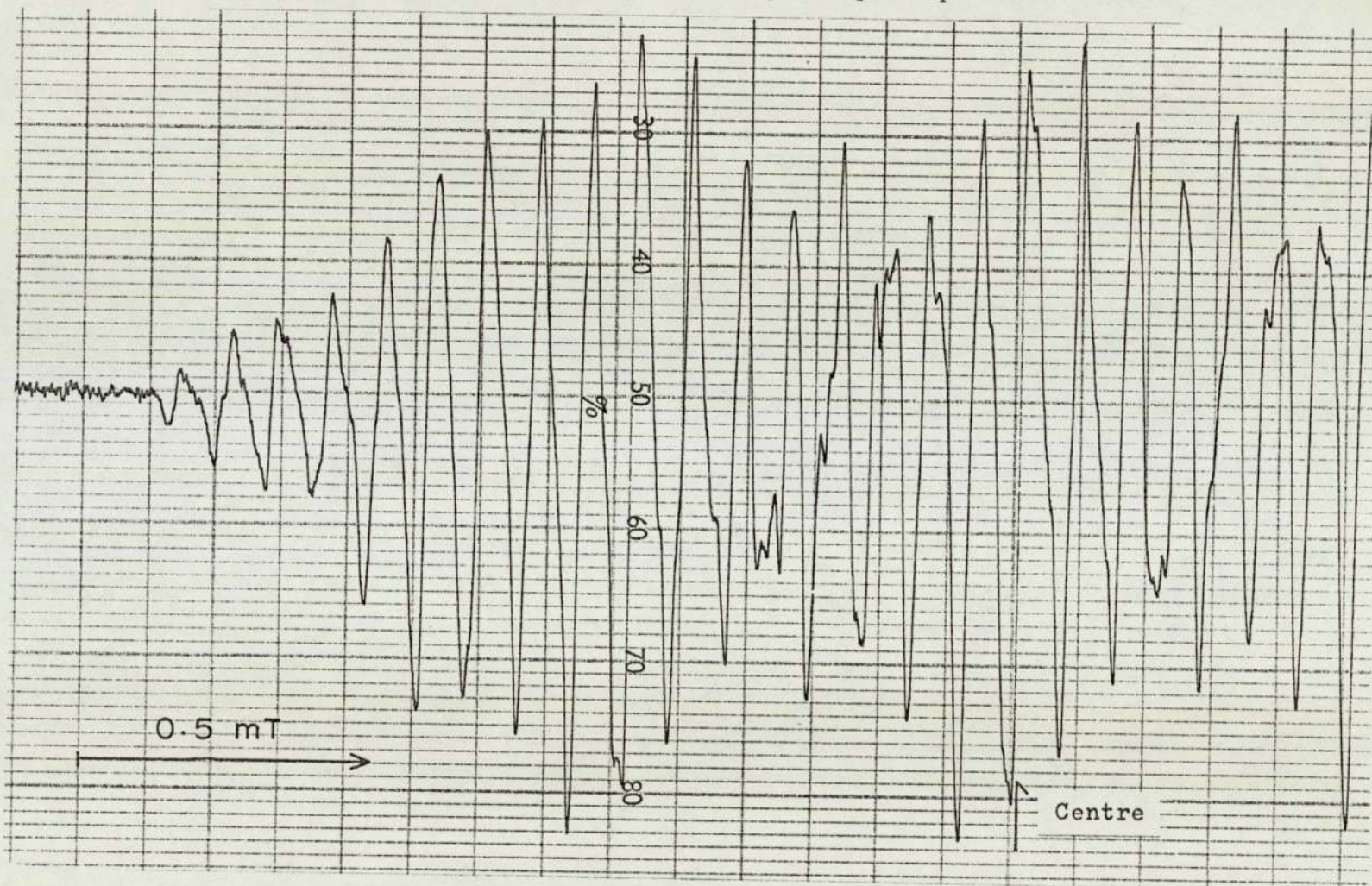
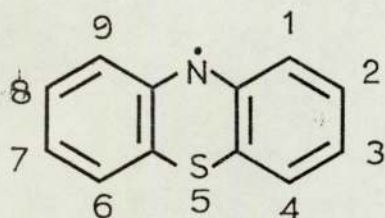


Figure 6.1

$$a^N = 0.705 \text{ mT}$$

$$a_{3,7}^H = 0.366 \text{ mT}$$



$$a_{1,9}^H = 0.285 \text{ mT}$$

$$a_{2,8}^H = 0.095 \text{ mT}$$

$$a_{4,6}^H = 0.095 \text{ mT}$$

(XXIV)

ethanol yields the same radical (XXIV) but the ESR spectrum is somewhat different which they attribute to solvent effects.

When the reaction between phenothiozine and TCBQ or TBBQ is carried out in 50% ethanoic acid the ESR spectrum is rather different from that described above is shown in figure 6.2. A similar spectrum was obtained by Gilbert et alia (99) from the oxidation of phenothiazine in acid solution. This spectrum was attributed to the phenothiazine radical-cation (XXV).

From the foregoing it would appear that the quinone is acting as an hydrogen abstraction reagent rather than an electron acceptor. However, immediately after mixing the two reactants in acetonitrile a narrow singlet can also be detected visually on the display oscilloscope



The ESR spectrum of a solution of phenothiazine  
and 3,3',5,5'-tetrachloro-4,4'-biphenone  
in 50% ethanoic acid

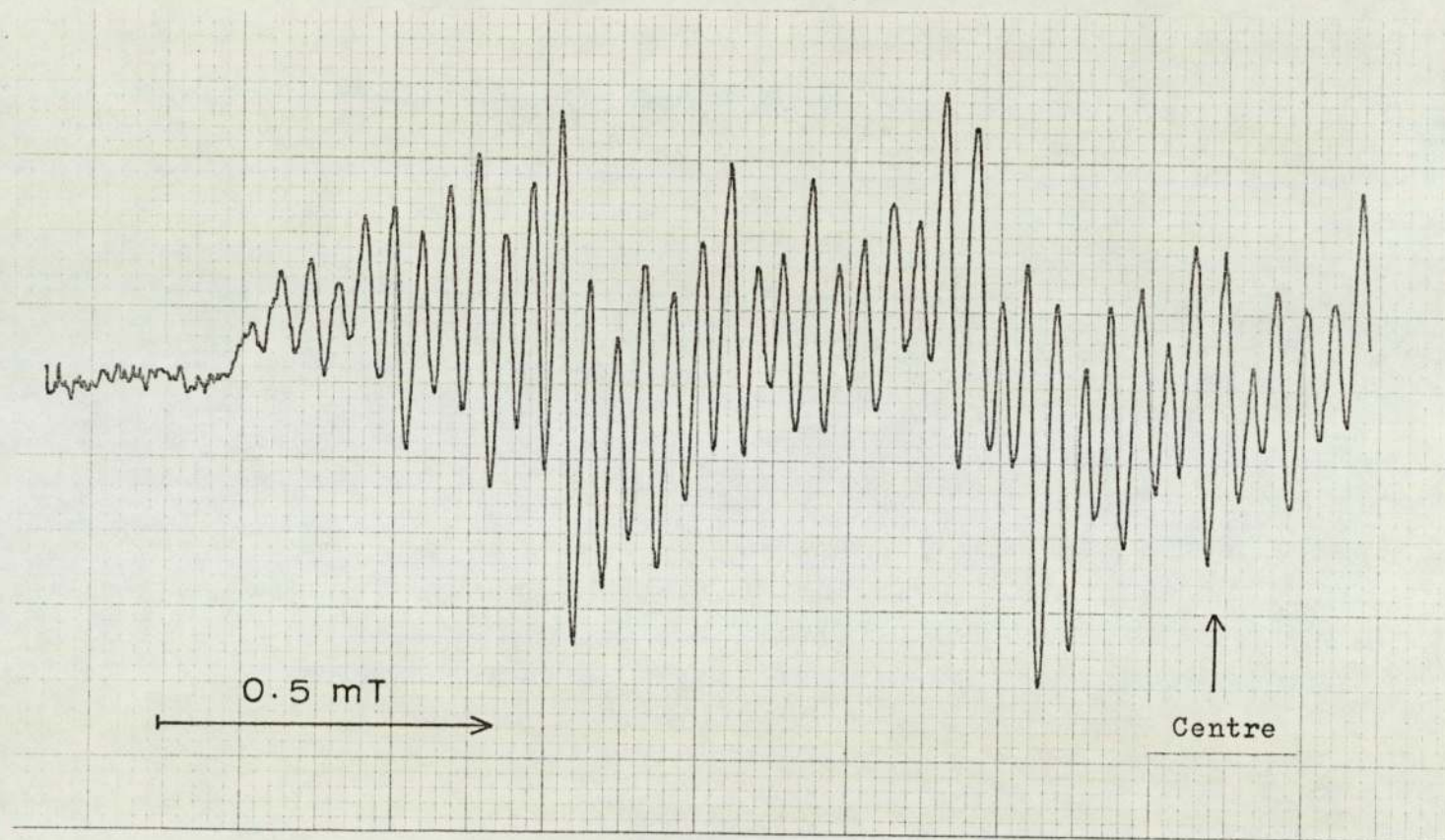
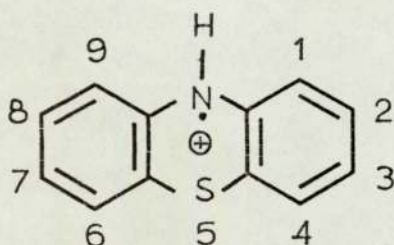


Figure 6.2

$$a^{\text{N}} = 0.652 \text{ mT}$$

$$a_{\text{NH}}^{\text{H}} = 0.736 \text{ mT}$$



$$a_{3,7}^{\text{H}} = 0.258 \text{ mT}$$

$$a_{1,9}^{\text{H}} = 0.123 \text{ mT}$$

$$a_{2,8}^{\text{H}} = 0.046 \text{ mT}$$

$$a_{4,6}^{\text{H}} = 0.046 \text{ mT}$$

(XXV)

superimposed on the more usual spectrum. It was found impossible to record this signal as within minutes of mixing the reactants it had disappeared. It would, therefore, seem that electron transfer might be taking place prior to a proton transfer. Jackson and Patel (98) have reported that phenothiazine reacts with strong electron acceptors in ethanol producing phenothiazinyl radicals together with radicals from the electron acceptor molecules. However, using ESR spectroscopy we were unable to detect any anion radicals from TCBQ, TBBQ or tetrachloro-1,4-benzoquinone.

## 7. CONCLUSIONS

Oxidation of biphenyl-4,4'-diol by 98% sulphuric acid containing a trace amount of hydrogen peroxide or potassium persulphate results in the production of a blue paramagnetic solution. The ESR signal from this solution is attributed to the 4,4'-biphenosemiquinone cation. The lack of any hyperfine coupling from the hydroxyl protons of this radical is interpreted in terms of a fast exchange of these protons with the acid. All other semiquinone cations, previously reported in the literature, exhibit an hyperfine coupling of the hydroxyl protons. When a mixture of aluminium chloride and nitromethane is used as the oxidising medium a blue paramagnetic solution is again obtained which is also attributed to the 4,4'-biphenosemiquinone cation but this time hyperfine coupling of the hydroxyl protons is observed.

When biphenyl-4,4'-diol is dissolved in the sulphuric acid prior to oxidation, sulphonation occurs. Addition of the oxidising agent produces a green paramagnetic solution containing the radical cation of 4,4'-biphenosemiquinone-3,3'-disulphonic acid. The monosulphonated cation of 1,4-benzosemiquinone can also be detected by ESR spectroscopy if 1,4-dihydroxybenzene is dissolved in sulphuric acid before the addition of the oxidising

agent. Both sulphonated and non-sulphonated radicals can also be detected using UV spectroscopy.

Reduction of 4,4'-biphenoquinone by dissolution in concentrated sulphuric acid yields a brown solution which contains the 4,4'-biphenosemiquinone cation. When dideuterosulphuric acid is used as the reaction medium there is a gradual change in the ESR spectrum from that attributed to the 4,4'-biphenosemiquinone cation to one consisting of five broad lines. This behaviour is interpreted as a stepwise exchange of the ring protons in positions 3,3',5 and 5' by deuterons. A variable temperature study of this phenomenon gives an activation energy for the overall process of  $73.3 \text{ kJ mol}^{-1}$ . 1,4-Benzoquinone behaves in a similar fashion but the process is much faster, the complete exchange is over within ten minutes of mixing a room temperature compared to three hours for 4,4'-biphenoquinone.

The 3,3',5,5'-tetrachloro- and 3,3',5,5'-tetrabromo-4,4'-biphenosemiquinone cations are easily obtained by dissolution of the corresponding quinone in sulphuric acid, the one-electron reduction being reversed by the addition of water. The ESR spectra of these cation radicals unlike the parent cation do show hyperfine coupling of the hydroxyl protons.

The cation of 3,3'-dimethyl-, 3,3',5,5'-tetramethyl and 3,3',5,5'-sec-butyl-4,4'-biphenosemiquinone produced by oxidation of the corresponding diols in aluminium chloride-nitromethane are stable at room temperature whereas the

3,3',5,5'-tetra-t-butyl analogue undergoes dealkylation to produce secondary radicals eventually culminating in the 4,4'-biphenosemiquinone cation. Secondary radicals are also produced in mixtures of sulphuric acid and nitromethane, however the final species is not the 4,4'-biphenosemiquinone cation but rather a species having three groups of four equivalent, two equivalent and two equivalent protons respectively, possibly the 3,3'-di-t-butyl-4,4'-biphenosemiquinone cation. In concentrated sulphuric acid alone the 3,3',5,5'-tetra-t-butyl-4,4'-biphenosemiquinone cation is stable, it's ESR spectrum showing hyperfine coupling due to both the ring and the hydroxyl protons.

The variation of the hyperfine coupling constants of 3,3',5,5'-tetramethyl-4,4'-biphenosemiquinone anion with the composition of the solvent mixture is interpreted in terms of an equilibrium between the semiquinone anions and hydrogen-bonded complexes of these anions with the hydroxylic solvent. Application of the solvent effect theory of Gendell, Freed and Fraentel to the equilibrium assuming that only monosolvated complexes exist and that the lifetimes of the radical species are short compared to the differences in hyperfine splittings gives a satisfactory agreement with the experimental results. Further, the equilibrium constant for the process calculated from the experimental results varies with the aprotic solvent used. This variation is correlated with the electron-donating power of the solvent,  $\Delta\nu_D$ , as measured by Kagiya et alia. An increase in the  $\Delta\nu_D$ -value of the solvent leads to a decrease in the concentration of the

hydrogen-bonded complexes. The anion of 3,3',5,5'-tetraisopropyl-4,4'-biphenosemiquinone behaves in a similar way whereas the insensitivity of the hyperfine coupling constants of the 3,3',5,5'-tetra-t-butyl-derivative to the solvent composition is attributed to the greater steric hindrance shown by the bulky t-butyl groups around the carbonyl oxygen atoms.

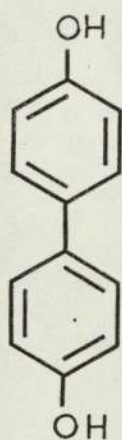
Changes in the hyperfine coupling constants between the anion and cation of 4,4'-biphenosemiquinone and between unsolvated and solvated anions of 3,3',5,5'-tetramethyl-4,4'-biphenosemiquinone are consistent with qualitative molecular orbital predictions.

Both 3,3',5,5'-tetrachloro- and 3,3',5,5'-tetrabromo-4,4'-biphenosemiquinone react with phenothiazine producing phenothiazinyl radicals in acetonitrile, 1,4-dioxan, dimethoxyethane or ethanol. When ethanoic acid is the solvent phenothiazine cation radicals are produced. It is not clear whether the process is one of electron transfer or hydrogen abstraction.

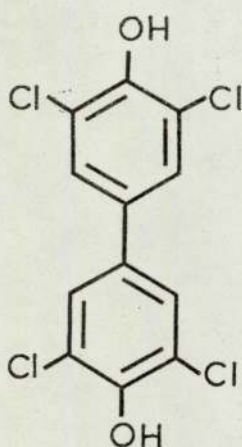
## APPENDIX 1

### NOMENCLATURE

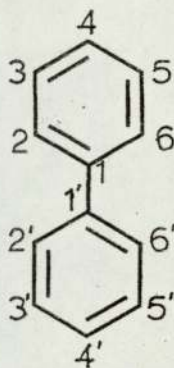
The chemical literature abounds with a variety of names for compound (XXVI) which can and indeed often does lead to some confusion when substituted derivatives are considered. Thus one may find (XXVI) called 4,4'-



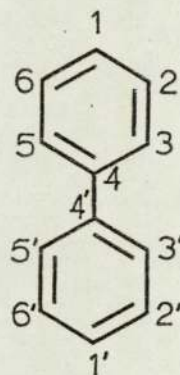
(XXVI)



(XXVII)



(XXVIII)

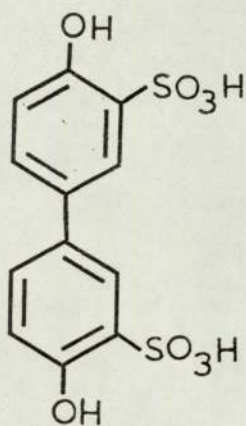


(XXIX)

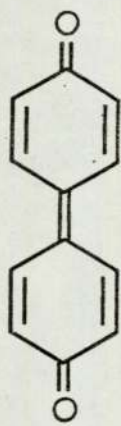
dihydroxybiphenyl, 4,4'-biphenol, p,p'-biphenol (used by Chemical Abstracts prior to 1966) or biphenyldiol (if numbers are present they may appear before or after the stem) also the prefix bi- may be replaced by di-. A result of this is that a substituted compound such as

(XXVII) can have two sets of numbers for the substituents depending on whether it is named as a derivative of biphenyl (XXVIII) or biphenol (XXIX).

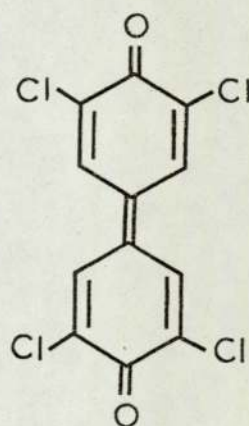
The system adopted in this thesis is based on the IUPAC rules (100) and allowing for the American convention for the positioning of numbers, it is the one now used by Chemical Abstracts. Thus compounds (XXVI) and (XXVII) are named as biphenyl-4,4'-diol and 3,3',5,5'-tetrachlorobiphenyl-4,4'-diol respectively. However, it should be noted that compound (XII) is written as 4,4'-dihydroxybiphenyl-3,3'-disulphonic acid since  $\text{SO}_3\text{H}$  ranks before OH in the list of principal groups (101).



(XII)



(XXX)



(XXXI)

Compound (XXX) is nearly always referred to in the literature as diphenoquinone and the substituents are numbered according to (XXIX) which makes compound (XXXI) 2,2',6,6'-tetrachlorodiphenoquinone. Since we are



concerned with semiquinone radicals which may be derived from either the diol or the corresponding quinone it would seem logical to keep the same numbering system for the quinone as the one used for the diol. The IUPAC report (102) suggests that a quinone should be named according to the aromatic hydrocarbon from which it is derived. Therefore, we refer to (XXX) as 4,4'-biphenoquinone and thus (XXXI) becomes 3,3',5,5'-tetrachloro-4,4'-biphenoquinone.

APPENDIX 2

ESRIM:

A Computer Program for the Simulation of ESR Spectra

'BEGIN'

'COMMENT' ESRSIM IS A PROGRAM FOR THE SIMULATION OF  
ESR SPECTRA ARISING FROM 1 TO 4 GROUPS OF  
EQUIVALENT ATOMS WITH A NUCLEAR SPIN OF 1/2  
OR 1 USING THE PAGE PACKAGE OF ALGOL GRAPHIC  
PROCEDURES

A.G.WHEWAY

JAN 1972

COMMENCEMENT OF PAGE;

```
'REAL' BREAK, XIN, YIN, XFACTOR, YFACTOR, CURRX, CURRY, STX,  
STY, FINX, FINY, HGT, STP, SLOP;  
'INTEGER' PAGES;  
'BOOLEAN' PAGING, OFFPAGE, TOPT, NEGX, NEGY, POSX, POSY;  
'PROCEDURE' CLOSEPLOT; 'EXTERNAL';  
'PROCEDURE' OPENPLOT; 'EXTERNAL';  
'PROCEDURE' STRARR(A, N, S); 'ARRAY' A; 'INTEGER' N; 'STRING' S;  
'EXTERNAL';  
'PROCEDURE' HGPDASHLN(X0, Y0, XI, YI, DI); 'VALUE' X0, Y0, XI, YI,  
DI; 'REAL' X0, Y0, XI, YI, DI; 'EXTERNAL';  
'PROCEDURE' HGPSYMBL(X, Y, HT, BCD, THETA, N); 'VALUE' X, Y, HT,  
THETA, N; 'INTEGER' N; 'ARRAY' BCD; 'REAL' X, Y, HT, THETA;  
'EXTERNAL';  
'PROCEDURE' HGPNUMBER(X, Y, HT, FL, THETA, I, IP, IQ); 'VALUE' X,  
Y, HT, FL, THETA, I, IP, IQ; 'INTEGER' I, IP, IQ; 'REAL' X, Y, HT,  
FL, THETA; 'EXTERNAL';  
'PROCEDURE' HGLOT(X, Y, A, B); 'REAL' X, Y; 'INTEGER' A, B;  
'EXTERNAL';  
'PROCEDURE' AXES(X0, Y0, DX, DY, XLAB, YLAB, NXCHARS, NYCHARS, MX,  
NX, MY, NY);  
'VALUE' X0, Y0, DX, DY, NXCHARS, NYCHARS, MX, NX, MY, NY;  
'INTEGER' NXCHARS, NYCHARS, MX, NX, MY, NY;  
'REAL' X0, Y0, DX, DY;  
'ARRAY' XLAB, YLAB;  
'BEGIN'  
'REAL' AX, AY, PX, PY, X, Y, R;  
AY:=('IF' Y0 > (FINY-STY)*0.6 'THEN' 2*HGT 'ELSE' -2*HGT;  
R:=('IF' NX=0 'THEN' (MX+2)/2 'ELSE' (MX+NX+3)/2)*0.83  
*HGT;  
VECTOR(X0, ('IF' NEGY 'THEN' STY 'ELSE' Y0, X0, ('IF' POSY 'THEN'  
FINY 'ELSE' Y0));  
VECTOR(('IF' NEGX 'THEN' STX 'ELSE' X0, Y0, ('IF' POSX 'THEN'  
FINX 'ELSE' X0, Y0));  
'FOR' X:=('IF' NEGX 'THEN' STX 'ELSE' X0)  
'STEP' DX  
'UNTIL' ('IF' POSX 'THEN' FINX 'ELSE' X0)  
'DO'  
'BEGIN'  
HGLOT(X*XFACTOR, Y0*YFACTOR+HGT/4, 3, 0);  
HGLOT(X*XFACTOR, Y0*YFACTOR-HGT/4, 2, 0);  
HGPNUMBER(X*XFACTOR-R, Y0*YFACTOR+AY, HGT, X, 0, 0,  
MX, NX);  
'END';  
AX:=('IF' X0 > (FINX-STX)*0.60 'THEN' 2*HGT 'ELSE' -2*HGT;  
R:=('IF' NY=0 'THEN' (MY+2)/2 'ELSE' (MY+NY+3)/2)*0.83  
*HGT;  
'FOR' Y:=('IF' NEGY 'THEN' STY 'ELSE' Y0)
```

```

'STEP'DY
'UNTIL'('IF'POSY'THEN'FINY'ELSE'Y0)
'DO'
'BEGIN'
  HGLOT(X0*XFACTOR+HGT/4,Y*YFACTOR,3,0);
  HGLOT(X0*XFACTOR-HGT/4,Y*YFACTOR,2,0);
  HGPNUMBER(X0*XFACTOR+AX,Y*YFACTOR-R,HGT,Y,90,0,
  MY,NY);
'END';
PX:=( 'IF'AX<0'THEN'(FINX+X0)/2'ELSE'(X0+STX)/2)*
XFACTOR-(NXCHARS/2)*0.83*HGT;
PY:='IF'AY<0'THEN'Y0*YFACTOR-3.5HGT'ELSE'
Y0*YFACTOR+3.5*HGT;
HGPSYMBL(PX,PY,HGT,XLAB,0,NXCHARS);
PX:='IF'AX<0'THEN'X0*XFACTOR-3.5HGT'ELSE'X0*XFACTOR
+3.5HGT;
PY:=( 'IF'AY<0'THEN'(FINY+Y0)/2'ELSE'(Y0+STY)/2)*
YFACTOR-(NYCHARS/2)*0.83*HGT;
HGPSYMBL(PX,PY,HGT,YLAB,90,NYCHARS);
'END' OF AXES;

'PROCEDURE' BORDER;
'BEGIN'
  VECTOR(STX,STY,FINX,STY);
  TO POINT(FINX,FINY);
  TO POINT(STX,FINY);
  TO POINT(STX,STY);
'END' OF BORDER;

'PROCEDURE' BROKEN(I);
'INTEGER'I;
BREAK:='IF'I<1'THEN'0.0'ELSE'0.5;

'PROCEDURE' CHANGE STEP(N);
'VALUE'N; 'REAL'N;
STP:=N;

'PROCEDURE' CHARACTER HEIGHT(HT);
'VALUE'HT; 'REAL'HT;
HGT:=HT*YFACTOR;

'PROCEDURE' CHANGE PAGE SIZE TO(XINCHES,YINCHES);
'VALUE'XINCHES,YINCHES; 'REAL'XINCHES,YINCHES;
'BEGIN'
  XIN:='IF'XINCHES>100'THEN'100'ELSE'XINCHES;
  YIN:='IF'YINCHES> 25'THEN' 25'ELSE'YINCHES;
'END' OF CHANGE PAGE SIZE TO;

'PROCEDURE' CURVFUNC(F,XA,XB);
'VALUE'XA,XB; 'REAL','PROCEDURE'F; 'REAL'XA,XB;
'BEGIN'
  'REAL' X,DX;
  'REAL' B;
  B:=BREAK; BREAK:=0;
  DX:=(FINX-STX)/(STP*XIN);
  VECTOR(XA,F(XA),XA+DX,F(XA+DX));
  'FOR'X:=XA+2*DX'STEP'DX'UNTIL'XB'DO'TO POINT(X,F(X));
  BREAK:=B;
'END' OF CURVFUNC;

```

```

'PROCEDURE' ELLIPSE(X,Y,A,B,DEG,PHI);
  'VALUE' A,B,X,Y,DEG,PHI; 'REAL' A,B,X,Y,DEG,PHI;
  'BEGIN'
    'REAL' TH;
    'REAL' 'PROCEDURE' XDASH(TH); 'REAL' TH;
    XDASH:=(A*COS(TH)+X)*COS(PHI);
    'REAL' 'PROCEDURE' YDASH(TH); 'REAL' TH;
    YDASH:=(B*SIN(TH)+Y)*COS(PHI);
    PHI:=DEG*3.14159/180;
    VECTOR(XDASH(0),YDASH(0),XDASH(0.1),YDASH(0.1));
    'FOR' TH:=0.1 'STEP' 0.1 'UNTIL' 6.38 'DO'
      TO POINT(XDASH(TH),YDASH(TH));
  'END' OF ELLIPSE;

'PROCEDURE' FINISH PLOTTING;
  'BEGIN'
    PAPER THROW; PRINT(PAGS,3,0);
    WRITETEXT('('PAGESZOFZGRAPHICALZOUTPUTZ
    GENERATED')');
    CLOSEPLOT;
  'END' OF FINISH PLOTTING;

'PROCEDURE' LIMITS(XMIN,YMIN,XMAX,YMAX);
  'VALUE' XMIN,YMIN,XMAX,YMAX;
  'REAL' XMIN,YMIN,XMAX,YMAX;
  'BEGIN'
    'PROCEDURE' PAGE NUMBER;
      'BEGIN'
        'ARRAY' PAGE[1:2];
        STRARR(PAGE,4,('PAGE'));
        HGPSYMBL(STX*XFACOR+0.5,FINY*YFACTOR+1.0,0.2,
        PAGE,0,4);
        HGPNUMBER(STX*XFACOR+1.3,FINY*YFACTOR+1.0,
        0.2,PAGS,0,0,2,0);
      'END' OF PAGE NUMBER;
    STX:=XMIN; STY:=YMIN; FINX:=XMAX; FINY:=YMAX;
    XFACOR:=XIN/(FINX-STX);
    YFACTOR:=YIN/(FINY-STY);
    HGLOT(STX*XFACOR,FINY*YFACTOR+2.0,0,4);
    'IF' PAGS=1 'AND' PAGING 'THEN' PAGE NUMBER;
  'END' OF LIMITS;

'PROCEDURE' MOVE TYPE TO(X,Y);
  'VALUE' X,Y; 'REAL' X,Y;
  'BEGIN'
    HGLOT(X*XFACOR,Y*YFACTOR,3,0);
    CURRX:=X; CURRY:=Y;
  'END' OF MOVE TYPE TO;

'PROCEDURE' NEXT PAGE;
  'BEGIN'
    'PROCEDURE' PAGE NUMBER;
      'BEGIN'
        'ARRAY' PAGE[1:2];
        STRARR(PAGE,4,('PAGE'));
        HGPSYMBL(STX*XFACOR+0.5,FINY*YFACTOR+1.0,0.2,
        PAGE,0,4);
        HGPNUMBER(STX*XFACOR+1.3,FINY*YFACTOR+1.0,
        0.2,PAGS,0,0,2,0);
      'END' OF PAGE NUMBER;
  'END' OF NEXT PAGE;

```

```

      'END' OF PAGE NUMBER;
HGLOT((FINX*XFACTOR)+2.0,(FINY*YFACTOR)+2.0,3,0);
HGLOT(STX*XFACTOR,FINY*YFACTOR+2.0,0,4);
PAGS:=PAGS+1;
  'IF' PAGING 'THEN' PAGE NUMBER;
  HGLOT(STX*XFACTOR,FINY*YFACTOR+2.0,3,0);
'END' OF NEXT PAGE;

'PROCEDURE' NUMBER PAGE(B);
  'BOOLEAN' B;
  PAGING:=B;

'PROCEDURE' PLOT(X,Y,N);
  'VALUE' X,Y; 'REAL' X,Y; 'INTEGER' N;
  'BEGIN'
    'REAL' XF,YF;
    'SWITCH' S:=S1,S2,S3,S4,S5,S6,S7;
    'PROCEDURE' DIAMOND(X,Y,D);
      'VALUE' X,Y,D; 'REAL' X,Y,D;
      'BEGIN'
        'INTEGER' I;
        HGLOT((X+D)*XF,Y*YF,3,0);
        'FOR' I:=1,2'DO'
          'BEGIN'
            HGLOT(X*XF,(Y+D)*YF,2,0);
            HGLOT((X-D)*XF,Y*YF,2,0);
            HGLOT(X*XF,(Y-D)*YF,2,0);
            HGLOT((X+D)*XF,Y*YF,2,0);
          'END';
        'END' OF DIAMOND;
    'PROCEDURE' CROSS(X,Y,D);
      'VALUE' X,Y,D; 'REAL' X,Y,D;
      'BEGIN'
        'INTEGER' I;
        HGLOT((X+D)*XF,(Y+D)*YF,3,0);
        'FOR' I:=1,2'DO'
          'BEGIN'
            HGLOT((X-D)*XF,(Y-D)*YF,2,0);
            HGLOT((X-D)*XF,(Y+D)*YF,3,0);
            HGLOT((X+D)*XF,(Y-D)*YF,2,0);
            HGLOT((X+D)*XF,(Y+D)*YF,3,0);
          'END';
        'END' OF CROSS;
    'PROCEDURE' PLUS(X,Y,D);
      'VALUE' X,Y,D; 'REAL' X,Y,D;
      'BEGIN'
        HGLOT(X*XF,Y*YF,3,0);
        HGLOT((X+D)*XF,Y*YF,2,0);
        HGLOT((X-D)*XF,Y*YF,2,0);
        HGLOT(X*XF,Y*YF,2,0);
        HGLOT(X*XF,(Y+D)*YF,2,0);
        HGLOT(X*XF,(Y-D)*YF,2,0);
        HGLOT(X*XF,Y*YF,2,0);
      'END' OF PLUS;
  XF:=XFACTOR; YF:=YFACTOR;
  'IF' X>FINX'OR'X<STX'OR'Y>FINY'OR'Y<STY'THEN'
  'GOTO' FIN;
  'GOTO' SEN1;

```

```

S1:          PLUS(X,Y,HGT/2);
            'GOTO'FIN;
S2:          CROSS(X,Y,HGT/2.828);
            'GOTO'FIN;
S3:          PLUS(X,Y,HGT/2); CROSS(X,Y,HGT/2.828);
            'GOTO'FIN;
S4:          PLUS(X,Y,HGT/2); DIAMOND(X,Y,HGT/2);
            'GOTO'FIN;
S5:          CROSS(X,Y,HGT/2.828); DIAMOND(X,Y,HGT/2);
S6:          PLUS(X,Y,HGT/2); DIAMOND(X,Y,HGT/2);
            CROSS(X,Y,HGT/2.828);
            'GOTO'FIN;
S7:          DIAMOND(X,Y,HGT/2); DIAMOND(X,Y,HGT/20);
FIN:        'END' OF PLOT;

```

```

'PROCEDURE' REMOVE AXIS(N);
  'INTEGER'N;
  'BEGIN'
    'IF'N=-2'THEN'NEGX:='FALSE';
    'IF'N=-1'THEN'NEGY:='FALSE';
    'IF'N= 2'THEN'POSX:='FALSE';
    'IF'N= 1'THEN'POSY:='FALSE';
    'IF'N= 0'THEN'NEGX:=POSX:=NEGY:=POSY:='TRUE';
  'END' OF REMOVE AXIS;

```

```

'PROCEDURE' START PLOTTING;
  'BEGIN'
    PAGING:='TRUE';
    OFFPAGE:=TOPT:='FALSE';
    PAGES:=1; BREAK:=0; XIN:=7.5; YIN:=7.5; HGT:=0.1;
    STP:=20;
    OPENPLOT;
  'END' OF START PLOTTING;

```

```

'PROCEDURE' TO POINT(X1,Y1);
  'VALUE'X1,Y1; 'REAL'X1,Y1;
  'BEGIN'
    'REAL' AX1,AX2,AY1,AY2;
    TOPT:='TRUE';
    AX1:=CURRX; AY1:=CURRY; AX2:=X1; AY2:=Y1;
    VECTOR(AX1,AY1,AX2,AY2);
  'END' OF TO POINT;

```

```

'PROCEDURE' TYPE NUMBER(P,M,N);
  'VALUE'P,M,N; 'REAL'P; 'INTEGER'M,N;
  'BEGIN'
    HGPNUMBER(CURRX*XFACOR,CURRY*YFACOR,HGT,P,0,0,M,N);
  'END' OF TYPE NUMBER;

```

```

'PROCEDURE' TYPE TEXT(A,N);
  'ARRAY'A; 'INTEGER'N;

```

```

'BEGIN'
  HGPSYMBL(CURRX*XFACTOR, CURRY*YFACTOR, HGT, A, 0.0, N);
'END' OF TYPE TEXT;

'PROCEDURE' VECTOR(X1, Y1, X2, Y2);
  'VALUE' X1, Y1, X2, Y2; 'REAL' X1, Y1, X2, Y2;
  'BEGIN'
    'REAL' DI, CX1, CX2, CY1, CY2;
    'PROCEDURE' ADJUST(A, B, C, D, FS);
      'VALUE' C, D, FS; 'REAL' A, B, C, D, FS;
      'BEGIN'
        A:=FS;
        B:=(FS-C)/SLOP+D;
        OFFPAGE:='TRUE';
      'END' OF ADJUST;
    DI:='IF' BREAK=0 'THEN' 0.0 'ELSE' 0.5;
    SLOP:='IF' ABS((X2-X1)*XFACTOR)<1E-5 'THEN'
      (Y2-Y1)/(XFACTOR*1E-5) 'ELSE' (Y2-Y1)/(X2-X1);
    CX1:=X1; CX2:=X2; CY1:=Y1; CY2:=Y2;
    'IF' (CX1>FINX 'AND' CX2>FINX) 'OR' (CX1<STX 'AND' CX2<STX)
    'OR' (CY1>FINY 'AND' CY2>FINY) 'OR' (CY1<STY 'AND' CY2<STY)
    'THEN' 'GOTO' FIN;
    'IF' CX2>FINX 'THEN' ADJUST(CX2, CY2, CX1, CY1, FINX);
    'IF' CX1<STX 'THEN' ADJUST(CX1, CY1, CX1, CY1, STX);
    'IF' CX1>FINX 'THEN' ADJUST(CX1, CY1, CX2, CY2, FINX);
    'IF' CX2<STX 'THEN' ADJUST(CX2, CY2, CX2, CY2, STX);
    'IF' CY2>FINY 'THEN' ADJUST(CY2, CX2, CY1, CX1, FINY);
    'IF' CY1<STY 'THEN' ADJUST(CY1, CX1, CY1, CX1, STY);
    'IF' CY1>FINY 'THEN' ADJUST(CY1, CX1, CY2, CX2, FINY);
    'IF' CY2<STY 'THEN' ADJUST(CY2, CX2, CY2, CX2, STY);
    'IF' CX1=CX2 'AND' CY1=CY2 'AND' 'NOT' TOPT 'THEN'
    CX1:=CX1-0.001/XFACTOR;
    'IF' 'NOT' TOPT 'THEN'
    HGPDASHLN(CX1*XFACTOR, CY1*YFACTOR, CX2*XFACTOR,
    CY2*YFACTOR, DI);
    'ELSE'
    'BEGIN'
      'IF' OFFPAGE 'THEN'
      HGPlot(CX2*XFACTOR, CY2*YFACTOR, 3, 0)
      'ELSE'
      HGPlot(CX2*XFACTOR, CY2*YFACTOR, 2, 0);
    'END';
  'END' OF VECTOR AND PAGE;

FIN:
  CURRX:=X2; CURRY:=Y2;
  OFFPAGE:=TOPT:='FALSE';
'END' OF VECTOR AND PAGE;

'REAL' X, XA, XB, XMIN, XMAX, DX, YMIN, YMAX, LW;
'INTEGER' C, D, Q, CONTROL, NUMBER;
'REAL' 'PROCEDURE' SIGMA(Z, I, P);
  'REAL' Z; 'INTEGER' I, P;
  'BEGIN'
    'REAL' SUM;
    SUM:=0;
    'FOR' I:=0 'STEP' 1 'UNTIL' P 'DO'
    SUM:=SUM+Z;
    SIGMA:=SUM;
  'END' OF SIGMA;

```



```

'REAL' 'PROCEDURE' MINMAX(FX);
  'REAL' 'PROCEDURE' FX;
  'BEGIN'
    'REAL' Y;
    YMIN:=YMAX:=0;
    'FOR' X:=XA 'STEP' DX 'UNTIL' XB 'DO'
      'BEGIN'
        Y:=FX(X);
        'IF' Y>YMAX 'THEN' YMAX:=Y 'ELSE'
        'IF' Y<YMIN 'THEN' YMIN:=Y;
      'END';
    'END' OF MINMAX;

'PROCEDURE' PMULTIPLICITIES(A,B,N,R,D);
  'INTEGER' 'ARRAY' A,B; 'INTEGER' N,R,D;
  'BEGIN'
    'INTEGER' I,J;
    'FOR' I:=0 'STEP' 1 'UNTIL' N 'DO'
      'FOR' J:=- (N+1) 'STEP' 1 'UNTIL' N+1 'DO'
        A[I,J]:=0;
        A[0,0]:=1;
        'IF' N=0 'THEN' 'GOTO' TRIVIAL;
        'FOR' I:=1 'STEP' 1 'UNTIL' N 'DO'
          'FOR' J:=-1 'STEP' 2 'UNTIL' 1 'DO'
            A[I,J]:=A[I-1,J-1]+A[I-1,J+1];
TRIVIAL:
        'FOR' R:=0 'STEP' 1 'UNTIL' N 'DO'
          B[D,R]:=A[N,2*R-N];
    'END' OF PMULTIPLICITIES;

'PROCEDURE' DNMULTIPLICITIES(A,B,N,R,D);
  'INTEGER' 'ARRAY' A,B; 'INTEGER' N,R,D;
  'BEGIN'
    'INTEGER' I,J;
    'FOR' I:=1 'STEP' 1 'UNTIL' N 'DO'
      'FOR' J:=- (N+1) 'STEP' 1 'UNTIL' N+1 'DO'
        A[I,J]:=0;
        A[1,-1]:=A[1,0]:=A[1,1]:=1;
        'IF' N=1 'THEN' 'GOTO' TRIVIAL;
        'FOR' I:=2 'STEP' 1 'UNTIL' N 'DO'
          'FOR' J:=-1 'STEP' 1 'UNTIL' 1 'DO'
            A[I,J]:=A[I-1,J-1]+A[I-1,J]+A[I-1,J+1];
TRIVIAL:
        'FOR' R:=0 'STEP' 1 'UNTIL' 2*N 'DO'
          B[D,R]:=A[N,R-N];
    'END' OF DNMULTIPLICITIES;

START PLOTTING;
NEWSPEC:
Q:=READ;
'BEGIN'
  'INTEGER' 'ARRAY' N,R[1:Q];
  'REAL' 'ARRAY' SPIN,K[1:Q];
  'FOR' D:=1 'STEP' 1 'UNTIL' Q 'DO'
    N[D]:=READ;
  'FOR' D:=1 'STEP' 1 'UNTIL' Q 'DO'
    SPIN[D]:=READ;

```

```

'BEGIN'
  'INTEGER' 'ARRAY' 'N(0:N(1)), -(N(1)+1):(N(1)+1)),
  B(1:0,0:2*N(1));
  'COMMENT' 'N(1) MUST HAVE THE LARGEST VALUE FOR THE
  ABOVE DECLARATIONS TO BE CORRECT;
  'REAL' 'PROCEDURE' GAUSSTWO(X);
    'REAL' X;
    GAUSSTWO:=-SIGMA(SIGMA(B(1,RC(1))*B(2,RC(2))/LW*(X
    -(N(1)*SPIN(1)-RC(1))*K(1)-(N(2)*SPIN(2)-RC(2))*K(
    2))*EXP(-LN(2)/LW+2*(X-(N(1)*SPIN(1)-RC(1))*K(1)-
    (N(2)*SPIN(2)-RC(2))*K(2)),2),RC(1),N(1)*2*SPIN(1)
    ),RC(2),N(2)*2*SPIN(2));

  'REAL' 'PROCEDURE' LORENTZTWO(X);
    'REAL' X;
    LORENTZTWO:=-SIGMA(SIGMA(B(1,RC(1))*B(2,RC(2))/LW*
    (X-(N(1)*SPIN(1)-RC(1))*K(1)-(N(2)*SPIN(2)-RC(2))*
    K(2))/((1+((X-(N(1)*SPIN(1)-RC(1))*K(1)-(N(2)*SPI
    N(2)-RC(2))*K(2))/LW))2),2),RC(1),N(1)*2*SPIN(1),
    RC(2),N(2)*2*SPIN(2));

  'REAL' 'PROCEDURE' GAUSSTHREE(X);
    'REAL' X;
    GAUSSTHREE:=-SIGMA(SIGMA(SIGMA(B(1,RC(1))*B(2,RC(2)
    )*B(3,RC(3))/LW*(X-(N(1)*SPIN(1)-RC(1))*K(1)-(N(2)
    )*SPIN(2)-RC(2))*K(2)-(N(3)*SPIN(3)-RC(3))*K(3))*E
    XP(-LN(2)/LW+2*(X-(N(1)*SPIN(1)-RC(1))*K(1)-(N(2)
    )*SPIN(2)-RC(2))*K(2)-(N(3)*SPIN(3)-RC(3))*K(3)),2)
    ,RC(1),N(1)*2*SPIN(1),RC(2),N(2)*2*SPIN(2),RC(3),
    N(3)*2*SPIN(3));

  'REAL' 'PROCEDURE' LORENTZTHREE(X);
    'REAL' X;
    LORENTZTHREE:=-SIGMA(SIGMA(SIGMA(B(1,RC(1))*B(2,R
    C(2))*B(3,RC(3))/LW*(X-(N(1)*SPIN(1)-RC(1))*K(1)-(N
    (2)*SPIN(2)-RC(2))*K(2)-(N(3)*SPIN(3)-RC(3))*K(3))
    /((1+((X-(N(1)*SPIN(1)-RC(1))*K(1)-(N(2)*SPIN(2)-
    RC(2))*K(2)-(N(3)*SPIN(3)-RC(3))*K(3))/LW))2),2),R
    C(1),N(1)*2*SPIN(1),RC(2),N(2)*2*SPIN(2),RC(3),N(
    3)*2*SPIN(3));

  'REAL' 'PROCEDURE' GAUSSFOUR(X);
    'REAL' X;
    GAUSSFOUR:=-SIGMA(SIGMA(SIGMA(SIGMA(B(1,RC(1))*B(
    2,RC(2))*B(3,RC(3))*B(4,RC(4))/LW*(X-(N(1)*SPIN(1)-
    RC(1))*K(1)-(N(2)*SPIN(2)-RC(2))*K(2)-(N(3)*SPIN(3)
    )-RC(3))*K(3)-(N(4)*SPIN(4)-RC(4))*K(4))*EXP(-LN(2)
    )/LW+2*(X-(N(1)*SPIN(1)-RC(1))*K(1)-(N(2)*SPIN(2)
    )-RC(2))*K(2)-(N(3)*SPIN(3)-RC(3))*K(3)-(N(4)*SPIN(
    4)-RC(4))*K(4)),2),RC(1),N(1)*2*SPIN(1),RC(2),N(2)
    )*2*SPIN(2),RC(3),N(3)*2*SPIN(3),RC(4),N(4)*2*SPI
    N(4));

  'REAL' 'PROCEDURE' LORENTZFOUR(X);
    'REAL' X;
    LORENTZFOUR:=-SIGMA(SIGMA(SIGMA(SIGMA(B(1,RC(1))*
    B(2,RC(2))*B(3,RC(3))*B(4,RC(4))/LW*(X-(N(1)*SPIN(1)
    )-RC(1))*K(1)-(N(2)*SPIN(2)-RC(2))*K(2)-(N(3)*SPIN
  
```

```

(3)-R(3))*K(3)-(N(4)*SPIN(4)-R(4))*K(4))/(1+((X
-(N(1)*SPIN(1)-R(1))*K(1)-(N(2)*SPIN(2)-R(2))*K
2)-(N(3)*SPIN(3)-R(3))*K(3)-(N(4)*SPIN(4)-R(4))*
K(4))/L(1)+2)+2),R(1),N(1)*2*SPIN(1),R(2),N(2)*2
*SPIN(2),R(3),N(3)*2*SPIN(3),R(4),N(4)*2*SPIN
4);

```

```

'SWITCH' S:=GTWO,GTHREE,GFOUR,LTWO,LTHREE,LFOUR;
'SWITCH' SS:=GCTWO,GCTHREE,GCFOUR,LCTWO,LCTHREE,LCFOUR;
'FOR'D:=1'STEP'1'UNTIL'Q'DJ'
'IF'SPIN(D)=1'THEN'DNMULTIPLICITIES(A,B,N(D),R(D),D)
'ELSE'
PMULTIPLICITIES(A,B,N(D),R(D),D);

```

ALTERHFS:

```

'FOR'D:=1'STEP'1'UNTIL'Q'DJ'
K(D):=READ;
XA:=READ; DX:=READ; XB:=READ;

```

ADJUSTLINEW:

```
LW:=READ;
```

CHANGESHAPE:

```

C:=READ;
'GOTO'S(C);

```

GTWO:

```

MINMAX(GAUSSTWO);
'GOTO'CARRYON;

```

GTHREE:

```

MINMAX(GAUSSTHREE);
'GOTO'CARRYON;

```

GFOUR:

```

MINMAX(GAUSSFOUR);
'GOTO'CARRYON;

```

LTWO:

```

MINMAX(LORENTZTWO);
'GOTO'CARRYON;

```

LTHREE:

```

MINMAX(LORENTZTHREE);
'GOTO'CARRYON;

```

LFOUR:

```

MINMAX(LORENTZFOUR);

```

CARRYON:

```

CHANGE PAGE SIZE TO(9,6);
CHANGE STEP(50);
XMIN:=READ; XMAX:=READ; NUMBER:=READ;
LIMITS(XMIN,YMIN,XMAX,YMAX);
'GOTO'SS(C);

```

GCTWO:

```

CURVFUNC(GAUSSTWO,XMIN,XMAX);
'GOTO'NEXT;

```

GCTHREE:

```

CURVFUNC(GAUSSTHREE,XMIN,XMAX);
'GOTO'NEXT;

```

GCFOUR:

```

CURVFUNC(GAUSSFOUR,XMIN,XMAX);
'GOTO'NEXT;

```

LCTWO:

```

CURVFUNC(LORENTZTWO,XMIN,XMAX);
'GOTO'NEXT;

```

```

LCTHREE:
    CURVFUNC(LORENTZTHREE,XMIN,XMAX);
    'GOTO'NEXT;
LCFOUR:
    CURVFUNC(LORENTZFOUR,XMIN,XMAX);
NEXT:
    MOVE TYPE TO(XMAX,YMAX);
    TYPE NUMBER(NUMBER,3,0);
    NEXT PAGE;
    CONTROL:=READ;
    'IF'CONTROL=1'THEN''GOTO'CARRYON;
    'IF'CONTROL=2'THEN''GOTO'CHANGESHAPE;
    'IF'CONTROL=3'THEN''GOTO'ADJUSTLINEW;
    'IF'CONTROL=4'THEN''GOTO'ALTERHFS;
    'END';
    'END';
    'IF'CONTROL=5'THEN''GOTO'NEWSPEC
    'ELSE'
    WRITETEXT('('('C')'PROGRAM%COMPLETED')');
    FINISH PLOTTING;
    'END' OF PROGRAM;

```

APPENDIX 3

MOLORB 2:

A computer Program for the Calculation of HMO and  
McLachlan Modified HMO Spin Densities for Conjugated  
Free Radicals

'BEGIN'

'COMMENT' MOLORB 2 IS A PROGRAM FOR THE CALCULATION OF  
HMO AND MCLACHLAN MODIFIED HMO SPIN DENSITIES  
OF CONJUGATED FREE RADICALS

A.G.WHEWAY  
MARCH 1972;

'REAL' H,H1,H2,DH,K,K1,K2,DK;  
'INTEGER' N,ROT,I,J,R,S,ORB;  
'BOOLEAN' EIVEC,EIGENVEC,RHOVAL;  
'ARRAY' TITLE[1:20],DATE[1:10];  
'PROCEDURE' INSTRARR(STR,A);  
  'String' STR; 'ARRAY' A; 'EXTERNAL';  
'PROCEDURE' ARRTEXT(A);  
  'ARRAY' A; 'EXTERNAL';  
'PROCEDURE' JACOBI(N,EIVEC,A,D,V,ROT);  
  'VALUE' N,EIVEC; 'INTEGER' N,ROT; 'BOOLEAN' EIVEC;  
  'ARRAY' A,D,V;  
  'BEGIN'

    'REAL' SM,C,S,T,H,G,TAU,THETA,TRESH;  
    'INTEGER' P,Q,I,J;  
    'ARRAY' B,Z[1:N];

PROGRAM:

  'IF' EIVEC 'THEN'  
    'FOR' P:=1 'STEP' 1 'UNTIL' N 'DO'  
      'FOR' Q:=1 'STEP' 1 'UNTIL' N 'DO'  
        VIP,QJ:='IF' P=Q 'THEN' 1.0 'ELSE' 0.0;  
        'FOR' P:=1 'STEP' 1 'UNTIL' N 'DO'  
          'BEGIN'  
            B[P]:=D[P]:=A[P,P];  
            Z[P]:=0;  
          'END';  
        ROT:=0;  
        'FOR' I:=1 'STEP' 1 'UNTIL' 50 'DO'

SWP:

  'BEGIN'  
    SM:=0;  
    'FOR' P:=1 'STEP' 1 'UNTIL' N-1 'DO'  
      'FOR' Q:=P+1 'STEP' 1 'UNTIL' N 'DO'  
        SM:=SM+ABS(A[P,Q]);  
        'IF' SM=0 'THEN' 'GOTO' OUT;  
        TRESH:='IF' I<4 'THEN' 0.2\*SM/N+2 'ELSE' 0.0;  
        'FOR' P:=1 'STEP' 1 'UNTIL' N-1 'DO'  
          'FOR' Q:=P+1 'STEP' 1 'UNTIL' N 'DO'  
            'BEGIN'  
              G:=100\*ABS(A[P,Q]);  
              'IF' I>4 'AND' ABS(D[P])+G=ABS(D[P]) 'AND'  
              ABS(D[Q])+G=ABS(D[Q]) 'THEN' A[P,Q]:=0  
              'ELSE'  
              'IF' ABS(A[P,Q])>TRESH 'THEN'  
                'BEGIN'  
                  H:=D[Q]-D[P];  
                  'IF' ABS(H)+G=ABS(H) 'THEN' T:=A[P,Q]/H  
                  'ELSE'  
                  'BEGIN'  
                    THETA:=0.5\*H/A[P,Q];

```

      T:=1/(ABS(THETA)+SQRT(1+THETA*2));
      'IF' THETA<0 'THEN' T:=-T;
'END' OF COMPUTING TAN OF ROTATION ANGLE;
C:=1/SQRT(1+T*2);
S:=T*C;
TAU:=S/(1+C);
H:=T*A[P,Q];
Z[P]:=Z[P]-H;
Z[Q]:=Z[Q]+H;
D[P]:=D[P]-H;
D[Q]:=D[Q]+H;
A[P,Q]:=0;
'FOR' J:=1 'STEP' 1 'UNTIL' P-1 'DO'
'BEGIN'
  G:=A[J,P]; H:=A[J,Q];
  A[J,P]:=G-S*(H+G*TAU);
  A[J,Q]:=H+S*(G-H*TAU);
'END' OF CASE 1 LESS THAN OR EQUAL TO J<P;
'FOR' J:=P+1 'STEP' 1 'UNTIL' Q-1 'DO'
'BEGIN'
  G:=A[P,J]; H:=A[J,Q];
  A[P,J]:=G-S*(H+G*TAU);
  A[J,Q]:=H+S*(G-H*TAU);
'END' OF CASE P<J<Q;
'FOR' J:=Q+1 'STEP' 1 'UNTIL' N 'DO'
'BEGIN'
  G:=A[P,J]; H:=A[Q,J];
  A[P,J]:=G-S*(H+G*TAU);
  A[Q,J]:=H+S*(G-H*TAU);
'END' OF CASE Q<J LESS THAN OR EQUAL TO N;
'IF' EIVEC 'THEN'
'FOR' J:=1 'STEP' 1 'UNTIL' N 'DO'
'BEGIN'
  G:=V[J,P]; H:=V[J,Q];
  V[J,P]:=G-S*(H+G*TAU);
  V[J,Q]:=H+S*(G-H*TAU);
'END' OF CASE V;
  ROT:=ROT+1;
'END' OF ROTATE;
'END';
'FOR' P:=1 'STEP' 1 'UNTIL' N 'DO'
'BEGIN'
  D[P]:=B[P]:=B[P]+Z[P];
  Z[P]:=0;
'END' OF P;
'END' OF SWP;
OUT:
'END' OF JACOBI;

'PROCEDURE' SWAP(A,B);
'REAL' A,B;
'BEGIN'
  'REAL' S;
  S:=A; A:=B; B:=S;
'END' OF SWAP;

```

```

'PROCEDURE' SORTOP(D,V,N);
  'REAL' 'ARRAY' D,V;
  'INTEGER' N;
  'BEGIN'
    'COMMENT' SORT IN ASCENDING ORDER BY SHELL METHOD;
    'INTEGER' A,K,H,L,H1,L1,P;
    A:=1;
REPEAT:
  A:=2*A;
  K:=N/'A;
  'IF' K=0 'THEN' 'GOTO' EXIT;
  L:=1; H:=K+1;
CONTINUE:
  'IF' H>N 'THEN' 'GOTO' REPEAT;
  L1:=L; H1:=H;
COMPARE:
  'IF' D[L1]>D[H1] 'THEN'
  'BEGIN'
    SWAP(D[L1],D[H1]);
    'FOR' P:=1 'STEP' 1 'UNTIL' N 'DO'
      SWAP(V[P],L1,V[P],H1);
    L:=L-K;
    'IF' L'GE' 1 'THEN'
    'BEGIN'
      H:=H-K;
      'GOTO' COMPARE;
    'END';
  'END';
NEXT:
  L:=L1+1;
  H:=H1+1;
  'GOTO' CONTINUE;
EXIT:
  'END' OF SORTOP;

```

```

'REAL' 'PROCEDURE' SIGMA(X,I,M,N);
  'VALUE' M,N; 'INTEGER' I,M,N; 'REAL' X;
  'BEGIN'
    'REAL' SUM;
    SUM:=0;
    'FOR' I:=M 'STEP' 1 'UNTIL' N 'DO'
      SUM:=SUM+X;
    SIGMA:=SUM;
  'END' OF SIGMA;

```

```

N:=READ; ORB:=READ;
H1:=READ; DH:=READ; H2:=READ;
K1:=READ; DK:=READ; K2:=READ;
EIVEC:=READBOOLEAN; EIGENVEC:=READBOOLEAN;
RHOVAL:=READBOOLEAN;
INSTRARR(('**'),'TITLE);
INSTRARR(('**'),'DATE);

```

```

WRITETEXT(('('205')'*****
('C 205')'MOLECULARZORBITAL%CALCULATIONS('C 205')'
*****'));

```



```

NEWLINE(2); SPACE(20);
ARRTEXT(TITLE);
NEWLINE(2); SPACE(20);
ARRTEXT(DATE);
PAPERTHROW;
'BEGIN'
  'COMMENT' START OF INNER BLOCK;
  'ARRAY' D,SPINDEN,RHO[1:N], A,V,PI[1:N,1:N];
  'REAL''PROCEDURE' ATOM POLARISABILITY(M,N,S,R);
    'VALUE'M,N,S,R;
    'INTEGER'M,N,S,R;
    ATOM POLARISABILITY:=4*SIGMA(SIGMA(V[M,R]*V[N,R]*
    V[M,S]*V[N,S]/(D[S]-D[R]),S,8,14),R,1,7);

  'REAL''PROCEDURE' RHO VALUE(I,J);
    'VALUE'I,J;
    'INTEGER'I,J;
    RHO VALUE:=SPINDEN[I]+1.2*SIGMA(PI[I,J]*SPINDEN[J],
    J,1,14);

  'PROCEDURE' PRINT EIGENVALUES AND VECTORS;
  'BEGIN'
    WRITETEXT('('('C')'H=)');
    PRINT(H,1,2);
    WRITETEXT('('('S')'K=)');
    PRINT(K,1,2);
    WRITETEXT('('('C 40S')'EIGENVECTORS)');
    WRITETEXT('('('C 3S')'EIGENVALUESZZZZZ1'('11S
    ') '2'('11S') '3'('11S') '4'('11S') '5'('11S') '6'('
    11S') '7')');
    'FOR'I:=1'STEP'1'UNTIL'N'DO'
  'BEGIN'
    NEWLINE(1); SPACE(5);
    PRINT(D[I],1,4);
    'FOR'J:=1'STEP'1'UNTIL'7'DO'
    PRINT(V[J,I],4,4);
  'END';
    WRITETEXT('('('C 3S')'EIGENVALUESZZZZZZ8'('11S
    ') '9'('11S') '10'('10S') '11'('10S') '12'('10S') '13
    '('10S') '14')');
    'FOR'I:=1'STEP'1'UNTIL'N'DO'
  'BEGIN'
    NEWLINE(1); SPACE(5);
    PRINT(D[I],1,4);
    'FOR'J:=8'STEP'1'UNTIL'14'DO'
    PRINT(V[J,I],4,4);
  'END';
  'END' OF PRINT EIGENVALUES AND VECTORS;

  'PROCEDURE' PRINT RHO VALUES;
  'BEGIN'
    WRITETEXT('('('C 3S')'RHOZVALUES)');
    NEWLINE(1);
    'FOR'I:=1'STEP'1'UNTIL'7'DO'
    PRINT(RHO[I],5,4);
    NEWLINE(1);

```

```

      'FOR' I:=8 'STEP' 1 'UNTIL' 14 'DO'
      PRINT(RHO[I],5,4);
    'END' OF PRINT RHO VALUES;

'PROCEDURE' SUMMARISE;
  'BEGIN'
    WRITETEXT('('('C 17S')'RHO'('7S')'SPINZDENSITY')');
    'FOR' I:=1,2,3,4,13 'DO'
      'BEGIN'
        RHO[I]:=RHO VALUE(I,J);
        NEWLINE(1);
        SPACE(4);
        PRINT(I,2,0);
        SPACE(5);
        PRINT(RHO[I],1,4);
        SPACE(5);
        PRINT(SPINDEN[I],1,4);
      'END';
    'END' OF SUMMARISE;

'FOR' H:=H1 'STEP' DH 'UNTIL' H2 'DO'
'FOR' K:=K1 'STEP' DK 'UNTIL' K2 'DO'
'BEGIN'
  'FOR' I:=1 'STEP' 1 'UNTIL' N 'DO'
  'FOR' J:=1 'STEP' 1 'UNTIL' I 'DO'
  'COMMENT' THE NEXT 4 STATEMENTS ABOUT THE ARRAY
            AC(I,J) ARE CORRECT ONLY FOR THE
            DIPHENQUINODIMETHANE SYSTEM;
  AC(I,J):=AC(J,I):=0.0;
  AC(1,2):=AC(1,6):=AC(1,7):=AC(2,1):=AC(2,3):=AC(3,2):=AC
  3,4):=AC(4,3):=AC(4,5):=AC(5,4):=AC(5,6):=AC(6,1):=AC(6,
  5):=AC(7,1):=AC(7,8):=AC(7,12):=AC(8,7):=AC(8,9):=AC(9,8
  ):=AC(9,10):=AC(10,9):=AC(10,11):=AC(11,10):=AC(11,12):
  =AC(12,7):=AC(12,11):=1.0;
  AC(13,13):=AC(14,14):=H;
  AC(4,13):=AC(13,4):=AC(10,14):=AC(14,10):=K;
  JACOBI(N,EI,VEC,A,D,V,ROT);
  'FOR' I:=1 'STEP' 1 'UNTIL' N 'DO'
  D[I]:=-D[I];
  'IF' EI,VEC 'THEN' SORTOP(D,V,N)
  'ELSE'
  'BEGIN'
    WRITETEXT('('('C')'EIGENVALUES')');
    'FOR' I:=1 'STEP' 1 'UNTIL' N 'DO'
      'BEGIN'
        NEWLINE(1);
        PRINT(D[I],5,4);
      'END';
    'GOTO' EIGENVALUES ONLY;
  'END';
  'IF' EIGENVEC 'THEN' PRINT EIGENVALUES AND VECTORS;
  'FOR' I:=1 'STEP' 1 'UNTIL' N 'DO'
  'FOR' J:=1 'STEP' 1 'UNTIL' N 'DO'
  PII(I,J):=PI(J,I):=ATOM POLARISABILITY(I,J,S,R);
  'FOR' I:=1 'STEP' 1 'UNTIL' N 'DO'
  SPINDEN[I]:=V(I,ORB)**2;

```

```
'IF' RHOVAL 'THEN'  
'BEGIN'  
  'FOR' I:=1 'STEP' 1 'UNTIL' N 'DO'  
    RHO(I,J):=RHO VALUE(I,J);  
    PRINT RHO VALUES;  
  'END'  
  'ELSE' SUMMARISE;  
EIGENVALUES ONLY:  
  'END' OF K;  
  'END' OF INNER BLOCK;  
'END' OF PROGRAM;
```

## BIBLIOGRAPHY

1. L. MICHAELIS, J. Biol. Chem. 92, 211 (1931).
2. L. MICHAELIS, Chem. Revs. 16, 243 (1935).
3. L. MICHAELIS, M.P. SCHUBERT, R.K. REBER, J.A. KUCK  
and S. GRANICK, J. Am. Chem. Soc. 60, 1678 (1938).
4. L. MICHAELIS and M.P. SCHUBERT, Chem. Revs. 22,  
437 (1938).
5. L. MICHAELIS, Ann. N.Y. Acad. Sci. 40, 39 (1940).
6. L. MICHAELIS and S. GRANICK, J. Am. Chem. Soc.  
70, 624 (1948).
7. B. VENKATARAMAN and G.K. FRAENKEL, J. Chem. Phys.  
23, 988 (1955).
8. R. HOSKINS, J. Chem. Phys. 23, 1975 (1955).
9. T.J. STONE and W.A. WATERS, J. Chem. Soc. 1964, 4302.
10. T.J. STONE and W.A. WATERS, J. Chem. Soc. 1965, 1488.
11. I. YAMAZAKI and L.H. PIETTE, J. Am. Chem. Soc. 87,  
986 (1965).
12. T.E. GOUGH, Trans. Faraday Soc. 62, 2321 (1966).
13. B.E. LAND and G. PORTER, Proc. Chem. Soc. 1960, 84.
14. J.R. BOLTON and A. CARRINGTON, Proc. Chem. Soc.  
1961, 385.
15. Y. MATSUNAGA and C.A. McDOWELL, Can. J. Chem.  
38, 1158 (1960).
16. Y. MATSUNAGA, Can. J. Chem. 38, 1172 (1960).
17. W.F. FORBES and P.D. SULLIVAN, J. Am. Chem. Soc.  
88, 2862 (1966).

18. J. BOURDON and M. CALVIN, U.S. Atomic Energy  
Comm. UCRL-3466 (1965).
19. A. STREITWIESER, "Molecular Orbital Theory for  
Organic Chemists", Wiley, New York 1961, 252.
20. L.F. FIESER, J. Am. Chem. Soc. 52, 5204 (1930).
21. HEILBRON and BUNBURY, "Dictionary of Organic  
Compounds", Eyre and Spottiswoode, London 1965.
22. G. MAGATTI, Ber. 13, 224 (1880).
23. K.H. KONIG, W. SCHULZE and G. MOLLER, Chem. Ber.  
93, 554 (1960).
24. J. MOIR, S. African J. Sci. 9, 322 (1912).
25. B.R. BROWN and A.R. TODD, J. Chem. Soc. 1954, 1280.
26. V. BALOGH, M. FETIZON and M. GOLFIER, Angew. Chem.  
Internat. Edn. 8, 444 (1969).
27. T.H. COFFIELD, A.H. FILBEY, G.G. ECKE and A.J. KOLKA,  
J. Am. Chem. Soc. 79, 5019 (1957).
28. M. PIANKA, J. Chem. Soc. (C) 1967, 2618.
29. H. BROCKMANN and A. DORLARS, Chem. Ber. 85, 1180  
(1952).
30. W.H. HUNTER and G.H. WOLLETT, J. Am. Chem. Soc.  
43, 135 (1921).
31. J. MOIR, J. Chem. Soc. 91, 1305 (1907).
32. HILGER and WATTS, "Microspin X-Band Instruction  
Manual", Hilger and Watts, London 1964, Book I.
33. HILGER and WATTS, "Instruction Manual for Variable  
Temperature Gas Flow System W910, Hilger and Watts,  
London 1967.
34. HILGER and WATTS, "Microspin X-Band Instruction  
Manual", Hilger and Watts, London 1964, Book IV.

35. F. GROVES, "PAGE, A Package of Algol Graphic Procedures for the ICL 1905 Computer", Department of Chemistry, The University of Aston in Birmingham Nov. 1971.
36. P.B. AYSCOUGH: "Electron Spin Resonance in Chemistry", Methuen, London 1967, p. 440.
37. H. RUTISHAUSER, Numerische Mathematik 9, 1 (1966).
38. A.S. HOUSEHOLDER, "Principles of Numerical Analysis", McGraw-Hill, New York 1953, p. 160.
39. C.A. COULSON and H.C. LONGUET-HIGGINS, Proc. Roy. Soc. A191, 39 (1947).
40. A.D. McLACHLAN, Mol. Phys. 3, 233 (1960).
41. Y.YOKOZAWA and I. MIYASHITA, J. Chem. Phys. 25, 796 (1956).
42. E. DE BOER and S.I. WEISSMAN, J. Chem. Phys. 26, 963 (1957).
43. A. CARRINGTON, J. Chem. Soc. 1959, 947.
44. J. BOLTON and A. CARRINGTON, Proc. Chem. Soc. 1961, 174.
45. J.A. BRIVATI, R. HULME and M.C.R. SYMONS, Proc. Chem. Soc. 1961, 384.
46. J.R. BOLTON, A. CARRINGTON and J. dos SANTOS-VEIGA, Mol. Phys. 5, 465 (1962).
47. M.J. STEPHEN and G.K. FRAENKEL, J. Chem. Phys. 32, 1435 (1960).
48. J.R. BOLTON and A. CARRINGTON, Mol. Phys. 5, 161 (1962).
49. J.R. BOLTON, A. CARRINGTON and P.F. TODD, Mol. Phys. 6, 169 (1963).
50. W.F. FORBES and P.D. SULLIVAN, Can. J. Chem. 44, 1501 (1966).

51. H.M. BUCK, W. BLOEMHOFF and L.J. OOSTERHOFF,  
Tetrahedron Letters, 1960 (9), 5.
52. A.B. BARABAS, W.F. FORBES and P.D. SULLIVAN, Can.  
J. Chem. 45, 267 (1967).
53. P.D. SULLIVAN, J. Am. Chem. Soc. 89, 4294 (1967).
54. W.F. FORBES and P.D. SULLIVAN, Can. J. Chem. 46,  
325 (1968).
55. P.D. SULLIVAN and J.R. BOLTON, J. Am. Chem. Soc.  
90, 5366 (1968).
56. P. MARKLEW, Undergraduate Project Report University  
of Aston in Birmingham 1973.
57. M.L. RANDOLPH, Rev. Sci. Instr. 31, 949 (1960).
58. A. NISHINAGA, P. ZIEMEK and T. MATSUURA, Tetrahedron  
Letters 1969 (55), 4905.
59. P.D. SULLIVAN, J. Mag. Resonance 5, 438 (1971).
60. M. ADAMS, M.S. BLOIS and R.H. SANDS, J. Chem. Phys.  
28, 774 (1958).
61. H. TSUBOMURA, K. KIMURA, H. YAMADA and M. KATO,  
Tetrahedron Letters 1965 (47), 4217.
62. H. YAMADA and K. KIMURA, J. Chem. Phys. 51, 5733  
(1969).
63. J. PETRANEK, J. PILAR and O. RYBA, Collect. Czech.  
Chem. Comm. 35, 2571 (1970).
64. F. GERSON, "High Resolution ESR Spectroscopy",  
Wiley, New York 1970, p.96.
65. E.W. STONE and A.H. MAKI, J. Chem. Phys. 36, 1944  
(1962).
66. M.R. DAS and B. VENTKATARAMAN, J. Chem. Phys. 35,  
2262 (1961).
67. J. GENDELL, J.H. FRIED and G.K. FRAENKEL, J. Chem.  
Phys. 37, 2832 (1962).

68. M.R. DAS and G.K. FRAENKEL, *J. Chem. Phys.* 42, 1350 (1965).
69. M. KARPLUS and G.K. FRAENKEL, *J. Chem. Phys.* 35, 1312 (1961).
70. E.W. STONE and A.H. MAKI, *J. Am. Chem. Soc.* 87, 454 (1965).
71. W.M. GULICK, Jr. and D.H. GESKE, *J. Am. Chem. Soc.* 88, 4119 (1966).
72. M. BROZE, Z. LUZ, and B.L. SILVER, *J. Chem. Phys.* 46, 4891 (1967).
73. J. BURGESS and M.C.R. SYMONS, *Quart. Rev.* 22, 276 (1968).
74. J. OAKES and M.C.R. SYMONS, *Trans. Faraday Soc.* 64, 2579 (1968).
75. E.M. KOSOWER, *J. Am. Chem. Soc.* 80, 3253 and 3267 (1958).
76. P. ACKERMANN, J.P. GERMAIN and H. ROBERT, *C.P. Acad. Sci. Ser. B* 271, 138 (1970).
77. T.H. CLAXTON and D. McWILLIAMS, *Trans. Faraday Soc.* 64, 2593 (1968).
78. H.M. McCONNELL, *J. Chem. Phys.* 24, 632 (1956).
79. H.M. McCONNELL and D.B. CHESNUT, *J. Chem. Phys.* 28, 107 (1958).
80. J.R. MORTON, *Chem. Rev.* 64, 453 (1964).
81. T. KAGIYA, Y. SUMIDA and T. INOUE, *Bull. Chem. Soc. Jap.* 41, 707 (1968).
82. H.M. McCONNELL, *J. Chem. Phys.* 24, 764 (1956).
83. R. BERSOHN, *J. Chem. Phys.* 24, 1066 (1956).
84. S.I. WEISSMAN, *J. Chem. Phys.* 25, 890 (1956).
85. H.S. JARRETT, *J. Chem. Phys.* 25, 1289 (1956).



86. H.M. McCONNELL, C. HELLER, T. COLE and R.W. FESSENDEN, J. Am. Chem. Soc. 82, 760 (1960).
87. A. STREITWIESER, "Molecular Orbital Theory for Organic Chemists", Wiley, New York 1961, p. 33.
88. A. CARRINGTON, F. DRAVNIKS and M.C.R. SYMONS, J. Chem. Soc. 1959, 947.
89. G. VINCOW and G.K. FRAENKEL, J. Chem. Phys. 34, 1333 (1961).
90. A. STREITWIESER, "Molecular Orbital Theory for Organic Chemists", Wiley, New York 1961, p. 131.
91. C.A. COULSON and V.A. CRAWFORD, J. Chem. Soc. 1953, 2052.
92. J.W. EASTMAN, G. ENGELSMA and M. CALVIN, J. Am. Chem. Soc. 84, 1339 (1962).
93. I. ISENBERG and S.L. BAIRD Jr., J. Am. Chem. Soc. 84, 3803 (1962).
94. N.H. KOLODNY and K.W. BOWERS, J. Am. Chem. Soc. 94, 1113 (1972).
95. K. MARUYAMA, S. SUZUE and J. OSUGI, Bull. Chem. Soc. Jap. 44, 1161 (1971).
96. Y. IIDA, Bull. Chem. Soc. Jap. 45, 105 (1972).
97. Y. MATSUNAGA and Y. NARITA, Bull. Chem. Soc. Jap. 45, 408 (1972).
98. C. JACKSON and N.K.D. PATEL, Tetrahedron Letters 1967, 2255.
99. B.C. GILBERT, P. HANSON, R.O.C. NORMAN and B.T. SUTCLIFFE, Chem. Comm. 1966, 166.
100. IUPAC, "Nomenclature of Organic Chemistry, Section C", Butterworths, London 1965, p. 76.
101. R.S. CAHN, "An Introduction to Chemical Nomenclature", Butterworths, London 1968, p. 48.

102. IUPAC, "Nomenclature of Organic Chemistry, Section C", Butterworths, London 1965, p. 11.

### ACKNOWLEDGEMENTS

The author acknowledges with gratitude the guidance and encouragement given him by his supervisor, Dr. D.A.F. Munday, throughout the course of the work presented in this thesis.

The author is also indebted to Mr. P.D. Groves for much helpful advice regarding the computer programming.

Acknowledgement is made of the receipt of an S.R.C. Award, and of the facilities made available by the Department of Chemistry which made the work possible.